HYDRODYNAMICS OF LAMELLA CLARIFIERS IN WASTEWATER TREATMENT PLANTS

NGUYEN THE ANH

February 2020

THE UNIVERSITY OF KITAKYUSHU

GRADUATE SCHOOL OF ENVIRONMENTAL ENGINEERING

HYDRODYNAMICS OF LAMELLA CLARIFIERS IN WASTEWATER TREATMENT PLANTS

by

NGUYEN THE ANH

February 2020

This dissertation is submitted for the degree of Doctor of Engineering

DECLARATION

This dissertation is the result of my own work and contains no material which has been accepted for the award of any other degree or diploma in my name, in any university or other tertiary institution. It contains no material previously published or written by another person, except where due reference has been made in the text. This dissertation has not been previously submitted, in part or whole, to any university or other tertiary institution for any degree, diploma, or the other qualification.

Nguyen The Anh

February 2020

Kitakyushu, Japan

ACKNOWLEDGEMENTS

First and foremost, I would like to express my deepest gratitude to my supervisor, Associate Professor Mitsuharu Terashima. It has been a great honor to be his first Ph.D. student. His continuous supports and guidance helped me to reach the study accomplishment. His explanations were always simple but efficient, which enlightened many of the complex problems encountered during the research. I do appreciate his time and effort in revising my papers and thesis. Without his contribution, my research could never obtain such profound results.

Besides my supervisor, I would like to thank Professor Hidenari Yasui for his insightful comments throughout my study. His immense knowledge and integral perspective on the research helped me to sharpen my thinking. Following his suggestions, my complicated simulation results became clearer and more practical.

I am grateful to the other committee members, Professor You Ito, and Associate Professor Takumi Sasaki, The University of Kitakyushu, for their valuable comments and helpful suggestions on my research.

My sincere thanks also go to Professor Nguyen Viet Anh from the National University of Civil Engineering in Vietnam, who was my supervisor when I was an undergraduate and Master student. I would not achieve this point without his support and encouragement. I have learned a lot of things from him, both inside and outside the research field.

I would like to thank all members of Yasui-Terashima's laboratory for sharing both joyful and hard moments in my Ph.D. study. Special thanks go to Magnus So for his valuable support at the first stage of my research.

I greatly acknowledge the financial support from the Vietnam

International Education Development that made my Ph.D. work possible.

Last but not least, I would like to thank my family for their immersed love and encouragement during all these years of studying.

ABSTRACT

The sedimentation tank plays an important role in water and wastewater treatment systems. The effective performance of the settling tank contributes largely to the reduction of suspended solids (SS), which is an important parameter in the wastewater quality index. The treatment efficiency of settling tanks is influenced by many factors such as type of sedimentation tank, settling area, temperature conditions, sediment characteristics, the hydraulic regime in the tank, etc. Therefore, it is difficult to estimate the influences of boundary conditions on the performance of the settling tank.

In recent decades, the computational fluid dynamics (CFD) model has been widely used in sedimentation tank research. The CFD model is developed based on numerical methods in which influencing factors such as flow, turbulent, discrete settling are expressed through mathematical equations. Other influencing factors such as tank configuration, particle distribution were defined in boundary simulation conditions. In this study, the CFD model was applied to simulate the settling process taking place in primary and secondary settling tanks. In primary sedimentation tanks, installing lamella baffles is a promising alternative to increase the removal efficiency and reduce the footprint. All the guidelines for designing a lamella settling tank are mostly based on ideal settling assumptions. In this study, we conducted a simulation for lamella settling tanks to assess the effect of the increased settling area due to inclined plates, the shape of inclined plates on the suspended solids removal efficiency in tanks. Simulation results are used to build the relationship between the increased settling area and the increased capacity of the clarifier. In addition, this study also simulated sedimentation tanks with increasing the settling area by (i) increasing the number of inclined plates or (ii) increasing the width and/or (iii) increasing the length of the tank dimension. The research results help to optimize the design of sedimentation tanks and to achieve the desired sediment removal efficiency. The hydraulic process taking place in the tanks when changing the design parameters was also visualized. Based on the

findings, it is possible to evaluate the difference between simulation results by the CFD model and theoretical method. For secondary settling tanks, the study introduced a new concept for simulation of sediments in sedimentation tanks. Simulation is conducted with two scenarios of the conventional model and the proposed model. Simulation results were compared with experimental results to assess the suitability of the model for the settling process in the tank.

CONTENTS

LIST OF FIGURES

LIST OF TABLES

LIST OF ABBREVIATIONS

ABBREVIATIONS	DESCRIPTION
ASM	Activated sludge model
BOD_5	Biochemical oxygen demand at 5 days
COD	Chemical oxygen demand
CFD	Computational fluid dynamics
1D, 2D, 3D	1-dimensional, 2-dimensional, 3-dimensional
FTCs	Flow-through curves
MBBR	Moving bed biofilm reactor
MLSS	Mixed liquor suspended solids
RTD	Resident time distribution
SS	Suspended solids
UV	Ultraviolet
VOF	Volume of fluid
WTP	Water treatment plant
WWTP	Wastewater treatment plant

LIST OF SYMBOLS AND UNITS

ENGLISH SYMBOLS

A	Total settling area in the settling tank (m^2)
A_o	Surface area in the original settling tank (m^2)
A_0^*	Surface area of tank (m^2)
A_b	Horizontal projection area of the inclined plate (m^2)
A_L	Increased surface area by increasing the length of the tank (m^2)
A_W	Increased surface area by increasing the width of the tank (m^2)
A_δ	Increased settling area by installing inclined plates or increasing the length of the tanks or increasing the width of the tanks (m^2)
C	Chezy coefficient ($m^{1/2}/s$)
C_{in}^i	Concentration of particle group i (from 1 to 10) at the inlet (mg/L)
C_{out}^i	Concentration of particle group i (from 1 to 10) at the outlet (mg/L)
E_θ	Exit age distribution in terms of θ (-)
g	The acceleration of gravity (m/s^2)
Ha	Hazen number (-)
Ha^0	Hazen number in settling tank (-)
Ha^*	Hazen number in lamella settling tank (-)
H	Height of tank (m)
H_D	The depth of the tank (m)
H_L	Water level (m)

k	Dimensionless turbulent kinetic energy (-)
k_s	Settling slope (-)
L	Length of the original settling tank (m)
L_b	Length of the inclined plate (m)
L_m	The length from inlet to the monitoring position (m)
L_p	Horizontal projection length of the inclined plate (m)
L_δ	Increased length of the tank (m)
LV^*	Modified linear velocity in lamella settling tank ($m^3/(m^2 \cdot h)$)
LV_b	Linear velocity in the lamella settling tank in case α=1 ($m^3/(m^2/h)$)
LV_b^*	Linear velocity in the lamella settling tank in case $\alpha \neq 1$ ($m^3/(m^2/h)$)
LV_o	Linear velocity in the original settling tank ($m^3/(m^2 \cdot h)$)
LV_i	Linear velocity in the improved settling tank ($m^3/(m^2 \cdot h)$)
N	Number of tanks
n	Manning roughness ($s/m^{1/3}$)
n_b	Number of inclined plates in the lamella settling tank
N_p	Number of particle groups
P	The pressure (*Pa*),
p	Dimensionless pressure (-)
Q_b	Theoretical attainable flow rate in the lamella settling tank (m^3/h)
Q^*_b	Actual attainable flow rate in the lamella settling tank to maintain the same SS removal efficiency (m^3/h)
Q_o	Flow rate in the original settling tank (m^3/h)
ΔQ	Incremental change of flow rate (m^3/h)
Q_1	Outlet 1 flow rate (m^3/h)
R	Hydraulic radius (m)
Re	Reynolds number based on flow depth and nominal flow velocity (-)

$R_{(\theta)}$ Ideal curve (assuming that the flow within inclined plate at lamella settling tank is similar up-flow regime)

r_w The water volume fraction (-)

$r_{s,n}$ The SS volume fraction (-)

SV_i Settling velocity of particle group i (m/h or m/s)

SV_{0i} Maximum settling velocity of particle group i (m/h)

$SV_{90\text{-}i}$ Ideal settling velocity of particle group i in improved tank which had the η of 90% (m/h)

$SV^*_{90\text{-}i}$ Actual settling velocity of particle group i in improved tank which had the η of 90% (m/h)

t Time (s)

t^* Hydraulic retention time (s)

t_i Residence time of particle i (s)

t^*_m Hydraulic retention time at the monitoring position (h)

U Mean horizontal velocity (m/s)

U_c Average velocity of the cross (m/s)

u Dimensionless velocity component in x direction (-)

u_m^i The mixture flow velocity in the i-direction (m/s)

u_m^j The mixture flow velocity in the j-direction (m/s)

u_{Dw}^i The drift velocities for the water (m/s)

$u_{Ds,n}^i$ The drift velocities for the solids (m/s)

V Mean vertical velocity (m/s)

V_T	Volume of tank (m^3)
V_m	The volume of secondary settling tank from inlet to monitoring position (m^3)
W	Width of the original settling tank (m)
W_b	Width of the inclined plate (m)
W_δ	Increased width of the tank (m)
X	Sludge concentration (kg/m^3)
x	Horizontal coordinate (m)
x_f	Direction of flow (m)
x^i	The Cartesian coordinate in the i-direction (m)
x^j	The Cartesian coordinate in the j-direction (m)
y	Vertical coordinate (m)
$Y_{s,n}$	The SS mass fraction (-)

GREEK SYMBOLS

α	Effectiveness of baffle related to increased flow rate (from 0 to 1)
β	Effectiveness of increased δ to improve the η of small SV particle groups (from 0 to 1)
γ	Effectiveness of inclined plates on Hazen number (from 0 to 1)
∇^2	Laplacian operator
δ	Increased settling area (-)
ε	Turbulence dissipation rate (m^2/s^3)
η	SS removal efficiency of the tank (from 0 to 1)
η_i	SS removal efficiency of particle group i (from 0 to 1)
η_{oi}	Removal efficiency of particle group i in the original settling tank (-)
η_{bi}	Removal efficiency of particle group i in the lamella settling tank (-)
θ	Dimensionless time units (-)
λ	The ratio of increment and initial flow rate (-)
ν	Dimensionless kinematic molecular viscosity (-)
ν_{tv}	Turbulent viscosity (kg/m.s)
ν_t	Dimensionless turbulent eddy viscosity (-)
ρ	Density (kg/m^3)
ρ_m	The mixture density (kg/m^3)
ρ_w	The water density (kg/m^3)
ρ_s	The SS density (kg/m^3)

σ^2 Variance of a tracer curve or distribution function (s^2)

τ_m^{ji} The viscous stresses (Pa)

τ_{Tm}^{ji} The turbulent stresses (Pa)

τ_{Dm}^{ji} The diffusion stresses (Pa)

υ Dimensionless velocity component in y direction (-)

φ_i Suspended solid removal efficiency increased (-)

$\psi_{90\text{-o}}$ The ratio between $SV_{90\text{-}o}$ and LV_o

$\psi_{90\text{-}i}$ The ratio between $SV_{90\text{-}i}$ and LV_o

$\psi^*_{90\text{-}i}$ The ratio between $SV^*_{90\text{-}i}$ and LV_o

CHAPTER 1 GENERAL INTRODUCTION

1.1. OVERVIEW ON SEDIMENTATION TANK

The sedimentation tank plays an important role in water and wastewater treatment systems by settling suspended particles using gravity. The sedimentation tank contributes largely to the reduction of suspended solids (SS), which is an important parameter in wastewater quality index due to its association with large amounts of Chemical Oxygen Demand (COD) and nutrients [1]. In water treatment (**Fig 1.1**), sedimentation tanks are often used to remove suspended solids, turbidity, color, and increasing working time for filter tanks. In wastewater treatment (**Fig 1.2**), sedimentation tanks are usually designed before and after the biological reactor. The primary settling tank removes SS from wastewater influent to reduce the organic loading of the biological reactor. The secondary settling tank compresses and separates organic particulates (biomass), which are created in biological treatment reactors. In many countries, poor effluent quality has reported at 20 to 50% of wastewater treatment plants due to low-performance sedimentation [2]. In order to improve the treatment efficiency of the settling tank, it is necessary to understand the nature of the processes occurring internally in the settling tanks and identify factors affecting the hydraulic regime of the sedimentation tanks.

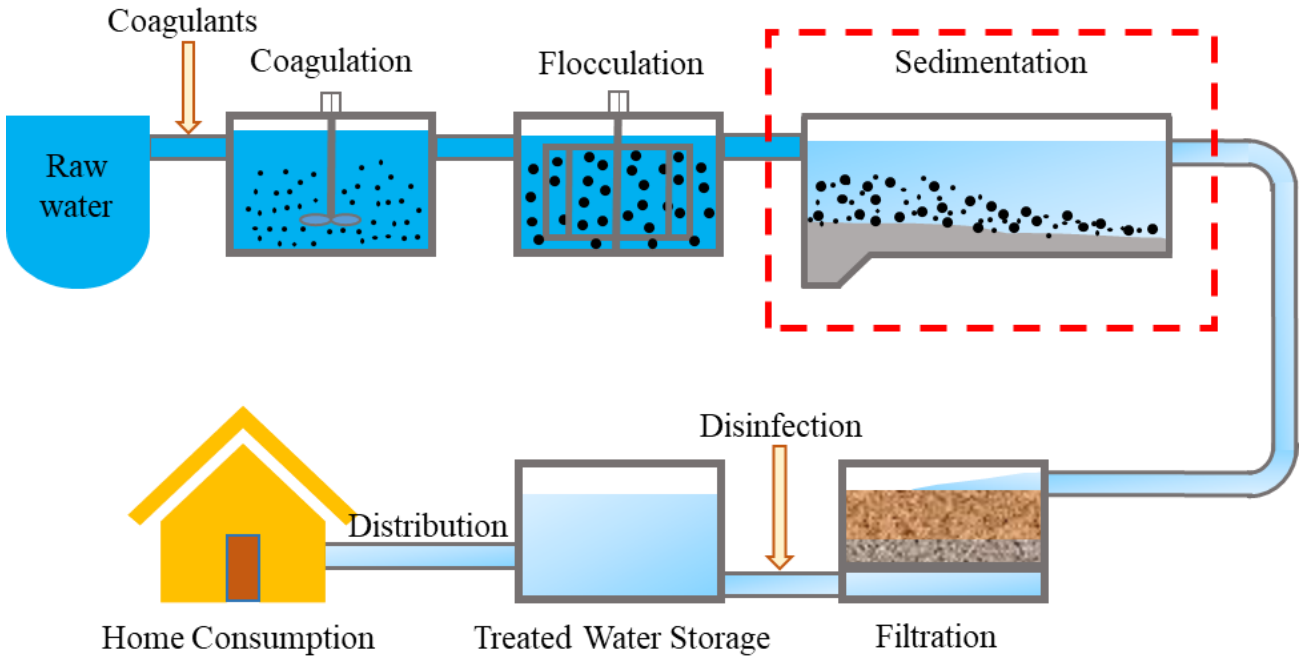

Fig 1.1 Water treatment process

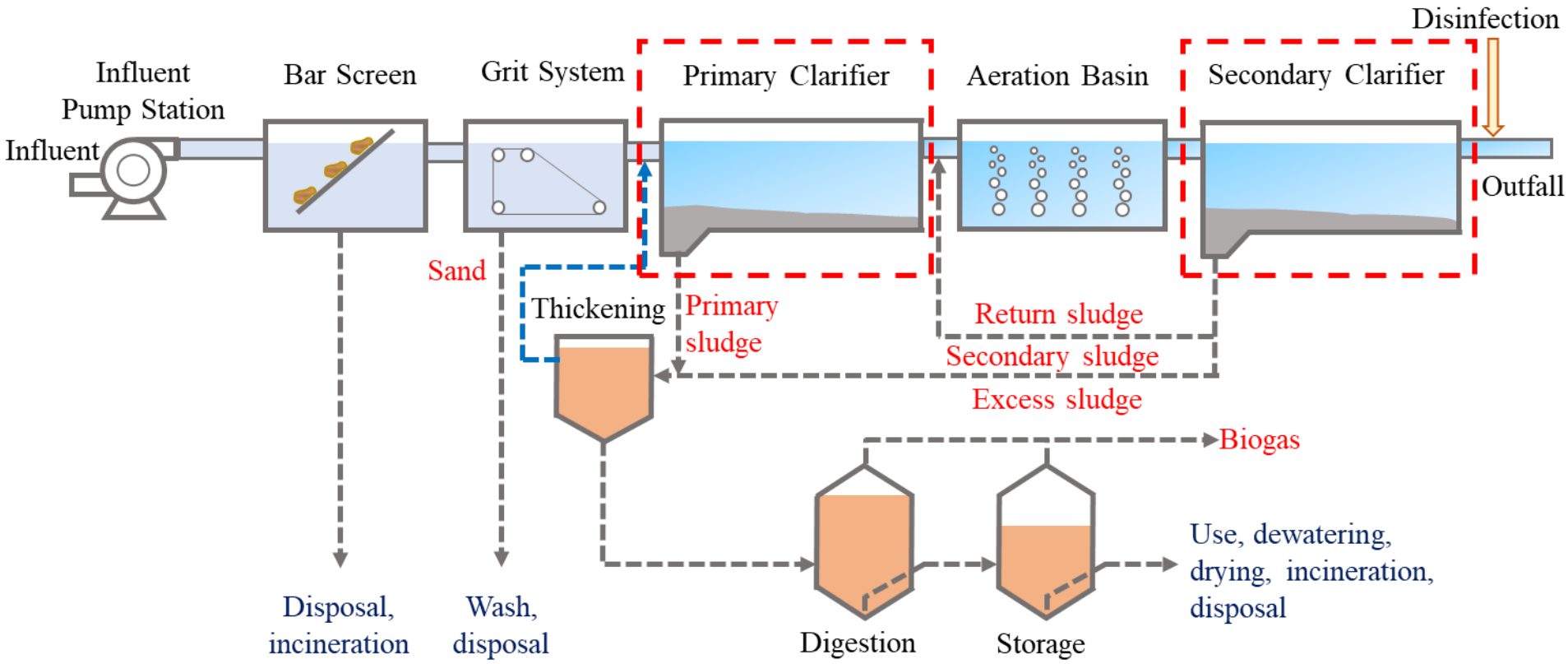

Fig 1.2 Wastewater treatment process

There are many factors needed to be taken into account, such as overflow rate, input SS content, the particle size distribution of SS, tank-type, etc. in designing the sedimentation tanks. However, in the conventional method, the calculation is based on the ideal linear velocity, which is calculated as the ratio of flow rate to the surface area. In the case of increasing flow rate, the surface area of the tank was needed to be increased proportionally to maintain the SS removal efficiency. Meanwhile, at the constant flow rate, the overall SS removal of the tank could be enhanced if the small particle groups were effectively separated.

However, the designing of a sedimentation tank based on ideal settling conditions could not reflect the real working conditions, resulting in the undesirable tank performance. The experimental models needed to be developed to refine the design process, which was time-consuming and costly, even though some parameters were experimentally unidentifiable.

Many researchers used empirical models to evaluate the treatment efficiency of sedimentation tanks and developed empirical equations employed for the design process. Christoulas, Yannakopoulos and Andreadakis, 1998 [3] built a relationship between SS removal efficiency and input SS concentration, overflow rate, and wastewater temperature using an experimental mathematical model. Jover-Smet, Martín-Pascual and Trapote, 2017 [4] built an experimental model for primary settling tanks to assess the impact of operational parameters, such as overflow rate, hydraulic retention time, and temperature on the SS and organic matter removal efficiency.

For the lamella settling tank, Leung, 1983 [5] studied the distribution of three-layer, stratified viscous channel flow between inclined plates. Demir, 1995 [6] investigated the optimum angle of the baffle in the lamellar settling tank at various linear velocities. Different types of tube settlers were examined by

Fujisaki and Terashi, 2005 [7] to obtain a higher solid separation capacity. McKean, 2010 [8] investigated the effectiveness of lamella settling tanks in the primary treatment of domestic wastewater. Study results indicated that the SS and Biochemical Oxygen Demand (BOD_5) removal efficiency in lamella settling tanks was improved compared to conventional primary settling tanks. Chintokoma, Machunda and Njau, 2015 [9] studied the optimization of sedimentation tanks using inclined plates to pre-treat highly turbid water. Research results for the laboratory scale sedimentation tanks showed that the sedimentation tanks with inclined plates are capable of pre-treating highly turbid water for ultra-filtration.

Computational fluid dynamics (CFD) models are developed based on mathematical equations to describe the flow regime (gas, water, or mixture), thereby studying details of the flow regime with parameters such as pressure, velocities, and fluxes. The CFD model has been in development since the late 1950s, initially being used in the development and manufacture of aerospace and military equipment. By the 1990s, CFD was developed for application in fluid flow simulations. The model is used for research on water and wastewater treatment.

A series of studies on flocculation, flotation, biological treatment, and disinfection were conducted using the CFD model. Bridgeman, Jefferson and Parsons, 2010 [10] successfully applied the CFD model to simulate the flocculation process for water treatment. The simulation used velocity gradient distribution, and turbulence dissipation rates demonstrate mixing efficiency in different jar test units. Terashima et al., 2009 [11] built a three-dimensional model in CFD to study the effect of quantifying mixing in a full-scale anaerobic digester. The simulation model was employed to determine the required time for complete mixing in a full-scale digester. Simulation results could be used for optimizing the feeding cycles for better digester

performance. Fayolle et al., 2007 [12] used the CFD tool to optimize aeration in the activated sludge processes. The simulation results were predicted the oxygen transfer characteristics in the aeration tanks and showed small differences from the experimental results. Rauen, Angeloudis and Falconer, 2012 [13] applied CFD in chlorine contact tank simulation. The study focused on the hydrodynamic process simulation to optimize the study of chlorine contact tanks. Simulations were performed under steady and unsteady conditions to assess the hydraulic regime in the chlorine contact tank.

To improve the design process, in recent decades, the CFD model has been widely applied in the simulation of sedimentation tanks. The model shows the process of taking place in a tank based on the mass and momentum conservation equations. The configuration and boundary conditions change in the settling tanks will be solved by the algorithms defined in the model to identify process influences in the tank. Therefore, the CFD model is used for the optimal design of the sedimentation as well as an in-depth study of the processes occurring inside the sedimentation. Using the CFD model in designs will reduce costs and time consuming compared to conventional designs [14].

There are many studies carried out for sedimentation tanks in wastewater treatment. Imam, McCorquodale and Bewtra, 1983 [15] presented a finite difference model of the vorticity transport stream equations to establish the vertical velocity field. Stamou et al., 1989 [16] used a numerical model to study the flow and settling process of SS in primary sedimentation tanks and compared the simulation results to those from the theoretical method. McCorquodale, 1991 [17] applied a numerical model to predict the influence of unsteady flow on sedimentation tank performance. Zhou, McCorquodale and Vitasovic, 1992 [18] investigated the influence of the settling zone flow pattern to settling tank performance. A practical mathematical model was used to predict the settling process of non-uniform particle size in class I settling

tanks in Jin, Guo and Viraraghavan, 2000 [19]. Ramalingam et al., 2012 [20] evaluated the effect of two important parameters in the 3D CFD model, namely discrete particle and the modification of the floc aggregation and floc break-up coefficients on the accuracy of the predictions of the CFD model. Ghawi and Kriš, 2012 [21] developed a complex CFD model to estimate the factors that impact deposition efficiency.

Lamella settling tanks are commonly employed in wastewater treatment systems today, thanks to saving the construction area. Extensive research on the performance and optimization of incline plates, as well as the mechanism of the sedimentation process in lamella settlers, were carried out. Kowalski, 2004 [22] compared the SS removal efficiency in the conventional tank and the lamella settling tank taking into account the density, viscosity and mass fraction of solid particles. CFD model was used in lamella sedimentation simulation to evaluate the effect of the tank configuration and operating variables on SS removal efficiency of sedimentation tanks (Shen and Yanagimachi, 2011) [23]. Tarpagkou and Pantokratoras, 2014 [24] proved that inclined plates improved the hydraulic regime by CFD simulating a full-scale system, rather than a part of the system as in previous research. The above-mentioned studies successfully predicted the SS removal efficiency in lamella settling tanks.

Studies on secondary settling tanks often focused on the main function of settling tanks to compress and separate sludge particles from the biological reactors. Therefore, the simulation of predicting the distribution of sludge in secondary settling tanks has been mentioned by many studies recently. Weiss et al., 2006a [25] investigated the sedimentation of activated sludge using a CFD model to simulate a full-scale circular secondary sedimentation, but the simulation results incorrectly predicted the sludge concentration in a larger distance from the inlet zone. Ramin [26] developed a new settling velocity

model that involved the effect of resistance, transient, and compression on sludge distribution. François et al., 2016 [27] studied activated sludge settling mechanisms using the experiment method. The results of a detailed activated sludge velocity profile were applied to build numerical models in the simulation settling process.

However, in the sedimentation tanks for water and wastewater treatment, there are no studies fully evaluating the actual effect of increased settling area on SS removal efficiency of tanks. In secondary sedimentation tanks for wastewater treatment, the settling velocity model used in current numerical simulations did not accurately predict the sludge distribution in the tank. Therefore, a sedimentation study was conducted to clarify these issues.

1.2 SCOPE AND OBJECTIVES

The study focused on the application of the CFD model in simulation of the settling process in the sedimentation tanks of water and wastewater treatment plants. Current design guidelines for sedimentation tanks are often based on assumptions about ideal settling conditions of suspended solids (SS) particles. However, the treatment efficiency of the tanks in operation was often different from the calculated results in the design. In this study, simulations for sedimentation tanks were conducted with varying conditions of the simulation.

The first simulation was conducted for lamella settling tanks with a different number of inclined plates and inclined plates configuration. The purpose was to evaluate the actual contribution of the settling area to the efficiency of SS removal and then compare it with the ideal formula in the design of the sedimentation tank. Moreover, the simulation also assessed the impact of the configuration of the inclined plates on the hydraulic regime and the performance of the tank.

The second simulation was carried out for lamella settling tanks and settling tanks without inclined plates, which have the same increased settling area. The purpose of the study was to assess the influence of hydraulic regimes on the SS efficiency removal in three types of tank configuration.

Secondary settling tanks were simulated with a conventional settling model and proposed settling model to assess the accuracy of the simulation settling model of sedimentation tanks.

The findings could provide useful information for the design and optimization of settling tanks. Besides, the results also increase the understanding of the hydraulic process taking place in a settling tank, which was considered a black box in sedimentation tank research.

1.3 DISSERTATION ORGANIZATION

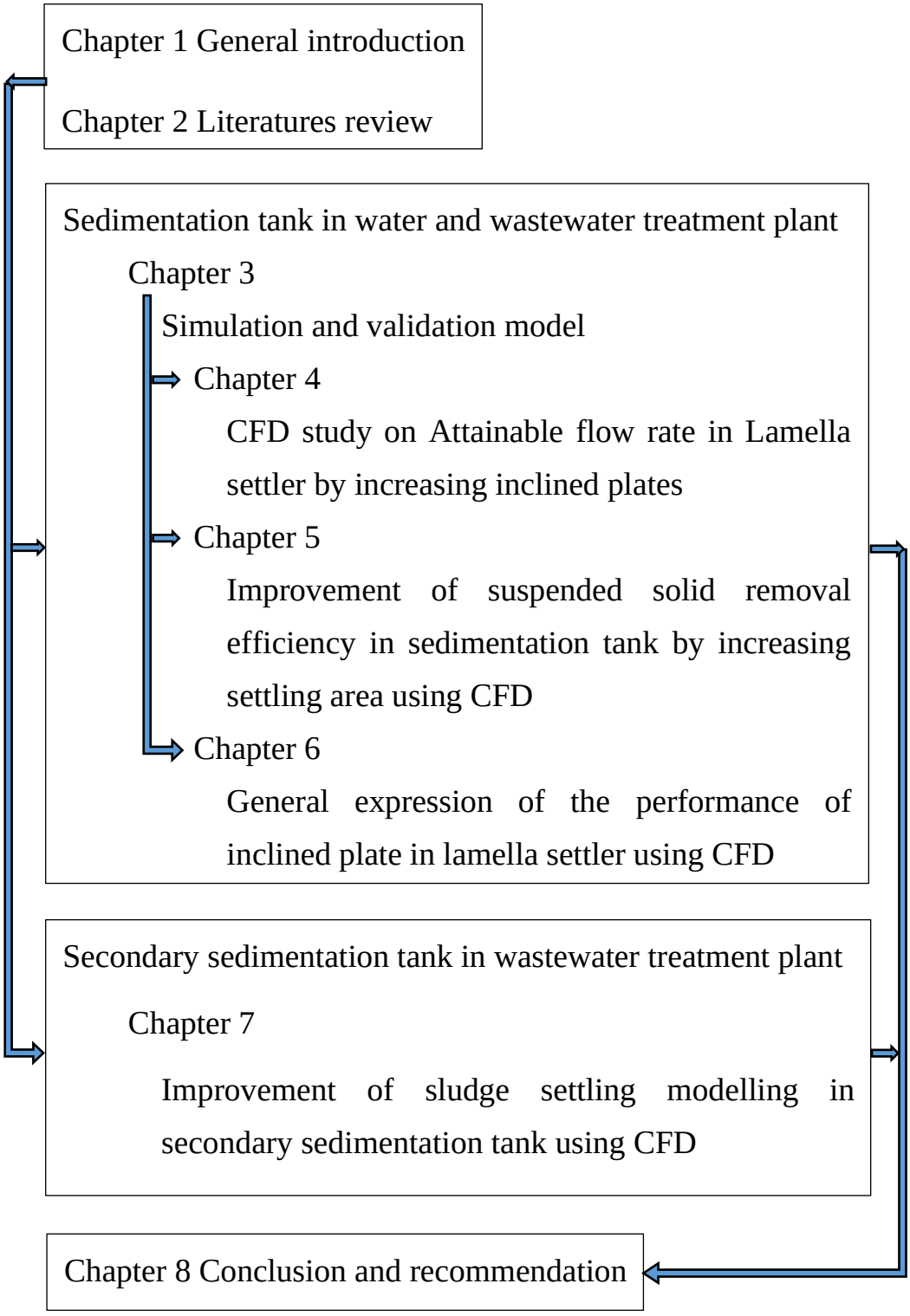

Fig 1.3 Structure of the dissertation

The structure of the dissertation is the following **Fig 1.3**. A brief description

of chapters 2-8 is given below.

Chapter 2: Literatures review

This chapter summarizes the study of sedimentation tanks used in wastewater treatment systems. The study presents the CFD model and its application in settling process simulation. Overview of previous studies using CFD in a simulation of conventional settling tanks and lamella settling tanks were

Chapter 3: Simulation and validation model

This study focuses on the simulation method used in CFDs to simulate settling tanks. Data from reference materials are used to calibrate the model to ensure accuracy for the simulation process. This simulation method is applied for similar simulations in subsequent chapters.

Chapter 4: Computational Fluid Dynamics Study on Attainable Flow Rate in a Lamella Settler by Increasing Inclined Plates

This chapter assesses the effect of the increased settling area due to the inclined plate to increase capacity for the tank. Tracer simulation was performed to evaluate the hydraulic regime in the tank when changing the number of inclined plates. The tracer simulation results have explained the real effect of the inclined plates in the lamella clarifier. The study also conducted a simulation of inclined plates with different configurations, thereby assessing the effect of inclined plates on removal efficiency when the area of inclined plates remained unchanged.

Chapter 5: Improvement of Suspended Solids Removal Efficiency in Sedimentation Tanks by Increasing Settling Area Using Computational Fluid Dynamics

In this chapter, simulation is conducted with different tank configurations.

Simulation results are used to evaluate the effect of the increased sedimentation area on the ability to remove small particles in the tank. The hydraulic regime in the tanks is assessed through the vertical flow velocity. The results in this chapter can be used for optimization in sedimentation tanks design.

Chapter 6: General expression of the performance of inclined plates in lamella settler using Computational Fluid Dynamics Method

This study assesses the influence of the increased settling area due to the inclined plates to the Hazen number and hydraulic parameters in lamella settling tanks. Assess the possibility of increasing the efficiency of suspended solids removal in the tank using inclined plates.

Chapter 7: Improvement of Sludge Settling Modelling in Secondary Sedimentation Tank Using CFD

This chapter focuses on improving the simulation method of the settling process in the secondary sedimentation tanks. Experimental results are used to calibrate and evaluate the validity of the model. Tracer simulations are performed to assess the effect of gravity flow on the hydraulic regime in sedimentation tanks.

Chapter 8: Conclusions and Recommendations

This chapter summarizes the main results in chapters 4-7 and the limitations of the model. Proposals are made for the next research direction to improve the model and application in the optimal design of the clarifier.

References

[1] G. A. Ekama *et al.*, "Secondary settling tanks: theory, modelling and operation.," in *IAWQ Scientific and Technical Report No. 6.*, London, 1997.

[2] L. Piirtola, B. Hultman, C. Andersson, and Y. Lundeberg, "Activated sludge ballasting in batch tests," vol. 33, no. 8, pp. 3–8, 1999.

[3] D. G. Christoulas, P. H. Yannakopoulos, and A. D. Andreadakis, "An empirical model for primary sedimentation of sewage," *Environ. Int.*, vol. 24, no. 8, pp. 925–934, 1998.

[4] M. Jover-Smet, J. Martín-Pascual, and A. Trapote, "Model of suspended solids removal in the primary sedimentation tanks for the treatment of urban wastewater," *Water (Switzerland)*, vol. 9, no. 6, 2017.

[5] W. F. Leung, "Lamella and Tube Settlers. 2. Flow Stability," *Ind. Eng. Chem. Process Des. Dev.*, vol. 22, no. 1, pp. 68–73, 1983.

[6] A. Demir, "Determination of settling efficiency and optimum plate angle for plated settling tanks," *Water Res.*, vol. 29, no. 2, pp. 611–616, 1995.

[7] K. Fujisaki and M. Terashi, "Improvement of settling tank performance using inclined tube settlers," vol. 80, pp. 475–484, 2005.

[8] T. McKean, "Novel Application of a Lamella Clarifier for Improved Primary Treatment of Domestic Wastewater," no. 118, pp. 119–124, 2010.

[9] G. C. Chintokoma, R. L. Machunda, and K. N. Njau, "Optimization of Sedimentation Tank Coupled with Inclined Plate Settlers as a Pre-treatment for High Turbidity Water," vol. 5, no. 17, pp. 11–24, 2015.

[10] J. Bridgeman, B. Jefferson, and S. A. Parsons, "The development and application of CFD models for water treatment flocculators," *Adv. Eng. Softw.*, vol. 41, no. 1, pp. 99–109, 2010.

[11] M. Terashima *et al.*, "CFD simulation of mixing in anaerobic digesters," *Bioresour. Technol.*, vol. 100, no. 7, pp. 2228–2233, 2009.

[12] Y. Fayolle, A. Cockx, S. Gillot, M. Roustan, and A. Héduit, "Oxygen transfer prediction in aeration tanks using CFD," *Chem. Eng. Sci.*, vol. 62, no. 24, pp. 7163–7171, 2007.

[13] W. B. Rauen, A. Angeloudis, and R. A. Falconer, "Appraisal of chlorine contact tank modelling practices," *Water Res.*, vol. 46, no. 18, pp. 5834–5847, 2012.

[14] D. L. Huggins, R. H. Piedrahita, and T. Rumsey, "Use of computational fluid dynamics (CFD) for aquaculture raceway design to increase settling effectiveness," *Aquac. Eng.*, vol. 33, no. 3, pp. 167–180, 2005.

[15] E. Imam, J. A. McCorquodale, and J. K. Bewtra, "Numerical modeling of sedimentation tanks," *J. Hydraul. Eng.*, vol. 109, no. 12, pp. 1740–1754, 1983.

[16] A. I. Stamou, E. W. Adams, and W. Rodi, "Modélisation numérique de l'écoulement et de la sedimentation dans des bassins de décantation primaires de forme rectangulaire," *J. Hydraul. Res.*, vol. 27, no. 5, pp. 665–682, 1989.

[17] J. A. McCorquodale, "Numerical Simulation of Unsteady Conditions in Clarifiers," *Water Poll. Res. J. Canada*, vol. 26, no. 2, pp. 201–222, 1991.

[18] S. Zhou, J. A. McCorquodale, and Z. Vitasovic, "Influences of density on circular clarifiers with baffles," *J. Environ. Eng. (United States)*, vol. 118, no. 6, pp. 829–847, 1992.

[19] Y. C. Jin, Q. C. Guo, and T. Viraraghavan, "Modeling of Class I settling tanks," *J. Environ. Eng.*, vol. 126, no. 8, pp. 754–760, 2000.

[20] K. Ramalingam *et al.*, "Critical modeling parameters identified for 3D CFD modeling of rectangular final settling tanks for New York City wastewater treatment plants," *Water Sci. Technol.*, vol. 65, no. 6, pp. 1087–1094, 2012.

[21] A. Ghawi and J. Kriš, “Improvement performance of secondary clarifiers by a computational fluid dynamics model,” *Slovak J. Civ. Eng.*, vol. 19, no. 4, pp. 1–11, 2012.

[22] W. P. Kowalski, “The method of calculations of the sedimentation efficiency in tanks with lamella packets,” *Arch. Hydroengineering Environ. Mech.*, vol. 51, no. 4, pp. 371–385, 2004.

[23] Y. Shen and K. Yanagimachi, “CFD-aided cell settler design optimization and scale-up: Effect of geometric design and operational variables on separation performance,” *Biotechnol. Prog.*, vol. 27, no. 5, pp. 1282–1296, 2011.

[24] R. Tarpagkou and A. Pantokratoras, “The influence of lamellar settler in sedimentation tanks for potable water treatment - A computational fluid dynamic study,” *Powder Technol.*, vol. 268, pp. 139–149, 2014.

[25] M. Weiss, B. G. Plosz, K. Essemiani, and J. Meinhold, “CFD modelling of sludge sedimentation in secondary clarifiers,” *WIT Trans. Eng. Sci.*, vol. 52, pp. 509–518, 2006.

[26] E. Ramin *et al.*, “A new settling velocity model to describe secondary sedimentation,” *Water Res.*, vol. 66, pp. 447–458, 2014.

[27] P. François, F. Locatelli, J. Laurent, and K. Bekkour, “Experimental study of activated sludge batch settling velocity profile,” *Flow Meas. Instrum.*, vol. 48, pp. 112–117, 2016.

CHAPTER 2 LITERATURES REVIEW

2.1. INTRODUCTION

Sedimentation tanks have existed for a long time in water and wastewater treatment systems. Sedimentation tanks play an important role in the wastewater treatment process, the cost of construction and operation of sedimentation tanks accounts for 30% of the investment cost of the treatment plant [28]. Therefore, research on sedimentation tanks has been the subject of much attention so far. Studies often focus on sedimentation processes occurring in the tank, factors affecting sediment efficiency such as tank configuration, flow regime, temperature, turbulent flow, etc. The purpose of the studies is to find out the nature of the settling processes occurring in the settling tanks, which can optimize the design and operation of sedimentation tanks to improve the efficiency of sediment removal. Recently, CFD models have been used to simulate settling processes using numerical solutions of mathematical equations. The CFD model has been built and developed by many researchers to complete the simulation. This chapter presents an overview of previous sedimentation research. It focuses on studies that use the CFD model in sedimentation tank simulation.

2.2. COMPUTATIONAL FLUID DYNAMICS

The pioneer of CFD was Richardson (1910) when he applied approximate arithmetical solution by finite differences of physical in calculating the stresses in a masonry dam. The early simulation process using hand calculation and the computer was very time-consuming but provided the ideas for the numerical research.

Later, with the rapid development of computer power, the numerical calculation was widely used to solve fluid problems. The 3D models appeared in lates 1960s in the aerospace and military fields, applying fluid dynamics in designing the submarines, helicopters, aircraft, and missiles, etc.

The Finite difference methods for Navier-Stokes equations and Finite element methods appeared in the 1970s. At this time, the Finite difference methods were only applicable to objects of rectangular and cubic sharps, while the finite element methods required much computer power. To overcome such limitations, the Finite volume methods were proposed by the CFD group at Imperial College in the 1970s, that provided solutions of the Navier Stokes Momentum Equations. Further, Launder and Spalding, 1974 presented a Standard k-ε turbulence model in which the turbulent flow with high Reynolds numbers was described. These achievements allowed fluid dynamics to be programmed and solved using computers, distinguishing the CFD with other traditional methods.

The CFD was applied in a vast majority of industries in the 1980s. Until then, the simple structure grid of CFD could not effectively solve the unstructured boundary and wall conditions. Further, due to the limited computing power, the convergence speed was very low. The 3D simulation of complex geometric objects was time-consuming.

Started in the 1980s, the commercial CFD software, for example, ANSYS, was introduced on the market, allowing the users to define the geometry, physical, and chemical properties of the fluids with the specific initial

boundary conditions. The illustration on input data requirements and available output data were presented as follows:

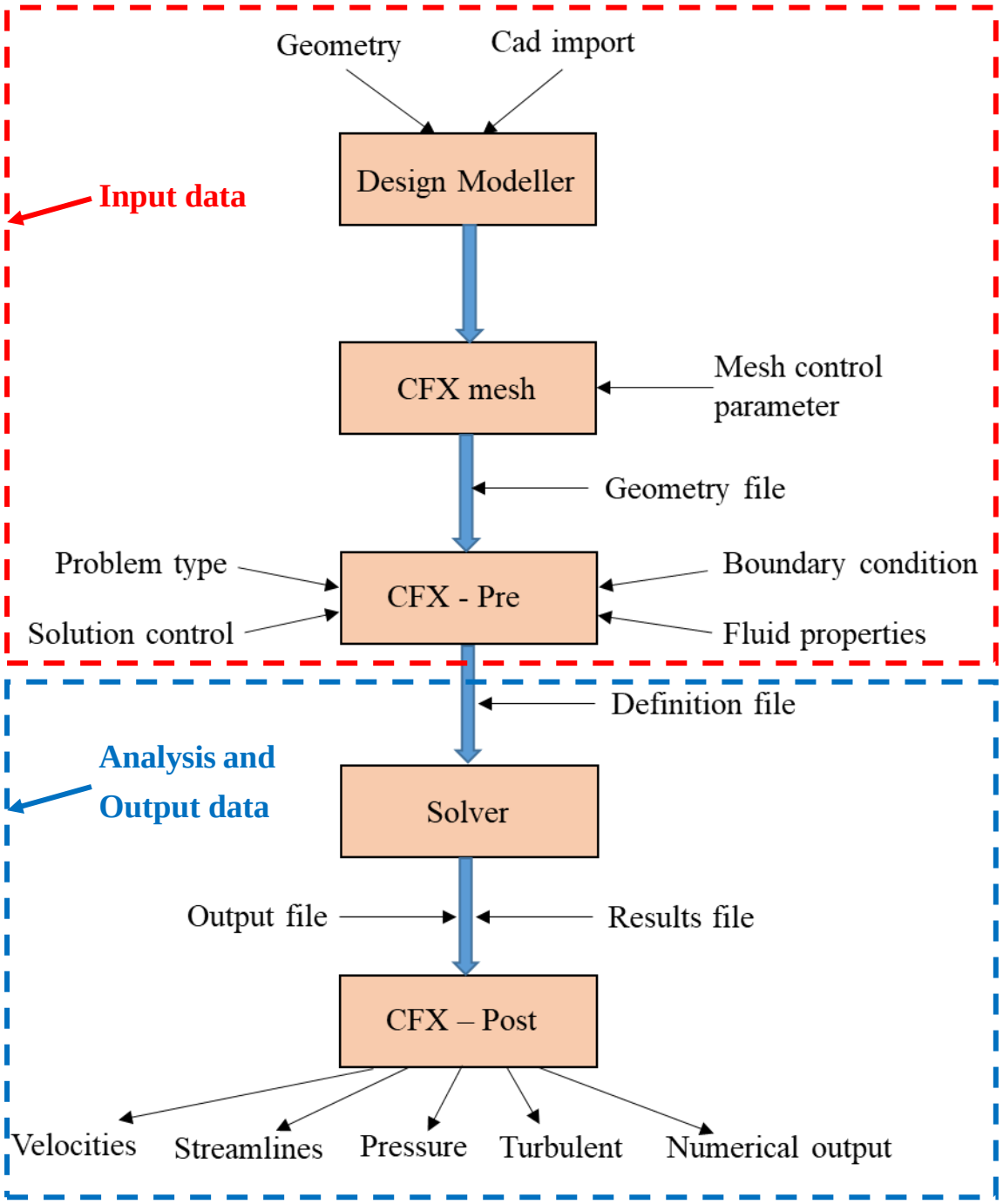

Fig 2.1 Input and output data of commercial CFD software

Based on the sets of mathematical equations, such as the continuity equation, Navier-Stokes equation, and energy equation, etc., the flow regime of gas,

water, or the mixture could be described. The details of the flow regime (velocities, pressures, and fluxes) could be analyzed at a spatial and temporal resolution that is difficult and/or expensive to achieve by other means (observation, direct measurement, and inference). CFD enables scientists and engineers to perform ‘numerical experiments’ (i.e., computer simulations) in a ‘virtual flow laboratory.’ As illustrated below, the velocity vector, velocity streamlines, and contour plots of the fluids could be visualized in the simulation (**Fig 2.2**).

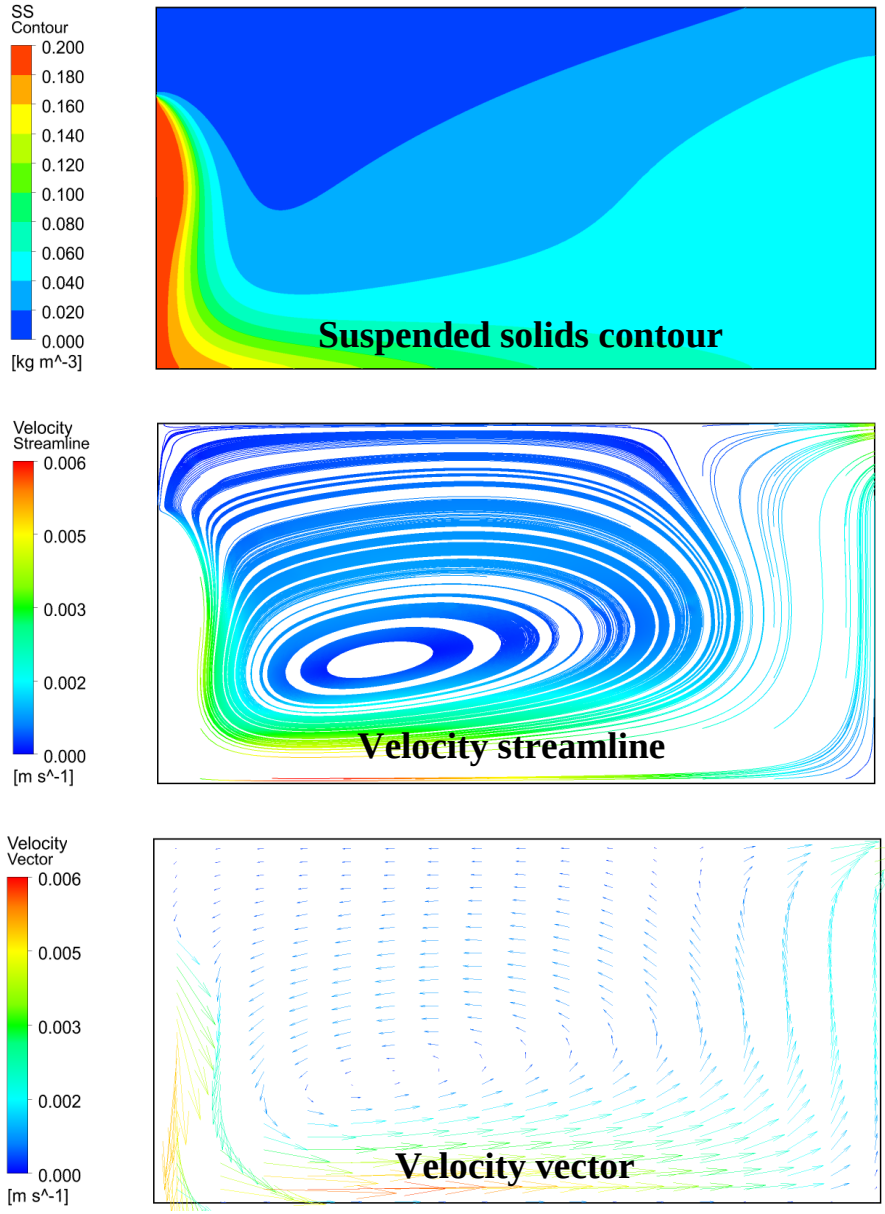

Fig 2.2 Visualization of fluids properties in CFD modelling

2.3. APPLICATION OF CFD IN WATER AND WASTEWATER FIELD

Nowadays, with the development of computer technology, the CFD model has been successfully applied in many fields, including water and wastewater treatment. This section aimed to summarize the general application of CFD in water engineering. The detailed application in sedimentation and lamella settling tanks were provided in the next sections.

2.3.1 In water treatment

The CFD software studies in water treatment covered the overall process, from the raw water reservoir, treatment facilities, clear well, and distribution network. By using CFD, the complex hydrodynamic conditions of the water treatment, which resulted from the combination of physical, chemical, and biological processes, were revealed. From such findings, the optimization of the existing water treatment facilities, as well as the novel design criteria, could be proceeded.

The water treatment processes include a series of units, aiming to remove the impurities from water. Successful performance of the whole process engages with different flow regimes in those unit treatment processes. The units involved in the water treatment process, their objectives of treatment, as well as the flow regime together with possibilities for CFD modelling were summarized in the tables below (**Table 2.1** and **Table 2.2**).

Most of those treatment processes were carried out in a turbulent flow regime. The two-equation turbulence models could solve such flow regime, in which the turbulent velocity and length scales are determined via the solution of two separate transport equations. The first equation is for turbulent kinetic energy, k, while the second one is for the turbulence length scale or some equivalent parameter (ε, the dissipation of turbulence kinetic energy per unit time, or ω, the rate at which turbulent energy is dissipated). The turbulence models are now available in CFD commercial packages.

Table 2.1 Principle units in the water treatment process [29]

Treatment process	Description	Purpose
Raw water storage	Bulk storage of water > 1 day.	Backup supply to WTW in the event of source pollution. Some solids removal via sedimentation.
Coagulation	Chemical (trivalent inorganic coagulant) dose and short (<30s) rapid mix.	Destabilization of water via neutralization of colloidal material charge and precipitation of soluble compounds.
Flocculation	Slow, extended (15-45 mins) mix.	Encourage agglomeration of particles to form mass fractal aggregates (“flocs”) up to 1000 μm.
Clarification	Sedimentation or flotation (via dissolved air injection) of larger flocs.	Solids removal.
Filtration	Flow-through porous granular media	Removal of smaller flocs and particles (<100 μm)
Disinfection	Chemical (chlorine, UV) dose and storage (chlorine only).	Killing or inactivation of potentially harmfully microorganisms

Table 2.2 Flow regime and possible CFD modelling approach

Flow characteristics	Treatment process	CFD Modelling approach
Turbulent flow	Open channel flow	2-equation turbulence models
	Pipe flow	Renolds stress model
	Mixing chambers	Large-eddy simulation
		Direct numerical simulation
Laminar flow	Settlement tanks	Laminar flow model

Flow characteristics	Treatment process	CFD Modelling approach
Multiphase flow	Coagulation	Eulerian multiphase model
	Flocculation	Lagrangian particle model
	Settlement	
	Flotation	
	Filtration	
	Disinfection	
Rotating flow	Mixing chambers	Sliding mesh
	Flocculation	Multiple reference frames

The findings on CFD studies on the units of water treatment processes were presented hereafter.

2.3.1.1 Flocculation

In 2010, Bridgeman et al. [29] applied the CFD to simulate the jar test and lab-scale/full-scale flocculators.

Flocculation is the aggregation of small particles into larger flocs that facilitated their settlement under gravity. The flocs size is the decisive factor controlling the performance of the process. Flocs size is found to be influenced by the turbulence energy dissipation rate and floc strength, which could be estimated by the velocity gradient. In CFD modeling, the actual power dissipated at any point in the mixing vessel could be simulated under the real hydrodynamic regime. For instance, the local power consumption nearby the impeller could be several orders of magnitude higher than the remaining parts of the vessels. The good mixing performance could be expressed by the even distribution of the velocity gradient within the vessel. Opposingly, poor performance, such as bypass or dead zone, could also be revealed. At the same mixing speed, the performance of the circular section vessel was found to be better than the one of the circular section vessel, which was indicated by the more even distribution of turbulence dissipation rates.

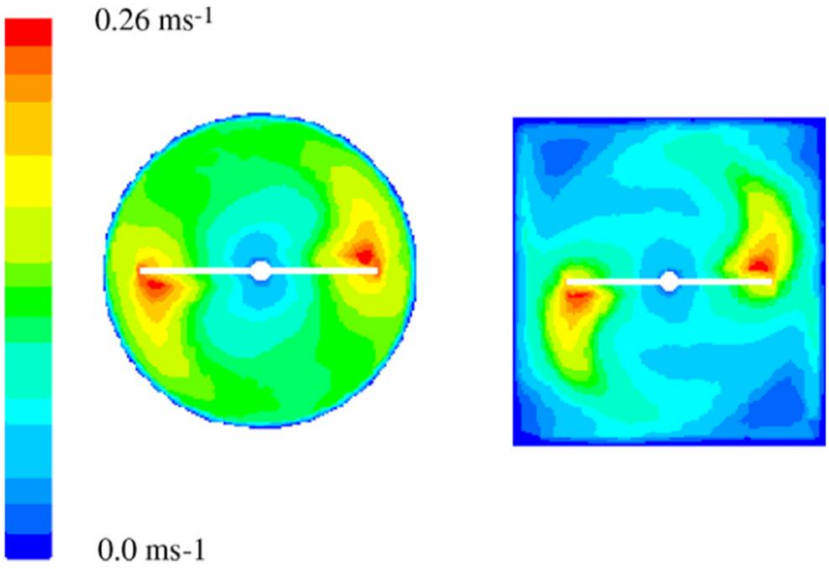

Fig 2.3 Contour of velocity magnitude of cylinder and rectangular vessels used in jar test

For the full-scale mechanical flocculator, the mixing speed, rather than the flow rate, considerably affected the distribution of the local velocity gradient. Due to the density current, the dead zones and recirculation loops were found in each flocculator chamber and between baffles.

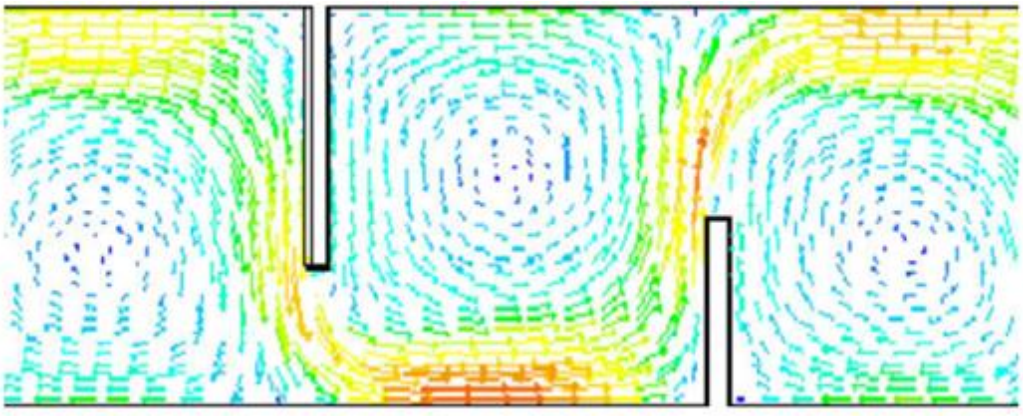

Fig 2.4 Velocity vector along the center line of the channel

2.3.1.2 Rapid sand filtration

The hydrodynamics behavior of rapid sand filtration was investigated by several studies. Rapid sand filtration aimed at removing the small suspended

solids particles presenting in the water after the settling process. The CFD studies addressed the pressure drop in rapid sand filtration [30]. The results indicated that the pressure drop due to the underdrain system might be contributed up to 11% of the total pressure drops, while the pressure drop in the sand filter accounted for nearly 85%, and about 4% of the pressure drop was in the inlet and outlet pipe. Comparing to the perforated plates without nozzles, the use of nozzles resulted in the reduction of the pressure drop, due to the decrease in the water velocity in the lower part of the sand filter.

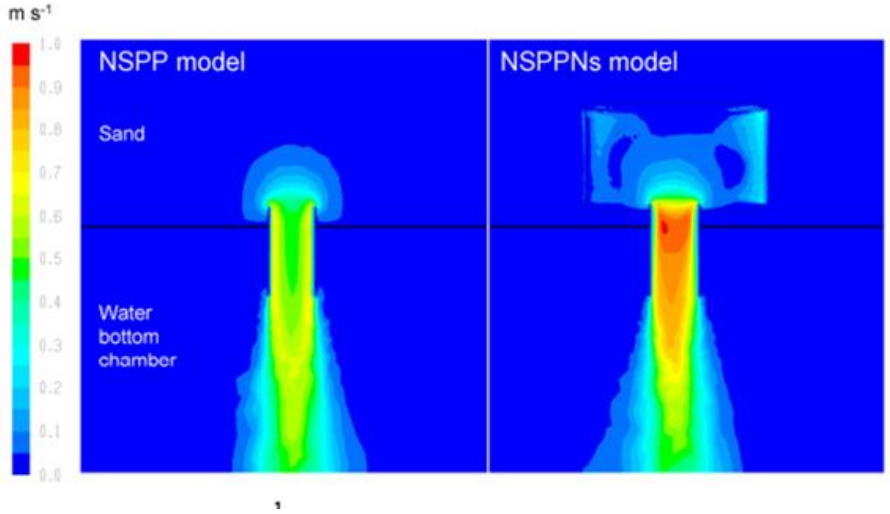

Fig 2.5 Velocity magnitude in a vertical cross section through the tube (NSPP model) and nozzle symmetry plane (NSPPNs model). The horizontal black line corresponds to the upper part of the perforated plate (NSPP model) or the sand media (NSPPNs model). Below the black line is water bottom chamber of the filter.

2.3.1.3 Service reservoir

Different studies have been carried out to investigate the performance of the service reservoir using CFD software. Service reservoirs were built to provide the dual function of balancing supply with demand and provision of the adequate head to maintain pressure throughout the distribution network [31].

CFD has been used to study the behavior of a range of service reservoirs with

a rectangular plan form by Hoi (2001). Detailed analysis of flow distribution and water age suggests that tanks with horizontal inlets are better mixed when compared with vertical top water level inlets. With increasing length to width ratio, the flow characteristics of tanks with vertical inlets increasingly resemble plug flow.

A major water-quality concern in a potable water service reservoir is the potential loss of chlorine residual, which is closely related to the flow pattern. Simulation results suggest that manipulating the valve located at the inlet can lead to the evolution and migration of the vortices in the service reservoir, which would then allow water with prolonged age to flow out of the reservoir. Adding the baffle wall to the reservoir also minimizes the probability of seriously diminished water quality resulting from poor mixing and excessive aging [32].

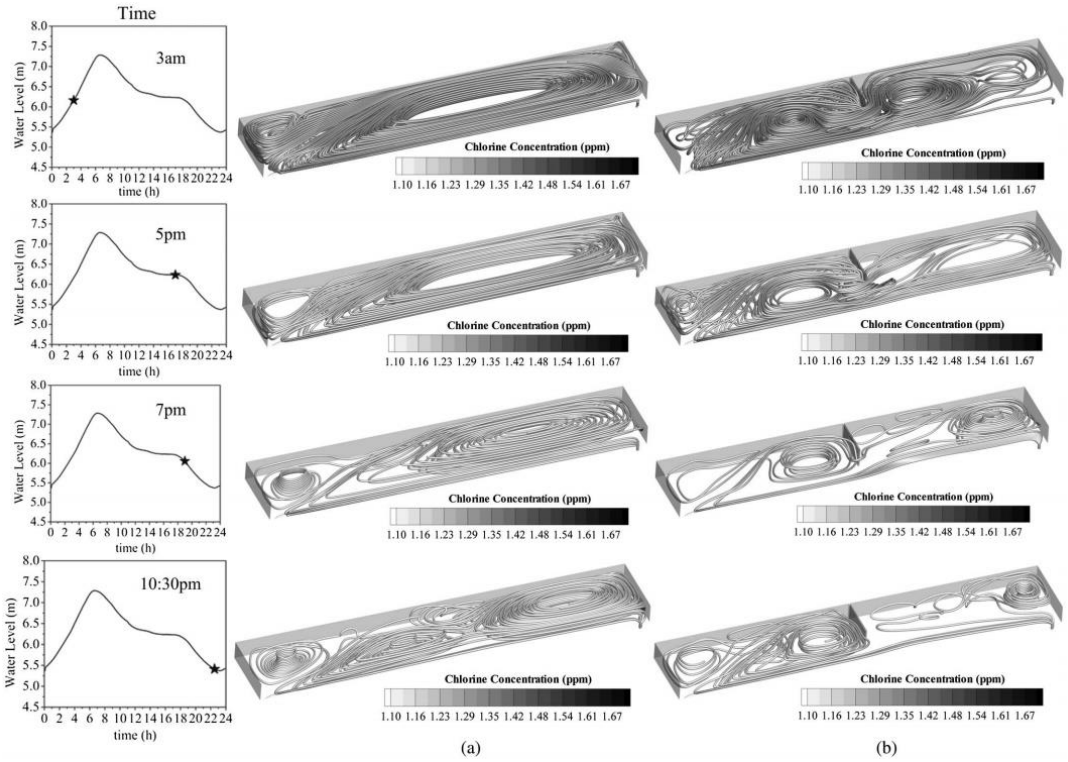

Fig 2.6 Comparisons of streamline distributions for service reservoirs at various time instants under flow condition with turnover: (a) without baffle wall; (b) with baffle wall

2.3.1.4 Distribution network

CFD studies on water distribution network mainly focused on the particle dispersion and deposition along the pipelines. Even drinking water distribution network is designed to transport only dissolved matters; it is almost impossible to exclude the suspended solid particles, which might result from the water source origins, treated water, biofilm grown in the pipeline or corrosion. In 2005 [33], Hossain demonstrated the particle distribution along the pipe and particle deposition at different cross-sections. Particle concentration was seen high at the bottom wall in the pipe flow before entering the bends, but for the downstream of bend, the deposition was not seen high at the bottom as seen in upstream of bend rather inner side of the bend wall (600 skewed from bottom).

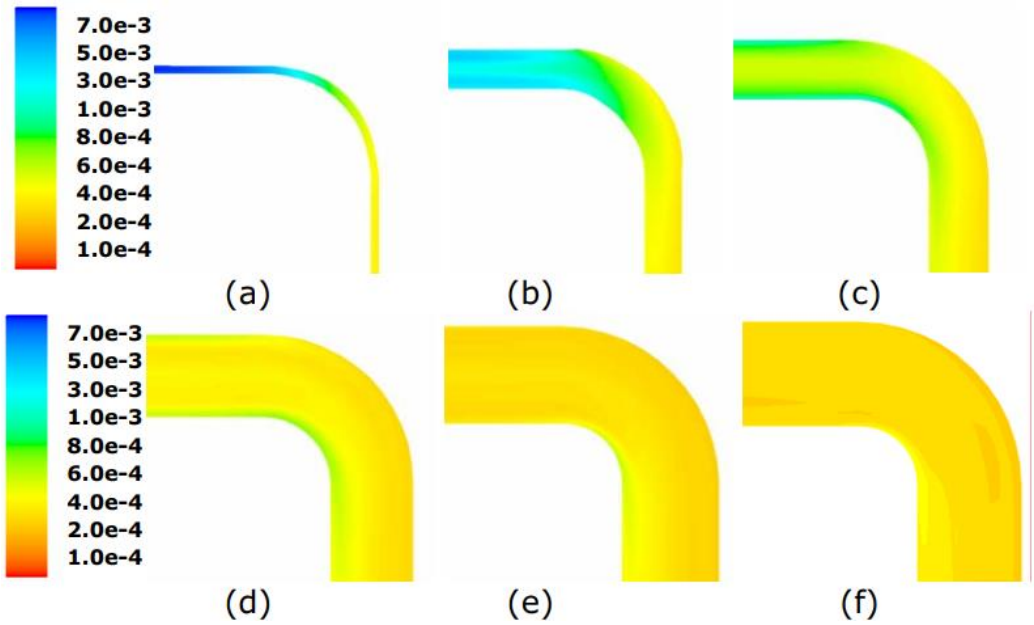

Fig 2.7 Contour of volume fraction of total particles at different heights (a, b, c, d, e, and f are for at 1, 5, 10, 20, 30, and 50 mm measured from bottom, respectively) for the velocity of 0.05 ms^{-1}.

The larger particles clearly showed deposition near the bottom of the wall except downstream. As expected, the smaller particles showed less tendency of deposition, and this was more pronounced at higher velocity. Due to the

high streamline curvature and associated centrifugal force acting on the fluid at different depths, the particles became well mixed and resulted in a homogeneous distribution near the bend regions. The hydrodynamic behavior of particles flowing in a turbulent unsteady state flowing through a horizontal pipe was also studied. Results showed that after a certain length of pipe and period after downward velocity gradient, when the velocity was constants over time, the shear stress was sufficiently high enough to cause the particle deposition on and roll along the bottom wall of the pipe wall and created a secondary group of particle peak.

2.3.2 In wastewater treatment

The art-of-knowledge on the application of CFD modelling on the wastewater treatment was critically reviewed by Samstag et al., 2016 [34]. The following section summarized the main findings of this study.

The paper presented around plant unit processes where CFD has been used and which are particularly promising for future applications.

2.3.2.1 Flow splitting and evaluation of head losses

Flow splitting is a critical unit operation that enables balanced flow to multiple units across a range of flows. Hassan et al., 2014 present results from CFD analysis on a tapered longitudinal manifold and a uniform longitudinal manifold. Two manifold configurations were tested at different inlet flows, and results suggested that the tapered manifold provided relatively equal flow distribution compared with the uniform longitudinal manifold. Knatz, 2005 indicated that the influent direction relative to the channel might impact the results.

Tong et al., 2009 used CFD to investigate balancing the flow through a wide range of manifold geometries. Results showed that optimal flow uniformity could be achieved by expansion of the cross-sectional area, linear or non-linear tapering of the distribution manifold or varying the cross-sectional area of the outflow channels modifications (**Fig 2.8**)

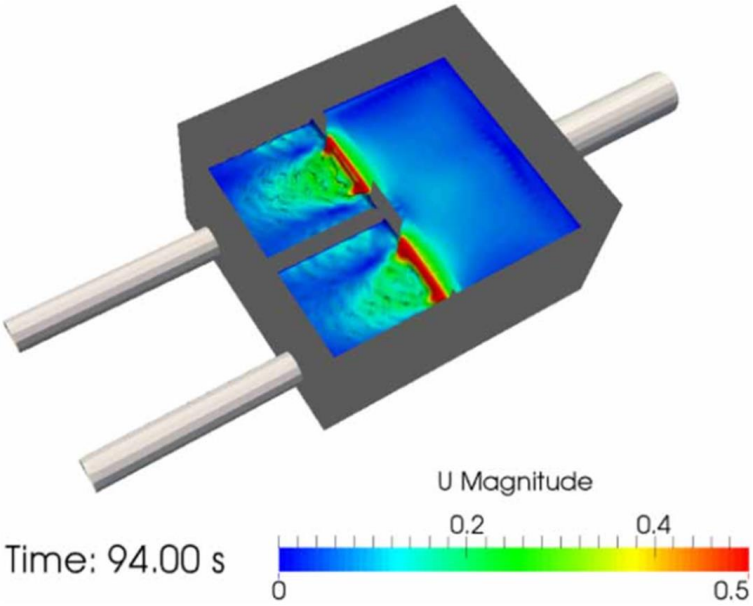

Fig 2.8 Surface velocity profile for a flow splitter from open source CFD software (Source: Marques, 2015)

2.3.2.2 Grit removal

Grit chambers use gravity or centrifugal sedimentation to separate large, dense particles from raw wastewater. While the principles are relatively simple, the multiphase nature and multiple mechanisms can make an analysis complex. The sizing of grit removal channels based on ideal settling behavior. Much of current practice, however, relies on manufacturer's recommendations without an analytical basis

McNamara et al., 2012 present a comprehensive evaluation of three different types of grit removal tank geometries: forced vortex, detritor, and lamella. Grit particles of nine different diameters were converted to a continuous distribution equation and modelled with specific gravities of 2.65 based on silica sand and 1.5 based on laboratory samples from field installations and a sphericity ratio of 0.65. Multiphase (water and air) simulations were carried out to steady state prior to the injection of grit particles into the inlet stream.

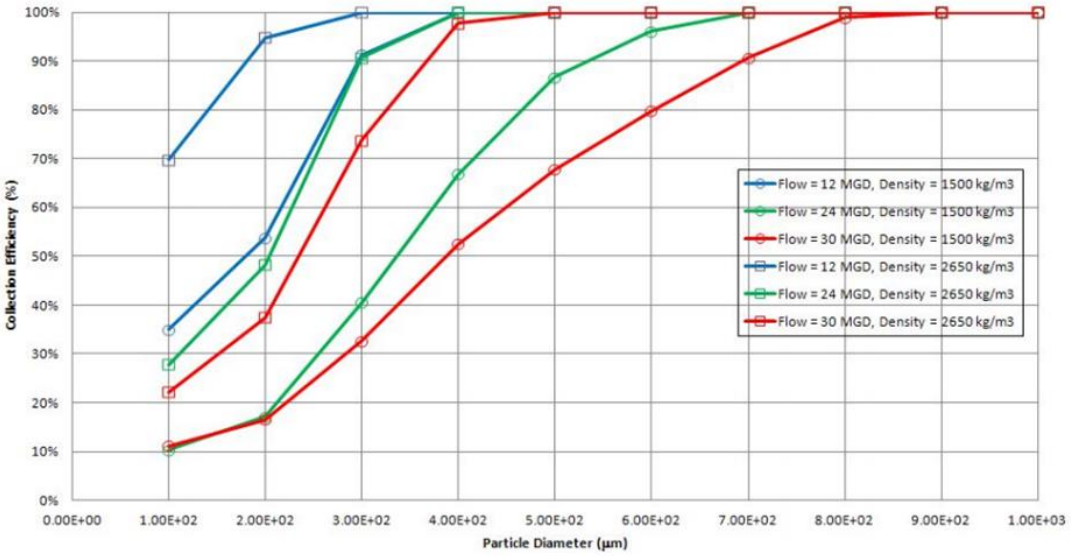

Fig 2.9 Simulated Forced Vortex Collection efficiency

2.3.2.3 Suspended growth process

The focus on suspended growth (flocculent) systems have been in activated sludge basins. Activated sludge tanks have a broad range of functionality, including nutrient and carbon removal, pathogen destruction, and removal of micropollutants. They are also generally compartmentalized, have large recycle streams, and are critically dependent on multiphase contact and effective hydraulics.

A very comprehensive review is provided by Karpinska & Bridgeman, 2016, for CFD of activated sludge reactors. This includes a critical review of (1) Reynolds averaged Navier-Stokes (RANS) simulations, (2) turbulence models, and (3) multiphase modelling, with a strong focus and discussion of the need to move to coupled CFD-biokinetic modelling.

Within the area of mixing modelling, efforts have been made in activated sludge tanks by estimation of velocity and solids profiles. Samstag et al., 2012 showed that if density couple was not included, mechanical mixing in an activated sludge reactor was significantly overestimated. They used a 3D commercial CFD model with the multiphase simulation of water and air and

an active scalar transport model for solids calibrated to field tests. Le Moullec et al., 2008 used a multiphase 2D Euler-Euler scheme and simulation of particle tracking in a Lagrangian reference frame using a commercial CFD package to model velocity profiles and RTD in an aerated channel whose characteristics had been previously measured at laboratory scale (Potier et al., 2005).

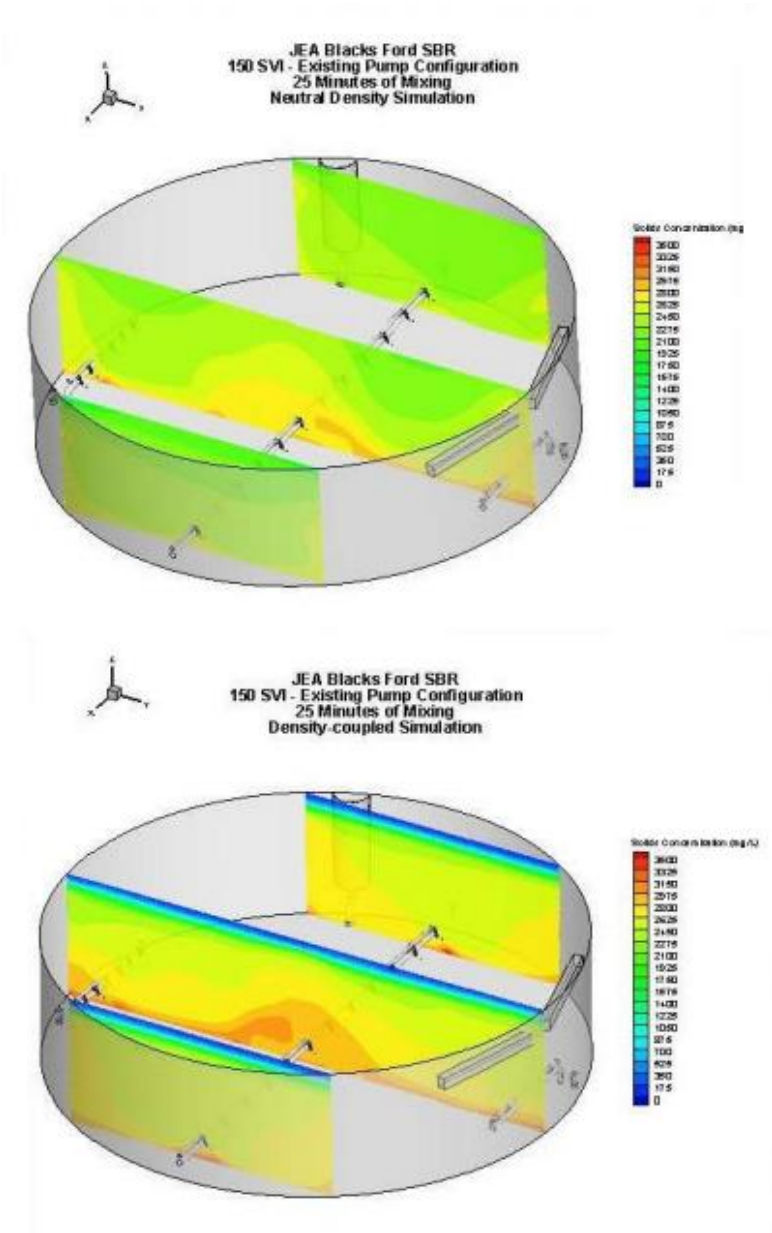

Fig 2.10 Comparison of Solids Profiles from Density-coupled and Neutral Density Models (Samstag et al., 2012)

Laursen, 2006 completed a very comprehensive study of the hydrodynamic and biokinetic modelling of activated sludge applied to full-scale WWTP case studies. Commercial software was used to develop full 3D CFD simulations of three different full-scale aeration tank geometries. Features included: (1) biokinetic modelling using the ASM3 model (Henze et al., 2000), (2) active density coupling of solids concentrations, (3) liquid turbulence simulated by k-ε and shear strain transport models with air bubbles and sludge flocs modelled using a zero equation model, (4) air diffusers modelled as bubbly flow calibrated to detailed laboratory velocity and air fraction measurements, (5) propeller mixer modelled by both sliding mesh and momentum source models, and (6) calibrated viscosity models. Interesting practical problems were considered in three case studies.

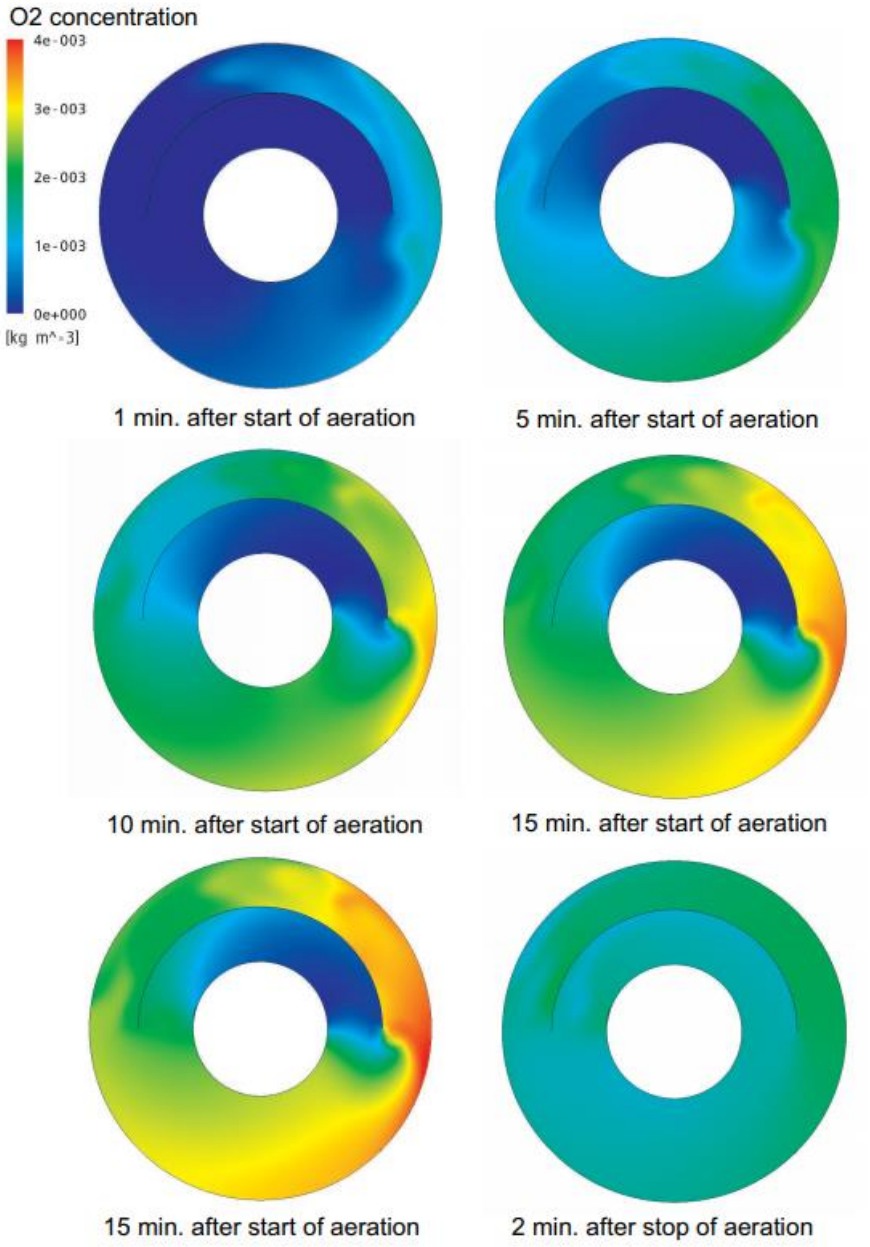

Fig 2.11 Plots of the distribution of soluble oxygen concentration at 3m depth at different time steps during the aeration process (Laursen, 2006)

2.3.2.4 Attached growth process

The CFD multiscale model of the reaction and mass transport processes in a sponge carrier media was carried out by Magnus, 2014 [35]. The study divided the sponge carrier media process into four spatial scales: reactor, sponge, biofilm, and individual organisms. In this way, the individual scales were

modelled separately, and the connection between different scales was solved by a proper set of boundary conditions. Firstly, an aerated sponge Moving Bed Biofilm Reactor was modelled by conducting a fluid dynamic and particle dynamic simulation, where sponge and air bubbles were simulated as particles. From the results, a pressure gradient boundary condition for the internal flow was developed. Secondly, a model of bio-clogging was performed by investigating the interaction of the biofilm growth and detachment with the porous structure of the sponge carrier media. The interaction was solved by the Lattice Boltzmann Methods of hydraulic and mass transfer coupled with Individual-based Modelling of the biofilm, where individual cells were modelled as particles.

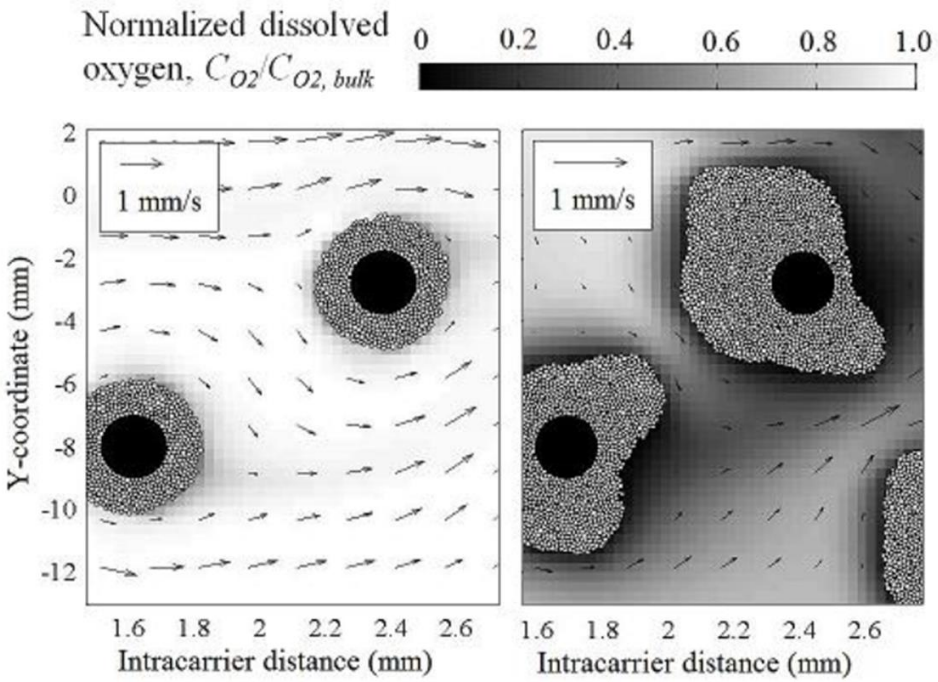

Fig 2.12 Simulation on biofilm formation at different stages

Finally, from the analysis and generalizations of the results, a simple model for engineering purposes was developed with empirical relations of internal biologging. By a new definition of a critical porosity for bio-clogging, the model could be calibrated with experimental results.

2.3.2.5 Disinfection

CFD modelling of ultraviolet (UV) reactors is fast becoming a standard approach for characterizing, designing, and trouble-shooting the UV disinfection performance. Moreover, growing confidence in numerical models that have been validated with extensive bio dosimetry data has led UV manufacturers to use the tool as part of an on-line algorithm for dose monitoring. Numerical UV disinfection models are complex and require the proper execution of several components so that the numerical results can be used for the analysis of a UV process. UV disinfection models can be divided into three major components. These major components include: (a) fluid flow/turbulence model, (b) fluence rate distribution model, and (c) microbial transport model. As the name implies, the fluid flow/turbulence model involves characterizing the spatial variations in fluid flow and turbulent mixing that occurs in the UV reactor. The fluence rate model involves characterizing the spatial variations in the UV light intensity in the UV reactor. Finally, the microbial transport model involves characterizing the movement of the microorganisms through the UV reactor.

2.4. CLASSIFICATION OF SEDIMENTATION TANKS

Sedimentation tanks play an important role in water and wastewater treatment. Sedimentation tanks are used to remove SS particles due to gravity. Sedimentation tanks have a simple structure but high SS removal efficiency, so it is still widely applied in treatment systems. Zhang, 2014 [36] showed that the settling process could remove 70-80% of suspended solids. In water treatment, settling tanks are usually arranged in front of the filtration tanks to remove large particles from flocculation tanks. In wastewater treatment, according to the purpose of treatment, sedimentation tanks are usually classified into primary settling tanks and secondary settling tanks. Primary sedimentation tanks are located before biological or chemical treatment facilities. Primary settling tanks remove most inorganic sludge, such as sand, natural solid particle, grit, and a portion of organic particles that reduce the effectiveness of biological treatment. Secondary settling tanks are placed after biological or chemical treatment works. The function of the secondary settling tanks is to compress and remove small particles or biological sludge, such as microbiological membranes or activated sludge generated from the previous biological treatment facility.

According to shape and flow direction, settling tanks are classified into four common types: horizontal sedimentation tanks, circular sedimentation tanks, vertical flow sedimentation tanks, and lamella sedimentation tanks

2.4.1 Horizontal sedimentation tank

Horizontal sedimentation tanks are rectangular in plan, in which the length is many times larger than the width (**Fig 2.13**). Wastewater inflow through the tank horizontally at a slow velocity, so the tank has a high treatment efficiency. However, horizontal sedimentation tanks require a large construction area.

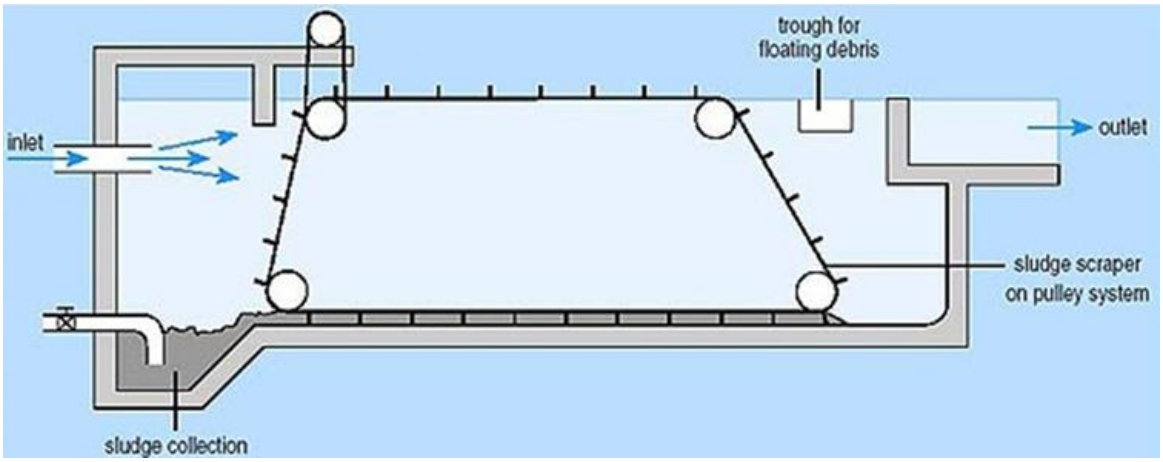

Fig 2.13 Horizontal sedimentation tank [37]

2.4.2 Vertical flow sedimentation tank

Sedimentation tanks with flow inlets are located at the bottom of the tanks, and clean water is collected on the surface (**Fig 2.14**). The flow direction arranged in opposite with the gravity direction, so the SS particles are well removed.

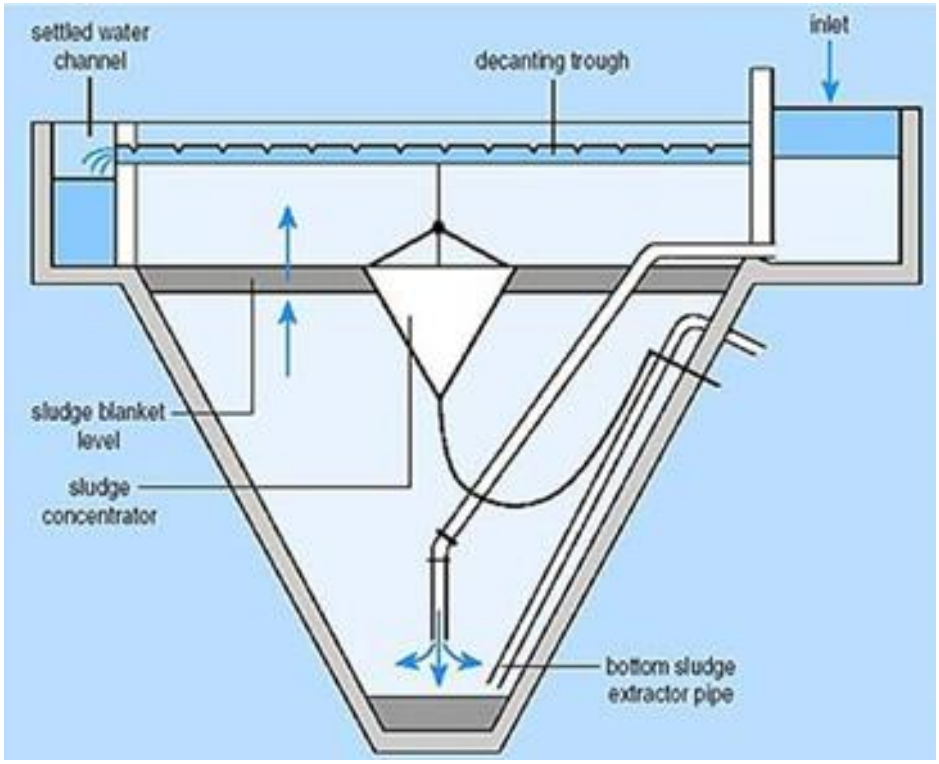

Fig 2.14 Vertical flow sedimentation tank [37]

2.4.3 Circular sedimentation tank

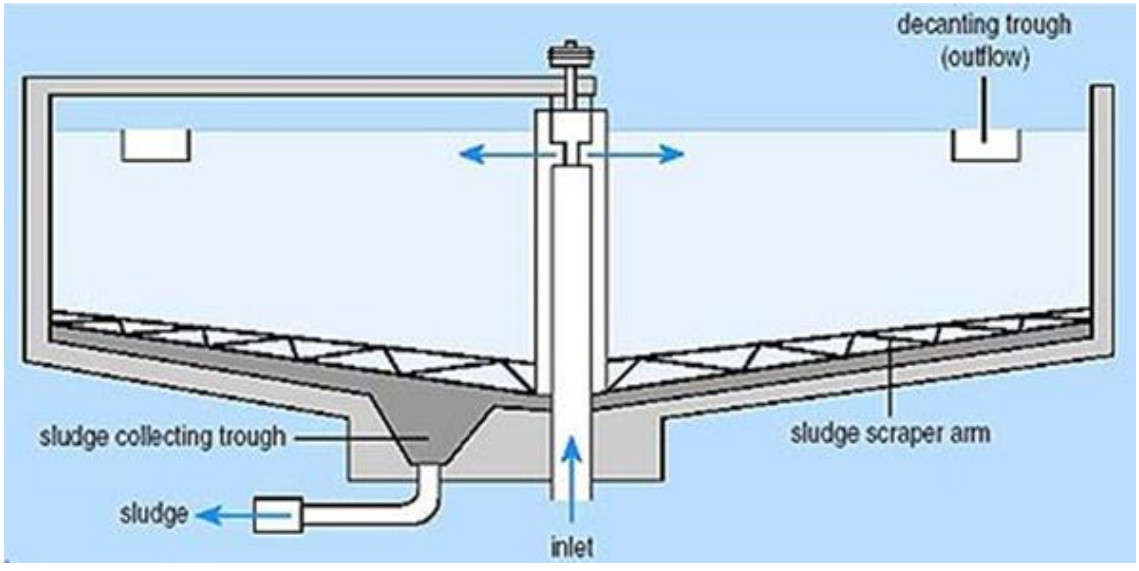

Fig 2.15 Circular sedimentation tank [37]

The working principle of the tank is like a horizontal sedimentation tank, but the water distribution pipe is arranged in the center of the tank (**Fig 2.15**).

After the settling process, water is collected in troughs arranged around the tank wall.

2.4.4 Lamella settling tank

The inclined plates are installed in the settling tanks with small distances between two parallel plates (**Fig 2.16**). Typically, water is flowing through the inclined plate from the bottom up to reduce the settling distance of particles and increase the SS removal efficiency. Recent studies show that lamella sedimentation tanks have a high treatment efficiency and a small footprint. Therefore, lamella sedimentation tanks are considered as the best option for the design or renovation of sedimentation tanks.

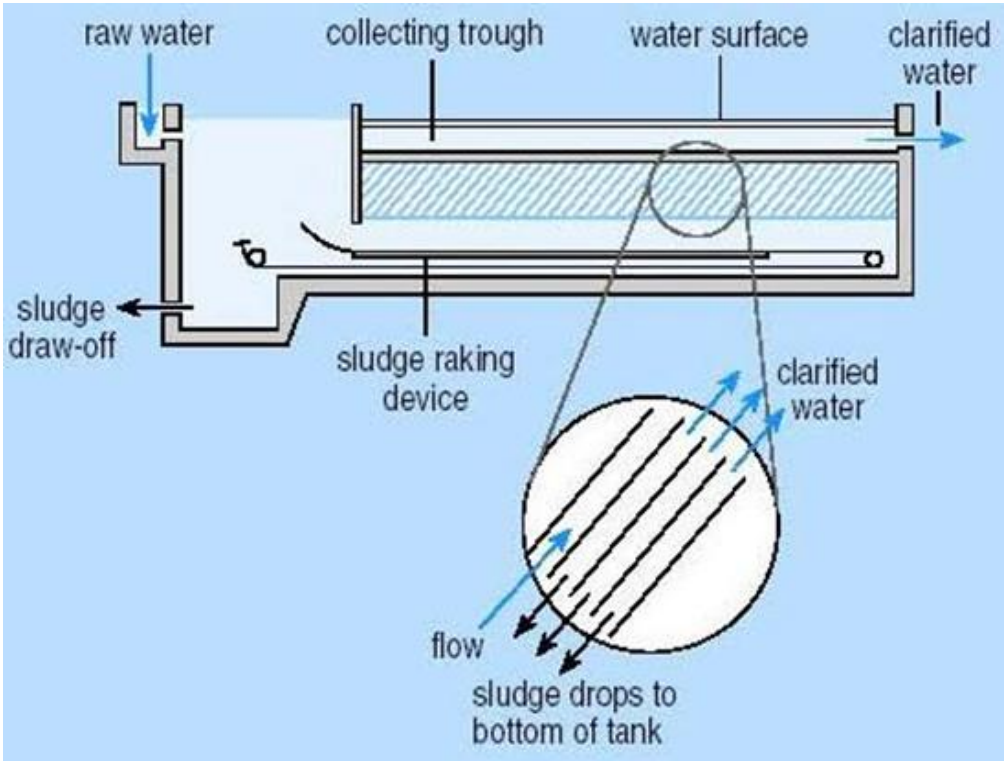

Fig 2.16 Lamella settling tank [37]

2.5. STUDY ON SIMULATION SEDIMENTATION TANKS

The CFD model was applied to simulate secondary sedimentation tanks in the late 1970s. As one pioneer in numerical simulation of sedimentation tank, Larsen, 1977 [38] applied CFD simulation to several sedimentation tanks, although with simplification and conceptualization, he still shown several major hydraulic phenomena of sedimentation tank, such as “density waterfall” due to heavier fluid sink into the bottom of sedimentation tank soon after entering, bottom current and surface return current.

Sedimentation simulations focused on developing models based on numerical methods. The mathematical equations were built so that the simulation results reflect the actual process taking place under operating conditions.

Imam, McCorquodale and Bewtra, 1983 [15] presented a finite difference model of the vorticity transport stream equations to establish the vertical velocity field. The physical model was used to determine the eddy viscosity. The simulation results were verified with experimental results. The Alternating Direction Implicit method was applied to analyze the vorticity transport in the model. The two-dimensional model was used to simulate suspended solids deposition using the same equations for the vorticity transport. This study simulated for sedimentation tanks with reaction baffle submergence to evaluate the effectiveness of suspended solids removal. Simulation results indicated that the efficiency of suspended solids removal predicted by the simulation model was always lower than that predicted by the Camp-Dobbins method in **Fig 2.17**.

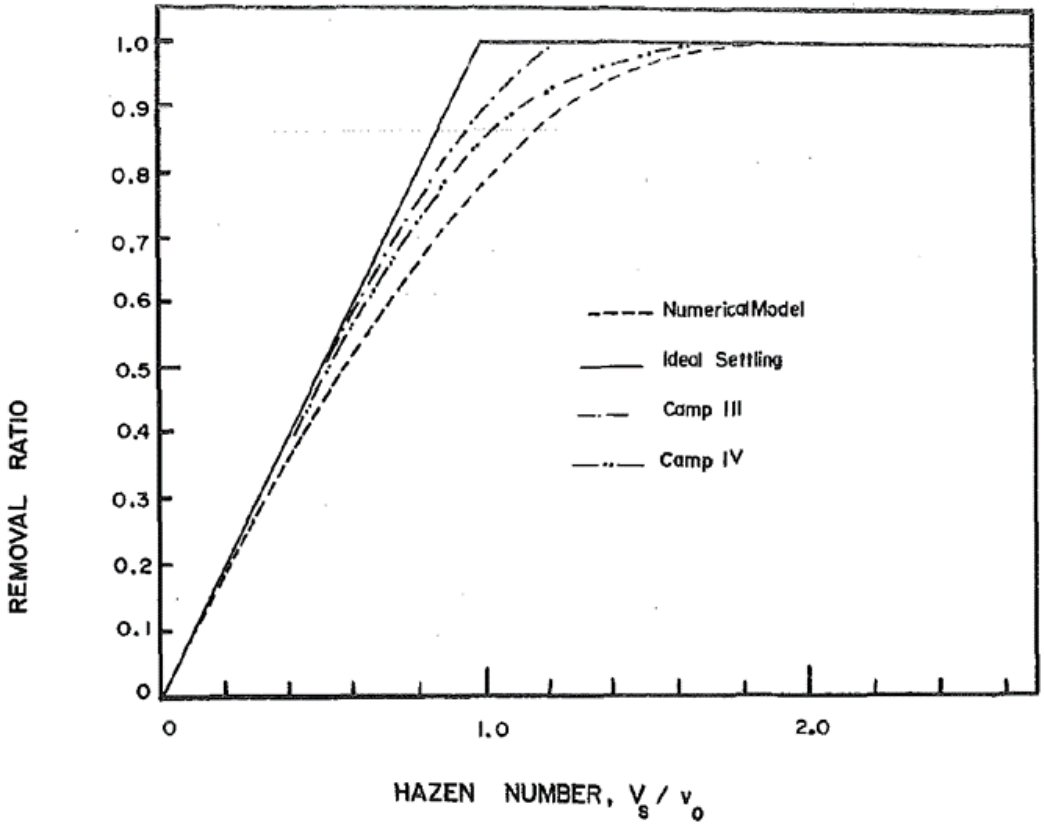

Fig 2.17 Comparison of Predicted Removal Ratios for Various Methods

Stamou et al., 1989 [16] used a numerical model to study the flow and settling process of SS in primary sedimentation tanks and compared the simulation results to those from the theoretical method. The model divided into two parts, in which the velocity and turbulent viscosity were simulated by using the flow model, and the suspended solids concentration field was modelled and determined by the suspended solids transport model. Thanks to the use of the k-ε turbulence model, the simulation results had been improved compared to previous numerical models because it calculated for each group of particles with different settling velocity and mass fraction ratio (**Fig 2.18**). This study identified the flow regime and the distribution of suspended solids distribution in the primary sedimentation tanks corresponding to changes in linear velocity and the settling velocity curves. The simulation results showed that a small difference between the simulation results and the measurement results were observed (**Table 2.3**).

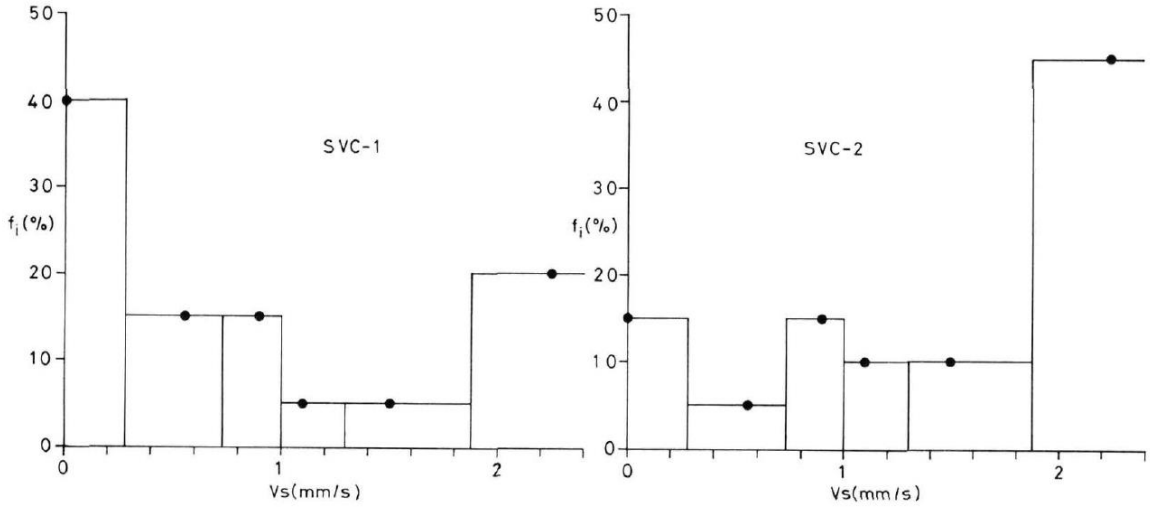

Fig 2.18 Settling velocity curves

Table 2.3 Predicted total removal efficiencies, experimental results, and results of other models

Model	Overflow rate = OR (m/d)		
	37	60	110
Ideal settling	60.0	57.2	46.6
Dobbin's model	53.5	47.0	35.9
Complete mixing	43.0	37.0	28.6
Cam's theory	59.4	55.5	45.5
Abdel-Gawad and McCorquodale's model	-	48.5	-
Present model	54.4	49.4	37.5
Measured	57.0	47.0	34.0

A numerical model was applied to predict the influence of unsteady flow in a center-fed circular clarifier on the tank performance by McCorquodale, 1991 [17]. The study conducted simulations for two cases. The flow rate changed at a constant MLSS concentration for case one, and the MLSS was increased suddenly for another one. The simulation results showed that SS removal efficiency of the clarifier was greatly affected by the unsteadiness of the flow. In Zhou, McCorquodale and Vitasovic, 1992 [18], the influence of the inlet densiometric Froude number to the SS concentration distribution and the

velocity secondary sedimentation tank was studied. Numerical simulation was applied to describe the settling process by using conservation equations, *k-ε* turbulence models, and the equation for suspended solids transporting. The study focused on assessing the effect of settling zone flow pattern, the density current at the bottom, upward flow at the outlet, and the recirculation to the inlet densiometric Froude number. The performance of the sedimentation tank was also assessed based on the hydraulic regime in the tank. Simulation results were compared with measurement results and physical model data with small differences in SS removal efficiency (**Fig 2.19**)

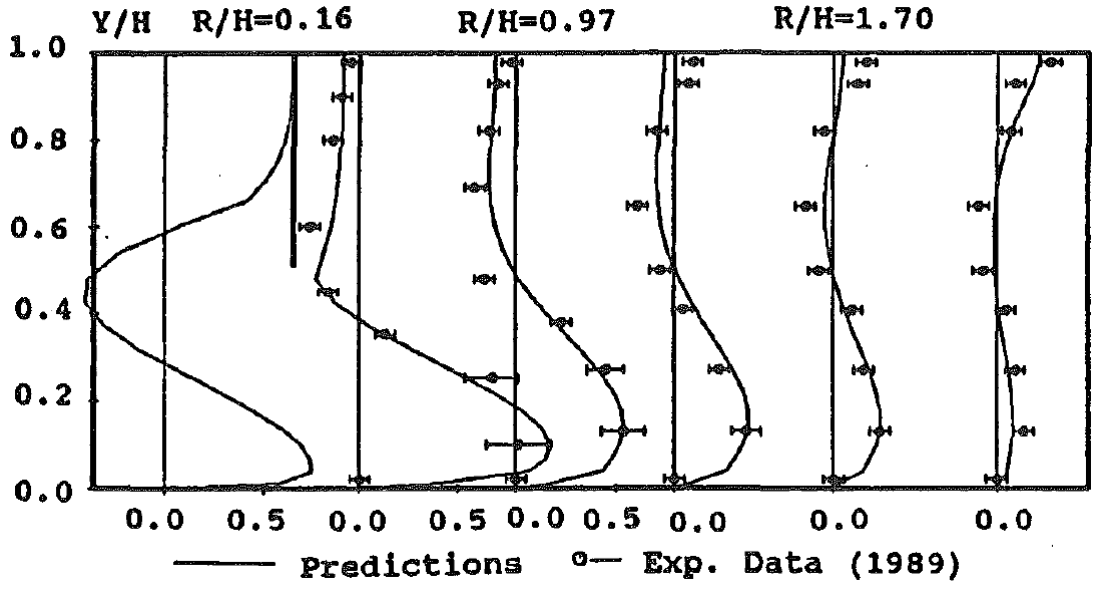

Fig 2.19 Comparison of Predicted Velocity Profiles (Fr= 0.346) with Data of Scale Model (Fr = 0.34 and RAS = 0.45)

Zhou and Godo, 1995 [39] investigated the effect of temperature on flow regime in primary sedimentation tanks. The algebraic stress model and the other versions using the conventional *k-ε* model were applied in the study. The comparison of prediction on velocity and temperature profiles with measurement results in physical models showed that the algebraic stress model was in good agreement with the physical model. Matko et al., 1996 [40] conducted simulation of the primary settling tank using three models, such as the mass flux model, lumped parameter model, and CFD models. The

simulation results indicated that the CFD model could predict the flow pattern in clarifiers more accurately than the mass flux and lumped parameter models. However, this research did not study the influence of the parameters such as particle density, particle size, particle flocculation, turbulent, mass diffusion on tank performance in CFD simulation. Jin, Guo and Viraraghavan, 2000 [19] applied a one-dimensional mathematical model with a stable, steady situation to study the settling of non-uniform particle size in Class I sedimentation tanks. The study better predicted the SS removal efficiency, the size distribution in sludge and influent SS, and sludge thickness in the tank compared to the conventional approaches. Besides, the numerical experiment used in this study has determined the effect of tank dimension, overflow rate, and retention time on the SS removal efficiency (**Table 2.4**).

Table 2.4 Experimental Conditions (El-Baroudi 1969)

Run (1)	Discharge, Q ($\times 10^{-4}$ m^3/s) (2)	Overflow rate, v ($\times 10^{-4}$ m/s) (3)	Detention time, t (min) (4)	Depth, h (m) (5)
1-7	2.21	3.88	8.8	0.205
2-3	1.26	2.22	25.0	0.333
2-4	1.58	2.77	22.0	0.366
2-5	1.89	3.32	18.3	0.365
2-8	3.0	5.26	11.6	0.366

Liu et al., 2008 [41] simulated tracer in primary settling tank using a modified k-ε two-layer model based Boussinesq' approximation to model the Reynolds stress and a hybrid finite analytic method. The simulation results indicated that the HFAM approach was suitable for the turbulent flow and mass transfer simulation (**Fig 2.21**). The velocity field distribution was accurately predicted by using the modified k-ε two-layer model.

Mohanaganham and Stephens, 2009 [42] modelled floating phase on settling tanks using the CFD model. In this study, Multi-phase simulations were employed for clay, sand, and a floating solid (density less than the continuous phase) as the secondary phases. The model presented both the settling as well as the floating of the secondary phases occurring in the tank (**Fig. 2.22** and **Fig 2.23**).

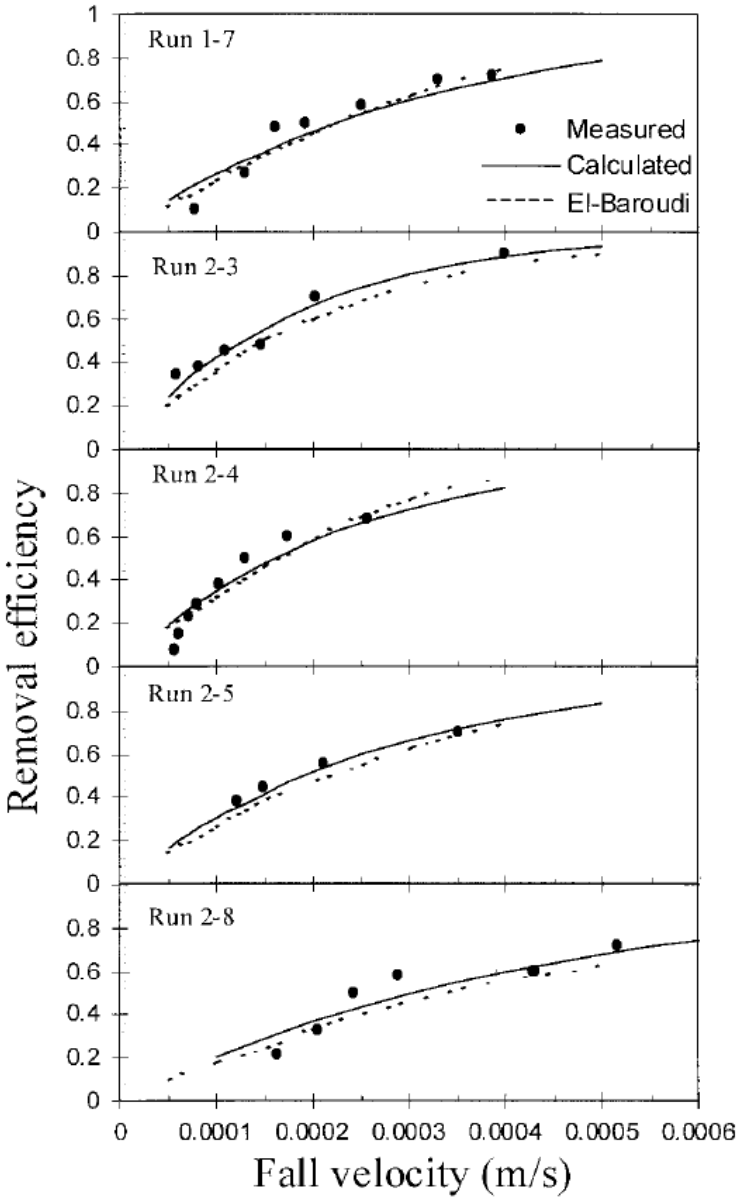

Fig 2.20 Measured and Simulated Removal Efficiency

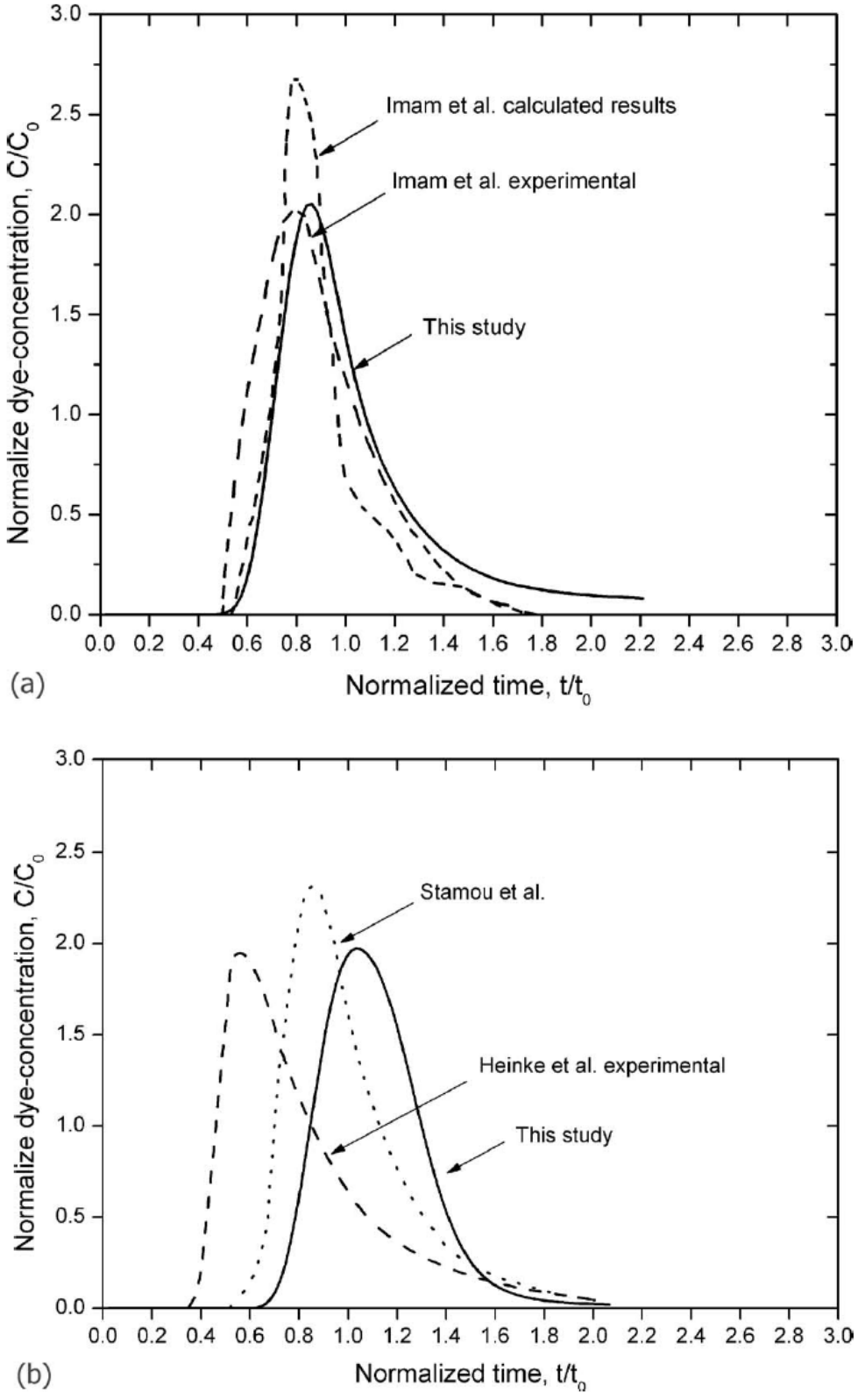

Fig 2.21 Comparison of predicted FTC with: (a)experimental results and numerical results of Imam et al. (1983); (b) experimental results of Heinke et al. (1977) and numerical results of Stamou et al. (1989)

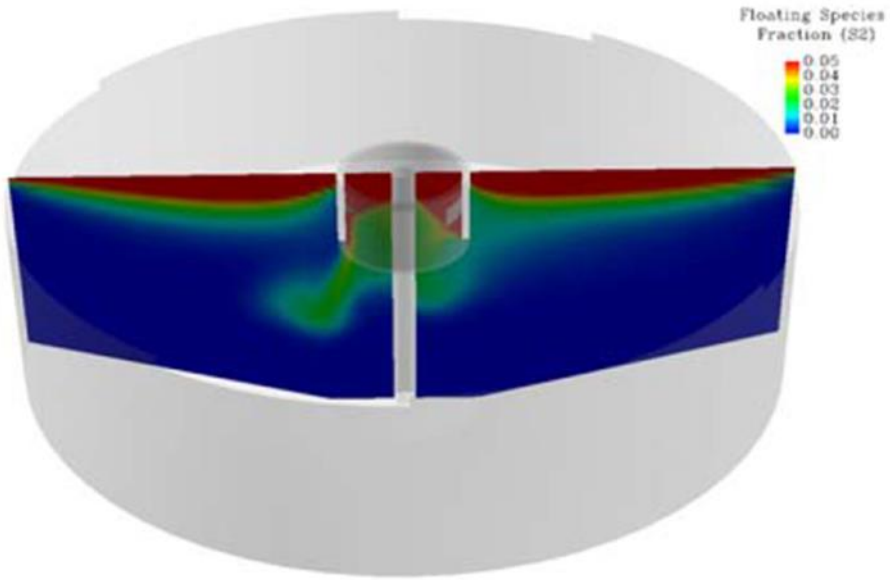

Fig 2.22 Fraction of floating phase in a vertical cross-section of the settling tank (S2)

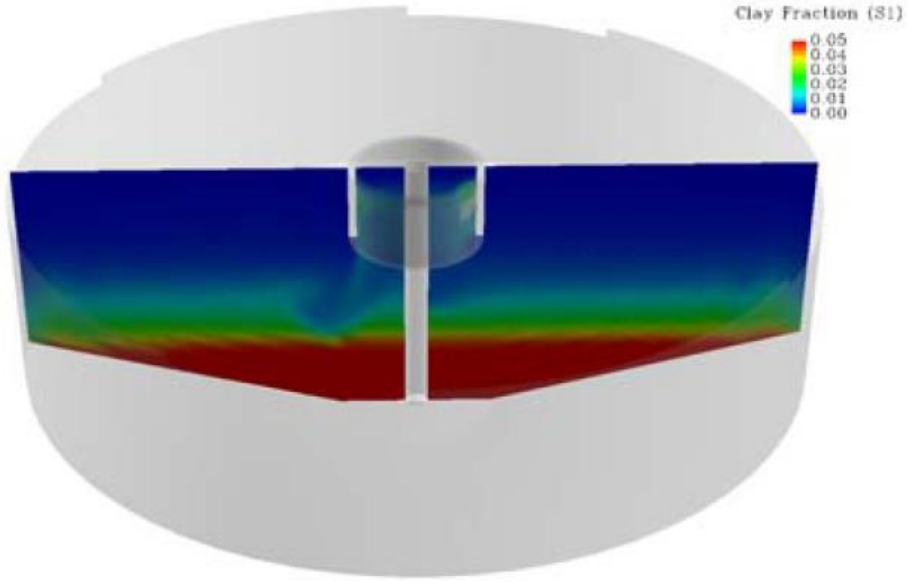

Fig 2.23 Solids fraction of clay in a vertical cross-section of the settling tank (S1)

Ramalingam et al., 2012 [20] evaluated the effect of two important parameters in the three-Dimensional CFD model, namely discrete particle and the modification of the floc aggregation and floc break-up coefficients on the accuracy of the predictions of the CFD model. Ghawi and Kriš, 2012 [21] developed a complex CFD model to estimate the factors that impact deposition efficiency.

Optimizing the tank configuration design to improve the hydraulic regime was conducted by many researchers. Krebs, Vischer and Gujer, 1995 [43] proposed an improved inlet design of sedimentation tanks to enhance flow conditions and treatment efficiency (**Fig 2.24**). Study results indicated that the optimal inlet structure should be performed with different procedures for primary and secondary clarifiers. The design of the primary clarifier inlet should consider the dissipation of kinetic energy, while the density current should be calculated in the design of the secondary clarifier inlet.

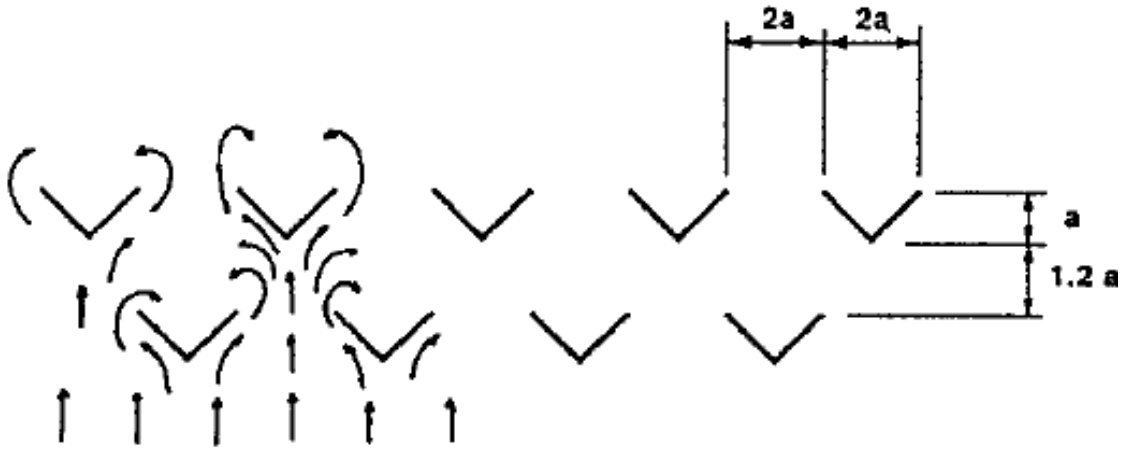

Fig 2.24 Arrangement of Angle Bars for Energy Dissipation (Typical a-Values Range 5-7 cm)

Firoozabadi, 2005 [28] investigated the influence of the inlet position and baffle configuration on treatment efficiency in primary settling tanks. Flow-Through Curves method was used to compare hydraulic regimes in different tanks. The best location for the inlet and the baffle position was determined in this study to reduce the dead zone and improve the hydraulic regime in the

sedimentation tank (**Table 2.5**). Goula et al., 2008 [44] evaluated the impacts of baffles in the inlet zone on the distribution of flow patterns and the influence of SS mass fraction on their removal efficiency (**Fig 2.25**). Ghawi and Jozef, 2008 [45] investigated the solution to improve the SS removal efficiency of the sedimentation tanks at the Hrinova water treatment plant using the CFD model. This study proposed installing a baffle in existing sedimentation tanks to improve the hydraulic regime in the tank and treatment efficiency (**Fig 2.26**). Simulation results for the modified sedimentation tank showed the improved removal efficiency as well as the capacity of the sedimentation tank due to the installing baffle. A small difference between the model-predicted results and the experimental results was observed.

Table 2.5 Total dead volume for various positions and heights.

Position-Baffle height	Total circulation volume	Position-Baffle height	Total circulation volume
1-3	555	4-3	715.5
1-5	637.5	4-5	882
2-3	648	5-3	622
2-5	807.5	5-5	710
3-3	476	6-3	589.5
3-5	483	6-5	655

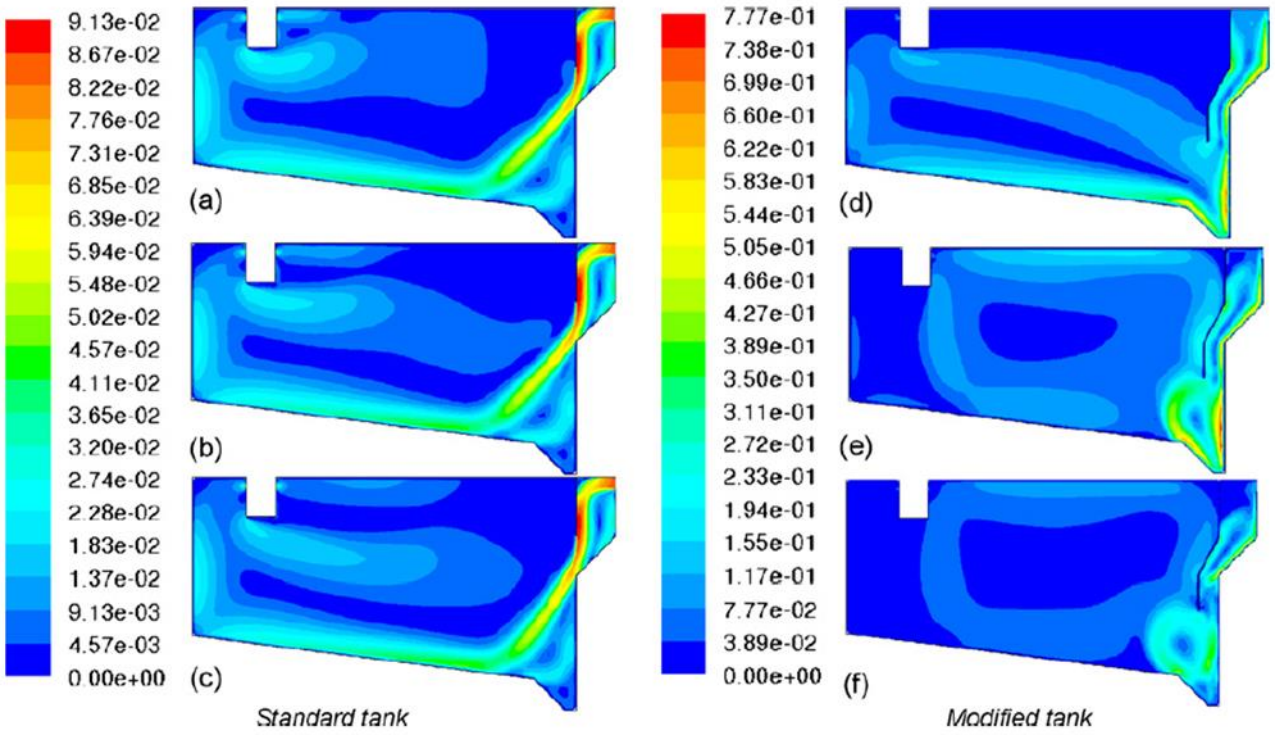

Fig 2.25 Contours of velocity (m/s) for the standard and the modified clarifier for particle class size 2 (a and d), 3 (b and e) and 4 (c and f).

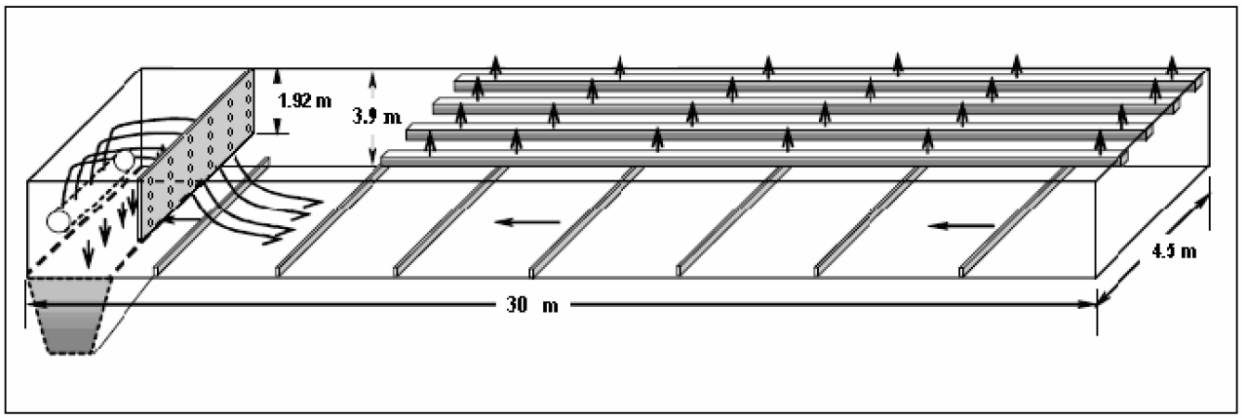

Fig 2.26 Tank with baffle and launder Modifications

Wang et al., 2008 [46] investigated the water flow field and SS distribution on a rectangular settling tank using three dimensions CFD model. Simulation results showed the hydraulic regime in the tank and the effect of inlet baffle length on SS settling in the tank. Rodríguez López et al., 2008 [47] analysed the hydrodynamic behaviour of the pilot-scale sedimentation tank under the

change of flow and types of feed. The tracer experiments were conducted to determine the residence times distribution in the settling tanks, and in order to build models to assess the hydrodynamic behaviour of the tanks. The results showed that a change in the arrangement of feed inlet could improve SS removal efficiency in the sedimentation tank. Al-Sammarraee and Chan, 2009 [48] evaluated the effect of vertical baffles on the SS removal efficiency in sedimentation tanks using 3-Dimensional simulation in the LES model. In the simulation model, the suspended solids were represented by 13 particle groups with different mean diameter and mass fraction (**Table 2.6**). The results showed that SS removal efficiency was increased as the number of baffles increased. The study results had an important contribution to the optimal design of sedimentation tanks in water treatment plants. In Tamayol, Firoozabadi and Ashjari, 2010 [49], the effect of the baffle on the flow regime in the secondary sedimentation tanks was studied. The position of the baffle was selected based on the influence of the buoyancy force. Simulation results showed that in high Reynolds numbers, flow regime and baffle position was not affected by the inlet Froude number.

Table 2.6 Particle classes of flow in the sedimentation basin

Particle class	Mean diameter (μm)	Mass fraction	Mass flow rate (kg/s)
1	20	0.025	0.00125
2	50	0.027	0.00135
3	80	0.039	0.00195
4	120	0.066	0.0033
5	170	0.095	0.00475
6	200	0.115	0.00575
7	250	0.126	0.0063
8	350	0.124	0.0062
9	450	0.113	0.00565
10	550	0.101	0.00505

Particle class	Mean diameter (μm)	Mass fraction	Mass flow rate (kg/s)
11	650	0.077	0.00385
12	750	0.057	0.00285
13	850	0.04	0.002
		1.00	0.05025

Liu et al., 2010 [50] employed two-dimensional laser Doppler velocimetry and numerical model to optimize the design parameters of rectangular primary settling tanks. The flow field in the tank was more affected by the variation of the reaction baffle height compared to the change of the flow rate (**Fig. 2.27**)

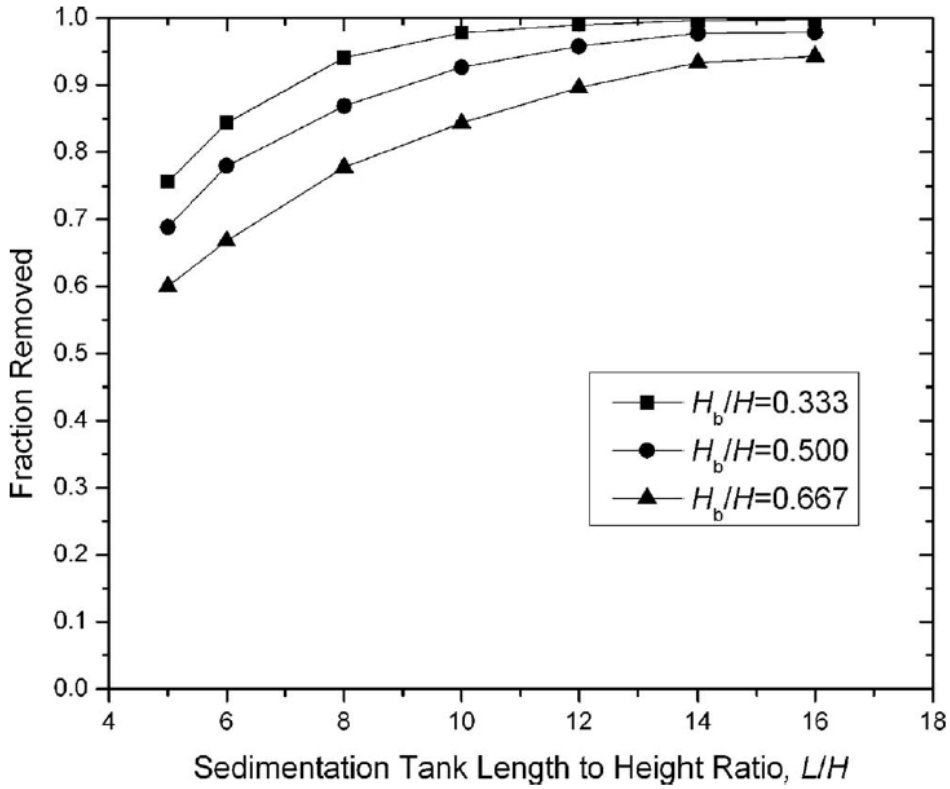

Fig 2.27 Effect of length-to-height ratio on solids removal

Asgharzadeh, 2011 and Shahrokhi, 2011 [51], [52] investigated the reduction of dead zones and recirculation zones in cases where a different number of baffles were installed at the bottom of the tank. The parameters of flow pattern and the Flow-Through Curves (FTCs) method were applied to estimate the effects of the number of baffles on the performance of the primary

sedimentation tank in Shahrokhi, 2011. Analysis of simulation results indicated that the hydraulic efficiency of the sedimentation tank was improved by increasing the number of baffles in a suitable position (**Fig 2.28**), which helps to reduce the recirculation zone and create a uniform flow pattern in the tank. Similar results were recorded in the measurement data.

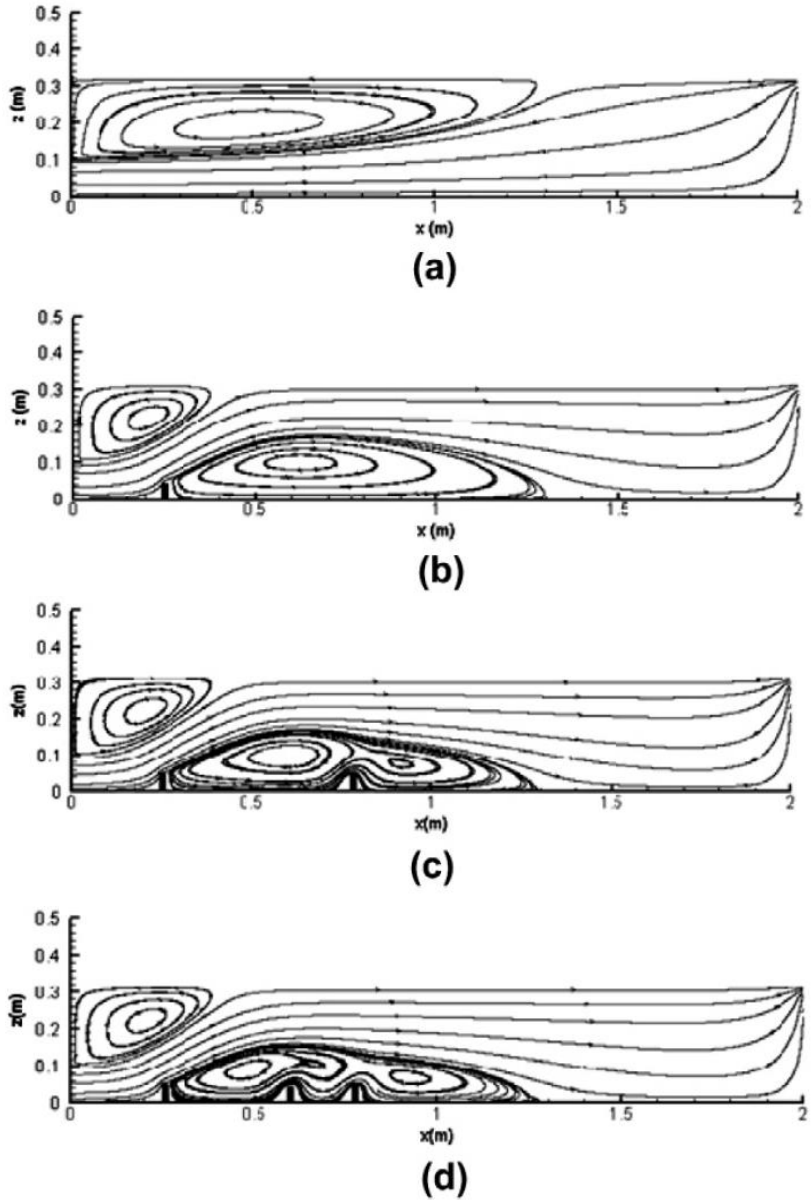

Fig 2.28 Computed streamlines for baffle height ($H_b/H = 0.18$) (a) no baffle (b) case (1) (c) case (4) (d) case (9).

Gong et al., 2011 [53] conducted a three-dimensional model in CFD to optimize the performance of final settling tanks. The study investigated the influence of different baffle arrangements, sludge withdrawal mechanisms, and loading alternatives to the capture efficiency of SS. Moreover, the study developed the flocculation sub-model and the relationship of the flocculation coefficients in the known parker equation to the initially mixed liquor SS concentration. Shahrokhi et al., 2012 [54] studied the effect of a different number of baffles on the hydraulic efficiency of rectangular primary settling tanks using numerical simulation models. The simulation results showed that the hydraulic performance was improved by increasing the number of baffles in the appropriate position. Heydari et al., 2013 [55] focused on assessing the effect of short-circuiting in the tank on treatment efficiency. This study conducted simulations on the angle of the baffle at the bottom of the settling tank to reduce the vortex zone. The results indicated that the angle of the baffle at 60° has a minimum magnitude of circulation volume leading to increased sedimentation efficiency (**Fig 2.29**)

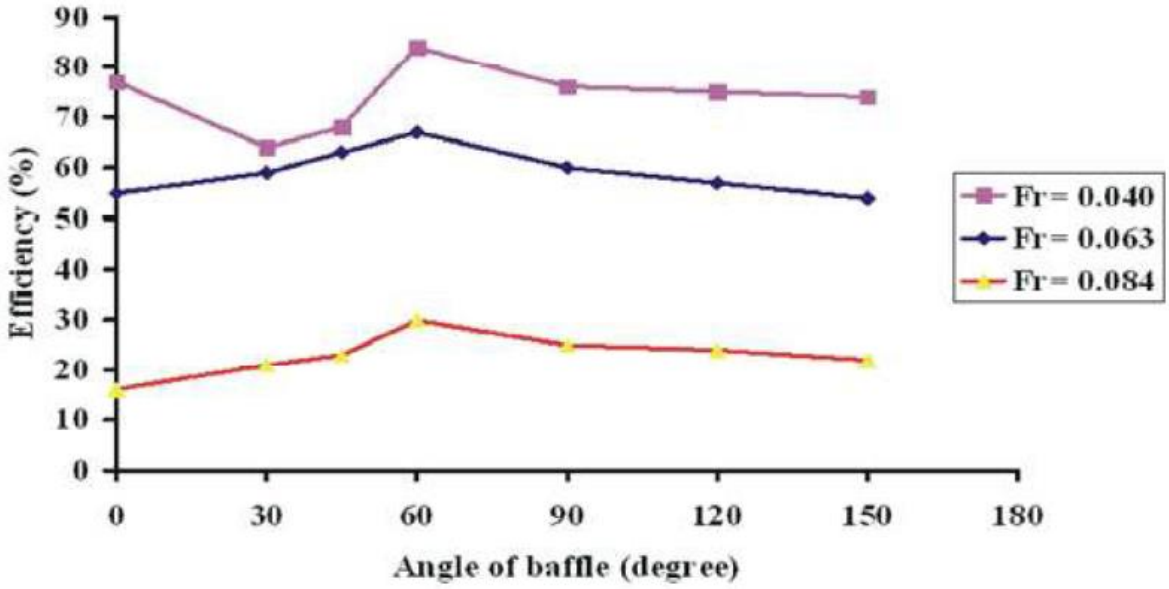

Fig 2.29 The removal efficiency for different angle

Lee, 2017 [56] investigated the influence of the double perforated baffles on SS removal efficiency in the rectangular secondary sedimentation tanks using the CFD simulation model. The simulation results showed that the SS

treatment efficiency was improved better in the tank with baffles compared to the tank without baffles (**Fig 2.30**). Experimental data from 48 settling tanks with double perforated baffles installed confirmed the role of baffles in reducing effluent turbidity.

However, some studies still employed empirical models to evaluate the performance of sedimentation tanks under operating conditions. As a result, empirical equations to determine the relationship between SS removal efficiency and boundary conditions have been developed. The tracer method was used to evaluate the hydraulic efficiency of sedimentation tanks in Kuoppamäki, 1977 [57]. However, in this study, the relationship between SS removal efficiency and hydraulic behaviour expressed in terms of the tracer test results was not established.

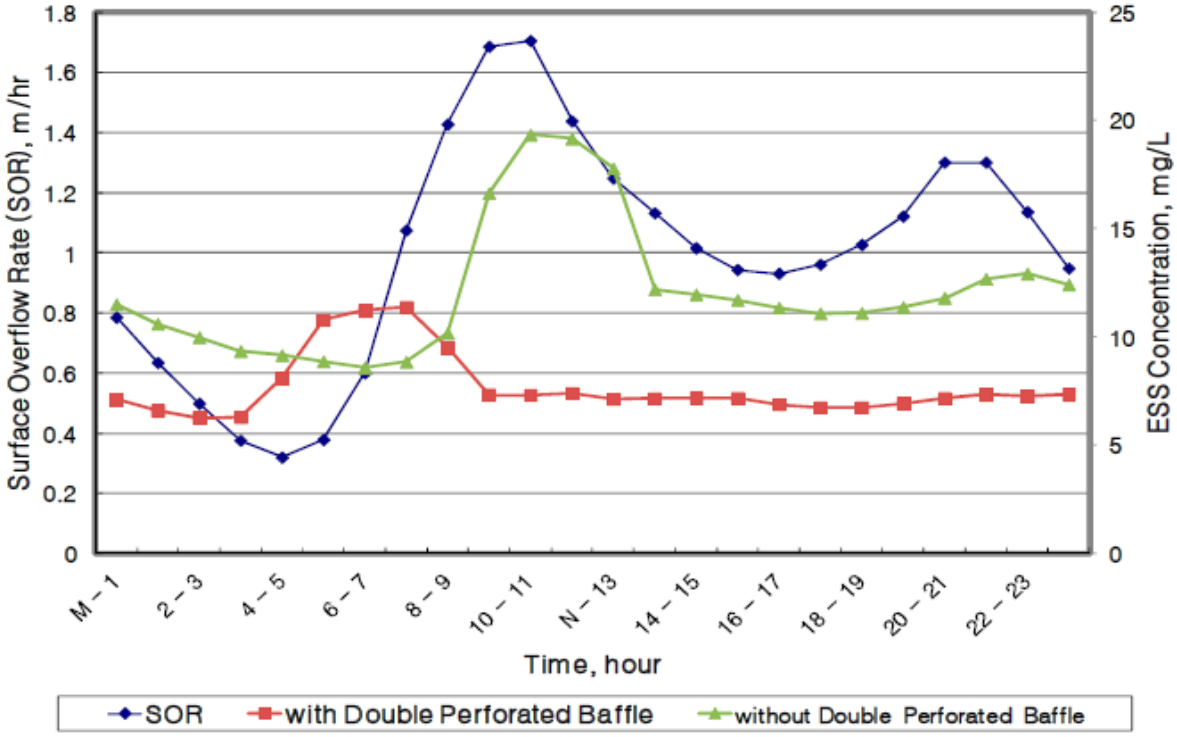

Fig 2.30 CFD simulation results of the rectangular secondary clarifier under diurnal variations of surface overflow rate.

Christoulas, Yannakopoulos and Andreadakis, 1998 [3] applied an empirical model to study the primary settling tank in operating conditions. The study has

developed an empirical mathematical formula for the relationship between SS removal efficiency and overflow rate, influent SS concentration, and sewage temperature based on measurement data from three different pilot-scale sedimentation tanks (**Fig 2.31**). The study also showed the relationship between the influent SS concentration and chemical oxygen demand removal efficiencies. Jover-Smet, Martín-Pascual and Trapote, 2017 [4] built an experimental model for primary settling tanks to assess the impact of operational parameters, such as overflow rate, hydraulic retention time, and temperature on the SS and organic matter removal efficiency. The research developed an empirical mathematical model relating the SS removal efficiency to overflow rate, influent SS concentration, and wastewater temperature. Conserva et al., 2019 [58] studied the effect of biological processes on the sludge characteristics and the settling efficiency in the secondary sedimentation tanks. The results showed that the settling efficiency was greatly affected by the reactor conditions in the tank.

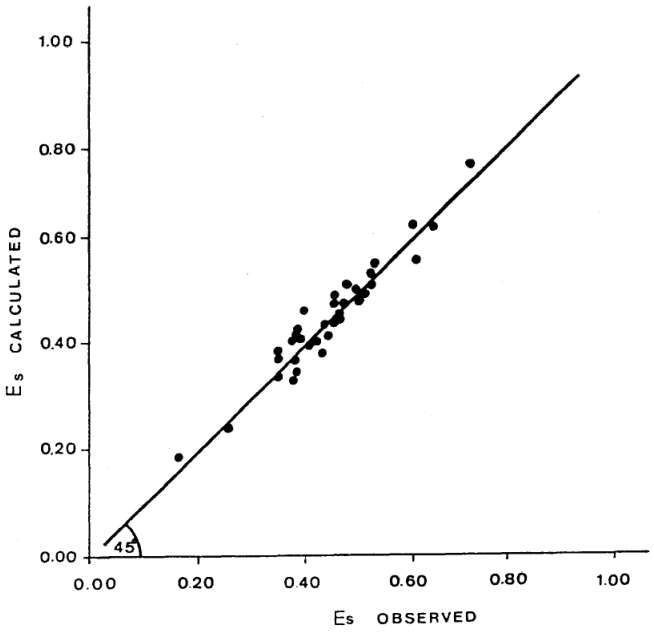

Fig 2.31 Calculated and observed E_S values.

2.6. STUDY ON SIMULATION LAMELLA SETTLING TANK

An effective way to increase the settling tanks' performance is to introduce inclined plates to increase the settling area and improve the hydraulic regime. Extensive research on the performance and optimization of incline plates, as well as the mechanism of the sedimentation process in lamella settlers, were carried out.

The sedimentation regime among inclined plates was studied in several papers. Leung and Probsteln, 1983 [59] studied the behaviour of the above three layers (**Fig. 2.32**), and they developed equations that represent the velocity profiles for each layer.

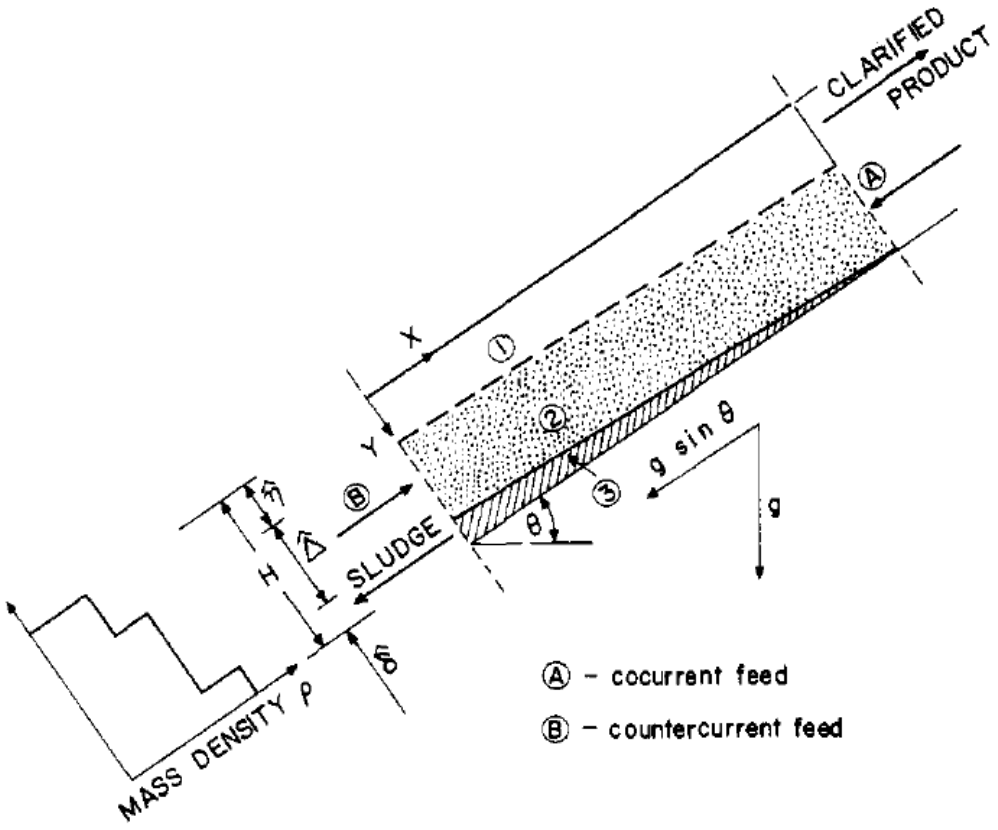

Fig 2.32 Three-layer model of lamella and tube settlers.

Continuing with this research direction, Leung, 1983 [5] investigated the distribution of three-layer, stratified viscous channel flow between inclined

plates.

Some studies are focusing on evaluating the effect of the inclined plate configuration on the treatment efficiency of the tank. Demir, 1995 [6] investigated the optimum angle of the baffle in the lamellar settling tank at various linear velocities. The results in **Fig 2.33** indicated that the optimum plate angle, which provides the highest suspended solids removal efficiency (α_{opt}) is 50 °.

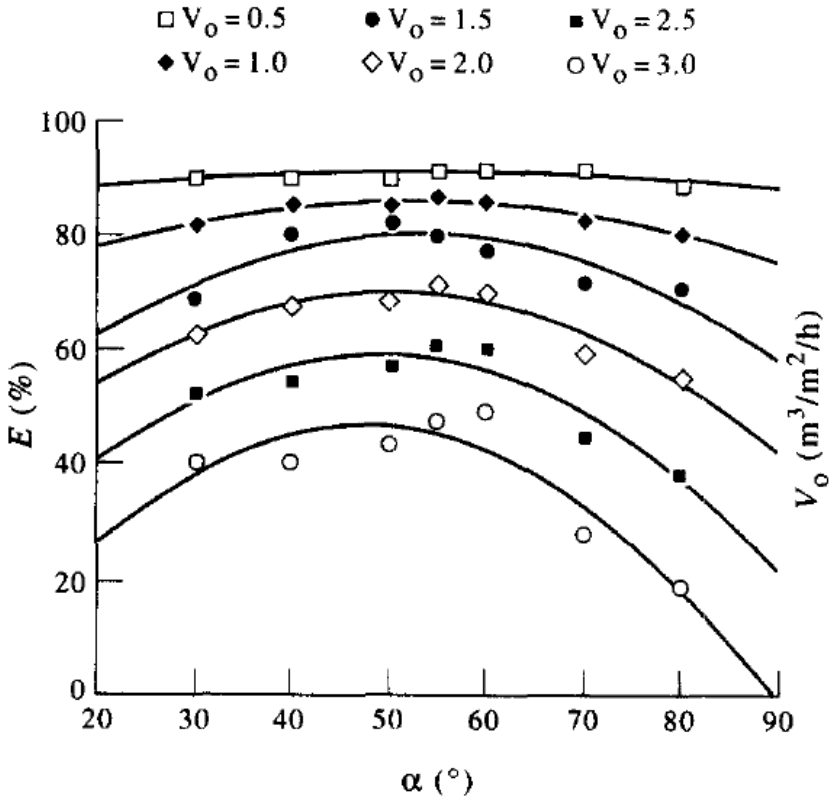

Fig 2.33 The sedimentation efficiencies, which were obtained in various angles (α) for different surface loading rates (V_o; $m^3/(m^2 \cdot h)$)

Fujisaki and Terashi, 2005 [7] examined different types of tube settlers to obtain a higher solid separation capacity **(Fig 2.34).**

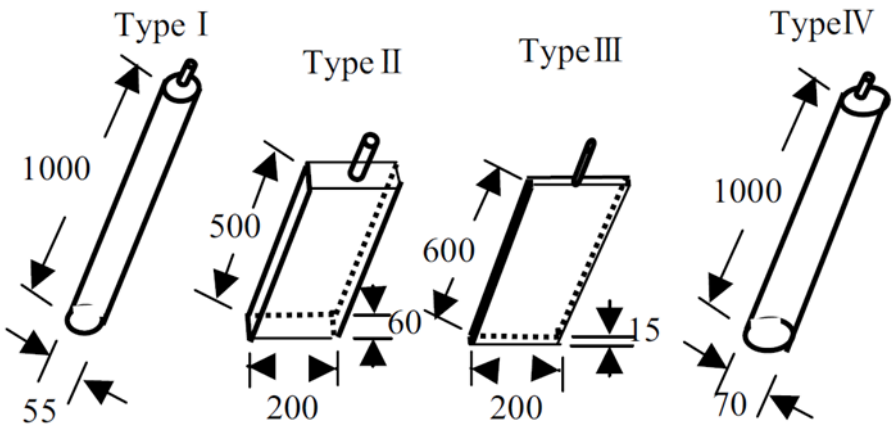

Fig 2.34 Types of tube settlers (unit: mm).

Experimental methods were employed to determine the treatment efficiency of lamella sedimentation tanks. However, the limitation of this method is not to show the hydrodynamic regime in the tank. McKean, 2010 [8] investigated the effectiveness of lamella settling tanks in the primary treatment of domestic wastewater. Study results indicated that the SS and BOD_5 removal efficiency in lamella settling tanks was improved compared to conventional primary settling tanks (**Fig 2.35**)

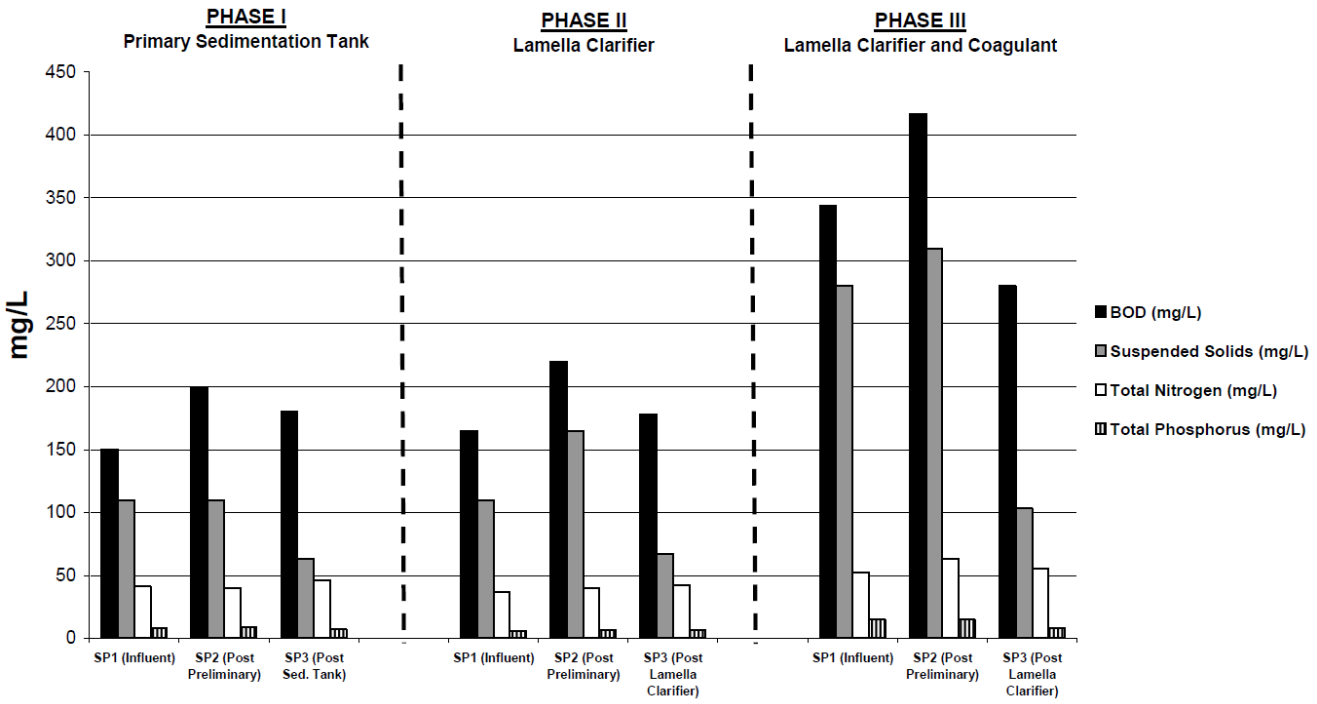

Fig 2.35 Evaluation of the performance of the primary sedimentation tank

Chintokoma, Machunda and Njau, 2015 [9] studied the optimization of sedimentation tanks using inclined plates to pre-treat highly turbid water. Research results for the laboratory scale sedimentation tanks showed that the sedimentation tanks with inclined plates are capable of pre-treating highly turbid water for ultra-filtration. Lee, 2015 [60] investigated the role of inclined plates in clarifier tanks for SS removal efficiency. The experimental results showed that the SS removal efficiency was different from that calculated by Standards for Water Works due to the Boycott effect.

In recent years, with the rapid development of computer technology, the study of the hydraulic regime in lamella sedimentation tanks has been conducted to predict the settling processes occurring in tanks accurately. Kowalski, 2004 [22] compared the SS removal efficiency in the conventional tank and the lamella settling tank taking into account the density, viscosity and mass fraction of solid particles. Sarkar, Kamilya and Mal, 2007 [61] conducted a simulation of sedimentation tanks using inclined plates to evaluate treatment

efficiency. The simulation was performed under a series of geometric parameters affecting the hydraulic regime in the tank, such as distance between plates, length of the plate, plate angle, number of inclined plates, particle diameter, the roughness of plate. Simulation formulas were developed to evaluate the treatment efficiency of lamella settling tanks under various dynamic conditions. The study results had an important contribution in optimizing the dynamic conditions to produce the highest treatment efficiency in the lamella settling tanks (**Table 2.7**).

Table 2.7 Optimal geometric parameters of the sedimentation tanks

Series no.	Variable	Corresponding value of efficiency (values in italics shows the optimal parameters)				
GS-1	α	40°	45°	50°	55°	60°
	E(%)	14.69	25.91	22.89	19.65	13.13
GS-2	l_p/w_p	25	27	29	31	33
	E(%)	25.05	27.81	29.01	28.13	27.70
GS-3	ε_p/w_p	0.00114	0.00221	0.00367	0.00500	0.00657
	E(%)	25.32	27.81	30.84	31.84	31.02
GS-4	n_p	6	8	10	12	14
	E(%)	27.22	29.40	31.01	32.31	33.12
GS-5	d_s/w_p	0.0075	0.0150	0.0210	0.0300	0.045
	E(%)	32.16	34.15	35.83	36.98	34.45

Burgos Flores et al., 2009 [62] applied the Rebhun and Argaman model and the several-reactors-in-series model to predict the hydraulic regime in lamella settling tanks. Comparing the experimental results and the predicted model results showed that the two models mention-above did not predict well stagnations and short-circuited area in the tanks. Shen and Yanagimachi, 2011 [23] studied the effect of tank structure design and operating parameters on SS removal efficiency. Tarpagkou and Pantokratoras, 2014 [24] proved that inclined plates improved the hydraulic regime by simulating a full-scale

system, rather than a part of the system as in previous research.

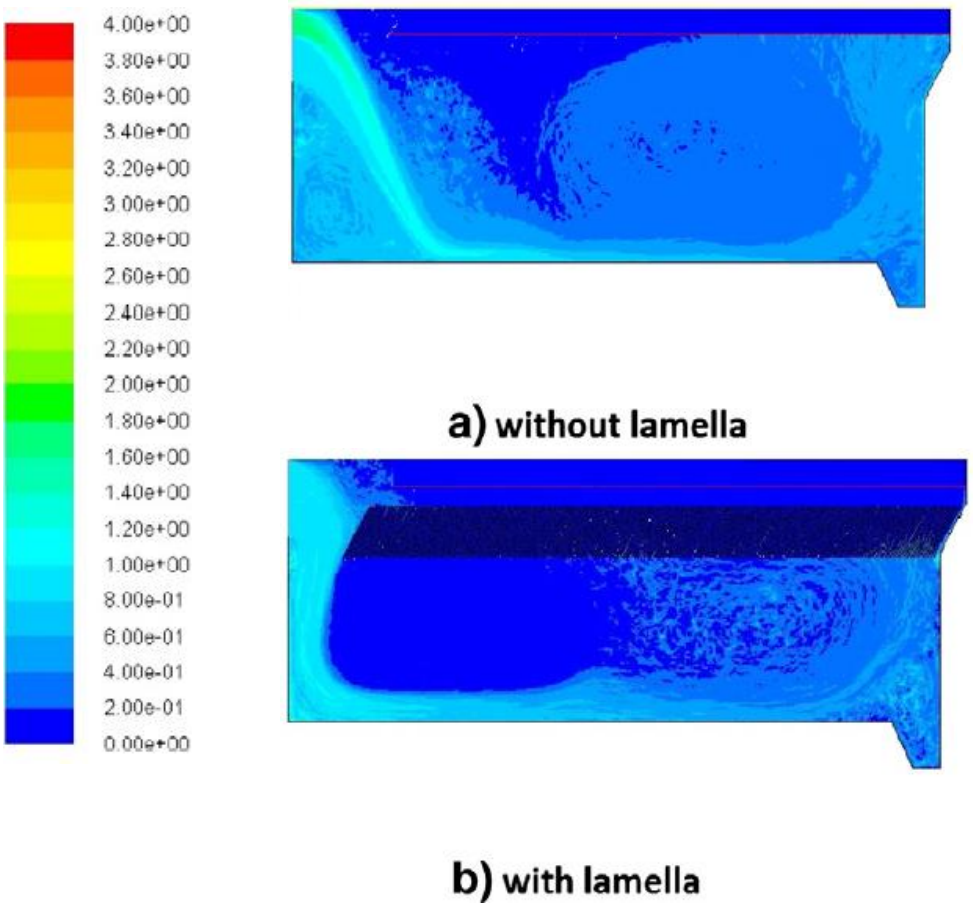

Fig 2.36 Concentration contours (kg/m^3) for a) conventional design and b) design with lamellar settlers.

Yu, Liu and Cui, 2016 [63] investigated the hydraulic regime in the lamella settling tank using CFD software. The *k-ε* turbulent model was applied to simulate the hydraulic characteristics in tanks. The study calculated the head loss of the tube settler due to numerical simulation. These studies used the CFD simulation model to optimize the design in lamella sedimentation tanks.

The application of computational fluid dynamics (CFD) to simulate the settling process has been widely accepted due to its visualization capabilities and data on the hydraulic regime under different conditions of geometry and flow pattern, density and vortex zone, mass fraction and settling velocity of particles.

2.7. CONCLUSIONS

This chapter presents an overview of the situation of sedimentation tanks in water and wastewater treatment. The research was conducted by many different methods, such as experimental models, mathematical simulation models, and a combination of two models. These methods focused on studying the processes taking place in the sedimentation tank to evaluate the performance of the tank and the main influencing factors. The research conducted by the experimental method requires a lot of time and cost for the implementation process. Meanwhile, research using mathematical models on computers is popular in research on sedimentation tanks today. The rapid development of computer technology has dealt with complex simulation problems in a short time at a low cost. Many recent studies show that the CFD model is employed for simulation of sedimentation tanks with high accuracy. Simulation results are presented in many different forms to help employees have an overview of the processes occurring in the tank. Therefore, the CFD model is employed for the simulation of sedimentation tanks in the following chapters.

References

[3] D. G. Christoulas, P. H. Yannakopoulos, and A. D. Andreadakis, “An empirical model for primary sedimentation of sewage,” *Environ. Int.*, vol. 24, no. 8, pp. 925–934, 1998.

[4] M. Jover-Smet, J. Martín-Pascual, and A. Trapote, “Model of suspended solids removal in the primary sedimentation tanks for the treatment of urban wastewater,” *Water (Switzerland)*, vol. 9, no. 6, 2017.

[5] W. F. Leung, “Lamella and Tube Settlers. 2. Flow Stability,” *Ind. Eng. Chem. Process Des. Dev.*, vol. 22, no. 1, pp. 68–73, 1983.

[6] A. Demir, “Determination of settling efficiency and optimum plate angle for plated settling tanks,” *Water Res.*, vol. 29, no. 2, pp. 611–616, 1995.

[7] K. Fujisaki and M. Terashi, “Improvement of settling tank performance using inclined tube settlers,” vol. 80, pp. 475–484, 2005.

[8] T. McKean, “Novel Application of a Lamella Clarifier for Improved Primary Treatment of Domestic Wastewater,” no. 118, pp. 119–124, 2010.

[9] G. C. Chintokoma, R. L. Machunda, and K. N. Njau, “Optimization of Sedimentation Tank Coupled with Inclined Plate Settlers as a Pre-treatment for High Turbidity Water,” vol. 5, no. 17, pp. 11–24, 2015.

[15] E. Imam, J. A. McCorquodale, and J. K. Bewtra, “Numerical modeling of sedimentation tanks,” *J. Hydraul. Eng.*, vol. 109, no. 12, pp. 1740–1754, 1983.

[16] A. I. Stamou, E. W. Adams, and W. Rodi, “Modélisation numérique de l’écoulement et de la sedimentation dans des bassins de décantation primaires de forme rectangulaire,” *J. Hydraul. Res.*, vol. 27, no. 5, pp. 665–682, 1989.

[17] J. A. McCorquodale, “Numerical Simulation of Unsteady Conditions in

Clarifiers," *Water Poll. Res. J. Canada*, vol. 26, no. 2, pp. 201–222, 1991.

[18] S. Zhou, J. A. McCorquodale, and Z. Vitasovic, "Influences of density on circular clarifiers with baffles," *J. Environ. Eng. (United States)*, vol. 118, no. 6, pp. 829–847, 1992.

[19] Y. C. Jin, Q. C. Guo, and T. Viraraghavan, "Modeling of Class I settling tanks," *J. Environ. Eng.*, vol. 126, no. 8, pp. 754–760, 2000.

[20] K. Ramalingam *et al.*, "Critical modeling parameters identified for 3D CFD modeling of rectangular final settling tanks for New York City wastewater treatment plants," *Water Sci. Technol.*, vol. 65, no. 6, pp. 1087–1094, 2012.

[21] A. Ghawi and J. Kriš, "Improvement performance of secondary clarifiers by a computational fluid dynamics model," *Slovak J. Civ. Eng.*, vol. 19, no. 4, pp. 1–11, 2012.

[22] W. P. Kowalski, "The method of calculations of the sedimentation efficiency in tanks with lamella packets," *Arch. Hydroengineering Environ. Mech.*, vol. 51, no. 4, pp. 371–385, 2004.

[23] Y. Shen and K. Yanagimachi, "CFD-aided cell settler design optimization and scale-up: Effect of geometric design and operational variables on separation performance," *Biotechnol. Prog.*, vol. 27, no. 5, pp. 1282–1296, 2011.

[24] R. Tarpagkou and A. Pantokratoras, "The influence of lamellar settler in sedimentation tanks for potable water treatment - A computational fluid dynamic study," *Powder Technol.*, vol. 268, pp. 139–149, 2014.

[28] B. Firoozabadi, "Hydraulic performance of primary settling tanks," pp. 1–6, 2005.

[29] J. Bridgeman, B. Jefferson, and S. A. Parsons, "Computational Fluid Dynamics Modelling of Flocculation in Water Treatment: A Review," *Eng. Appl. Comput. Fluid Mech.*, vol. 3, no. 2, pp. 220–241, 2009.

[30] G. Arbat *et al.*, "Hydrodynamic behaviour of the underdrains in microirrigation sand media filters using CFD software," *Acta Hortic.*, vol. 1008, pp. 85–90, 2013.

[31] H. Yeung, "Modelling of service reservoirs," *J. Hydroinformatics*, vol. 3, no. 3, pp. 165–172, 2001.

[32] J.-M. Zhang, B. C. Khoo, H. P. Lee, C. P. Teo, N. Haja, and K. Q. Peng, "Numerical Simulation and Assessment of the Effects of Operation and Baffling on a Potable Water Service Reservoir," *J. Environ. Eng.*, vol. 139, no. March, pp. 341–348, 2013.

[33] "No Title." [Online]. Available: https://researchbank.swinburne.edu.au/file/7b8f18b0-2f6e-4498-87bc-951a77960948/1/Alamgir Hossain Thesis.pdf.

[34] R. W. Samstag *et al.*, "CFD for wastewater treatment: An overview," *Water Sci. Technol.*, vol. 74, no. 3, pp. 549–563, 2016.

[35] M. So, "Multiscale modelling of biofilm in sponge carrier media," The University of Kitakyushu, 2014.

[36] D. Zhang, "Optimize sedimentation tank and lab flocculation unit by CFD," Norwegian University of Life Sciences, 2014.

[37] The open university, "Potable water treatment." [Online]. Available: https://www.open.edu/openlearn/science-maths-technology/engineering-and technology/technology/potable-water-treatment/content-section-4.4. [Accessed: 03-Feb-2020].

[38] P. Larsen, "On the hydraulics of rectangular settling basins: experimental and theoretical studies," *Dep. Water Res. Eng. Lund Inst. Technol. Lund, Sweden.*, 1977.

[39] B. S. Zhou and A. M. Godo, "Short-circuiting and density interface in primary clarifiers," vol. 120, no. 9, pp. 1060–1080, 1995.

[40] T. Matko, N. Fawcett, A. Sharp, and T. Stephenson, "Recent progress in the numerical modelling of wastewater sedimentation tanks," *Process Saf. Environ. Prot.*, vol. 74, no. 4, pp. 245–258, 1996.

[41] B. C. Liu, J. Ma, S. H. Huang, D. H. Chen, and W. X. Chen, "Two-dimensional numerical simulation of primary settling tanks by hybrid finite analytic method," *J. Environ. Eng.*, vol. 134, no. 4, pp. 273–282, 2008.

[42] K. Mohanarangam and D. Stephens, “Cfd Modelling of Floating and Settling Phases in Settling Tanks,” *Victoria*, no. December, pp. 1–7, 2009.

[43] P. Krebs, D. Vischer, and W. Gujer, “Inlet-structure design for final clarifiers,” *J. Environ. Eng. (United States)*, vol. 121, no. 8, pp. 558–564, 1995.

[44] A. M. Goula, M. Kostoglou, T. D. Karapantsios, and A. I. Zouboulis, “A CFD methodology for the design of sedimentation tanks in potable water treatment. Case study: The influence of a feed flow control baffle,” *Chem. Eng. J.*, vol. 140, no. 1–3, pp. 110–121, 2008.

[45] A. H. Ghawi and K. Jozef, “Improving Performance of Horizontal Sedimentation Tanks,” *ResearchGate*, no. December, 2008.

[46] X. Wang, L. Yang, Y. Sun, L. Song, M. Zhang, and Y. Cao, “Three-dimensional simulation on the water flow field and suspended solids concentration in the rectangular sedimentation tank,” *J. Environ. Eng.*, vol. 134, no. 11, pp. 902–911, 2008.

[47] P. Rodríguez López, A. G. Lavín, M. M. Mahamud López, and J. L. Bueno de las Heras, “Flow models for rectangular sedimentation tanks,” *Chem. Eng. Process. Process Intensif.*, vol. 47, no. 9–10, pp. 1705–1716, 2008.

[48] M. Al-Sammarraee and A. Chan, “Large-eddy simulations of particle sedimentation in a longitudinal sedimentation basin of a water treatment plant. Part 2: The effects of baffles,” *Chem. Eng. J.*, vol. 152, no. 2–3, pp. 315–321, 2009.

[49] A. Tamayol, B. Firoozabadi, and M. A. Ashjari, “Hydrodynamics of secondary settling tanks and increasing their performance using baffles,” *J. Environ. Eng.*, vol. 136, no. 1, pp. 32–39, 2010.

[50] B. Liu, J. Ma, L. Luo, Y. Bai, S. Wang, and J. Zhang, “Design of Rectangular Primary Settling Tanks,” *J. Environ. Eng.*, no. May, pp. 501–507, 2010.

[51] H. Asgharzadeh, B. Firoozabadi, and H. Afshin, “Experimental investigation of effects of baffle configurations on the performance of a

secondary sedimentation tank," *Sci. Iran.*, vol. 18, no. 4 B, pp. 938–949, 2011.

[52] M. Shahrokhi and F. Rostami, "The Computational Modeling of Baffle Configuration in the Primary Sedimentation Tanks," *Flow3D2.Propagation.Net*, vol. 6, pp. 392–396, 2011.

[53] M. Gong *et al.*, "Development of a flocculation sub-model for a 3-D CFD model based on rectangular settling tanks," *Water Sci. Technol.*, vol. 63, no. 2, pp. 213–219, 2011.

[54] M. Shahrokhi, F. Rostami, M. A. Md Said, S. R. Sabbagh Yazdi, and Syafalni, "The effect of number of baffles on the improvement efficiency of primary sedimentation tanks," *Appl. Math. Model.*, vol. 36, no. 8, pp. 3725–3735, 2012.

[55] M. M. Heydari, M. S. Bajestan, H. A. Kashkuli, and H. Sedghi, "The effect angle of baffle on the performance of settling basin," *World Appl. Sci. J.*, vol. 21, no. 6, pp. 829–837, 2013.

[56] B. Lee, "Evaluation of double perforated baffles installed in rectangular secondary clarifiers," *Water (Switzerland)*, vol. 9, no. 6, 2017.

[57] R. Kuoppamäki, "The applicability of tracer techniques for studies on sewage treatment process dynamics," *Int. J. Appl. Radiat. Isot.*, vol. 28, no. 10–11, pp. 833–837, 1977.

[58] S. Conserva, F. Tatti, V. Torretta, N. Ferronato, and P. Viotti, "An integrated approach to the biological reactor-sedimentation tank system," *Resources*, vol. 8, no. 2, 2019.

[59] W. F. Leung and R. F. Probsteln, "Lamella and Tube Settlers. 1. Model and Operation," *Ind. Eng. Chem. Process Des. Dev.*, vol. 22, no. 1, pp. 58–67, 1983.

[60] B. Lee, "Experimental study to evaluate design procedure and proposed improvement measures for clarifier with inclined plates," *Environ. Eng. Res.*, vol. 20, no. 3, pp. 298–305, 2015.

[61] S. Sarkar, D. Kamilya, and B. C. Mal, "Effect of geometric and process variables on the performance of inclined plate settlers in treating

aquacultural waste," *Water Res.*, vol. 41, no. 5, pp. 993–1000, 2007.

[62] D. Burgos-Flores, A. Martín-Domínguez, I. R. Martín-Domínguez, M. Pérez-Tello, and M. T. Alarcon-Herrera, "Mathematical modelling of lamella plate settle hydraulics," *Proc. Inst. Civ. Eng. Water Manag.*, vol. 162, no. 4, pp. 251–259, 2009.

[63] Y. Yu, D. Liu, and X. Cui, "Study on Hydraulic Characteristic of the Tube Settler," no. Mcae, pp. 128–131, 2016.

CHAPTER 3 SIMULATION AND VALIDATION MODEL

3.1. INTRODUCTION

In this study, the CFD model was built for simulation of the settling process in sedimentation tanks. The model was developed based on the digitization of influencing factors by mathematical equations, using algorithms to solve parameters related to research purposes. Input information includes data and assumptions provided for the model, and the processing is done thanks to the theoretical and mathematical constructs of the model. The simulation results are translated from mathematical analysis to useful information for evaluation according to the model building objectives. However, the assumptions and mathematical equations included should be checked for appropriateness for each specific study. Therefore, model validation is an essential step before conducting the simulation. The model modification aims to create a simulation environment like the environment in real working conditions. The adjustment of the model is made based on the simulation with empirical measurement data. Simulation results are compared with experimental measurement results, so there is a solution to adjust the model accordingly. In order to improve the accuracy of the model, the calibration should be conducted with many different measurement data sets. The model after calibration will be used for simulation for similar research purposes.

3.2. MATERIALS AND METHOD

3.2.1 Numerical modelling methods

In this study, the CFD model was chosen to conduct a dynamic study on sedimentation tanks. The Algebraic Slip Model was selected for simulation of the velocity profile and the concentration distribution of SS. A mass fraction equation represents each dispersed component, and a relative movement is allowed between these components in the continuous phase [42]. Turbulence in the liquid phase was modelled using the *k-ε* model, which successfully simulated the sedimentation tank in previous studies [64]. The hydrodynamic and flow behavior in the sedimentation tanks were modelled in two dimensions. In this study, the commercial software CFX 18.0 (in ANSYS) was used to perform CFD modelling. The hexahedral meshes were generated by ANSYS meshing for numerical calculations.

3.2.2 Model equations

In the CFD model, the hydrodynamic and the settling process are simulated based on equations such as continuity equations, fluid momentum equations, mass transport equations, turbulence modelling equations, and conservation laws.

A bulk continuity equation is derived by summing equation (3.1):

$$\frac{\partial \rho_m}{\partial t} + \frac{\partial \left(\rho_m u_m^i \right)}{\partial x^i} = 0 \tag{3.1}$$

A bulk momentum equation by summing equation (3.2):

$$\frac{\partial \left(\rho_m u_m^i \right)}{\partial t} + \frac{\partial \left(\rho_m u_m^j u_m^i \right)}{\partial x^j} = -\frac{\partial p}{\partial x^i} + \frac{\partial \left(\tau_m^{ji} + \tau_{Tm}^{ji} + \tau_D^{ji} \right)}{\partial x^j} + \rho_m g \tag{3.2}$$

where

t: time (s),

x^i: the Cartesian coordinate in the i-direction (m),

u_m^i: the mixture flow velocity in the i-direction (m/s),

x^j: the Cartesian coordinate in the j-direction (m),

u_m^j: the mixture flow velocity in the j-direction (m/s),

ρ_m: the mixture density (kg/m^3),

P: the pressure (*Pa*),

g: the acceleration of gravity (m/s^2).

The τ_m^{ji} , τ_{Tm}^{ji} and τ_{Dm}^{ji} are the viscous, turbulent, and apparent diffusion stresses, respectively.

Using the subscripts m, w, and s, n to denote quantities for the mixture, water phase, and particle groups of solids, respectively, we write the equations for the properties of the mixture as follows [65]:

$$\rho_m = r_{\mathrm{w}}\rho_{\mathrm{w}} + \rho_s \sum_{n=1}^{N_p} r_{s,n} \tag{3.3}$$

$$u_m^i = \frac{1}{\rho_m}\left[r_{\mathrm{w}}\rho_{\mathrm{w}} u_{\mathrm{w}}^i + \rho_s \sum_{n=1}^{N_p} r_{s,n} u_{s,n}^i \right] \tag{3.4}$$

$$\tau_m^{ji} = r_w \tau_w^{ji} + \sum_{n=1}^{N_p} r_{s,n} \tau_{s,n}^{ji} = r_w \mu_w \left(\frac{\partial u_w^i}{\partial x^j} + \frac{\partial u_w^j}{\partial x^i} \right) + \sum_{n=1}^{N_p} r_{s,n} \tau_{s,n}^{ji} \tag{3.5}$$

$$\tau_{Tm}^{ji} = \mu_{tm} \left(\frac{\partial u_m^i}{\partial x^j} + \frac{\partial u_m^j}{\partial x^i} \right) - \frac{2}{3} \delta^{ji} \rho_m k_m \tag{3.6}$$

$$\tau_{Dm}^{ji} = -\rho_w r_w u_{Dw}^i u_w^j - \rho_s \sum_{n=1}^{N} r_{s,n} u_{Ds,n}^i u_{s,n}^j \tag{3.7}$$

where

N_p: number of particle groups,

u_{Dw}^i: the drift velocities for the water $u_{Dw}^i = u_w^i - u_m^i$ (m/s),

$u_{Ds,n}^i$: the drift velocities for the solids $u_{Ds,n}^i = u_{s,n}^i - u_m^i$ (m/s),

ρ_w: the water density (kg/m^3),

ρ_s: the SS density (kg/m^3),

r_w: the water volume fraction (-),

$r_{s,n}$: the SS volume fraction ($r_{s,n} = Y_{s,n} \frac{\rho_m}{\rho_s}$) (-),

$Y_{s,n}$: the SS mass fraction (-)

In Equation (3.6) we apply the Boussinesq approximation for the calculation of the Reynolds (turbulent) stresses, where δ^{ji} is the Kronecker delta (δ^{ji}=1

for i = j and $\delta^{ji} = 0$ for i $\neq$ j), μ_{tm} is the eddy viscosity of the mixture and k_m is the turbulent kinetic energy; the k_m and μ_{tm} were determined by the k-ε model.

3.2.3 Data set for validation

In this study, two data sets were selected from the two papers by Stamou et al., 1989 and Liu et al., 2010 to validate the model.

3.2.3.1 Model equation used in Stamou et al., 1989

Continuity equation

$$\frac{\partial U}{\partial x} + \frac{\partial V}{\partial y} = 0 \tag{3.8}$$

x-momentum equation

$$\frac{\partial U^2}{\partial x} + \frac{\partial VU}{\partial y} = -\frac{1}{\rho}\frac{\partial P}{\partial x} + \frac{\partial}{\partial x}\left(\nu_{tv}\frac{\partial U}{\partial x}\right) + \frac{\partial}{\partial y}\left(\nu_{tv}\frac{\partial U}{\partial y}\right) + \frac{\partial}{\partial y}\left(\nu_{tv}\frac{\partial V}{\partial x}\right) + \frac{\partial}{\partial x}\left(\nu_{tv}\frac{\partial U}{\partial x}\right) \tag{3.9}$$

y-momentum equation

$$\frac{\partial UV}{\partial x} + \frac{\partial V^2}{\partial y} = -\frac{1}{\rho}\frac{\partial P}{\partial y} + \frac{\partial}{\partial x}\left(\nu_{tv}\frac{\partial V}{\partial x}\right) + \frac{\partial}{\partial y}\left(\nu_{tv}\frac{\partial V}{\partial y}\right) + \frac{\partial}{\partial x}\left(\nu_{tv}\frac{\partial U}{\partial y}\right) + \frac{\partial}{\partial y}\left(\nu_{tv}\frac{\partial V}{\partial y}\right) \tag{3.10}$$

The distribution of eddy viscosity (ν_t) is determined with the k-ε turbulence model.

where

U: mean horizontal velocity

V: mean vertical velocity

x: horizontal coordinate

y: vertical coordinate

v_{tv}: turbulent viscosity

ρ: density

P: pressure deviation from the hydrostatic

3.2.3.2 Model equations used in Jin et al., 2000 study

Flow equation

The differential equation describing the gradually varied flow in open channels is:

$$\frac{\partial H_L}{\partial x_f} + \frac{1}{2g}\frac{\partial U_c^{\,2}}{\partial x_f} + \frac{U_c^{\,2}}{C^2 R} = 0 \qquad (3.11)$$

Where

x_f: direction of flow

U_c: average velocity of the cross

H_L: water level

R: hydraulic radius

C: Chezy coefficient

$$C = \frac{R^{1/6}}{n}$$

n: Manning roughness

g: the acceleration of gravity

3.2.3.3 Model equation used in Liu et al., 2010 study

Continuum equation

$$\frac{\partial u}{\partial x}+\frac{\partial v}{\partial y}=0 \tag{3.12}$$

x- momentum equation

$$\left(u-\frac{\partial \nu_t}{\partial x}\right)\frac{\partial u}{\partial x}+\left(\upsilon-2\frac{\partial \nu_t}{\partial y}\right)\frac{\partial u}{\partial y}= -\frac{\partial p}{\partial x}+\left(\nu_t+1/\mathrm{Re}\right)\nabla^2 u+\frac{\partial \nu_t}{\partial y}\frac{\partial \upsilon}{\partial x}-\frac{2}{3}\frac{\partial k}{\partial x} \tag{3.13}$$

y- momentum equation

$$\left(u-\frac{\partial \nu_t}{\partial x}\right)\frac{\partial \upsilon}{\partial x}+\left(\upsilon-2\frac{\partial \nu_t}{\partial y}\right)\frac{\partial \upsilon}{\partial y}= -\frac{\partial p}{\partial y}+\left(\nu_t+1/\mathrm{Re}\right)\nabla^2 \upsilon+\frac{\partial \nu_t}{\partial x}\frac{\partial u}{\partial y}-\frac{2}{3}\frac{\partial k}{\partial y} \tag{3.14}$$

where

u: dimensionless velocity component in x direction

υ: dimensionless velocity component in y direction

x: horizontal coordinate

y: vertical coordinate

ν_t: dimensionless turbulent eddy viscosity

p: dimensionless pressure

Re: Reynolds number based on flow depth and nominal flow velocity

$$\mathrm{Re} = \frac{UH}{\nu}$$

U: mean horizontal velocity

v: dimensionless kinematic molecular viscosity

∇^2: Laplacian operator

$$\nabla^2 = \frac{\partial^2}{\partial x^2} + \frac{\partial^2}{\partial y^2}$$

k: dimensionless turbulent kinetic energy

The distribution of eddy viscosity (v_t) is determined with the k-ε turbulence model.

The model proposed in this study used the similar continuous and momentum equations like the ones in Stamou's and Liu's studies, in which the flow and settling process in tanks under different boundary conditions were described in 2D simulation. The effect of eddy viscosity was determined based on the k-ε turbulence model. Meanwhile, the model developed in Jin's study was 1D, in which the flow was calculated following the water level for an open channel.

3.2.3.4 The data set of Stamou et al., 1989

A rectangular settling tank was simulated at three linear velocities (LV) of 37, 60 and 110 m/d, and suspended particle concentration at influent of 0.2 kg/m^3. The particle distribution was divided into 6 particle groups with different fractions. For each particle group was solved with settling velocity (SV_i)

according to **Table 3.1**

Table 3.1 Settling velocity and mass fraction for each particle groups for Stamou's dataset

Group	1	2	3	4	5	6
fraction (%)	40	15	15	5	5	20
Settling velocity (mm/s)	0.063	0.30	0.72	1.04	1.51	2.25

3.2.3.5 The data set of Liu et al., 2010

A sedimentation tank was simulated with a linear velocity of 0.000977 m/s, detention time of 34 min, and suspended particle concentration at influent of 0.5 kg/m^3. The particle distribution and the corresponding settling velocities in the influent are listed in **Table 3.2**

Table 3.2 Settling velocity and mass fraction for each particle groups for Liu's dataset

Group	1	2	3	4	5	6	7	8
Fraction (%)	2	8	17	22	20	14	11	6
Settling velocity (mm/s)	0.0095	0.0536	0.299	1.34	5.36	17.20	40.40	82.80

3.2.4 Model geometry

Model validation was carried out with two datasets from literature reviews. The rectangular settling tanks were modelled in two-dimensions.

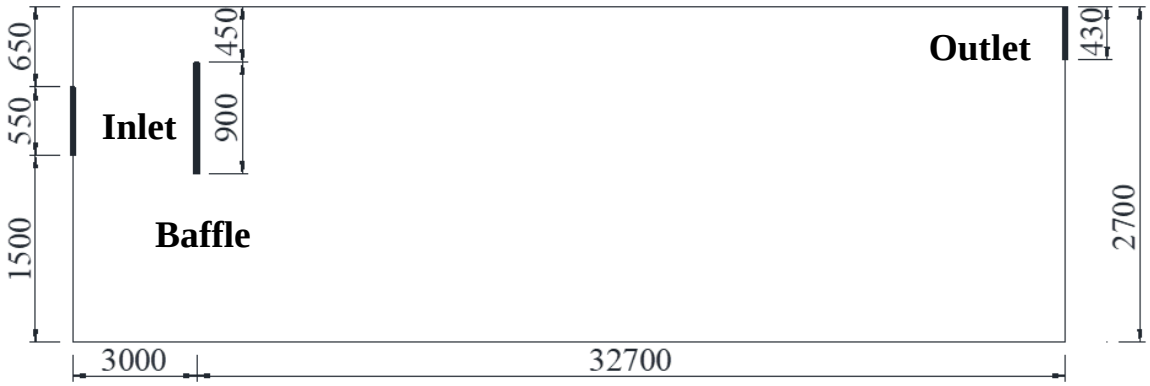

Fig 3.1 Geometry of the settling tank in modelling (Stamou et al., 1989)

The dimensions of this study settling tank are as follows: (L×H×W=35.7×2.7×0.02 m)

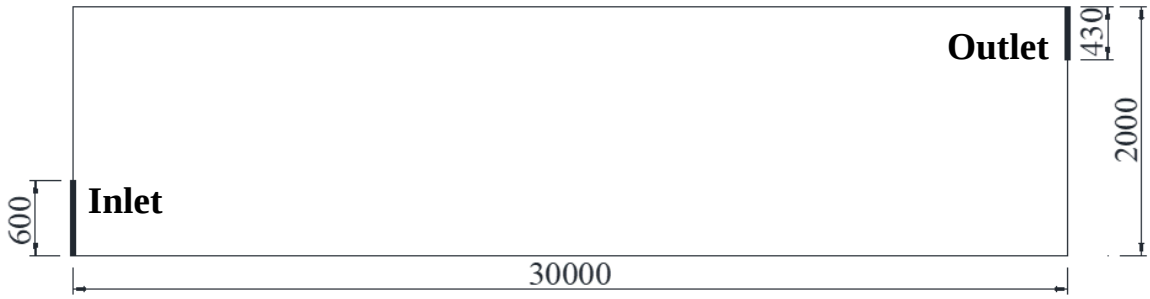

Fig 3.2 Geometry of the settling tank in modelling (Liu et al., 2010)

The dimensions of this study settling tank are as follows: (L×H×W=30.0×2.0×0.02 m)

3.2.5 Condition of simulation

In the model, the mass flow rate was selected at both the inlet and outlet. No slip wall was set for the bottom, the wall, or the baffles. The water-surface was best defined by the VOF method in some studies [66], [67], in case of simulating the complicated surface between two fluids (air and water). In this study, the surface was almost flat and simple, so the free slip wall was selected to setup the surface boundary condition. The water surface was assumed to be horizontal in the tank, which was also widely applied for simulation of settling

tanks in previous research [24], [68], [69]. The particles were set to be deposited only at the bottom, not on the wall or baffles.

The transient-type simulations were selected in this study. The initial time step was set at 5 seconds for the adaptive option in all calculations. For the numerical method, the advection scheme was upwind, and the transient scheme was set as second-order backward Euler.

3.2.6 Selection of appropriate mesh size

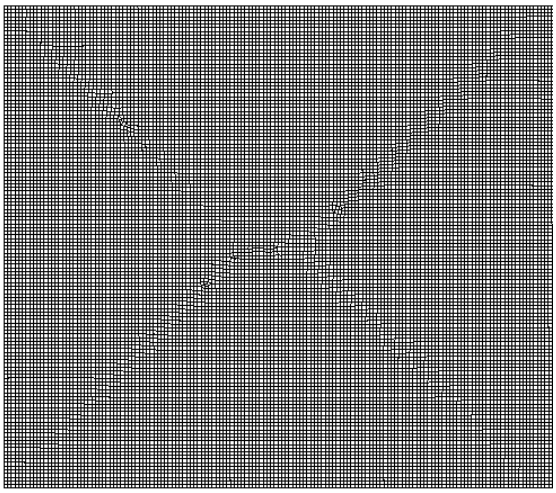

20 mm

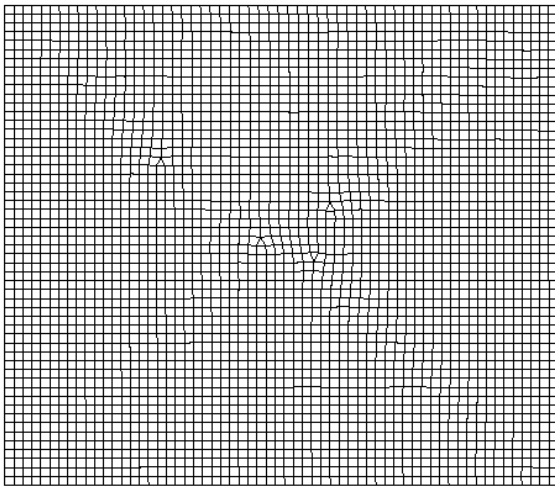

50 mm

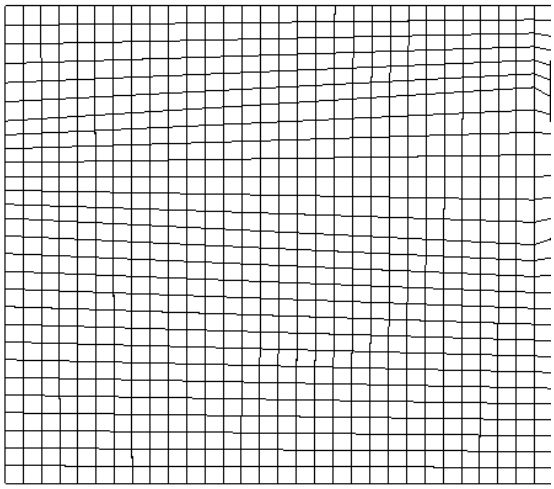

100 mm

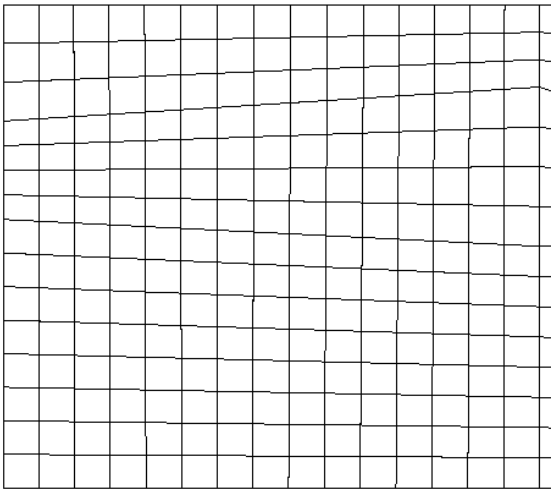

200 mm

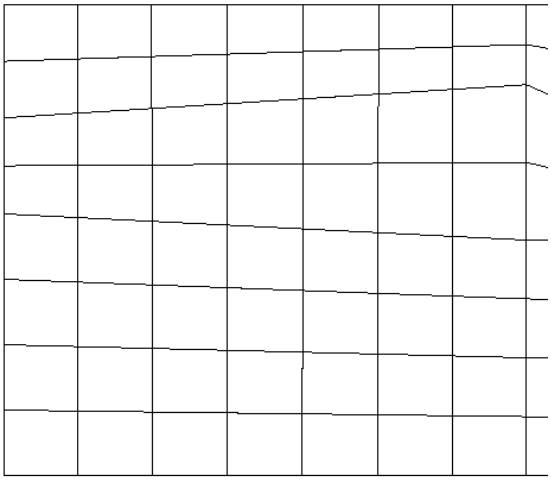

400 mm

Fig 3.3 Mesh sizes in the model

In order to check the mesh sensitivity, different mesh sizes ranging from 20-400 mm (**Fig 3.3**), corresponding to 205,253 and 589 number of elements, were used to simulate SS removal efficiency in settling tank from the first data set (Stamou, 1989). By enlarging the mesh size, SS removal efficiency increased from 56.85 to 57.20% according to the results (**Table 3.3**). At mesh sizes of 20 and 50 mm, SS removal efficiencies were similar. Consequently, the 20 mm-mesh size was selected for conducting subsequent simulations, assuring to provide accurate results and reasonable simulation time.

Table 3.3 Simulation results for the mesh sensitivity

	Mesh size 1 (20 mm)	Mesh size 2 (50 mm)	Mesh size 3 (100 mm)	Mesh size 4 (200 mm)	Mesh size 5 (400 mm)
Nodes	413,856	71,092	19,032	4,550	1,360
Elements	205,253	34,848	9,151	2,102	589
SS removal efficiency (%)	56.85	56.87	57.03	57.12	57.20
Difference	0.00	0.04	0.31	0.47	0.62

3.3. RESULTS

3.3.1 Comparisons on suspended solids removal efficiency between simulation and measurement results for Stamou's dataset

Validation of the model was conducted by comparing the simulation results and the experimental data on flow and settling patterns in sedimentation tanks studied by Stamou et al.,1989 [16]. Using their configuration and the settling velocity curve of SS, a rectangular settling tank was simulated at three linear velocities (*LV*) of 37, 60, and 110 m/d. A good agreement between model simulation and experimental results was observed (**Fig 3.4**).

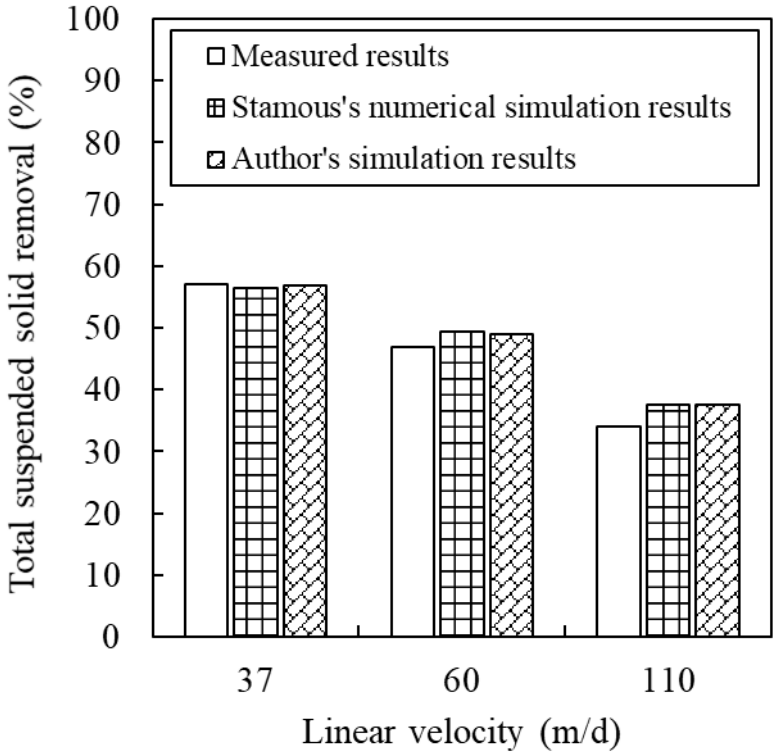

Fig 3.4 Comparison of measured and simulated results for Stamou's dataset.

3.3.2 Comparisons on suspended solids removal efficiency between simulation and measurement results for Liu's dataset

The solid particle removal efficiency was predicted using the ideal model, the model of Jin et al., 2000, the model of Liu et al., 2008, and the study simulation

results were shown in **Fig 3.5**. The total removal efficiency predicted by study results, Jin et al., and Liu et al., was less than the ideal model, which is reasonable because the flow was not uniform due to influences of the inlet and outlet, etc.

As a result, the proposed model was suited for modelling the settling process in sedimentation tanks.

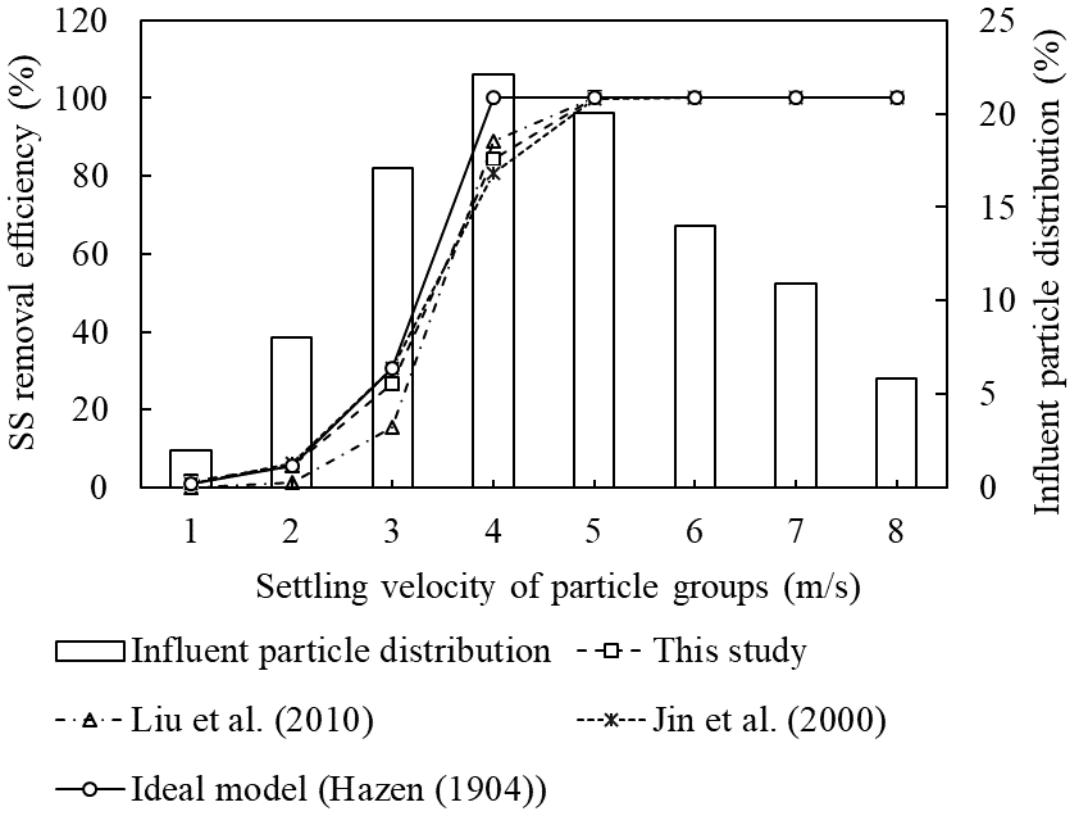

Fig 3.5 Comparison of simulation results for Liu's dataset.

3.4. CONCLUSIONS

The comparison results showed a small difference between simulation results in the research model and simulation results and measurements from reference documents. Therefore, the simulation methods established in CFDs are suitable for the simulation of settling processes in sedimentation tanks. The model after calibration was used for simulation in the sedimentation tanks in this study.

References

[16] A. I. Stamou, E. W. Adams, and W. Rodi, “Modélisation numérique de l’écoulement et de la sedimentation dans des bassins de décantation primaires de forme rectangulaire,” *J. Hydraul. Res.*, vol. 27, no. 5, pp. 665–682, 1989.

[24] R. Tarpagkou and A. Pantokratoras, “The influence of lamellar settler in sedimentation tanks for potable water treatment - A computational fluid dynamic study,” *Powder Technol.*, vol. 268, pp. 139–149, 2014.

[42] K. Mohanarangam and D. Stephens, “Cfd Modelling of Floating and Settling Phases in Settling Tanks,” *Victoria*, no. December, pp. 1–7, 2009.

[64] Ghawi, “Application of Computational Fluid Dynamics modelling to a horizontal sedimentation tank,” no. April, 2017.

[65] A. Stamou and A. Gkesouli, “Modeling settling tanks for water treatment using computational fluid dynamics,” *J. Hydroinformatics*, vol. 17, no. 5, pp. 745–762, 2015.

[66] Y. L. Liu, W. L. Wei, B. Lv, and X. F. Yang, “Research on optimal radius ratio of impellers in an oxidation ditch by using numerical simulation,” *Desalin. Water Treat.*, vol. 52, no. 13–15, pp. 2811–2816, 2014.

[67] W. Wei, Y. Liu, and B. Lv, “Numerical simulation of optimal submergence depth of impellers in an oxidation ditch,” *Desalin. Water Treat.*, vol. 57, no. 18, pp. 8228–8235, 2016.

[68] A. I. Stamou, G. Theodoridis, and K. Xanthopoulos, “Design of secondary settling tanks using a CFD model,” *J. Environ. Eng.*, vol. 135, no. 7, pp. 551–561, 2009.

[69] M. Weiss, B. G. Plosz, K. Essemiani, and J. Meinhold, “CFD modelling

of sludge sedimentation in secondary clarifiers," *WIT Trans. Eng. Sci.*, vol. 52, no. January 2009, pp. 509–518, 2006.

CHAPTER 4 COMPUTATIONAL FLUID DYNAMICS STUDY ON ATTAINABLE FLOW RATE IN A LAMELLA SETTLER BY INCREASING INCLINED PLATES

4.1. INTRODUCTION

The sedimentation tank plays an important role in water and wastewater treatment systems by settling suspended particles using gravity. The effective performance of the settling tank contributes largely to the reduction of suspended solids (SS) that enter into the filtration process. However, the low settling velocity (*SV*) desired in the settling tank requires a large surface area, which might be difficult in restricted areas.

Many studies have focused on the hydraulic regime in the settling tank. For example, in 1989, Stamou [16] used a numerical model to study the flow and settling process of SS in primary sedimentation tanks and compared the simulation results to those from the theoretical method. Goula [44] evaluated the impacts of baffles in the inlet zone on the distribution of flow patterns and the influence of SS mass fraction on their removal efficiency.

An effective way to increase the settling tanks' performance is to introduce inclined plates to increase the settling area and improve the hydraulic regime. Extensive research on the performance and optimization of incline plates, as well as the mechanism of the sedimentation process in lamella settlers, were carried out. Demir [6] investigated the optimum angle of the baffle in the lamellar settling tank at various linear velocities. Kowalski [22] compared the SS removal efficiency in the conventional tank and the lamella settling tank taking into account the density, viscosity, and mass fraction of solid particles. Different types of tube settlers were examined by Fujisaki and Terashi [7] to obtain a higher solid separation capacity. Leung [5] studied the distribution of three-layer, stratified viscous channel flow between inclined plates. The

above-mentioned studies successfully predicted the SS removal efficiency in lamella settling tanks.

Theoretically speaking, in the design of lamella settlers, a large assumption was made on the effectiveness of baffles, in which the entire horizontal projected area of inclined plates was considered to be involved in increasing the settling area in lamella settling tanks. Moreover, SS removal efficiency was assumed to be constant if the increase and/or decrease of settling area and flow rate were proportional [70], [71], because other factors such as vortex and density current have been considered as non-impacting ones. However, in the practical operation of lamella settlers, such factors should be taken into account as contributors to the SS removal efficiency. In experimental conditions, it is a big challenge to evaluate all factors affecting the settling process; that is the reason why the application of simulation is essential in the evaluation of the whole process.

The application of computational fluid dynamics (CFD) to simulate the settling process has been widely accepted due to its visualization capabilities and data on the hydraulic regime under different conditions of geometry and flow pattern, density and vortex zone, mass fraction and settling velocity of particles. Asgharzadeh [51] and Shahrokhi [52] investigated the reduction of dead zones and recirculation zones in cases where a different number of baffles were installed at the bottom of the tank. Similarly, Heydari et al., [55] conducted simulations on the angle of the baffle at the bottom of the settling tank to reduce the vortex zone. Ghawi and Kriš [72] developed a complex CFD model to estimate the factors that impact deposition efficiency. Tarpagkou [24] proved that inclined plates improved the hydraulic regime by simulating a full-scale system, rather than a part of the system as in previous research.

As mentioned above, to maintain the SS removal of the sedimentation tank, the surface area of the tank needed to be increased proportionally to the increase of flow rate. To remove the smallest particles with settling velocity of SV_o, the surface loading rate or linear velocity of the ideal sedimentation

tanks is calculated according to equation (4.1) and illustrated in **Fig 4.1**:

$$LV_o = \frac{Q_o}{A_o} \tag{4.1}$$

where

Q_o: flow rate of sedimentation tank (m^3/h)

LV_o: linear velocity of sedimentation tank (m/h)

A_o: surface area of sedimentation tank (m^2)

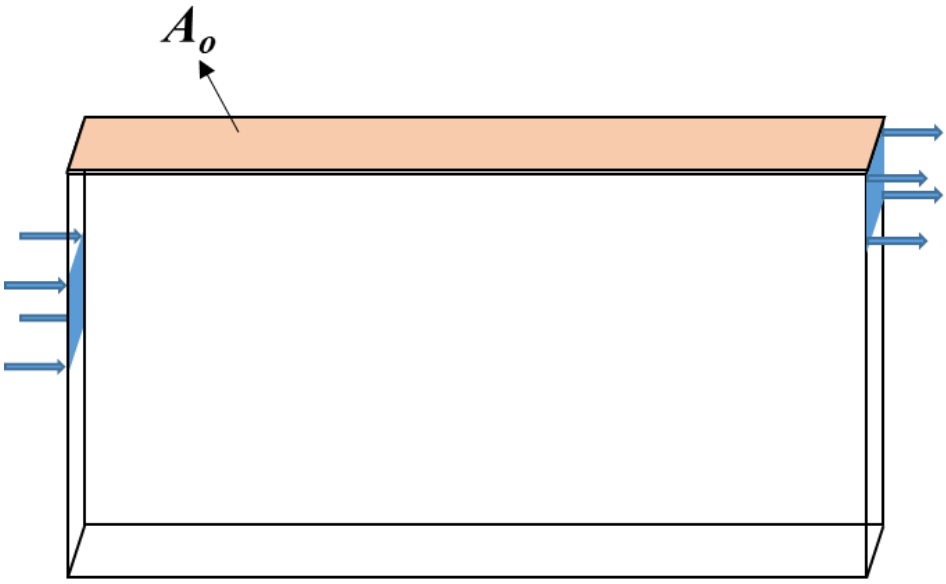

Fig 4.1 Sedimentation tank

From equation (4.1), to increase the flow rate (Q_o) while keeping LV_o constant, the surface area could be increased using the inclined plates (**Fig 4.2**). Then, the increased settling area by inclined plates will improve the capacity of the sedimentation tank according to the equation (4.2):

$$Q_b = LV_o \times (A_o + A_b) \tag{4.2}$$

where

Q_b: increased flow rate in lamella settling tank (m^3/h)

A_b: horizontal projection area of the inclined plate (m^2)

$$A_b = A_1 \times \cos\theta$$

δ: increased settling area ratio (-)

$$\delta = \frac{A_b}{A_o}$$

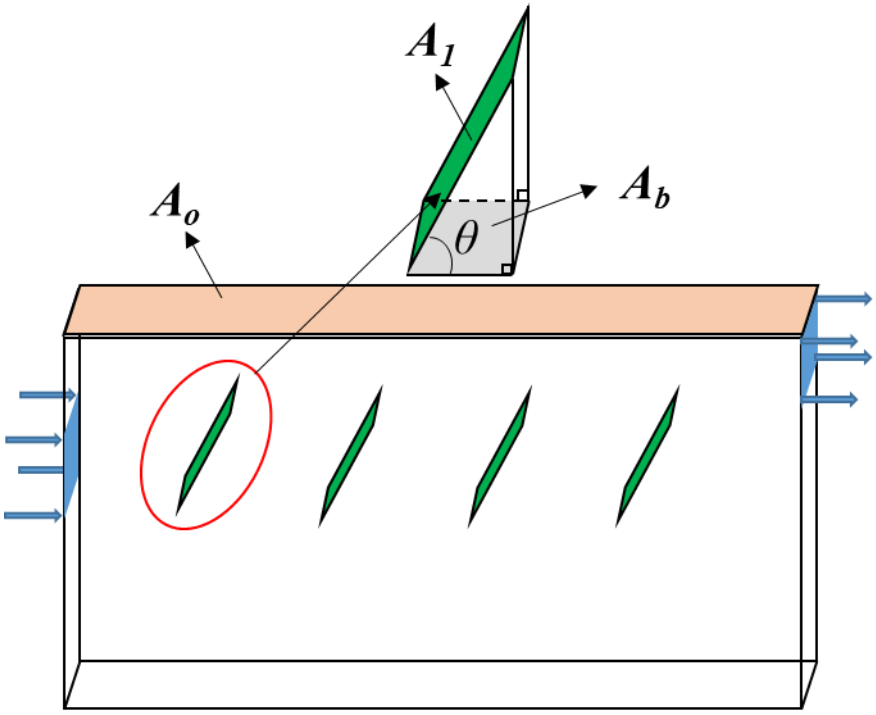

Fig 4.2 Lamella settling tank

Thus, in this study, lamella settling tanks were simulated using CFD to investigate the effectiveness of inclined plates on attainable flow rates in lamella settlers. This basic consideration is of great importance to SS removal efficiency and will be analyzed for different particle groups, flow patterns, and baffle configurations. The findings could provide useful information for the design and optimization of lamella settling tanks.

4.2. MATERIALS AND METHODS

4.2.1 Numerical modelling methods

The Algebraic Slip Model was selected for simulation of the velocity profile and the concentration distribution of SS. Each dispersed component is represented by a mass fraction equation, and a relative movement is allowed between these components in the continuous phase [42]. Turbulence in the liquid phase was modelled using the k-ε model, which successfully simulated the sedimentation tank in previous studies [64]. The hydrodynamic and flow behavior in the sedimentation tanks were modelled in two dimensions. In this study, the commercial software CFX 18.0 (in ANSYS) was used to perform CFD modelling. The hexahedral meshes were generated by ANSYS meshing for numerical calculations.

4.2.2 Model geometry

Simulations were performed using 9 tank configurations, assigned with the letters A to I, of the same dimensions (H×W×L = 2×0.02×4 m). All tanks were lamella settlers except for tank A which was a conventional settling tank without inclined plates. The investigation on the impacts of increased settling area to SS removal efficiency in lamella settling tanks was carried out on tanks B, C, D and E. A count of 4, 8 and 16 inclined plates of the same configuration were installed at a 60^{o} angle in tanks B, C and D respectively; longitudinal depth of 0.5 m; and spacing of 0.8, 0.4, and 0.2 m, respectively. In tank E, 16 baffles at a longitudinal depth of 1 m were introduced at 0.2 m apart. The influence of baffle configuration and flow pattern in lamella settlers was carried out in tanks D, F, G, H and I. Here, a different configuration of baffles was used at different depths and spacing as shown in **Fig 4.3.**

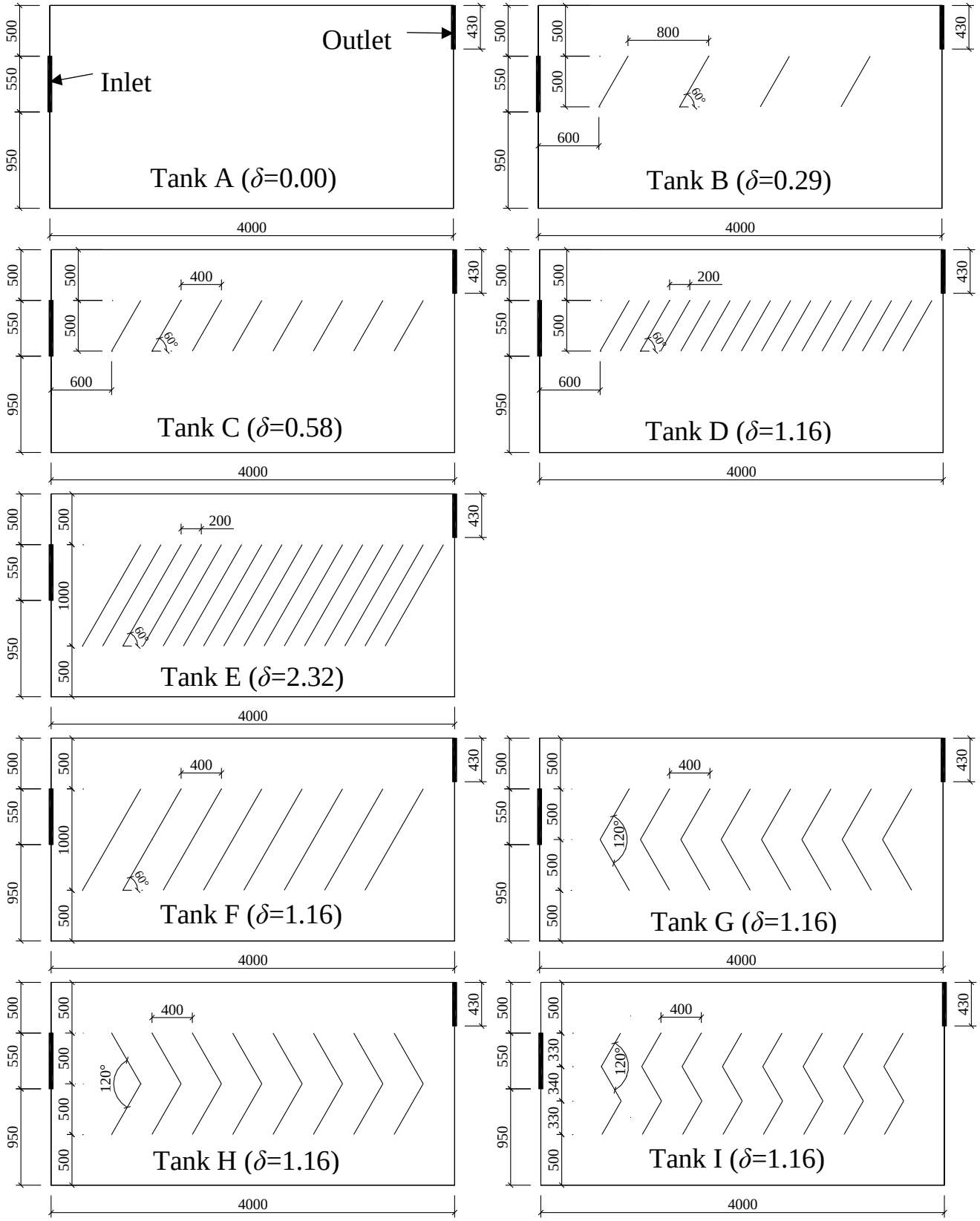

Fig 4.3 Geometry of settling tank and lamella settling tanks.

4.2.3 Boundary condition simulation

In sedimentation tank design, the *LV* commonly selected is between 1 and 2 $m^3/(m^2 \cdot h)$ [73], which corresponds to a flow rate of 0.08 to 0.16 m^3/h. Therefore, in this study, a primary sedimentation unit located in the wastewater treatment process was simulated under varying flow rates from 0.08 to 0.16 m^3/h, inlet 200 mg-SS/L, water density 998 kg/m^3 (at STP) and particle density of 1020 kg/m^3.

The mass and momentum option in the model were selected as the mass flow rate at both the inlet and outlet. No slip wall was set for the bottom, the wall, or the baffles. The free slip wall was established for the surface boundary condition; the particles were set to be deposited only at the bottom, not on the wall or baffles.

The transient-type simulations were selected to visualize the hydraulic regime in the tanks better. The initial time step was set at 5 seconds for the adaptive option in all calculations. For the numerical method, the advection scheme was upwind, and the transient scheme was set as second-order backward Euler.

4.2.4 Selection of appropriate mesh size

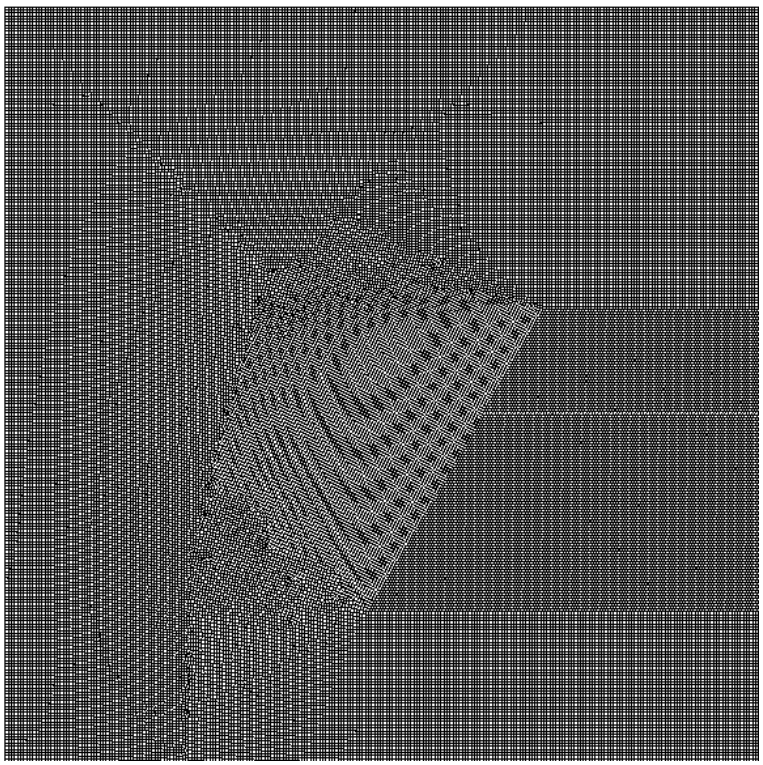

5 mm

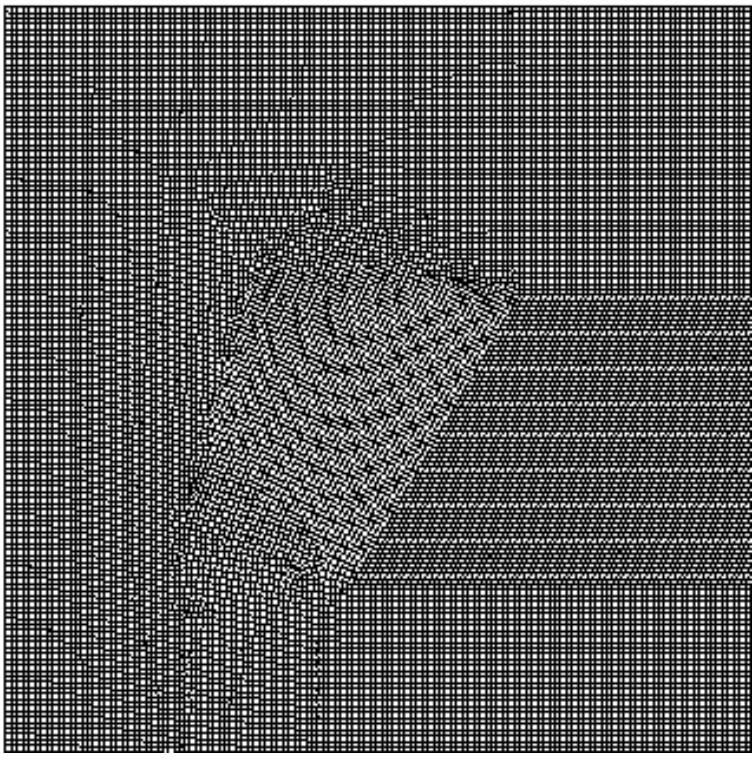

10 mm

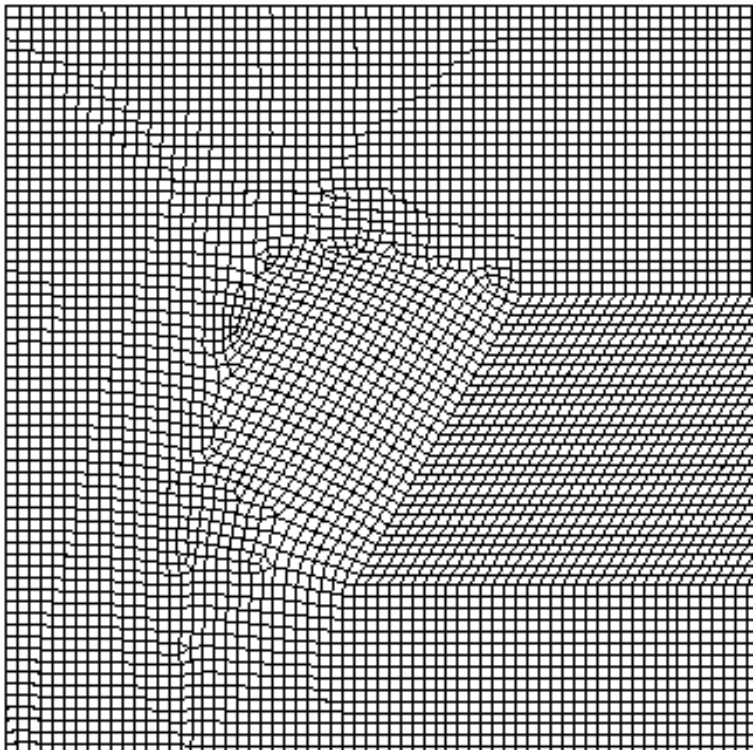

20 mm

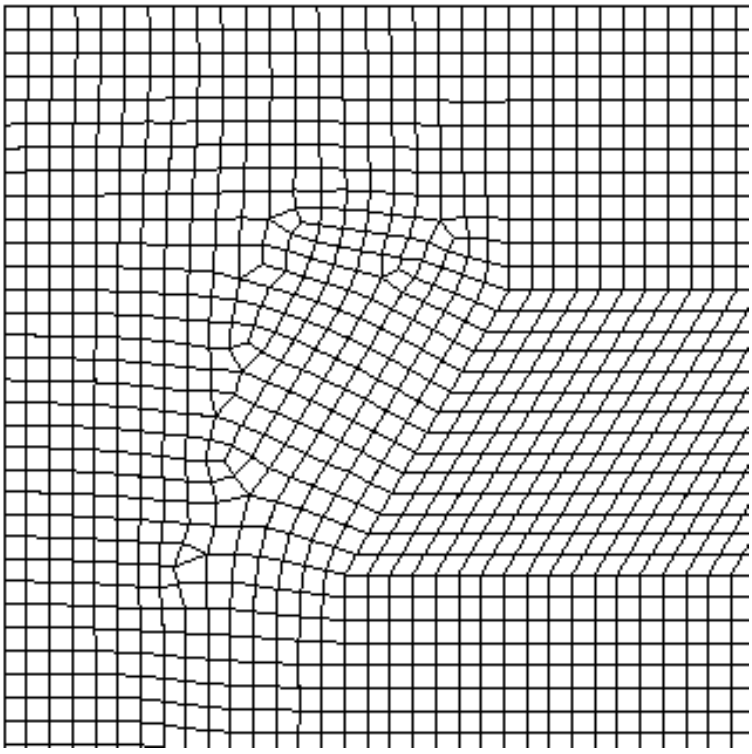

40 mm

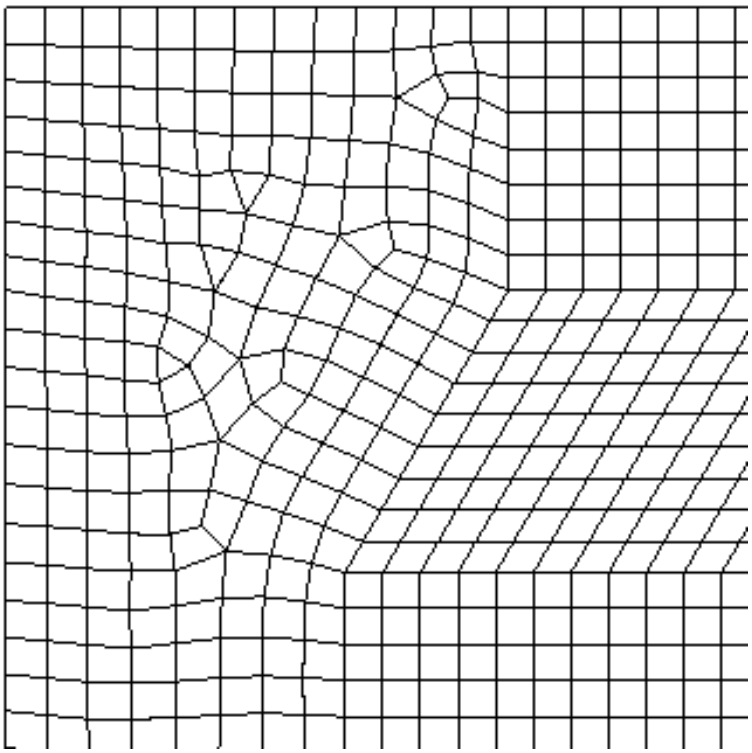

Fig 4.4 Mesh sizes in the model

In order to check the mesh sensitivity, different mesh sizes ranging from 5-80 mm (**Fig 4.4**), corresponding to 324,538 and 1,857 number of elements (**Table 4.1**), were used to simulate SS removal efficiency in lamella D (δ = 1.16). By enlarging the mesh size, SS removal efficiency decreased from 88 to 79% according to the results. At mesh sizes of 5, 10, and 20 mm, SS removal efficiencies were similar. Consequently, the 20 mm-mesh size was selected for conducting subsequent simulations, assuring to provide accurate results and reasonable simulation time.

Table 4.1 Simulation results for the mesh sensitivity

	Mesh size 1 (5 mm)	Mesh size 2 (10 mm)	Mesh size 3 (20 mm)	Mesh size 4 (40 mm)	Mesh size 5 (80 mm)
Nodes	651,364	164,230	41,682	10,362	3,888
Elements	324,538	81,532	20,550	5,035	1,857
SS removal efficiency (%)	87.82	87.79	87.16	83.16	79.09
Difference	0.00	0.03	0.75	5.31	9.94

4.2.5 Selection of appropriate groups of particles

In the CFD model, SS particles in the influent were grouped and represented by average settling velocities for simplification in **Table 4.2**. To verify the sensitivity of group numbers, the simulation of SS removal efficiency of lamella D (δ = 1.16) was conducted using different particle groups ranging from 1 to 20. By increasing particle groups, the SS removal efficiencies decreased from 95 to 87% (**Fig 4.5**). The groups from 10 to 20 provided results without much difference. Hence, 10 groups of particles were used for the following simulations.

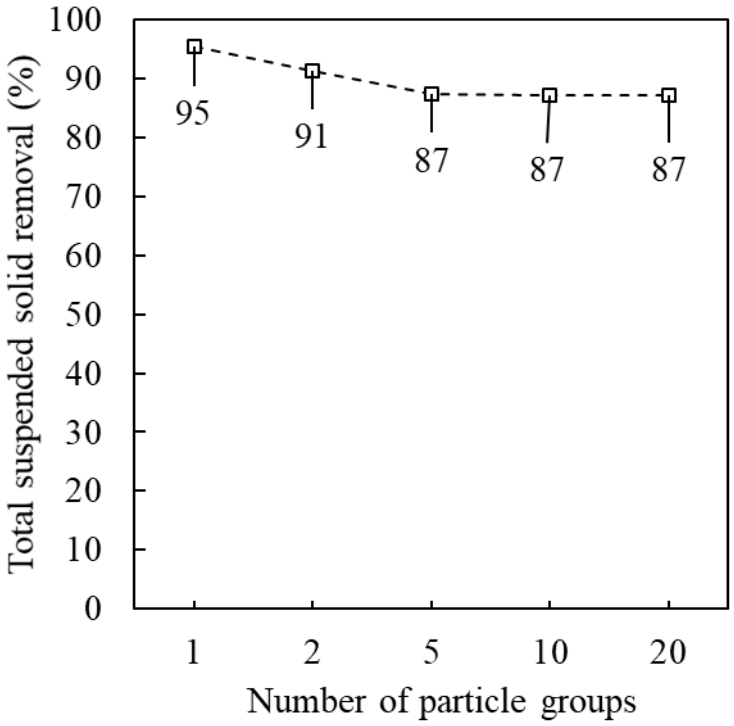

Fig 4.5 Sensitivity simulation on the number of particle groups

Table 4.2 Settling velocities for group number sensitivity test

1 group	Particle group No.	1								
	Settling velocity (mm/s)	0.52								
	Mass fraction	1.00								

2 groups	Particle group No.	1	2							
	Settling velocity (mm/s)	0.38	0.66							
	Mass fraction	0.50	0.50							

5 groups	Particle group No.	1	2	3	4	5				
	Settling velocity (mm/s)	0.24	0.38	0.52	0.66	0.80				
	Mass fraction	0.20	0.20	0.20	0.20	0.20				

10 groups	Particle group No.	1	2	3	4	5	6	7	8	9	10
	Settling velocity (mm/s)	0.21	0.28	0.35	0.42	0.49	0.56	0.63	0.69	0.76	0.83
	Mass fraction	0.1	0.1	0.1	0.1	0.1	0.1	0.1	0.1	0.1	0.1

20 groups	Particle group No.	1	2	3	4	5	6	7	8	9	10
	Settling velocity (mm/s)	0.19	0.23	0.26	0.30	0.33	0.36	0.40	0.43	0.47	0.50
	Mass fraction	0.05	0.05	0.05	0.05	0.05	0.05	0.05	0.05	0.05	0.05
	Particle group No.	11	12	13	14	15	16	17	18	19	20
	Settling velocity (mm/s)	0.54	0.57	0.61	0.64	0.68	0.71	0.75	0.78	0.82	0.85
	Mass fraction	0.05	0.05	0.05	0.05	0.05	0.05	0.05	0.05	0.05	0.05

4.2.6 Tracer simulation method

The hydraulic regime of the settling tanks was assessed using a tracer simulation. A total tracer amount of 5.15×10^{-7} kg was introduced into the inlet (flow rate, Q=0.08 m^3/h) for a period of 1s (pulse input). The data for tracer concentrations at the outlet was recorded to plot a residence time distribution and calculated *F-curve*. The value of 0.1 from *F-curve* corresponds to the normalized time θ_{10}, indicating that 10% of the tracer was discharged at the outlet. The parameter of θ_{10} relates to the degree of short-circuiting (Stamou, 2002 [74] and Terashima et al.,2013 [75]). At larger values of θ_{10}, a smaller degree of short-circuiting occurs.

4.2.7 Calculation of SS removal efficiency from simulation results

From simulation results, the SS removal efficiency of the tank was evaluated as:

$$\eta = \frac{\sum_{i=1}^{10} C_{in}^{i} - \sum_{i=1}^{10} C_{out}^{i}}{\sum_{i=1}^{10} C_{in}^{i}} \tag{4.3}$$

The SS removal efficiency for each group of particles was calculated as:

$$\eta_i = \frac{C_{in}^{i} - C_{out}^{i}}{C_{in}^{i}} \tag{4.4}$$

where

η: SS removal efficiency of the tank (from 0 to 1)

η_i: SS removal efficiency of particle group i (from 0 to 1)

C_{in}^{i}: concentration of particle group i (from 1 to 10) at the inlet (mg/L)

C_{out}^{i}: concentration of particle group i (from 1 to 10) at the outlet (mg/L)

The ratio of increased settling area by inclined plates was:

$$\delta = \frac{A_b}{A_o} \tag{4.5}$$

Where

δ: increase in settling area

A_o: surface area in original settling tank ($0.02\times4=0.08$ m^2)

A_b: horizontal projection area of the inclined plate

$$(A_b = n_b \cdot W_b \cdot L_b \cdot \cos 60^\circ)\ (\mathrm{m}^2)$$

where

n_b: number of inclined plates in the lamella settling tank

W_b: width of inclined plates (m)

L_b: length of inclined plates (m)

Table 4.3 contains the values for δ in the lamella settlers.

Table 4.3 Increased settling area in tanks.

Tanks	A	B	C	D	E	F	G	H	I
δ	0	0.29	0.58	1.16	2.32	1.16	1.16	1.16	1.16

4.2.8 Definition and calculation of the effectiveness of baffle related to increasing flow rate

According to the theory of sedimentation [70][71], *LV* in the sedimentation tank is calculated as:

$$LV_o = \frac{Q}{A_o} \tag{4.6}$$

Similarly, *LV* in the lamella settling tank was calculated as:

$$LV_b = \frac{Q_b}{A_o + A_b} \tag{4.7}$$

At present, it is assumed that if LV_o is equal to LV_b, the SS removal efficiency will be unchanged. A coefficient for the effectiveness of baffles (α) reflects the actual effect of the inclined plates on attainable flow rate to maintain a constant SS removal efficiency. The value of α=1 indicated that the entire horizontal projected area provided by inclined plates contributed to the increased settling area in the lamella tank. On the other hand, the value of α=0 indicated that there was no impact from baffles, as shown in equation (4.8).

$$LV_b^* = \frac{Q_b^*}{A_o + \alpha \cdot A_b} \tag{4.8}$$

Then, the relationship between settling areas and flow rates will be described as:

$$\frac{Q_b^*}{Q_o} = \frac{A_o + \alpha \cdot A_b}{A_o} \tag{4.9}$$

or

$$\frac{\Delta Q}{Q_o} = \frac{\alpha \cdot A_b}{A_o} \tag{4.10}$$

where

LV_o: linear velocity in the original settling tank ($m^3/(m^2 \cdot h)$)

LV_b: linear velocity in the lamella settling tank in case α=1 ($m^3/(m^2 \cdot h)$)

LV_b^*: linear velocity in the lamella settling tank in case $\alpha \neq 1$ ($m^3/(m^2 \cdot h)$)

Q_o: flow rate in the original settling tank (m^3/h)

Q_b: theoretical attainable flow rate in the lamella settling tank (m^3/h)

Q^*_b: actual attainable flow rate in the lamella settling tank to maintain the same SS removal efficiency (m^3/h)

α: effectiveness of baffle related to increased flow rate (from 0 to 1).

ΔQ: incremental change of flow rate, equal to $Q^*_b - Q_o$ (m^3/h)

4.3. RESULTS AND DISCUSSION

4.3.1 Improvement on SS removal efficiency (η) due to increased settling area (δ) from inclined plates

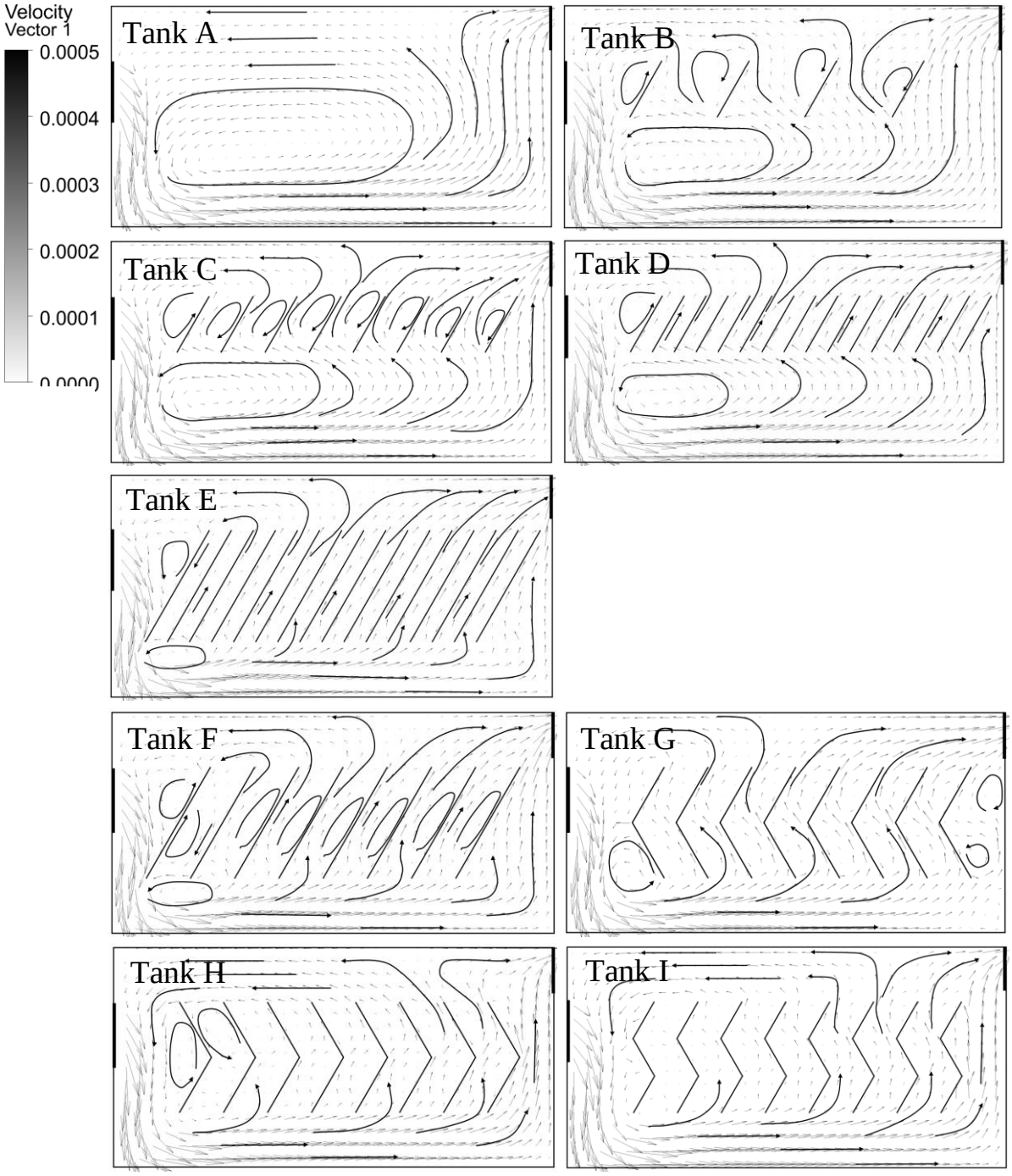

Fig 4.6 Vector of velocity for conventional tank and lamella settling tanks.

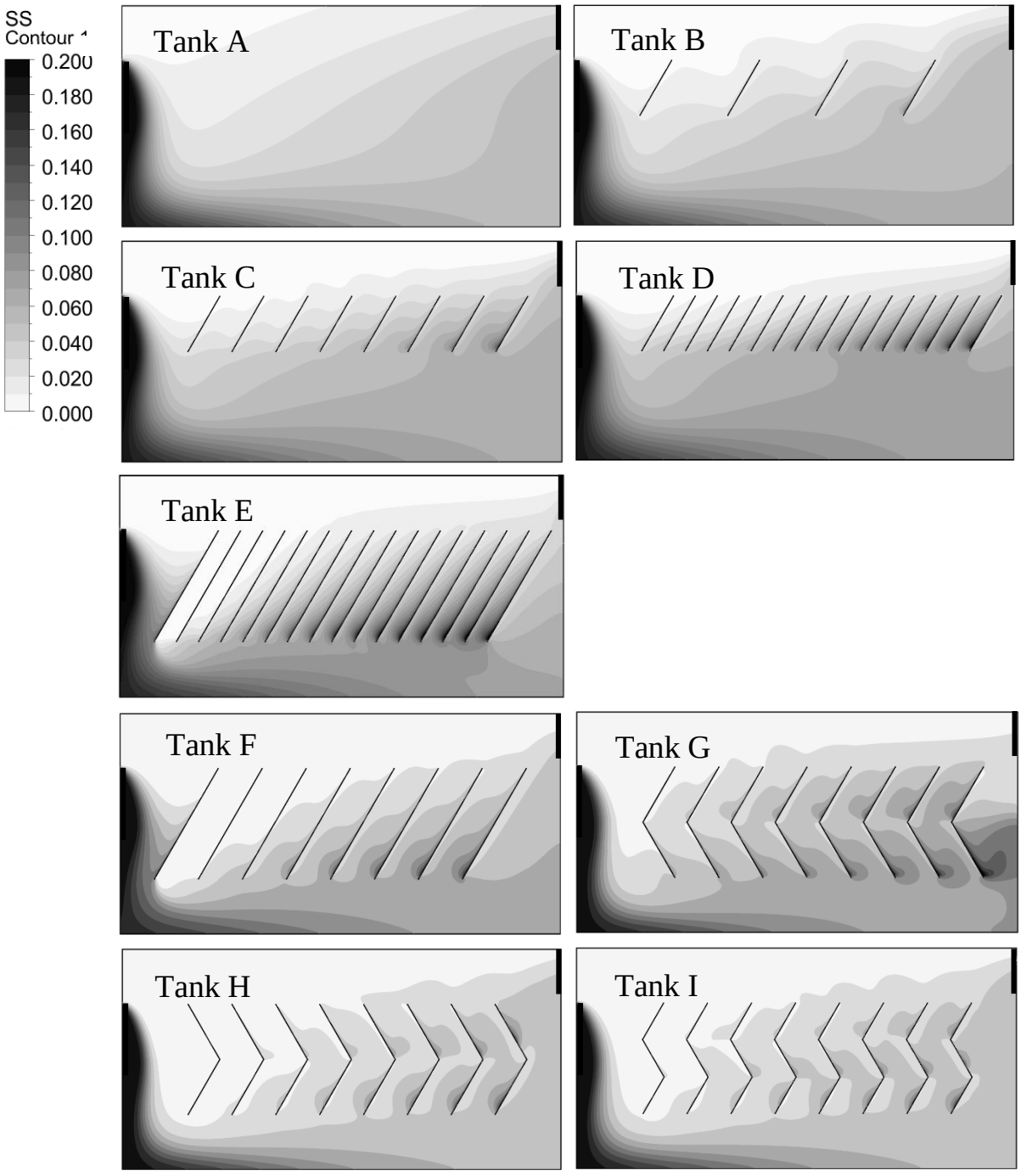

Fig 4.7 Contour of SS distribution for conventional tank and lamella settling tanks.

The velocity contour and SS distribution in the modelled tanks are shown in

Fig 4.6 and **Fig 4.7**. A large recirculation eddy area in the settling tank was observed. However, the vortex zones were reduced by half their size in lamella settlers and were located under the inclined plates. Some small vortex zones appeared between inclined plates in lamellas B and C and disappeared in lamellas D and E. The reduction of the vortex zone area in lamella settlers indicated an improvement in the hydraulic regime, as well as a more even upflow distribution among inclined plates. Furthermore, when the spacing between baffles was reduced, e.g., by 0.2 m, a higher concentration of SS was found on the baffles. This suggested that smaller spacing between plates played a role in retaining solids in the tanks. For similarly spaced plates, a clear improvement on the hydraulic pattern was observed in lamella E compared to lamella D. This was attributed to the plate length being doubled, and therefore a higher δ in lamella E. From lamella settlers B to E, larger clear water zones were observed, indicating that a better SS removal efficiency was achieved. For lamella settlers of the same settling area, such as tanks D, F, G, H and I, a modification of the baffle configuration influenced the flow pattern in the tanks. The highest retained SS was observed in tank G, as the hydraulic regime was favourable for SS removal. However, in tanks H and I, the flow patterns were identical to those of conventional settling tanks. As a result, the performance of these tanks was comparable. In tanks D and F, as the types of baffles were the same, the flow patterns were similar.

From the visualization of modelling results, it could be concluded that the number of baffles and their configuration and spacing influenced the SS removal efficiency to different extents. Therefore, the design of lamella settlers should focus on these parameters to optimize SS removal.

In the simulation, the flow rate was varied from 0.08 to 0.16 m^3/h. The influence of inclined plates to SS removal efficiency on each group of particles was investigated.

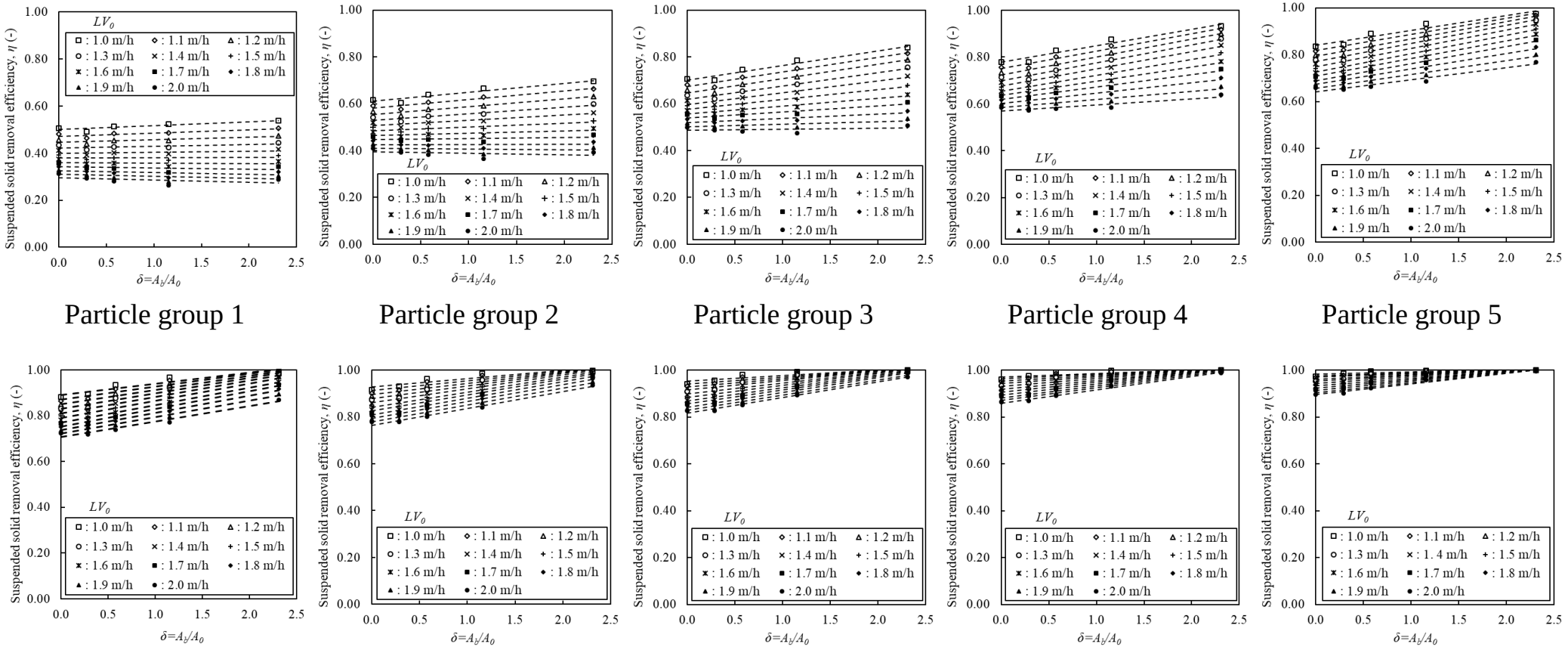

Particle group 1 | Particle group 2 | Particle group 3 | Particle group 4 | Particle group 5

Particle group 6 | Particle group 7 | Particle group 8 | Particle group 9 | Particle group 10

Fig 4.8 SS removal efficiency for each particle group.

In general, the more baffles installed (increased δ), the better the SS removal efficiency achieved for each particle group (η_i). As seen in **Fig 4.10**, for particle groups with small settling velocities (particle group 1, *SV*=0.21 mm/s), inclined plates were thought to have little impact on SS removal efficiency.

At a constant flow rate, as δ increased from 0 to 2.32, the largest improvement on SS removal efficiency was observed for particle groups 3 to 8 (*SV*=0.35 to 0.69 mm/s), at values of 12 and 8%. For particle groups 9 and 10 (*SV*=0.76 to 0.83 mm/s), no significant enhancement of SS removal efficiency was achieved due to the high inherent settling capacity of these particles.

On the other hand, at a constant δ, when the flow rate increased from 0.08 to 0.16 m^3/h, the SS removal efficiency was reduced for all particle groups. Specifically, for particle groups from 2 to 6 (*SV*=0.28 to 0.56 mm/s), the reduction of SS removal efficiency was similar in all studied tanks at about 20%. However, for particles groups 7 to 10 (*SV*=0.63 to 0.83 mm/s), the largest reduction of 10% was recorded, and the smallest between 1-5% was observed in lamella E. It suggests that particles of higher *SV* can be easily removed in lamella settling tanks without much influence from the flow rate.

Overall, a linear relationship between η and increased δ was observed. At a constant flow rate, by increasing δ from 0 to 2.32, η was increased up to a maximum 0.1 times. On the other hand, at a constant δ, represented by a defined value of δ, when the flow rate was doubled from 0.08 to 0.16 m^3/h, η was reduced to an average value of 0.18. It was suggested that η was more sensitive to flow rate than δ.

4.3.2 Relationship between increased flow rate and increased δ by inclined plates

As a theoretical calculation, a similar proportional increase and/or decrease of flow rate and settling area will result in the same SS removal efficiency. The equation relating the ratio of increment and initial flow rate $\lambda=\Delta Q/Q_0$, and

increased δ by inclined plates was presented by the linear equation $\lambda=\delta$.

As mentioned in section 2.4, *LV* in settling tank design was selected in the range of 1 to 2 $m^3/(m^2 \cdot h)$. In the CFD simulation, at the initial *LV* and flow rate values of 1 m/h and 0.08 m^3/h, respectively, the SS removal efficiency η was observed to be 0.82 in the settling tank. Consequently, the targeted SS removal efficiency η=0.82 was selected to investigate the effects of baffles on the attainable flow rate for the studied lamella settlers.

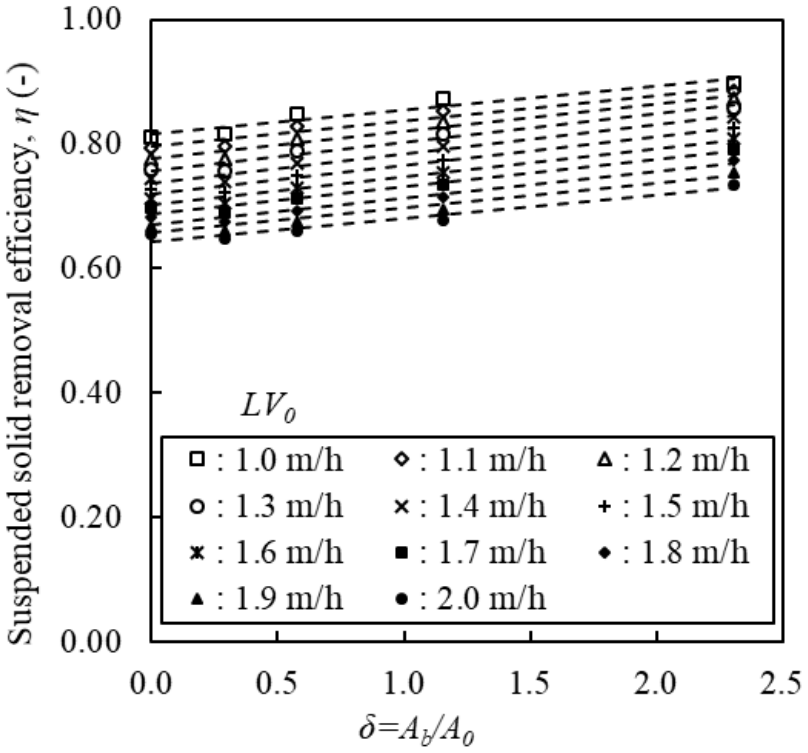

Fig 4.9 Relationship between total SS removal efficiency and δ increase.

From the results in **Fig 4.9**, the horizontal line λ=0.82 was plotted, and intersections with the other linear curves represented different values of flow rates corresponding to an increase in δ. Then, the relationship between λ and increased δ was plotted in **Fig 4.10**.

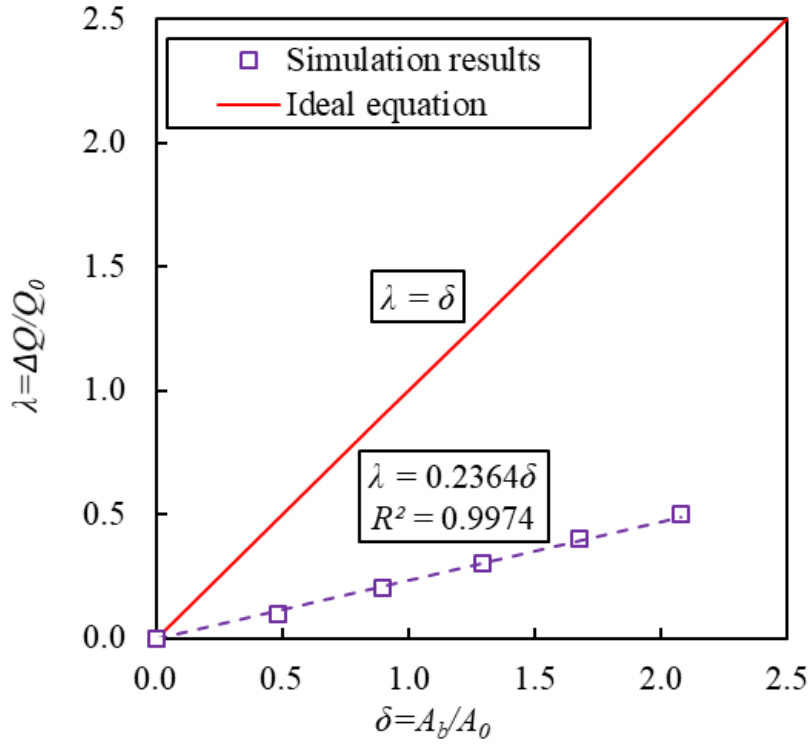

Fig 4.10 Relationship between increased flow rate and δ at η=0.82.

As seen in the figure, to maintain the same SS removal efficiency η=0.82, the ratio of λ/δ is 0.2364 (P-value <0.05), indicating that an increase in δ to 2.1-fold corresponded to an attainable flow rate of 1.5-fold. A significant difference between the ideal statement and simulation results was observed. This indicates that the application of the ideal equation (4.7) might provoke an erroneous prediction on η.

In the design of a sedimentation unit, a specific group of particles represented by *SV* will be selected as targets for removal. As an example, particle group 6 (*SV*=0.5 mm/s) was chosen at the desired SS removal efficiency of 89%. Applying a similar approach as above, the curve λ- δ was plotted in **Fig 4.11** for particle group 6. A higher performance on SS removal efficiency was observed. Specifically, δ needed to be increased by 2.04-fold in order to attain 1.8-fold of increased flow rate. This indicated that SS with varying *SV* would be influenced differently in the interrelation between λ and δ.

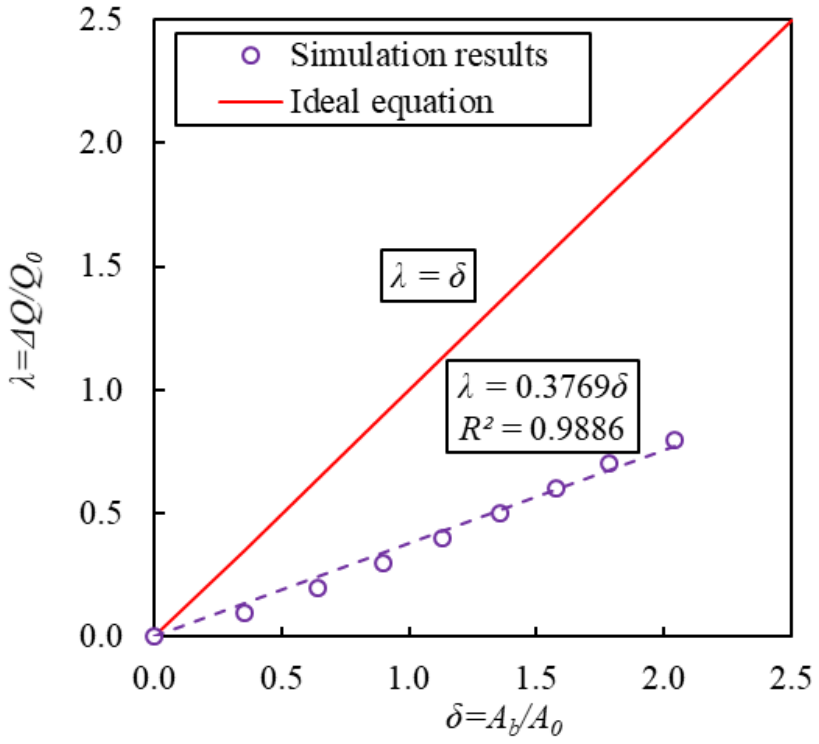

Fig 4.11 Relationship between increased flow rate and δ at η=0.89 for particle group 6.

The findings allowed the designers of lamella settlers to correctly select the targeted SS removal efficiency in terms of overall and/or specific particle groups.

The actual effects of inclined plates on attainable flow rate, represented by coefficient α, will be examined in the next section.

4.3.3 Effectiveness of inclined plates to increased flow rate at SS removal efficiency η=0.82

From **Fig 4.10** and equation (4.10), the effectiveness of baffles (α) could be determined from values of increased δ and $\lambda=\Delta Q/Q_0$. The mismatch of increase and/or decrease for flow rate and δ in maintaining the same η highlighted the small contribution of baffles on an increased flow rate. The effectiveness of baffles was estimated at only 23.64% (α=0.2364), which was significantly lower compared to the ideal value of α=1.

Specifically, the effectiveness of baffles on particle group 6 (*SV*=0.5 mm/s) is shown in **Fig 4.11** to be higher than the overall result that is shown in **Fig 4.10**. The SS removal efficiency reached 89%, and the value of α was 37.69% (α=0.3769). It can be concluded that the effectiveness of baffles was different for each particle group. In the operational condition, when particle characterization in the influent varied with time, the effectiveness of baffles on each particle would be useful in predicting the performance of a lamella settling tank.

4.3.4 Tracer simulation results

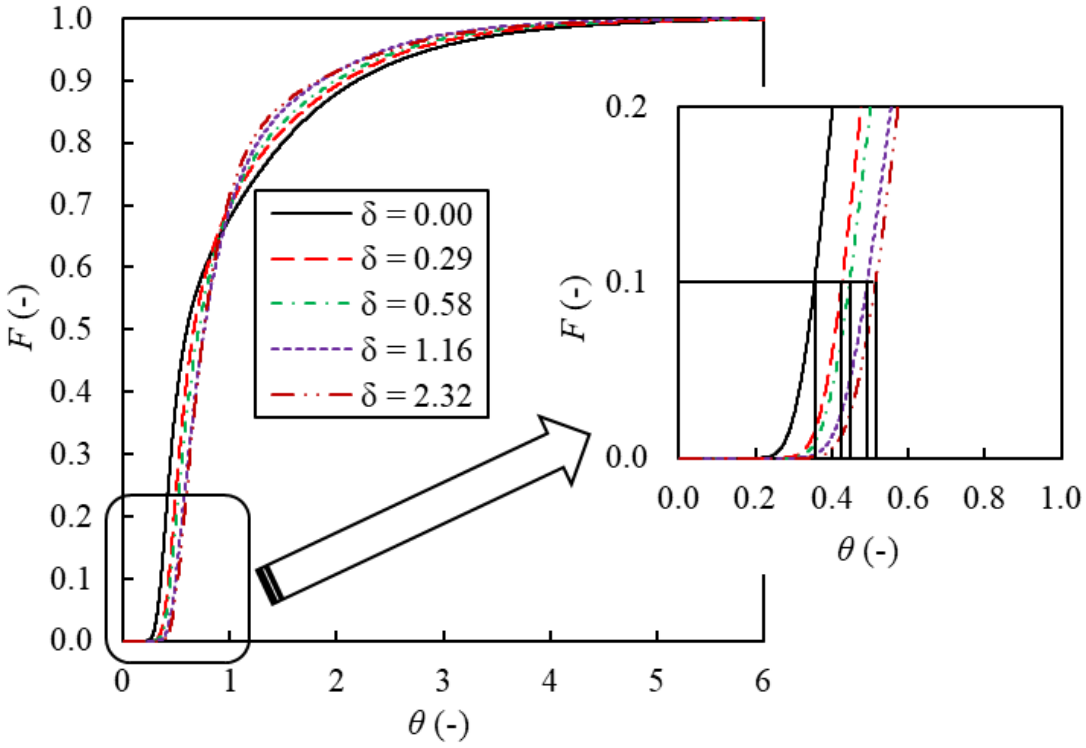

Fig 4.12 Calculated *F*-curve for tanks

From the results in **Fig 4.12**, the θ_{10} increased from 0.35 in tank A to 0.51 in tank E. The smaller value of θ_{10} indicated that short-circuiting could be reduced in the lamella settling tank. The baffles helped to improve the hydraulics in the lamella tank, leading to the enhancement of the settling process and SS removal efficiency.

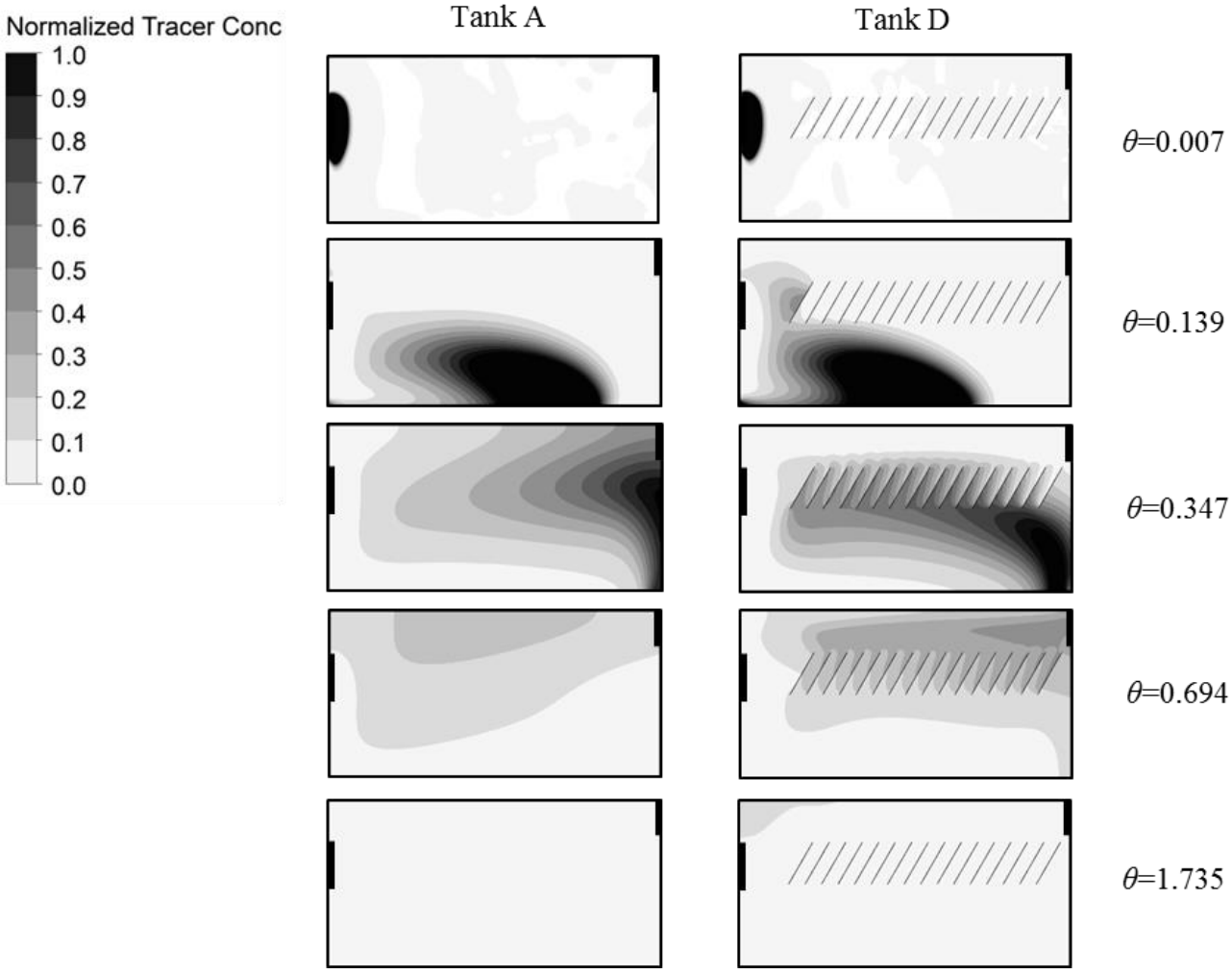

Fig 4.13 Tracer distribution in Tank A and Tank D

The distributions of tracer in tanks A and D are illustrated in **Fig 4.13**. In the period from $\theta = 0.007$ to 0.139, the distribution of the tracer was similar in the two tanks. However, at $\theta = 0.347$, the tracer reached the outlet in tank A but not in tank D. This is depicted in the figure where part of the tracer in tank A was discharged at the outlet. The longer residence time of the tracer in the lamella settling tank was the factor contributing to the high SS removal efficiency. Consequently, the SS removal efficiency in the lamella settling tank was higher compared to the one in the conventional setting tank.

4.3.5 Comparison on SS removal efficiency due to baffles configuration

The impacts of baffle configuration on SS removal efficiency were simulated. Five different types of baffles providing identical increased settling areas are introduced in **Fig 4.14**. The results show that tank G had the highest SS removal efficiency performance from 0.90 to 0.73, as the *LV* increased from 1 to 2 $m^3/(m^2 \cdot h)$. Under the same conditions, the lowest SS removal efficiency from 0.82 to 0.66 was observed in tanks H and I. In tanks D and F, there was no significant difference in performance. This was attributed to a similar baffle configuration and arrangement.

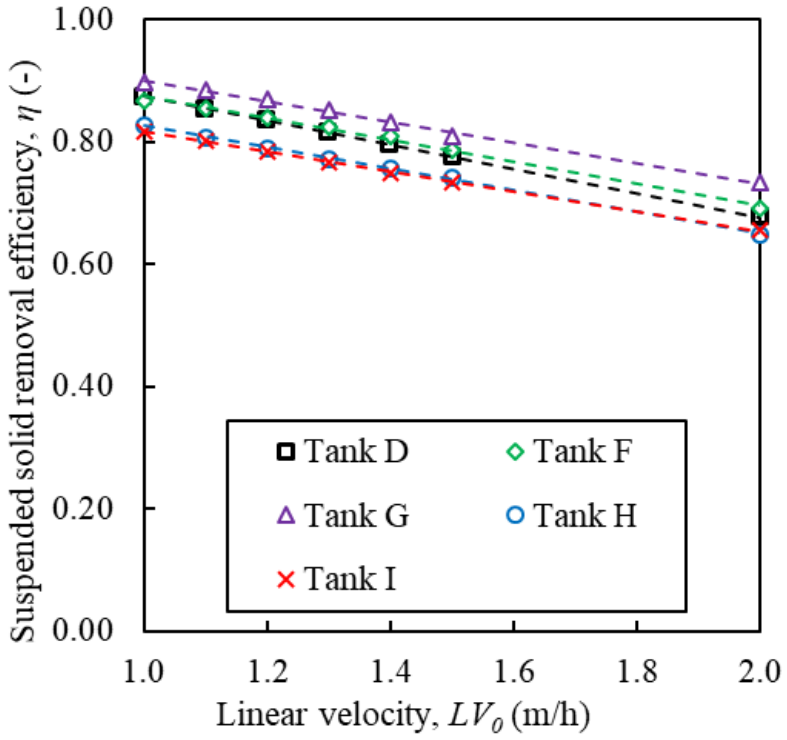

Fig 4.14 Relationship between SS removal efficiency and *LV*.

Interestingly, when identical baffle types were introduced at opposite positions, the SS removal efficiency in tank G was 10% higher than that of tank H. It indicated that the different flow patterns led to a variation in tank performance.

Consequently, SS removal efficiency in the lamella settlers depends on increased δ, baffle configuration, and flow pattern. These aspects should be taken into consideration in the optimization of lamella settling tanks.

In this study, it was assumed that all particles settled discretely. However, several researchers [53][20] suggested that the vortex in settling tanks might provoke the interaction and agglomeration among particles.

Further, the influences of some other parameters, such as a variation in tank depth and temperature, were not investigated. It is advised that future simulations consider these parameters to reflect the actual profile of lamella settling tanks better.

4.4. CONCLUSION

The study investigated the effectiveness of inclined plates in lamella settlers on attainable flow rate at constant SS removal efficiency. Simulation results revealed that baffles had different effects on the SS removal efficiency in each particle group, depending on the flow rate and *SV*, which might be difficult to characterize experimentally. Contradictory to the theoretical calculation, simulation results revealed a large difference in the proportion of increase and/or decrease in flow rate and settling area to maintaining the targeted SS removal efficiency. At the targeted SS removal efficiency of η=0.82, the increase of δ by 2.1-fold allowed the attainable flow rate to be increased 1.5-fold. The actual effectiveness of baffles on the increased flow rate was estimated to be 0.2364, significantly lower than the ideal value of α=1. The baffle configuration also proved to influence the flow pattern and, therefore, the SS removal efficiency of the tanks. Computational fluid dynamics modelling is useful in describing the profile of solid particles and can be effectively used to visualize the sedimentation process in the studied objects in reasonable simulation time. The computational fluid dynamics modelling can be used to accurately predict the SS removal efficiency in settling tanks and lamella settling tanks, and therefore can be used to optimize their design.

References

[5] W. F. Leung, “Lamella and Tube Settlers. 2. Flow Stability,” *Ind. Eng. Chem. Process Des. Dev.*, vol. 22, no. 1, pp. 68–73, 1983.

[6] A. Demir, “Determination of settling efficiency and optimum plate angle for plated settling tanks,” *Water Res.*, vol. 29, no. 2, pp. 611–616, 1995.

[7] K. Fujisaki and M. Terashi, “Improvement of settling tank performance using inclined tube settlers,” vol. 80, pp. 475–484, 2005.

[16] A. I. Stamou, E. W. Adams, and W. Rodi, “Modélisation numérique de l’écoulement et de la sedimentation dans des bassins de décantation primaires de forme rectangulaire,” *J. Hydraul. Res.*, vol. 27, no. 5, pp. 665–682, 1989.

[20] K. Ramalingam *et al.*, “Critical modeling parameters identified for 3D CFD modeling of rectangular final settling tanks for New York City wastewater treatment plants,” *Water Sci. Technol.*, vol. 65, no. 6, pp. 1087–1094, 2012.

[22] W. P. Kowalski, “The method of calculations of the sedimentation efficiency in tanks with lamella packets,” *Arch. Hydroengineering Environ. Mech.*, vol. 51, no. 4, pp. 371–385, 2004.

[24] R. Tarpagkou and A. Pantokratoras, “The influence of lamellar settler in sedimentation tanks for potable water treatment - A computational fluid dynamic study,” *Powder Technol.*, vol. 268, pp. 139–149, 2014.

[42] K. Mohanarangam and D. Stephens, “Cfd Modelling of Floating and Settling Phases in Settling Tanks,” *Victoria*, no. December, pp. 1–7, 2009.

[44] A. M. Goula, M. Kostoglou, T. D. Karapantsios, and A. I. Zouboulis, “A CFD methodology for the design of sedimentation tanks in potable water treatment. Case study: The influence of a feed flow control baffle,” *Chem. Eng. J.*, vol. 140, no. 1–3, pp. 110–121, 2008.

[51] H. Asgharzadeh, B. Firoozabadi, and H. Afshin, “Experimental investigation of effects of baffle configurations on the performance of a secondary sedimentation tank,” *Sci. Iran.*, vol. 18, no. 4 B, pp. 938–949, 2011.

[52] M. Shahrokhi and F. Rostami, “The Computational Modeling of Baffle Configuration in the Primary Sedimentation Tanks,” *Flow3D2.Propagation.Net*, vol. 6, pp. 392–396, 2011.

[53] M. Gong *et al.*, “Development of a flocculation sub-model for a 3-D CFD model based on rectangular settling tanks,” *Water Sci. Technol.*, vol. 63, no. 2, pp. 213–219, 2011.

[55] M. M. Heydari, M. S. Bajestan, H. A. Kashkuli, and H. Sedghi, “The effect angle of baffle on the performance of settling basin,” *World Appl. Sci. J.*, vol. 21, no. 6, pp. 829–837, 2013.

[64] Ghawi, “Application of Computational Fluid Dynamics modelling to a horizontal sedimentation tank,” no. April, 2017.

[70] Degrémont, *Water treatment handbook*, 7th edition. France, 2007.

[71] I. Metcalf and Eddy, *Wastewater Engineering: Treatment and Reuse*, Fourth edition. New York, USA: Mc Gram-Hill, 2003.

[72] Ghawi and J. Kri, “A Computational Fluid Dynamics Model of Flow and Settling in Sedimentation Tanks,” *Appl. Comput. Fluid Dyn.*, 2012.

[73] Japan Sewage Works Association, *Design Standard for Municipal Wastewater Treatment Plants*. Tokyo, Japan: Japan Sewage Works Association, 2013.

[74] A. I. Stamou, “Verification and application of a mathematical model for the assessment of the effect of guiding walls on the hydraulic efficiency of chlorination tanks,” *J. Hydroinformatics*, vol. 4, no. 4, pp. 245–254, 2002.

[75] M. Terashima, M. Iwasaki, H. Yasui, R. Goel, K. Suto, and C. Inoue, “Tracer experiment and RTD analysis of DAF separator with bar-type baffles,” *Water Sci. Technol.*, vol. 67, no. 5, pp. 942–947, 2013.

CHAPTER 5 IMPROVEMENT OF SUSPENDED SOLIDS REMOVAL EFFICIENCY IN SEDIMENTATION TANKS BY INCREASING SETTLING AREA USING COMPUTATIONAL FLUID DYNAMICS

5.1. INTRODUCTION

The sedimentation tank plays an important role in water and wastewater treatment systems by settling suspended particles using gravity. The effective performance of the settling tank contributes largely to the reduction of suspended solids (SS), which is an important parameter in the wastewater quality index. However, the low settling velocity (*SV*) desired in the settling tank requires a large surface area, which might be difficult in restricted areas. An effective way to increase the settling tanks' performance is to introduce inclined plates to increase the settling area and improve the hydraulic regime. Extensive research on the performance and optimization of inclined plates, as well as the mechanism of the sedimentation process in lamella settlers, were carried out. Demir [6] investigated the optimum angle of the baffle in the lamellar settling tank at various linear velocities. Kowalski [22] compared the SS removal efficiency in the conventional tank and the lamella settling tank taking into account the density, viscosity, and mass fraction of solid particles. Different types of tube settlers were examined by Fujisaki and Terashi [7] to obtain a higher solid separation capacity. Leung [5] studied the distribution of three-layer, stratified viscous channel flow between inclined plates. The above-mentioned studies successfully predicted the SS removal efficiency in lamella settling tanks.

Theoretically speaking, in the design of lamella settlers, a large assumption was made on the effectiveness of baffles, in which the entire horizontal projected area of inclined plates was considered to be involved in increasing

the settling area in lamella settling tanks. Moreover, SS removal efficiency was assumed to be constant if the increase and/or decrease of settling area and flow rate were proportional [70], [71], because other factors such as vortex and density current have been considered as non-impacting ones. However, in the practical operation of lamella settlers, such factors should be taken into account as contributors to the SS removal efficiency. In experimental conditions, it is a big challenge to evaluate all factors affecting the settling process; that is the reason why the application of simulation is essential in the evaluation of the whole process.

Many studies have focused on the hydraulic regime in the settling tank. For example, in 1989, Stamou [16] used a numerical model to study the flow and settling process of SS in primary sedimentation tanks and compared the simulation results to those from the theoretical method. Goula [44] evaluated the impacts of baffles in the inlet zone on the distribution of flow patterns and the influence of SS mass fraction on their removal efficiency.

The application of computational fluid dynamics (CFD) to simulate the settling process has been widely accepted due to its visualization capabilities and data on the hydraulic regime under different conditions of geometry and flow pattern, density and vortex zone, mass fraction and settling velocity of particles. Asgharzadeh [51]and Shahrokhi [52] investigated the reduction of dead zones and recirculation zones in cases where a different number of baffles was installed at the bottom of the tank. Similarly, Heydari [55] conducted simulations on the angle of the baffle at the bottom of the settling tank to reduce the vortex zone. Ghawi and Kriš [72] developed a complex CFD model to estimate the factors that impact deposition efficiency. Tarpagkou [24] proved that inclined plates improved the hydraulic regime by simulating a full-scale system, rather than a part of the system as in previous research. Nguyen [76] assessed the influence of inclined plates on attainable flow rate of the lamella settling tank, in which particle group with a removal efficiency of 89% in the original settling tank was selected to calculate the effectiveness of inclined plates (α). The results showed that the effectiveness

of inclined plates to attainable flow rate was significantly lower than the theoretical value.

As mentioned above, the overall performance of the tank could be improved if the separation of small particle groups were enhanced.

From equation (4.1), the settling area needs to be increased to reduce LV_o while keeping Q_o constant. Three options are proposed to increase the settling area as follows:

- Increasing number of inclined plates
- Increasing the length of the tank
- Increasing the width of the tank

According to the ideal equation (4.2), in case the increased settling area is equal, the SS removal efficiency would be the same in the cases as mentioned above.

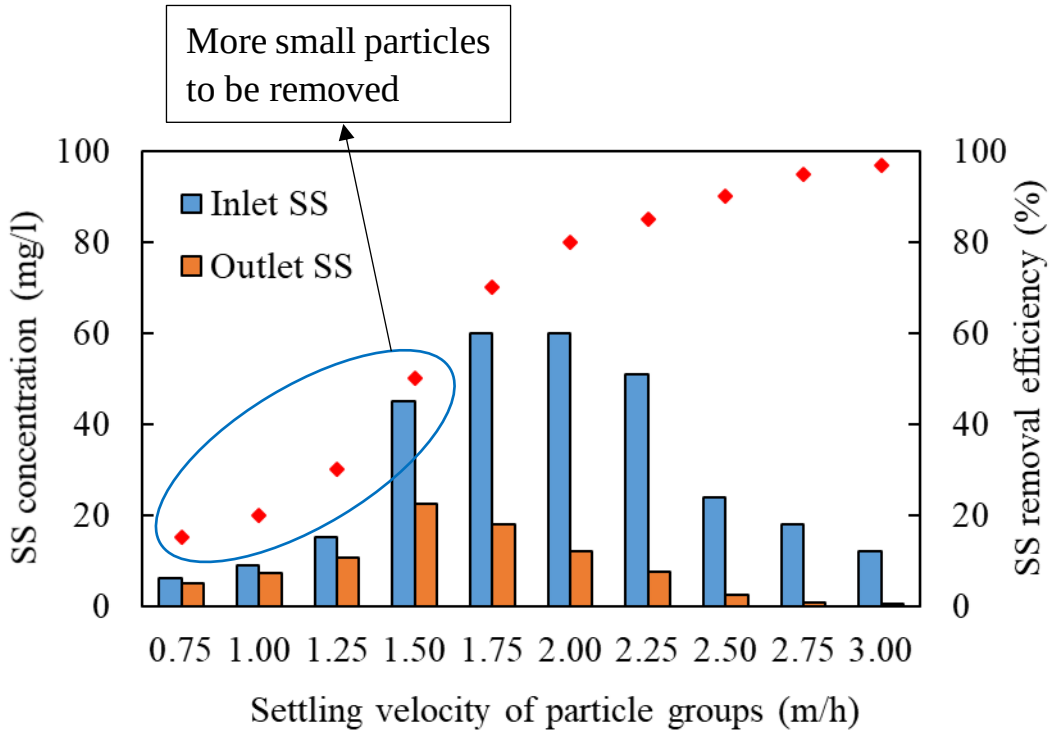

Fig 5.1 SS removal efficiency in the sedimentation tank

In this chapter, the CFD model is applied to simulate the effect of an increased

settling area to improve the SS removal efficiency of small groups in sedimentation tanks, which aimed to increase the overall performance of the tank. The research was carried out with several tank configurations. The research results help the designer to have a solution to improving performance in sedimentation tanks.

5.2. MATERIALS AND METHODS

5.2.1 Numerical modelling methods

The Algebraic Slip Model was selected for simulation of the velocity profile and the concentration distribution of SS. Each dispersed component is represented by a mass fraction equation, and a relative movement is allowed between these components in the continuous phase [42]. Turbulence in the liquid phase was modelled using the k-ε model, which successfully simulated the sedimentation tank in previous studies [64]. The hydrodynamic and flow behavior in the sedimentation tanks were modelled in two dimensions. In this study, the commercial software CFX 18.0 (in ANSYS) was used to perform CFD modelling. The hexahedral meshes were generated by ANSYS meshing for numerical calculations.

5.2.2 Model geometry

The study was conducted with three types of configuration:
In the first type of configuration: The settling tank size is maintained ($H \times W \times L$ = 2×0.02×4 m) with the increased settling area by increasing the number of inclined plates in the tank. The number of 4, 8 and 16 inclined plates of the same configuration were installed at a 60^o angle, which was widely applied in lamella settler design to obtain self-cleaning and high removal efficiency [71], in tanks B, C, and D respectively; longitudinal depth of 0.5 m; and spacing of 0.8, 0.4, and 0.2 m, respectively. Print tank E, 16 baffles at a longitudinal depth of 1 m, were introduced at 0.2 m apart.
In the second type of configuration: The width and height of the tank remain the same with original settling tank A ($H \times W$ = 2×0.02 m), the settling area is increased by increasing the length (L) of the tank from 4 to 5.2, 6.3, 8.6, and 13.2 m in tanks F, G, H and I respectively.
In the third type of configuration: The tank size was the same as in the settling tank A ($H \times W \times L$ = 2×0.02×4 m), the settling area is increased by raising the number of tanks from 1 to 3.32 tanks, which corresponded to the settling area

(δ) increased from 0 to 2.32. The flow rate into each tank was decreased from 1 to 3.32 times. The CFD modeling of this configuration was equivalent to the simulation of a settling tank with the width (W) increased.

Here, a different configuration was used, as shown in **Fig 5.2** and **Fig 5.3.**

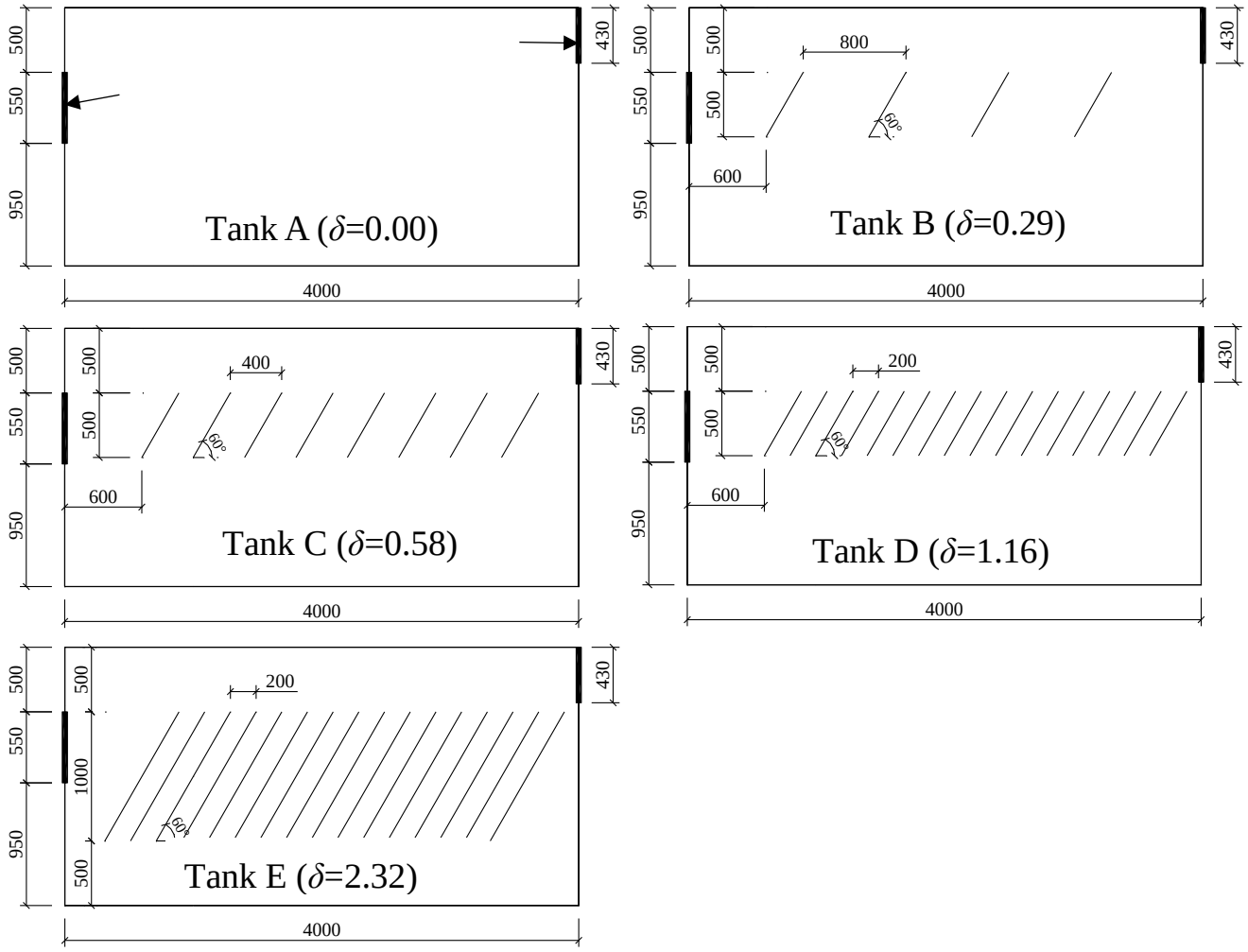

Fig 5.2 Cross section of settling tank and lamella settling tanks.

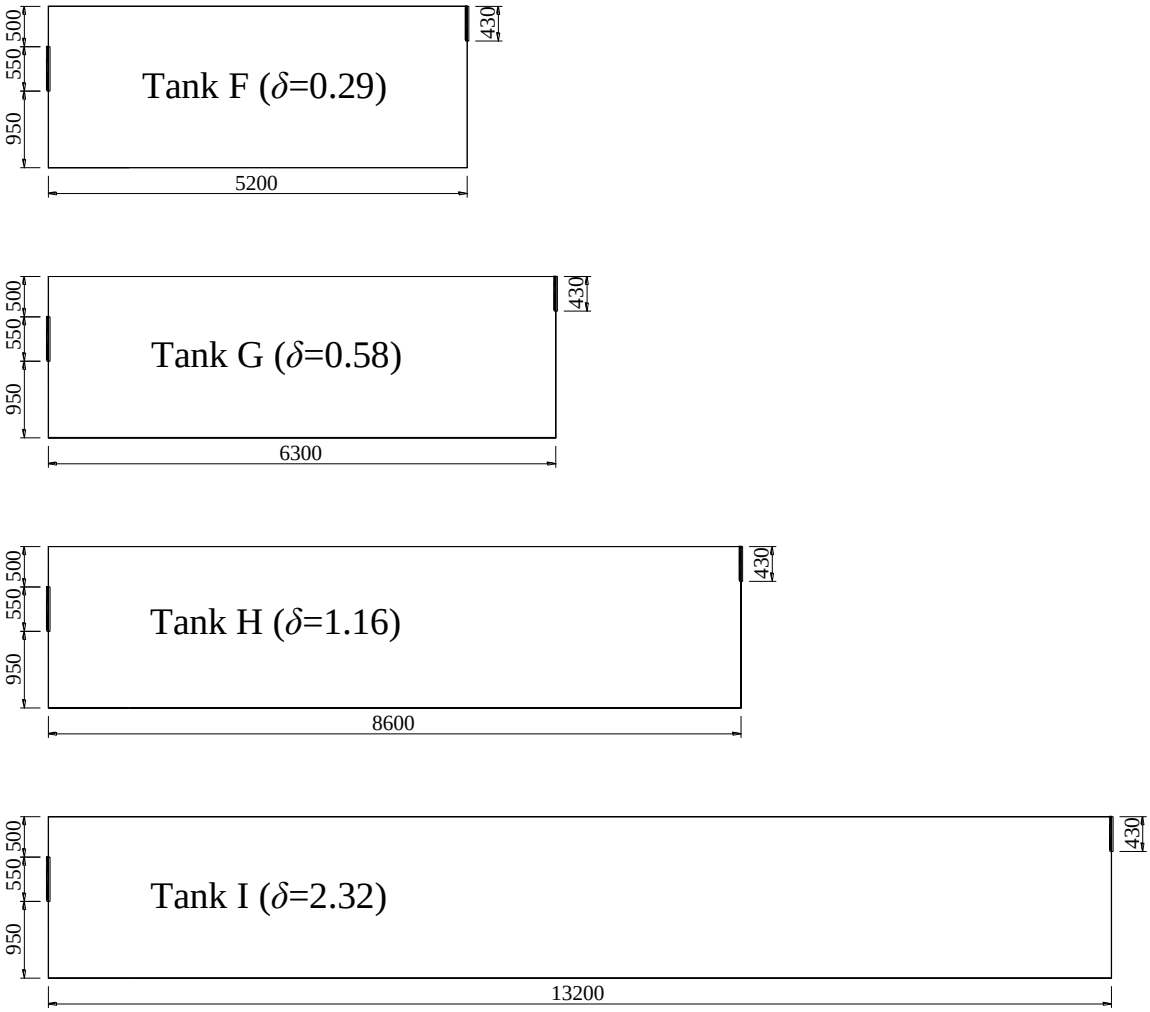

Fig 5.3 Cross section of settling tanks.

5.2.3 Boundary condition

In sedimentation tank design, the *LV* commonly selected is between 1 and 2 $m^3/(m^2 \cdot h)$ [73]. Therefore, in this study, a primary sedimentation unit located in the wastewater treatment process was simulated under the original *LV* of 1 $m^3/(m^2 \cdot h)$, inlet 200 mg-SS/L, water density 998 kg/m^3 and particle density of 1020 kg/m^3.

In the model, the mass flow rate was selected at both the inlet and outlet. No slip wall was set for the bottom, the wall, or the baffles. The water-surface was best defined by the VOF method in some studies [66] [67], in case of simulating the complicated surface between two fluids (air and water). In this study, the surface was almost flat and simple, so the free slip wall was selected to set up the surface boundary condition. The water surface was assumed to be horizontal in the tank, which was also widely applied for simulation of settling tanks in previous research [68] [24] [25]. The particles were set to be deposited only at the bottom, not on the wall or baffles.

The transient-type simulations were selected in this study. The initial time step was set at 5 seconds for the adaptive option in all calculations. For the numerical method, the advection scheme was upwind, and the transient scheme was set as second-order backward Euler.

5.2.4 Selection of appropriate mesh size

In order to check the mesh sensitivity, different mesh sizes ranging from 5-80 mm, corresponding to 324,538 and 1,857 number of elements (**Table 5.1**), were used to simulate SS removal efficiency in lamella D (δ = 1.16). By enlarging the mesh size, SS removal efficiency decreased from 88 to 79% according to the results. At mesh sizes of 5, 10, and 20 mm, SS removal efficiencies were similar. Consequently, the 20 mm-mesh size was selected for conducting subsequent simulations, assuring to provide accurate results and reasonable simulation time.

Table 5.1 Simulation results for the mesh sensitivity

	Mesh size 1 (5 mm)	Mesh size 2 (10 mm)	Mesh size 3 (20 mm)	Mesh size 4 (40 mm)	Mesh size 5 (80 mm)
Nodes	651,364	164,230	41,682	10,362	3,888
Elements	324,538	81,532	20,550	5,035	1,857
SS removal efficiency (%)	87.82	87.79	87.16	83.16	79.09
Difference	0.00	0.03	0.75	5.31	9.94

5.2.5 Selection of appropriate groups of particles

In the CFD model, SS particles in the influent were grouped and represented by average settling velocities for simplification in **Table 5.2**. To verify the sensitivity of group numbers, the simulation of SS removal efficiency of lamella D (δ = 1.16) was conducted using different particle groups ranging from 1 to 20. By increasing particle groups, the SS removal efficiencies decreased from 95 to 87%. The groups from 10 to 20 provided results without much difference. Hence, 10 groups of particles were used for the following simulations.

Table 5.2 Settling velocities for group number sensitivity test.

1 group	Particle group No.	1								
	Settling velocity (m/h)	1.88								
	Mass fraction	1.00								

2 groups	Particle group No.	1	2							
	Settling velocity (m/h)	1.38	2.38							
	Mass fraction	0.50	0.50							

5 groups	Particle group No.	1	2	3	4	5				
	Settling velocity (m/h)	0.88	1.38	1.88	2.38	2.88				
	Mass fraction	0.20	0.20	0.20	0.20	0.20				

10 groups	Particle group No.	1	2	3	4	5	6	7	8	9	10
	Settling velocity (m/h)	0.75	1.00	1.25	1.50	1.75	2.00	2.25	2.50	2.75	3.00
	Mass fraction	0.1	0.1	0.1	0.1	0.1	0.1	0.1	0.1	0.1	0.1

20 groups	Particle group No.	1	2	3	4	5	6	7	8	9	10
	Settling velocity (m/h)	0.69	0.81	0.94	1.06	1.19	1.31	1.44	1.56	1.69	1.81
	Mass fraction	0.05	0.05	0.05	0.05	0.05	0.05	0.05	0.05	0.05	0.05
	Particle group No.	11	12	13	14	15	16	17	18	19	20
	Settling velocity (m/h)	1.94	2.06	2.19	2.31	2.44	2.56	2.69	2.81	2.94	3.06
	Mass fraction	0.05	0.05	0.05	0.05	0.05	0.05	0.05	0.05	0.05	0.05

5.2.6 Calculation of SS removal efficiency from simulation results

The SS removal efficiency for each group of particles was calculated as:

$$\eta_i = \frac{C_{in}^i - C_{out}^i}{C_{in}^i} \tag{5.1}$$

where

η_i : SS removal efficiency of particle group i (from 0 to 1)

C_{in}^i : concentration of particle group i (from 1 to 10) at the inlet (mg/L)

C_{out}^i : concentration of particle group i (from 1 to 10) at the outlet (mg/L)

The settling area in a settling tank

$$A = A_o + A_\delta$$

$A_\delta = A_b$ or A_L or A_W

where

A: total settling area in the settling tank (m^2)

A_o: surface area in the original settling tank ($W \times L = 0.02 \times 4 = 0.08$ m^2)

A_δ: increased settling area by installing inclined plates or increasing the length of the tanks or increasing the width of the tanks as shown in **Fig 5.4**

A_b: horizontal projection area of the inclined plate ($A_b = n_b \times W_b \times L_p$) ($m^2$)

A_L: increased surface area by increasing the length of the tank ($A_L = L_\delta \times W$) (m^2)

A_W: increased surface area by increasing the width of the tank

$$(A_W = L \times W_\delta)\ (\mathrm{m}^2)$$

where

n_b: number of inclined plates in the lamella settling tank

W: width of the original settling tank (m)

W_b: width of the inclined plate (m)

W_δ: increased width of the tank (m)

L: length of the original settling tank (m)

L_p: horizontal projection length of the inclined plate

$$(L_p = L_b \times \cos 60^\circ)\ (\mathrm{m})$$

L_b: length of the inclined plate (m)

L_δ: increased length of the tank (m)

The ratio of increased settling area was:

$$\delta = \frac{A_\delta}{A_o} \tag{5.2}$$

where

δ: increased settling area

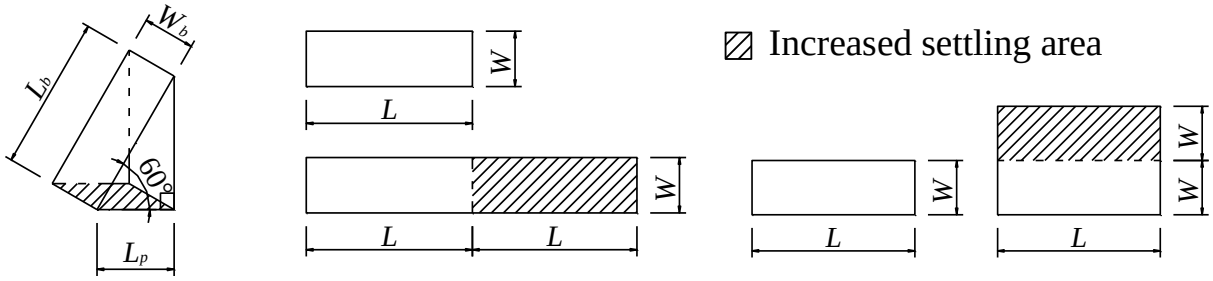

a) 3D view of inclined plate

b) Top view of settling tank with increasing the length

c) Top view of settling tank with increasing the width

Fig 5.4 The increased settling area of settling tank and lamella settling tanks.

5.2.7 Definition and calculation of the effectiveness of increased settling area related to ratio SV_{90}/LV_0 (ψ_{90})

According to the theory of sedimentation [70], [71], LV in the sedimentation tank is calculated as:

$$LV_o = \frac{Q_o}{A_o} \tag{5.3}$$

Similarly, LV in the lamella settling tank and settling tank when increased δ was ideally calculated as:

$$LV_i = \frac{Q_o}{A_o + A_\delta} \tag{5.4}$$

Ideally, it is assumed that when ratio SV_i/LV_i is constant, the η of the particle group will be unchanged. When 90% removal efficiency was considered [76], the settling velocity, with which the particle had the η of 90%, in the original settling tank was defined as $SV_{90\text{-}o}$.

$$\frac{SV_{90-o}}{LV_o} = \frac{SV_{90-i}}{LV_i} \tag{5.5}$$

or

$$SV_{90-i} = \frac{A_o \times SV_{90-o}}{A_o + A_\delta} = \frac{SV_{90-o}}{1 + \frac{A_\delta}{A_o}} = \frac{SV_{90-o}}{1+\delta} \tag{5.6}$$

A coefficient for the effectiveness of increased settling area (β) reflects the actual effect of the increased settling area by improving the η of small SV particle groups. The value of β=1 indicated that the entire increased settling area contributed to increasing the η of the particle group. On the other hand, the value of β=0 indicated that there was no impact from the increased settling area, as shown in equation (5.7).

Equation 5.6 should be:

$$SV^{*}_{90-i} = \frac{SV_{90-o}}{1+\beta\times\delta} \tag{5.7}$$

where

LV_o: linear velocity in the original settling tank ($m^3/(m^2\cdot h)$)

LV_i: linear velocity in the improved settling tank ($m^3/(m^2\cdot h)$)

Q_o: flow rate in the original settling tank (m^3/h)

$SV_{90\text{-}i}$: ideal settling velocity of particle group i in improved tank which had the η of 90% (m/h)

$SV^{*}_{90\text{-}i}$: actual settling velocity of particle group i in improved tank which had the η of 90% (m/h)

β: effectiveness of increased δ to improve the η of small SV particle groups (from 0 to 1).

In this study, particle group with η of 90% in original settling tank was selected to calculate the effect of δ on improving η of small SV particle groups by ratio $\psi_{90\text{-}i}$, which was the ratio between $SV_{90\text{-}i}$ in improved tank and LV_o.

In ideal condition: $$\psi_{90-i} = \frac{SV_{90-i}}{LV_o} \tag{5.8}$$

In actual condition: $$\psi^{*}_{90-i} = \frac{SV^{*}_{90-i}}{LV_o} \tag{5.9}$$

The relationship between ψ^{*}_{90-i} and δ was calculated:

$$\psi^{*}_{90-i} = \frac{SV^{*}_{90-i}}{LV_o} = \frac{SV_{90-o}}{(1+\beta\times\delta)\times LV_o} = \frac{\psi_{90-o}}{1+\beta\times\delta} \tag{5.10}$$

where

$\psi_{90\text{-}o}$: the ratio between $SV_{90\text{-}o}$ and LV_o.

5.3. RESULTS AND DISCUSSION

5.3.1 Relationship between SS removal efficiency (η) and increased settling area (δ)

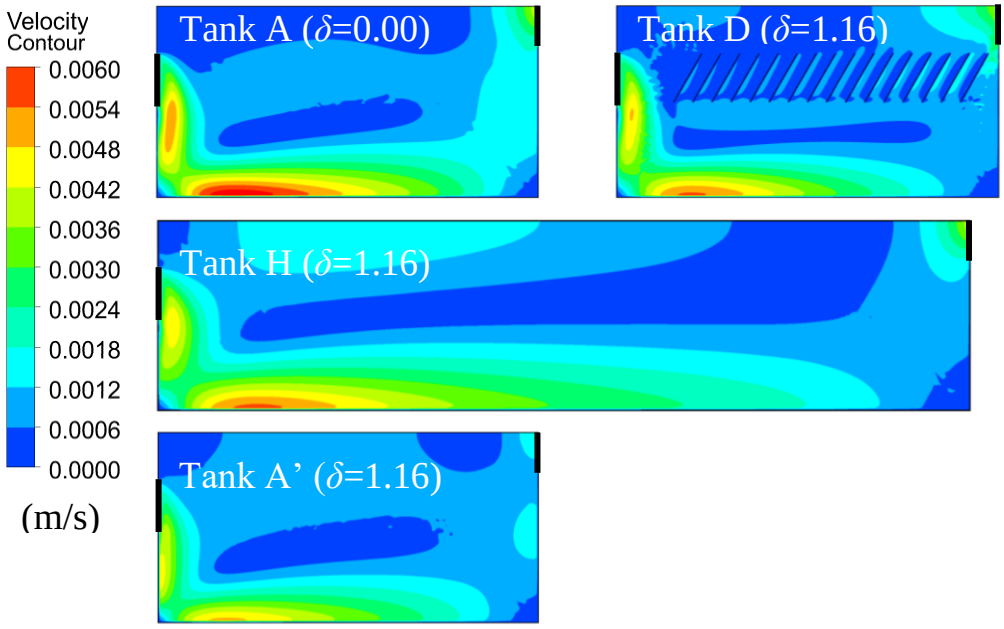

Fig 5.5 Contour of velocity for settling tanks and lamella settling tanks.

The contour plots of velocity in the modelled tanks with $\delta = 0$ and $\delta = 1.16$ are shown in **Fig 5.5**. In tank D, the small velocity zone (with blue colour) appeared in the middle of the inclined plates, resulting in easier settling of particles on the surface of inclined plates. These results indicated that the settling process was improved by inclined plates in tank D. In tank H, the small velocity zone was seen extending from the inlet to the outlet. The small velocity zone helps stabilize the settling process in the tank, thus improves particle removal efficiency. Moreover, the velocity near the outlet was seen lower compared to in tank A, which was also the reason for increasing the SS removal efficiency in this tank. In tank A', which had the same size as tank A, the flow rate into the tank decreased by 2.16 times compared to in tank A, so the velocity in the whole tank was lower than the one in tank A. Hence, the performance of particles removal was increased.

Figure 5.6, 5.7, and **5.8** showed the relationship between the increased settling area and the SS removal efficiency in the sedimentation tank.

The simulation results of SS removal efficiency in lamella settling tanks in **Fig 5.6** indicated that the more inclined plates installed (increased δ), the better the SS removal efficiency achieved for each particle group (η_i). For particle groups with small settling velocities (particle group 1, SV=0.75 m/h), inclined plates were thought to have little impact on SS removal efficiency. At a constant flow rate, as δ increased from 0 to 2.32, the largest improvement on η was observed for particle groups 3 to 7 (SV=1.25 to 2.25 m/h), at values of 12 and 8%. For particle groups 8 to 10 (SV=2.50 to 3.00 m/h), no significant enhancement of SS removal efficiency was achieved due to the high inherent settling capacity of these particles.

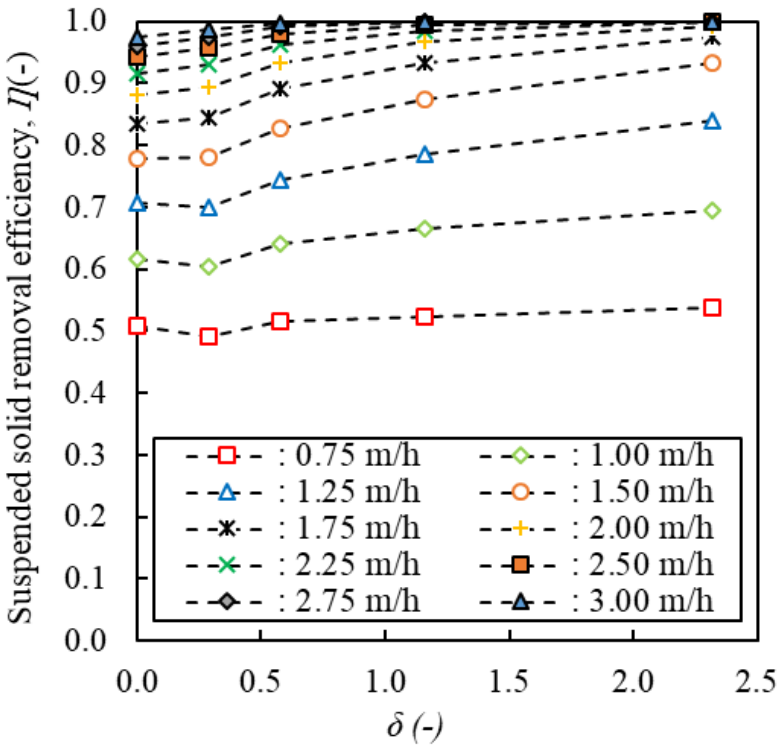

Fig 5.6 Relationship between η and δ for increased δ by installing inclined plates.

As shown in **Fig 5.7**, the η increased significantly in almost particle groups as

increasing the δ. With δ increasing from 0 to 2.32, there was a sharp increase in η for particles groups 1 to 7 (SV=0.75 to 2.25 m/h) with 41 to 8%, respectively. The high η was recorded in particle groups 8 to 10 (SV=2.50 to 3.00 m/h) in the original settling tank, so η only increased by 6 to 3% corresponding to these particle groups. Especially at δ = 2.32, particle groups were almost completely removed in the sedimentation tank.

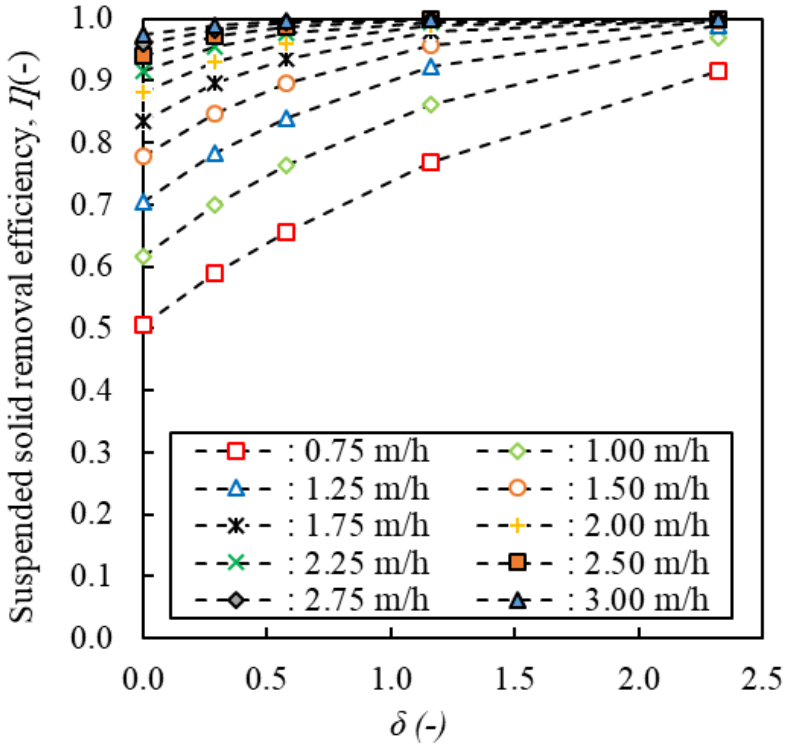

Fig 5.7 Relationship between η and δ for increased δ by increasing the length of the tank.

According to the simulation results in **Fig 5.8**, the η was observed to increase gradually for each particle group. For particle groups 1 to 2.32 (SV=0.75 to 2.25 m/h), the improvement of η increased with 25 to 8%, respectively. For particle groups 8 and 10 (SV=2.50 to 3.00 m/h), the improvement of SS removal efficiency was similar to two cases aforesaid.

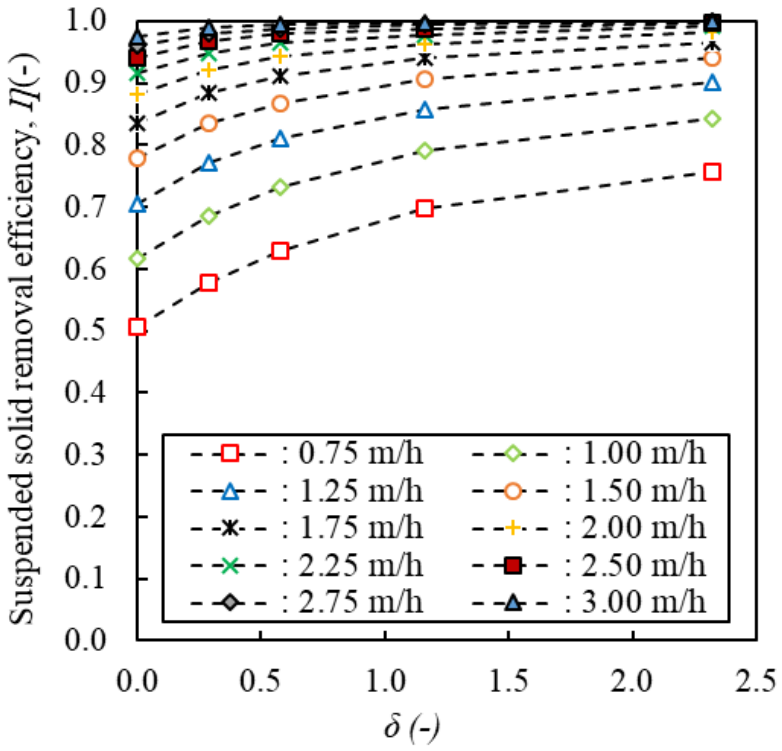

Fig 5.8 Relationship between η and δ for increased δ by increasing the width of the tank

Therefore, when the flow rate was constant, the increasing δ leads to enhance the removal efficiency of each particle group. With the same δ, the highest SS removal efficiency was observed in settling tanks with increased δ by increasing the length. In contrast, when the δ was increased by installing inclined plates, the SS removal efficiency was obtained at the lowest value. For each particle groups, the greater improvement of η was recorded in small *SV* particle groups, rather than the large one.

5.3.2 Effectiveness of δ to improve the η of small SV particle groups

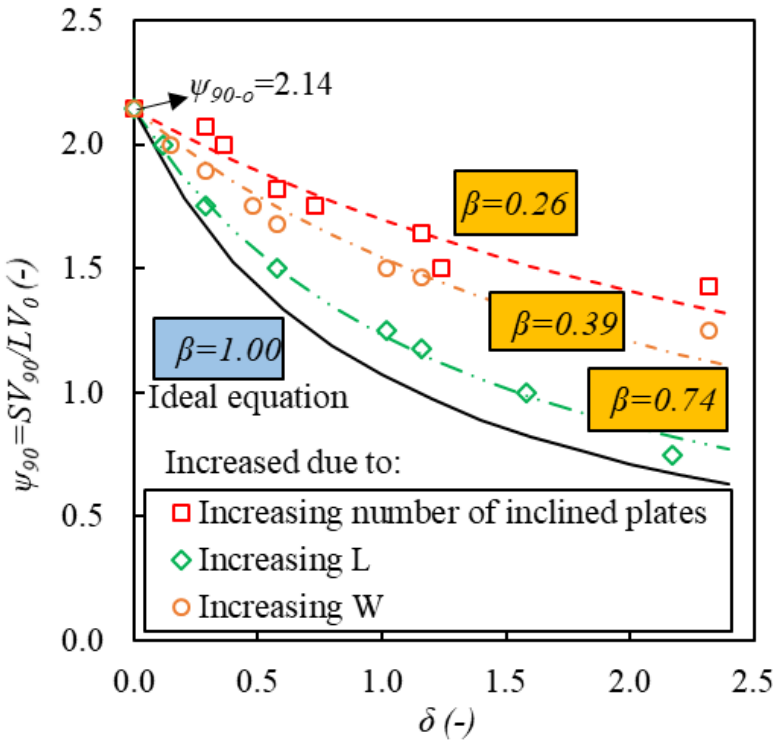

Fig 5.9 Relationship between ψ_{90} and δ at η=0.90.

To assess the effect of δ on removal efficiency of small SV particle groups, in this study, the particle group with a η of 90% corresponding to $SV_{90\text{-}o}$ = 2.14 m/h and $\psi_{90\text{-}o}$ = 2.14 in the original settling tank was selected. Based on the results in **Fig 5.6, 5.7,** and **5.8**, the ψ_{90} is calculated for other particle groups with the same η of 90% when the δ increased.

From the results in **Fig 5.6, 5.7,** and **5.8,** the horizontal line η =0.90 was plotted, and intersections with the other linear curves represented different values of SV corresponding to an increased δ. Then, the relationship between ψ_{90} and increased δ was plotted in **Fig 5.9**. When δ increased, it leads to a decrease in the ψ_{90}, which means that the increased δ enhances removal efficiency in small SV particle groups. For example, in ideal condition, when δ increased to 1, the ψ_{90} should decrease from 2.14 to 1.07 (2 times reduction) for all three cases. However**,** the ψ_{90} only decreased from 2.14 to 1.70, 1.23,

and 1.54 corresponding to increased δ by installing inclined plates, increasing the length, and increasing the width, respectively. Thus, the removal efficiency of the small *SV* particle group with ψ_{90} in case 2 was the best performance, the particle group with SV_{90} of 1.23 m/h was removed with η= 90% compared to the particle group with $SV_{90\text{-}o}$ of 2.14 m/h.

As the results in **Fig 5.9**, the coefficient β increased from 0.26 (increased δ by inclined plates) to 0.39 (increased δ by increasing the width) and 0.74 (increased δ by increasing the length), the results indicated that the increased δ by increasing the length was contributed the highest performance to small *SV* particle groups with a coefficient β of 0.74. However, this value was still smaller than the ideal value of β = 1.

In the previous study, Nguyen et al. [76] investigated the effect of increased δ by installing inclined plates to increase the attainable flow rate of the settling tank (α). The research results showed that the increased δ due to installing inclined plates only contributed 37.69% to increase the attainable flow rate. In this study, the effectiveness of the increased δ to the removal efficiency of small *SV* particle groups (β) was 26.10%, which was an insignificant difference compared to the α value. These findings revealed the actual contribution of inclined plates of about 30% to improve the η of small *SV* particle groups and increase the attainable flow rate, which was significantly lower than ideal calculation value.

5.3.3 Improvement on the hydraulic regime in settling tanks and lamella settling tanks

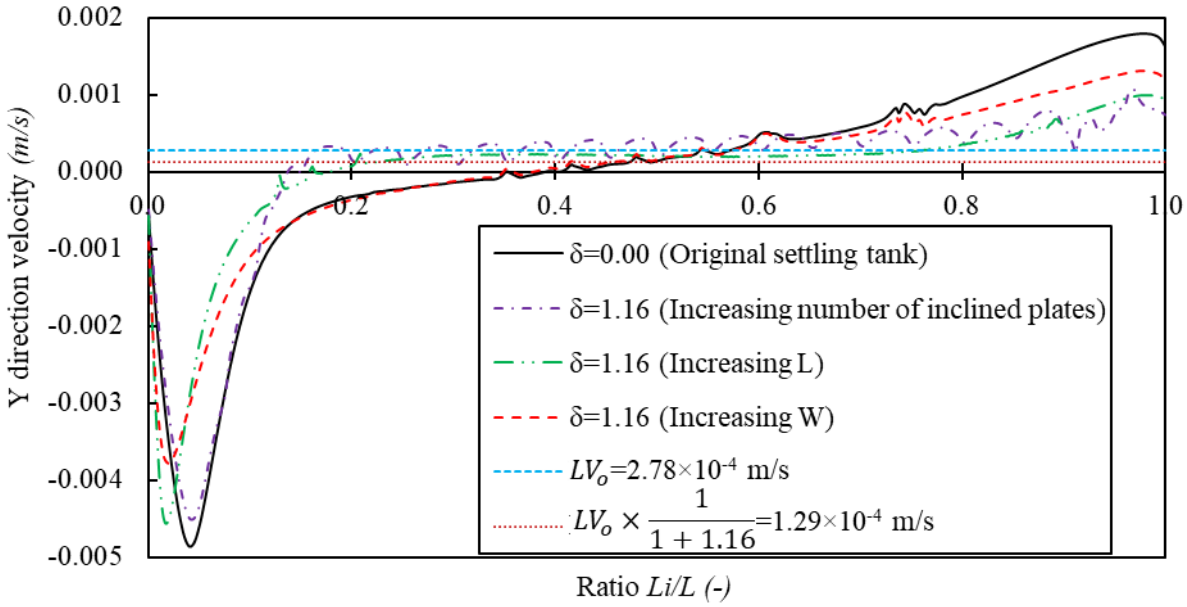

Fig 5.10 Y direction velocity at H=1m, δ = 0 and 1.16

In some studies [46], [77], a baffle plate was used to orient the inlet flow to the bottom of the settling tank. However, as illustrated by the simulation, even without the baffle plate, the difference between SS density and water temperature still created a downward flow, known as the density current [72], [78], as shown in **Fig 5.10**.

In order to clearly understand the effect of the hydraulic regime on the SS removal efficiency, the Y-direction velocity was compared between δ of 0 (in the original settling tank) and 1.16 (in three cases) at a depth of 1m.

Theoretically speaking, when δ increases to 1.16 corresponding to a decrease in *LV* with the same ratio, so the small *SV* particle group with *SV* higher than the decreased *LV* could be removed. The results in **Fig 5.10** indicated that the Y-direction velocity was different between other tanks with the same increased δ. In the case of increasing δ by installing the inclined plates, the velocity fluctuated in the middle of the tank. Nevertheless, the velocity nearby

the outlet zone was smaller than the one in the original settling tank. This result suggested that the η should be increased thanks to improving the hydraulic regime by installing inclined plates. In the tank with increased δ by increasing the width, the velocity was almost unchanged from inlet to the middle of the tank compared to the original settling tank, the velocity near the outlet zone slightly decreased, led to increasing η for small particle groups. Especially in the tank with increasing length, the velocity was stable and approximation the LV_o from inlet to near the outlet and the velocity near the outlet was lower compared to other cases. As a result, the effectiveness of δ to η (β=0.74) in this case was the highest. However, in three cases, the LV was decreased by 2.16 times, but a small reduction rate of velocity (lower than 2.16 times) was observed, so the coefficient β was always smaller compared to the ideal value of β=1.

From the study results, the best solution for improving SS removal efficiency in the settling tank was increasing the length. The disadvantage of this solution impossibility in the arrangement of the treatment plant due to area shape. In a further study, application the CFD model to estimate the effect of this type of configuration, as shown in **Fig 5.11,** on the treatment efficiency of the tank should be performed. Instead of reducing the LV by increasing the width, flow direction should be arranged in a zigzag way to have similar treatment efficiency to increase the length as above-mentioned. Thus, there is an optimal solution for the design of saving areas and easy organization layout of settling tanks.

a) Top view of settling tank with increasing the width

b) Top view of settling tank with increasing the length

Fig 5.11 Arrangement of settling tank layout

At present, the improvement of η of the lamella settlers is continuously evolved. A possible approach is to optimize the arrangement of inclined plates, for example, in parallel to the direction of the inlet flow [79], [80]. This scenario should be simulated to reveal the optimal placement of inclined plates. To better visualize the effects, the simulation in 3-dimensional should be carried out.

If the plates are installed in parallel to the inlet flow in the rectangular settling tank (see the configuration in **Fig 5.12**), the currents that go out of the lamella plates will create a non-uniform flow on the top of the plates. Consequently, the SS removal efficiency of the tank will be reduced. The plates installing in parallel to the inlet flow might not be the best arrangement; however, this scenario should be simulated in the future study.

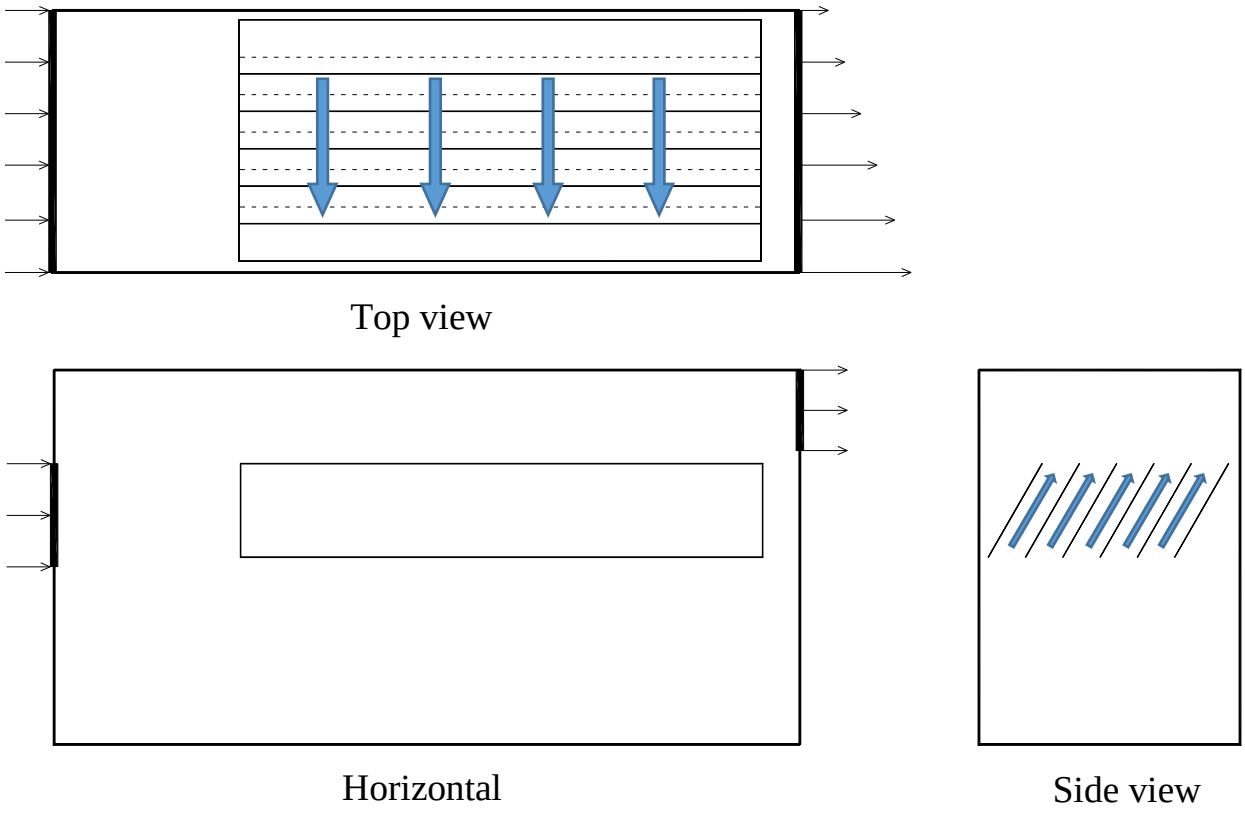

Fig 5.12 Cross section of lamella settling tank with inclined plates installing parallel to inlet flow

5.4. CONCLUSION

The research evaluated the effect of δ on improving SS removal efficiency in the settling tank with three different types of configuration. Simulation results show that the η could be improved by increasing the δ. Specifically, the particle group with $\psi_{90\text{-}o}$, the ratio of $SV_{90\text{-}o}$ to LV_o equal 2.14, was removed with 90% in the original settling tank. With the same removal efficiency, in ideal condition, the ψ_{90} decreases from 2.14 to 1.07 (2 times reduction) as increasing δ to 1 for all three cases. However, in this study, the δ increased to 1 by installing inclined plates, increasing the length, and increasing the width; the ψ_{90} only decreased from 2.14 to 1.70, 1.23, and 1.54, respectively. Therefore, the δ could enhance the removal efficiency of small SV particle groups, but the effectiveness of δ in increased η was significantly lower than the ideal value of β =1. It was noteworthy that the increased δ by increasing the length had the largest contribution to improve the η of small SV particle groups with β = 0.74. The result has important implications in the renovation design of settling tanks to get the best performance for the wastewater treatment plant.

References

[5] W. F. Leung, “Lamella and Tube Settlers. 2. Flow Stability,” *Ind. Eng. Chem. Process Des. Dev.*, vol. 22, no. 1, pp. 68–73, 1983.

[6] A. Demir, “Determination of settling efficiency and optimum plate angle for plated settling tanks,” *Water Res.*, vol. 29, no. 2, pp. 611–616, 1995.

[7] K. Fujisaki and M. Terashi, “Improvement of settling tank performance using inclined tube settlers,” vol. 80, pp. 475–484, 2005.

[16] A. I. Stamou, E. W. Adams, and W. Rodi, “Modélisation numérique de l’écoulement et de la sedimentation dans des bassins de décantation primaires de forme rectangulaire,” *J. Hydraul. Res.*, vol. 27, no. 5, pp. 665–682, 1989.

[22] W. P. Kowalski, “The method of calculations of the sedimentation efficiency in tanks with lamella packets,” *Arch. Hydroengineering Environ. Mech.*, vol. 51, no. 4, pp. 371–385, 2004.

[24] R. Tarpagkou and A. Pantokratoras, “The influence of lamellar settler in sedimentation tanks for potable water treatment - A computational fluid dynamic study,” *Powder Technol.*, vol. 268, pp. 139–149, 2014.

[25] M. Weiss, B. G. Plosz, K. Essemiani, and J. Meinhold, “CFD modelling of sludge sedimentation in secondary clarifiers,” *WIT Trans. Eng. Sci.*, vol. 52, pp. 509–518, 2006.

[42] K. Mohanarangam and D. Stephens, “Cfd Modelling of Floating and Settling Phases in Settling Tanks,” *Victoria*, no. December, pp. 1–7, 2009.

[44] A. M. Goula, M. Kostoglou, T. D. Karapantsios, and A. I. Zouboulis, “A CFD methodology for the design of sedimentation tanks in potable water treatment. Case study: The influence of a feed flow control baffle,” *Chem. Eng. J.*, vol. 140, no. 1–3, pp. 110–121, 2008.

[46] X. Wang, L. Yang, Y. Sun, L. Song, M. Zhang, and Y. Cao, “Three-dimensional simulation on the water flow field and suspended solids concentration in the rectangular sedimentation tank,” *J. Environ. Eng.*, vol. 134, no. 11, pp. 902–911, 2008.

[51] H. Asgharzadeh, B. Firoozabadi, and H. Afshin, “Experimental investigation of effects of baffle configurations on the performance of a secondary sedimentation tank,” *Sci. Iran.*, vol. 18, no. 4 B, pp. 938–949, 2011.

[52] M. Shahrokhi and F. Rostami, “The Computational Modeling of Baffle Configuration in the Primary Sedimentation Tanks,” *Flow3D2.Propagation.Net*, vol. 6, pp. 392–396, 2011.

[55] M. M. Heydari, M. S. Bajestan, H. A. Kashkuli, and H. Sedghi, “The effect angle of baffle on the performance of settling basin,” *World Appl. Sci. J.*, vol. 21, no. 6, pp. 829–837, 2013.

[64] Ghawi, “Application of Computational Fluid Dynamics modelling to a horizontal sedimentation tank,” no. April, 2017.

[66] Y. L. Liu, W. L. Wei, B. Lv, and X. F. Yang, “Research on optimal radius ratio of impellers in an oxidation ditch by using numerical simulation,” *Desalin. Water Treat.*, vol. 52, no. 13–15, pp. 2811–2816, 2014.

[67] W. Wei, Y. Liu, and B. Lv, “Numerical simulation of optimal submergence depth of impellers in an oxidation ditch,” *Desalin. Water Treat.*, vol. 57, no. 18, pp. 8228–8235, 2016.

[68] A. I. Stamou, G. Theodoridis, and K. Xanthopoulos, “Design of secondary settling tanks using a CFD model,” *J. Environ. Eng.*, vol. 135, no. 7, pp. 551–561, 2009.

[70] Degrémont, *Water treatment handbook*, 7th edition. France, 2007.

[71] I. Metcalf and Eddy, *Wastewater Engineering: Treatment and Reuse*, Fourth edition. New York, USA: Mc Gram-Hill, 2003.

[72] Ghawi and J. Kri, “A Computational Fluid Dynamics Model of Flow and Settling in Sedimentation Tanks,” *Appl. Comput. Fluid Dyn.*, 2012.

[73] Japan Sewage Works Association, *Design Standard for Municipal Wastewater Treatment Plants*. Tokyo, Japan: Japan Sewage Works Association, 2013.

[76] T. A. Nguyen, N. T. M. Dao, B. Liu, M. Terashima, and H. Yasui, “Computational fluid dynamics study on attainable flow rate in a lamella settler by increasing inclined plates,” *J. Water Environ. Technol.*, vol. 17, no. 2, pp. 76–88, 2019.

[77] Y. Liu, P. Zhang, and W. Wei, “Simulation of effect of a baffle on the flow patterns and hydraulic efficiency in a sedimentation tank,” *Desalin. Water Treat.*, vol. 57, no. 54, pp. 25950–25959, 2016.

[78] M. Patziger, H. Kainz, M. Hunze, and J. Józsa, “Influence of secondary settling tank performance on suspended solids mass balance in activated sludge systems,” *Water Res.*, vol. 46, no. 7, pp. 2415–2424, 2012.

[79] JFE Engineering Corporation, “Pretreatment sedimentation equipment - Inclined plate settling device,” 2019. [Online]. Available: http://www.jfe-eng.co.jp/products/environment/water_supply/sup02.html. [Accessed: 20-Sep-2008].

[80] SUEZ’s degremont, “SUEZ’s degremont® water handbook, Lamella sedimentation,” 2019. [Online]. Available: https://www.suezwaterhandbook.com/water-and-generalities/fundamental-physical-chemical-engineering-processes-applicable-to-water-treatment/sedimentation/lamellar-sedimentation. [Accessed: 20-Sep-2008].

CHAPTER 6 GENERAL EXPRESSION OF THE PERFORMANCE OF INCLINED PLATES IN LAMELLA SETTLER USING COMPUTATIONAL FLUID DYNAMICS

6.1. INTRODUCTION

The sedimentation tank plays an important role in water and wastewater treatment systems, which aims to remove settling particles in water by gravity. The effective performance of the settling tank contributes largely to the reduction of suspended solids (SS) that entered the filtration process. By installing inclined plates into settling tanks, the settling distances of the particles are reduced, and the laminar flow regime is created. The installation of inclined plates contributes to an increase in the settling area, hence improve settling ability. As a result, the lamella setting tank could achieve similar targeted SS removal efficiency at a lower footprint comparing to conventional settling tanks. However, the effectiveness of inclined plates in the lamella settling tank is not fully investigated.

The application of the Computational Fluid Dynamics (CFD) method on the settling process could enlighten the flow and hydraulic regime, as well as impact factors on settling efficiency of the sedimentation tanks. In 1989, Stamou [16] used a numerical model for studying the flow and settling process of suspended solids in primary sedimentation tanks and compared the simulation results with the theoretical method. Goula [44] used the CFD method to evaluate the effectiveness of baffles in the inlet zone on the distribution of flow patterns and the influence of mass fraction of suspended solids to their removal efficiency. Asgharzadeh and Shahrokhi [51] [52] investigated the reduction of the dead zone and recirculation zone by different

numbers of baffles installed at the bottom. Similarly, the simulation was conducted by Heydari [55] to improve settling efficiency by changing the angle of the baffle at the bottom of the settling tank. Ghawi and Kriš [72] simulated a complex model by using CFD to estimate effectiveness factors on deposition efficiency. These simulation results indicated that CFD provides accurate results comparing with experimental results. Using CFD for simulation of the sedimentation process could be time-saving and cost-effective.

There are many studies on the lamella settling tank. Leung [5] studied the distribution of 3 flow layers between two inclined plates. Demir [6] investigated the optimum angle of the baffle in the lamellar settling tank in changing the overflow rate. Kowalski [22] assessed the settling efficiency in the conventional tank and lamella settling tank taken into account the density, viscosity, and mass fraction of solid particles. Fujisaki and Terashi [7] used many types of tube settlers to improve the efficiency of the clarifier. The impact of the inclined plates on the mechanism of hydraulic in lamella settling tank and effectiveness of settling in the lamella settling tank was evaluated, comparing to full-scale conventional tank. Most of above-mentioned research were lab-scale studies and focused on the settling of particles in separate inclined plates. Further, the entire inclined plates were assumed to contribute to suspended solids removal efficiency. In this study, the effectiveness of baffle, specifically the fraction of horizontal projected area that engages in lamella performance will be investigated. Based on the ideal settling theory of Hazen, to evaluate the influence of increasing settling areas due to inclined plates on SS removal efficiency, by comparing simulation results of the conventional settling tank to lamella settling tanks with different numbers of inclined plates at the same working conditions. To visualize the change of hydraulic regime by varying the number of inclined plates and gaps between plates, therefore explain the better SS removal efficiency of lamella settling

tanks compared to the conventional settling tank

6.2. MATERIALS AND METHODS

6.2.1 Numerical modelling methods

The Algebraic Slip Model was selected for simulation of the velocity profile and the concentration distribution of SS. Each dispersed component is represented by a mass fraction equation, and a relative movement is allowed between these components in the continuous phase [42]. Turbulence in the liquid phase was modelled using the k-ε model, which successfully simulated the sedimentation tank in previous studies [64]. The hydrodynamic and flow behavior in the sedimentation tanks were modelled in two dimensions. In this study, the commercial software CFX 18.0 (in ANSYS) was used to perform CFD modelling. The hexahedral meshes were generated by ANSYS meshing for numerical calculations.

6.2.2 Geometry of modeling

The simulation was conducted on 4 tanks of the same size ($H \times W \times L$ = 2×0.2×4 m). The first tank was settling tank without an inclined plate. The following tanks were lamella settlers, of which 4, 8, and 16 plates were installed at 60^o angle and spacing of 0.8, 0.4, and 0.2 m, respectively (**Fig 6.1**). The ratio δ between the horizontal projection area of inclined plates (A_b) of lamella settlers and surface area (A_o) were 0.29, 0.58, and 1.16, respectively. The total settling area of lamella settlers was calculated as the sum of surface area and horizontal projection area of inclined plates ($A = A_o + A_b$).

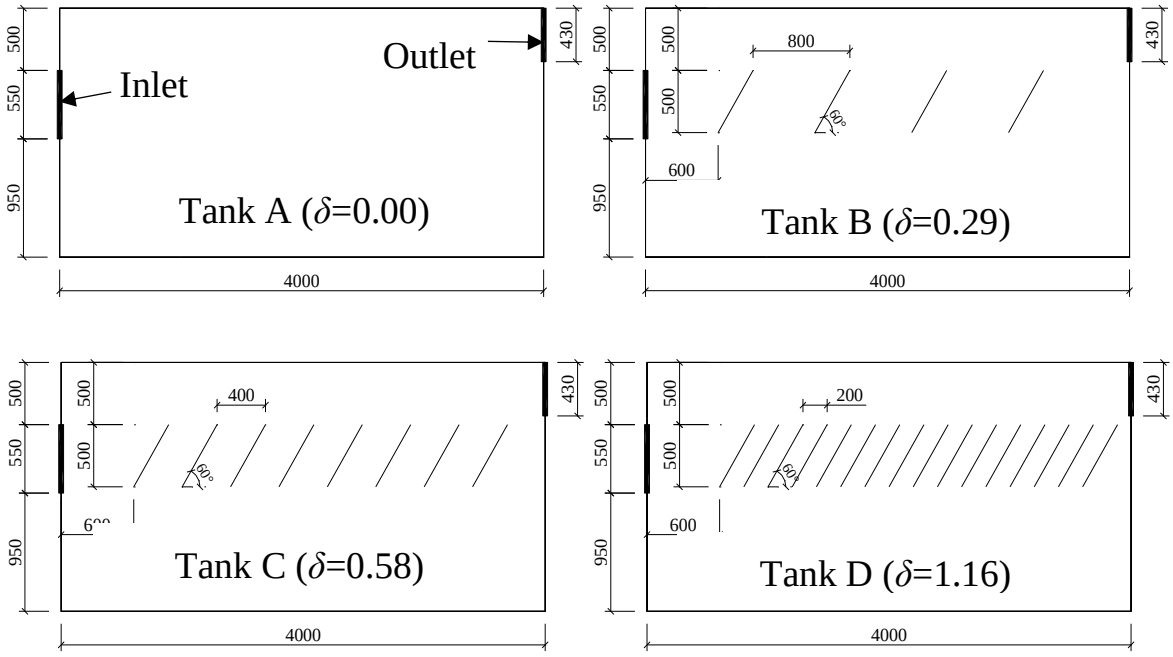

Fig 6.1 Geometry of settling tank and lamella settling tanks

6.2.3 Boundary condition

In sedimentation tank design, the *LV* commonly selected is between 1 and 2 $m^3/(m^2 \cdot h)$ [73]. Therefore, in this study, a primary sedimentation unit located in the wastewater treatment process was simulated under the original *LV* of 1 $m^3/(m^2 \cdot h)$, inlet 200 mg-SS/L, water density 998 kg/m^3 and particle density of 1020 kg/m^3.

In the model, the mass flow rate was selected at both the inlet and outlet. No slip wall was set for the bottom, the wall, or the baffles. The water-surface was best defined by the VOF method in some studies [66], [67], in case of simulating the complicated surface between two fluids (air and water). In this study, the surface was almost flat and simple, so the free slip wall was selected to set up the surface boundary condition. The water surface was assumed to be horizontal in the tank, which was also widely applied for simulation of settling tanks in previous research [24], [25], [68]. The particles were set to be deposited only at the bottom, not on the wall or baffles.

The transient-type simulations were selected in this study. The initial time step

was set at 5 seconds for the adaptive option in all calculations. For the numerical method, the advection scheme was upwind, and the transient scheme was set as second-order backward Euler.

6.2.4 Selection of appropriate mesh size

In order to check the mesh sensitivity, different mesh sizes ranging from 5-80 mm, corresponding to 324,538 and 1,857 number of elements (**Table 6.1**), were used to simulate SS removal efficiency in lamella D (δ = 1.16). By enlarging the mesh size, SS removal efficiency decreased from 80 to 74% according to the results. At mesh sizes of 5, 10, and 20 mm, SS removal efficiencies were similar. Consequently, the 20 mm-mesh size was selected for conducting subsequent simulations, assuring to provide accurate results and reasonable simulation time.

Table 6.1 Simulation results for the mesh sensitivity

	Mesh size 1 (5 mm)	Mesh size 2 (10 mm)	Mesh size 3 (20 mm)	Mesh size 4 (40 mm)	Mesh size 5 (80 mm)
Nodes	651,364	164,230	41,682	10,362	3,888
Elements	324,538	81,532	20,550	5,035	1,857
SS removal efficiency (%)	80.37	80.02	79.74	77.32	74.26
Difference	0.00	0.44	0.79	3.80	7.61

6.2.5 Selection of appropriate groups of particles

In the CFD model, SS particles in the influent were grouped and represented by average settling velocities for simplification in **Table 6.2**. To verify the sensitivity of group numbers, the simulation of SS removal efficiency of lamella D (δ = 1.16) was conducted using different particle groups ranging

from 1 to 20. By increasing particle groups, the SS removal efficiencies decreased from 97 to 80% (**Fig 6.2**). The groups from 10 to 20 provided results without much difference. Hence, 10 groups of particles were used for the following simulations.

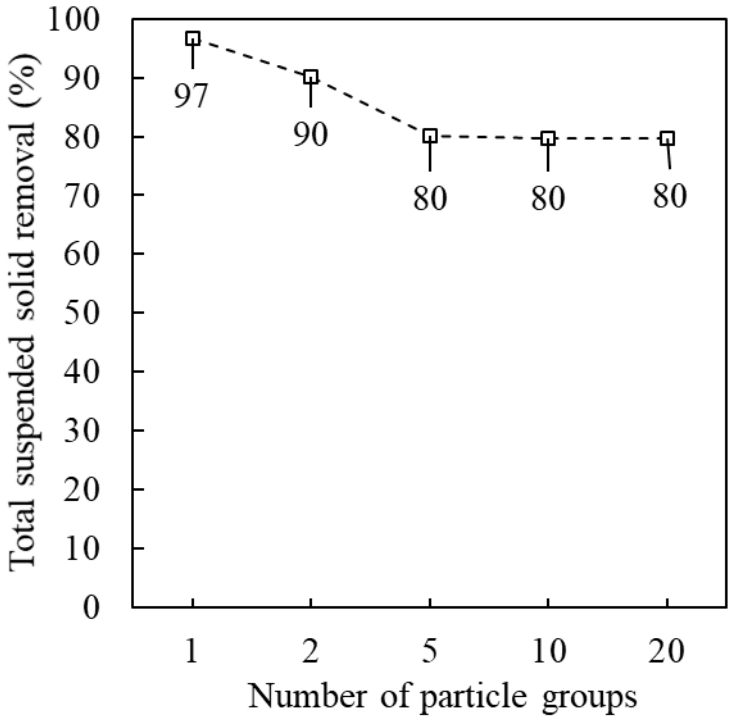

Fig 6.2 Sensitivity simulation on the number of particle groups

6.2.6 Tracer simulation method

The hydraulic regime of the settling tanks was assessed using a tracer simulation. A total tracer amount of 5.15×10^{-7} kg was introduced into the inlet (flow rate, Q=0.08 m^3 h^{-1}) for a period of 1s (pulse input). The data for tracer concentrations at the outlet was recorded to plot a residence time distribution and calculated *E-curve* and *R-curve*. (Terashima et al., 2013 [75]).

Table 6.2 Settling velocities for group number sensitivity test

1 group	Particle group No.	1								
	Settling velocity (mm/s)	0.63								
	Mass fraction	1.00								
2 groups	Particle group No.	1	2							
	Settling velocity (mm/s)	0.36	0.90							
	Mass fraction	0.50	0.50							
5 groups	Particle group No.	1	2	3	4	5				
	Settling velocity (mm/s)	0.10	0.35	0.63	0.90	1.18				
	Mass fraction	0.20	0.20	0.20	0.20	0.20				
10 groups	Particle group No.	1	2	3	4	5	6	7	8	9	10
	Settling velocity (mm/s)	0.07	0.14	0.28	0.42	0.56	0.69	0.83	0.97	1.11	1.25
	Mass fraction	0.1	0.1	0.1	0.1	0.1	0.1	0.1	0.1	0.1	0.1

20 groups	Particle group No.	1	2	3	4	5	6	7	8	9	10
	Settling velocity (mm/s)	0.05	0.09	0.10	0.17	0.24	0.31	0.38	0.45	0.52	0.59
	Mass fraction	0.05	0.05	0.05	0.05	0.05	0.05	0.05	0.05	0.05	0.05
	Particle group No.	11	12	13	14	15	16	17	18	19	20
	Settling velocity (mm/s)	0.66	0.73	0.80	0.87	0.94	1.01	1.08	1.15	1.22	1.28
	Mass fraction	0.05	0.05	0.05	0.05	0.05	0.05	0.05	0.05	0.05	0.05

6.2.7 Direct calculation of SS removal efficiency from simulation

From simulation results, the SS removal efficiency was directly evaluated for each group of particles as below.

$$\eta_i = \frac{C_{in}^i - C_{out}^i}{C_{in}^i} \tag{6.1}$$

where

η_i: suspended solid removal efficiency (from 0 to 1)

C_{in}^i : Concentration of particle group i in the inlet (mg/L)

C_{out}^i : Concentration of particle group i in the outlet (mg/L)

6.2.8 Definition of Hazen number

Hazen number is defined as the ratio between settling velocity (*SV*, m/s) and overflow rate (*LV*, m/s).

$$Ha = \frac{SV}{LV} \tag{6.2}$$

where

SV: settling velocity of particle group (m/h)

LV: Overflow rate ($m^3/(m^2 \cdot h)$)

6.2.9 Hazen number in the settling tank

In a conventional settling tank, the *LV* is defined as the ratio between flowrate

Q (m^3/h) and surface area in settling tank A_o (m^2). The equation is rewritten as below:

$$Ha^0 = \frac{SV}{LV_o} = \frac{SV}{\frac{Q}{A_o}} = \frac{SV \cdot A_o}{Q} \tag{6.3}$$

where

Q: flow rate (m^3/h)

A_o: surface area in settling tank (=0.2×4=0.8 m^2)

6.2.10 Hazen number in the lamella settling tank

In the lamella settling tank, the settling area includes the surface area of the settling tank and the effective settling area provided by inclined plates. The effectiveness of baffles was evaluated using the coefficient γ that reflects the actual effect of the inclined plates on the Hazen number.

$$Ha^* = \frac{SV}{LV^*} = \frac{SV}{\frac{Q}{(A_o + \gamma \cdot A_b)}} = \frac{SV \cdot (A_o + \gamma \cdot A_b)}{Q} \tag{6.4}$$

where

LV^*: Modified linear velocity in lamella settling tank ($m^3/(m^2 \cdot h)$)

γ: effectiveness of inclined plates on Hazen number

A_b: horizontal projection area of inclined plate

($A_b = n_b \times W_b \times L_b \times \cos 60^o$) ($m^2$)

n_b: number of inclined plates in the lamella settling tank

W_b: width of inclined plate (m)

L_b: length of inclined plate (m),

6.2.11 Calculation of effectiveness of inclined plates in the lamella settling tank

The improvement of SS removal efficiency of lamella settling tank compared to a conventional settling tank could be evaluated using the coefficient γ determined by the equation below:

$$\gamma = \frac{\left(\frac{Q \cdot Ha^*}{SV} - A_o \right)}{A_b} \tag{6.5}$$

In equation (6.5), A_o and A_b could be determined from theoretical calculations. The Ha^* obtained from simulation would help to determine the baffle effectiveness γ.

6.2.12 Analysis of Residence Time Distribution (RTD)

6.2.12.1 Determination of numbers of tanks

A variance of the E curve is equal to inverse number of N as follows:

$$\sigma^2 = \int_0^\infty (\theta - 1)^2 \cdot E_{(\theta)} d\theta \tag{6.6}$$

$$N = \frac{1}{\sigma^2} \tag{6.7}$$

where

θ: Dimensionless time units (–)

E_θ: exit age distribution in terms of θ (-)

6.2.12.2 Indirect calculation of suspended solid removal efficiency from tracer simulation

From RTD curve, the SS removal efficiency could be defined as below:

$$R_{(\theta i)} = \int_0^{\infty} R_{(\theta)} \cdot E_{(\theta)} d\theta \tag{6.8}$$

In which:

$$\theta_i = \frac{t_i}{t^*} \tag{6.9}$$

$$t_i = \frac{H_D}{SV_i} \tag{6.10}$$

$$H_D = \frac{V_T}{A_o^*} \tag{6.11}$$

where

V_T: Volume of tank (m^3)

A_o^*: surface area of tank (m^2)

H_D: the depth of tank (m)

SV_i: settling velocity of particle i (m/s)

t^*: hydraulic retention time (s)

t_i: residence time of particle i (s)

$R_{(\theta)}$: Ideal curve (assuming that the flow within inclined plate at lamella settling tank is similar up flow regime)

$$R_{(\theta)} = \begin{cases} 1 & (\theta < \theta_i) \\ 0 & (\theta > \theta_i) \end{cases}$$

Thus:

$$R_{(\theta_i)} = \int_0^{\theta_i} 1 \cdot E_{(\theta)} d\theta + \int_{\theta_i}^{\infty} 0 \cdot E_{(\theta)} d\theta \cong \sum_0^{\theta_i} E_{(\theta i)} \cdot \Delta\theta_i \tag{6.12}$$

Suspended solid removal efficiency increased

$$\varphi_i = \eta_{bi} - \eta_{oi} \tag{6.13}$$

where

η_{oi}: removal efficiency of particle group i in the original settling tank

η_{bi}: removal efficiency of particle group i in the lamella settling tank

6.3. RESULTS AND DISCUSSION

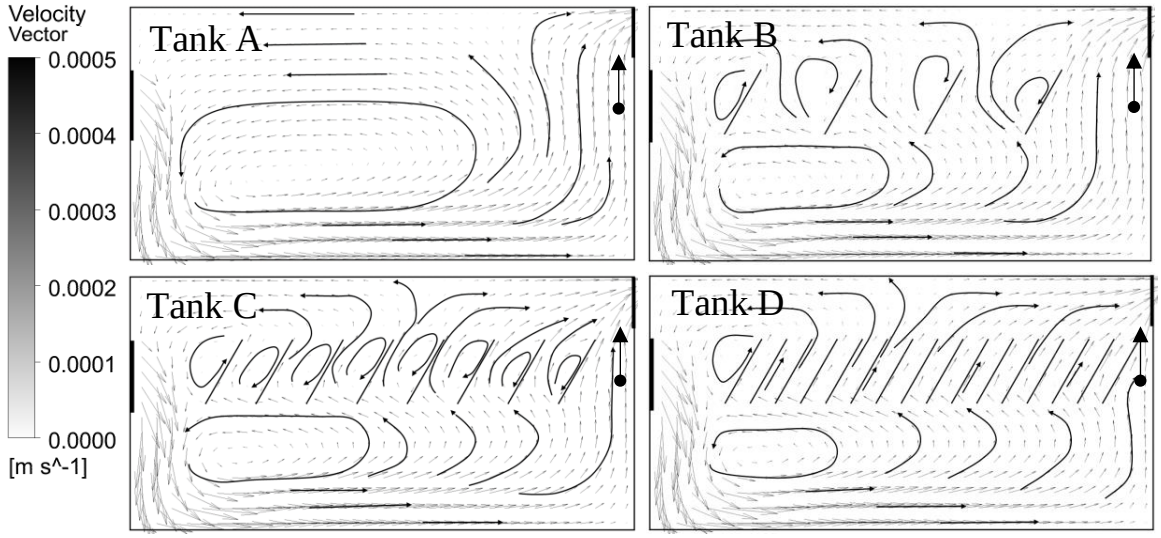

Fig 6.3 Vector of velocity for conventional tank and lamella settling tanks

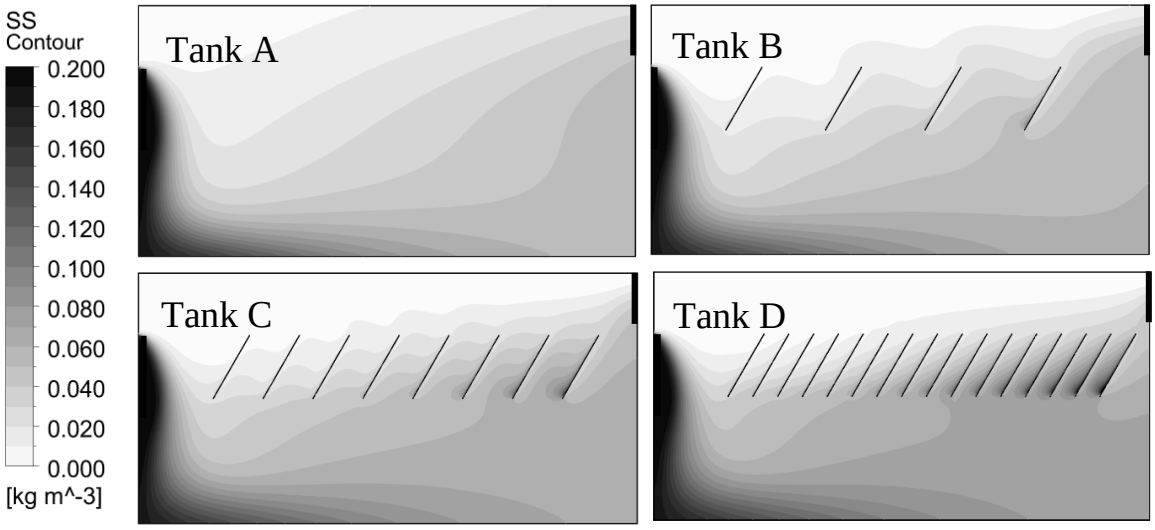

Fig 6.4 Contour of SS distribution for conventional tank and lamella settling tanks

6.3.1 Velocity contour and SS distribution

Velocity contour and SS distribution in the modelled tanks were visualized in **Fig 6.3** and **Fig 6.4**. A large recirculation eddy area closed to the top and outlet of the settling tank was observed. Meanwhile, these vortex zones were reduced

by half of the size in lamella settlers and located under the inclined plates. The maximum velocities in lamella settling tanks were reduced to be 2.97 mm/s (Tank D), 3.07 mm/s (Tank C), and 3.13 mm/s (Tank B), compared to 3.17 mm/s in settling tank (Tank A). Furthermore, suspended solids were observed deposition on inclined plates, which increased from Tank B to Tank D. The larger clear water zones were obtained when more inclined plates were installed.

6.3.2 Evaluation of the effectiveness of inclined plates in lamella settling tanks

As mentioned in paragraph 6.2.11, the effectiveness of inclined plates γ could be defined by obtaining accurate Ha^*.

The following sections investigate and compare the values of Hazen number in settling tank and lamella setting tanks within different scenarios (i) $\gamma = 0$, (ii) $\gamma = 1$, and (iii) accurate value of γ.

For each particle group, the SS removal efficiencies η were obtained from simulation, while the Hazen number is calculated from theoretical equations (6.2), (6.3) and (6.4). The curves between Hazen number and SS removal efficiency (curve Ha-η) was developed and discussed in the following sections.

6.3.2.1 Scenario 1: Inclined plates do not contribute to increasing of settling area ($\gamma = 0$)

In this scenario, it can be understood that lamella settlers and conventional settling tank should have identical curves of Ha^0-η. However, simulation results showed that lamella settlers improved solids settling. For the same value of Ha, the η in lamella settlers was almost higher than in the settling tank (**Fig 6.5**). Consequently, it is concluded that inclined plates contribute to the improvement of SS removal efficiency in lamella settling tanks; therefore,

γ could not be zero.

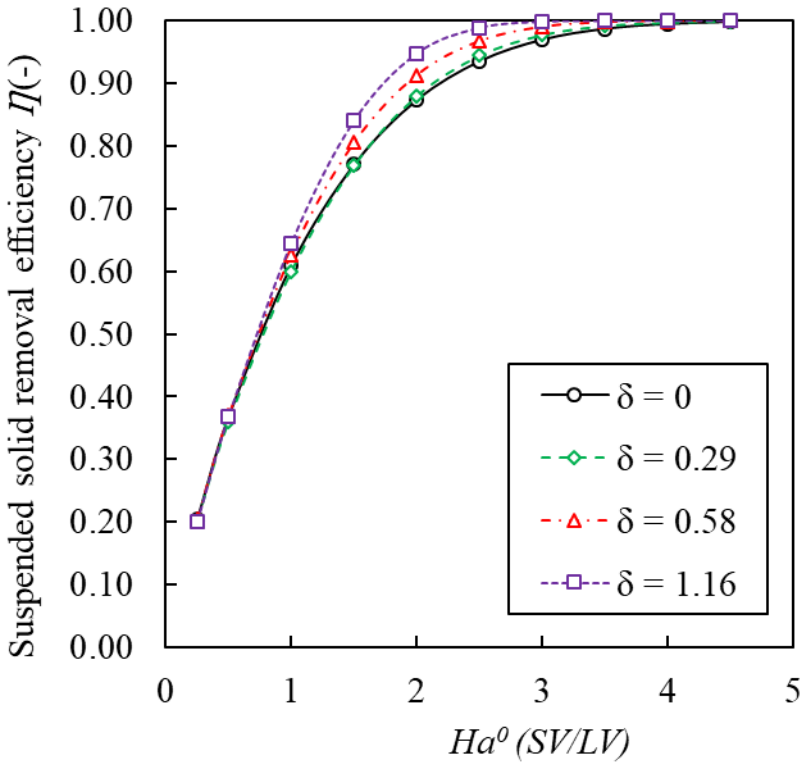

Fig 6.5 Curve *Ha-η* without the contribution of inclined plates

6.3.2.2 Scenario 2: Inclined plates entirely contribute to increasing of settling area (γ = 1)

In contrast to the previous scenario, here, it was assumed that the total horizontal projection area of inclined plates contributed to the increase of the settling area in lamella settling tanks. An improvement of SS removal efficiency was observed, as indicated by the increase of Hazen number for each particle group (**Fig 6.6**). As an example, particle group 3 in the settling tank was described by *Ha* of 1 and η of 0.61, while in Tank D (δ=1.16), these values were 2.16 and 0.65, respectively. However, in case *Ha* of particle group 3 was improved from 1 to 2.16, this corresponds to η of 0.9 in the settling tank. The results suggested that the *Ha'* in lamella settlers could not reach the calculated values, which means the accurate γ should less than 1.

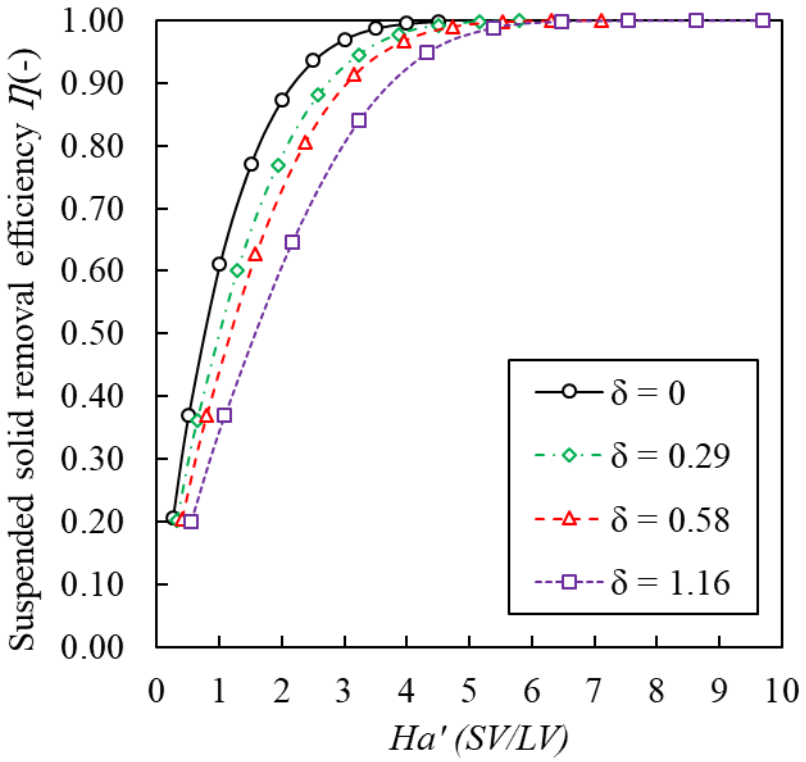

Fig 6.6 Curve *Ha-η* with a total contribution of inclined plates

6.3.2.3 Scenario 3: Accurate effectiveness of inclined plates to increase of settling area (accurate γ)

In this scenario, the actual improvement of settling capacity due to inclined plates, represented by an accurate value of α will be determined. As mentioned above, the increase of *Ha* number from Ha^0 to Ha^* for a particle group should agree with the improvement of η of such group in the settling tank (**Fig 6.7**). Hence, the curves Ha'-η should be converted into the curve Ha^0-η. For instance, particle group 3 in Tank D (δ=1.16) indicated the Ha^* of 1.11 and η of 0.65 on the curve Ha^0-η. Using this approach, the modified curves Ha'-η could be constructed and allowed to determine the accurate Ha^* and γ of lamella settlers.

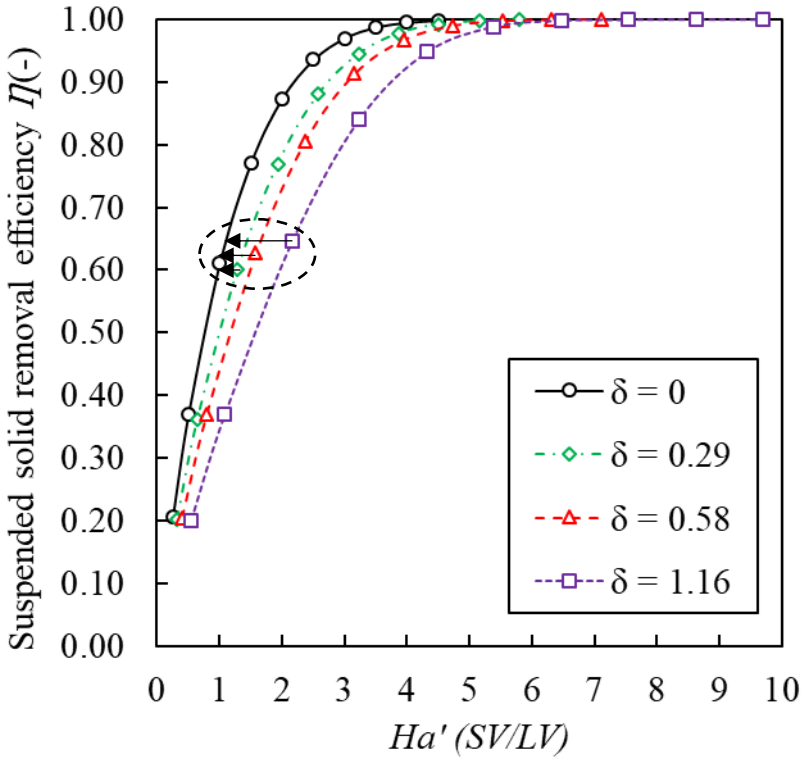

Before converting

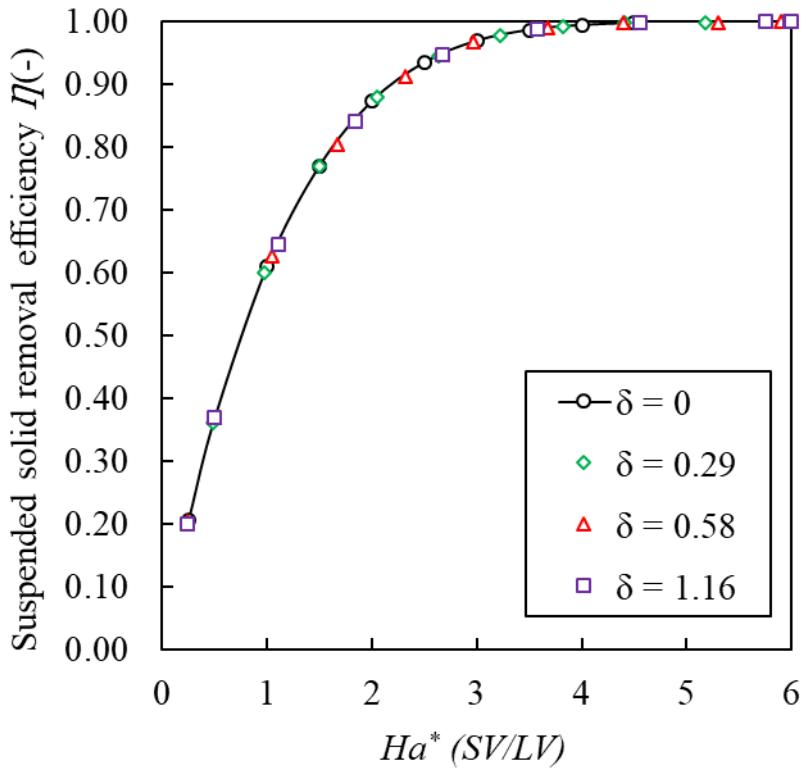

After converting

Fig 6.7 Curve *Ha-η* with an accurate contribution of inclined plates

6.3.3 Assessment the influence of inclined plates to Hazen number

The influence of inclined plates to Hazen number was shown in **Fig 6.8**. As observed, the calculation of coefficient γ provided acceptable results when the Ha number was lower than 3.5. When the Ha number was higher than 3.5, 4, and 4.5, which corresponding to δ = 1.16, 0.58, and 0.29 respectively, the calculated coefficient γ was inaccurate. It was because these particle groups had greater removal efficiencies than those of the largest particle group in the original clarifier. Therefore, the calculation of coefficient γ based on the predicted values from the curve of the original clarifier provided unreasonable value. For that reason, the discussion only focused on the particle groups with Hazen number lower than 3.5.

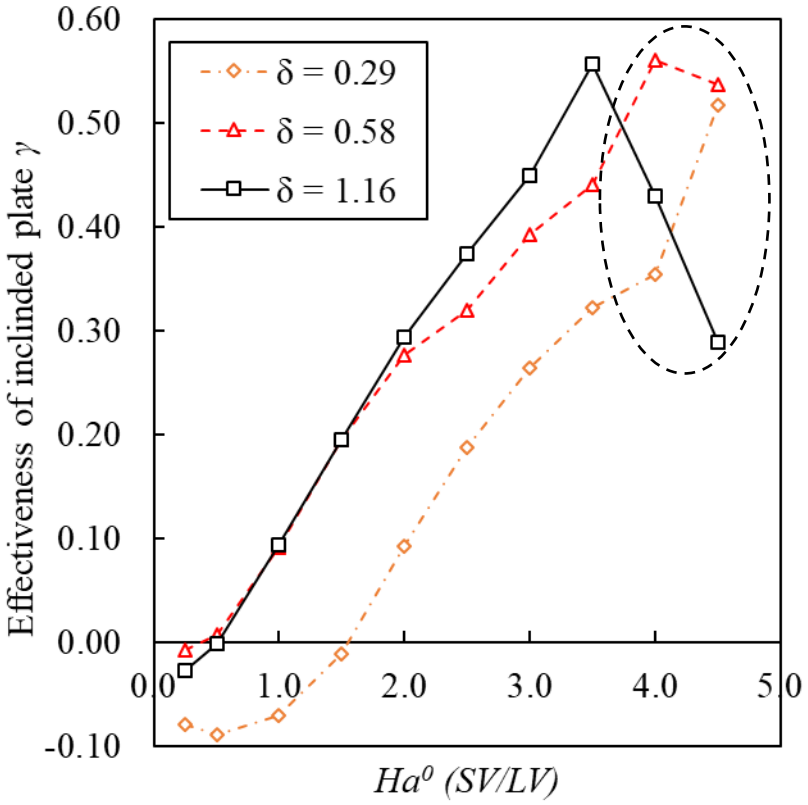

Fig 6.8 Influence of inclined plates to Hazen number

Simulation results showed that by installing more inclined plates (from 4 to 16 plates), the effectiveness of baffles could be increased. Surprisingly, the actual effectiveness of baffles is rather small (maximum 0.56) comparing to conventional design criteria (1.00) (**Fig 6.8**). Hence, the SS removal efficiency in operation might significantly lower than the designed one. In addition, inclined plates have different impacts on particle groups. Higher efficiencies were observed on particles with higher Hazen numbers. Settling tank design particularly focuses on particle groups having Hazen number from 2 to 4. As an example, for particle group with Hazen number of 3, the effectiveness of baffles increased from 26% to 45% as δ increased from 0.29 to 1.16.

6.3.4 Evaluation of hydraulic improvement due to inclined plates

6.3.4.1 Numbers of tanks

Tracer simulation results (**Fig 6.9** and **Fig 6.10**) showed the RTD curves and

numbers of tanks-in-series in settling tanks and lamella settlers. The elapsed time between the starting of tracer injection and its first appearance at the outlet were higher in lamella settlers than in settling tank, suggesting that the liquid resided longer in the tank and therefore reduced short-circuiting. Furthermore, the numbers of tanks were increased from 1.19 in settling tanks to be 2.05 in Tank D (δ=1.16), indicating an improvement of the hydraulic regime.

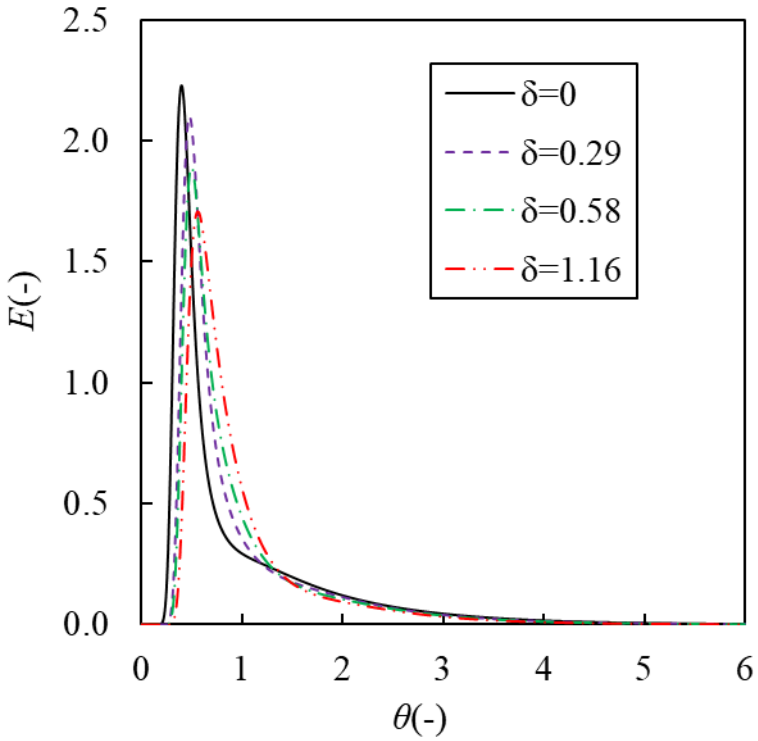

Fig 6.9 RTD curve from tracer results

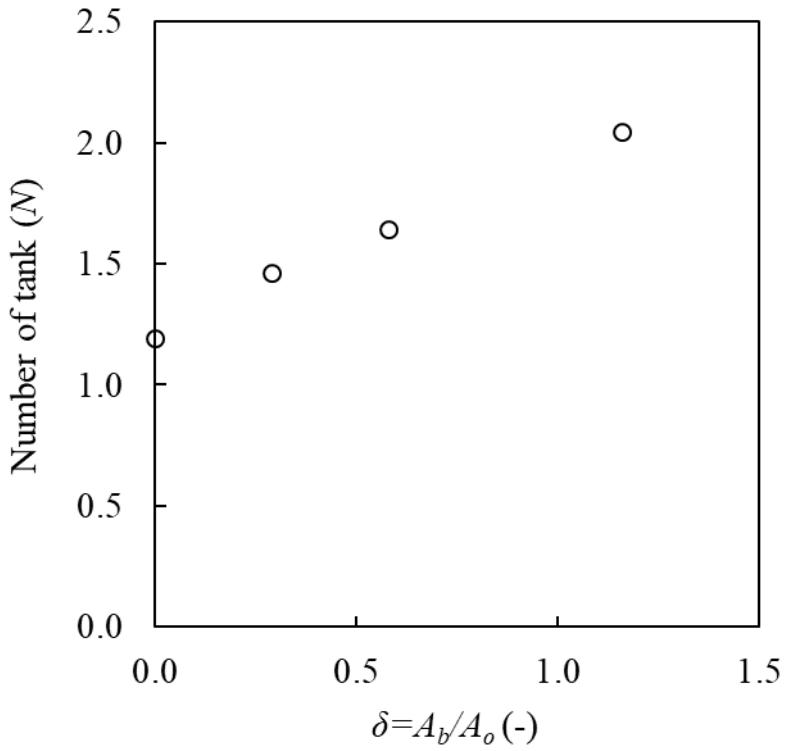

Fig 6.10 Relative between the number of tank (N) and δ

6.3.5 Comparison of suspended solid removal efficiency

The SS removal efficiency was calculated from direct simulation (equation (6.1)) and tracer simulation (equation (6.12)). As seen in **Fig 6.11**, the higher numbers of inclined plates to be installed, the better SS removal efficiency could be obtained. A good agreement between the two different approaches to SS removal efficiency indicated that the simulation was reliable.

The difference in SS removal efficiency between the tracer and direct simulations should be explained. As an illustration, for particles with *Ha*= 3 (**Fig 6.12**), the direct simulation indicated an increase of 3% of solids settling between Tank D (δ=1.16) and Tank A (δ=0.00), which was higher than nearly 2% obtained from tracer simulation. It should be noticed that tracer results reflect the flow pattern in the tanks. Hence, it was thought that the better hydraulic regime due to inclined plates was accounted for about 67% (2/3) in the total improvement on SS removal efficiency. For lamella settlers with

fewer baffles, e.g., δ=0.29, the SS removal efficiencies in two methods were similar and lower than the other lamella settlers. In this case, the hydraulic improvement might be the main factor for better solids settling.

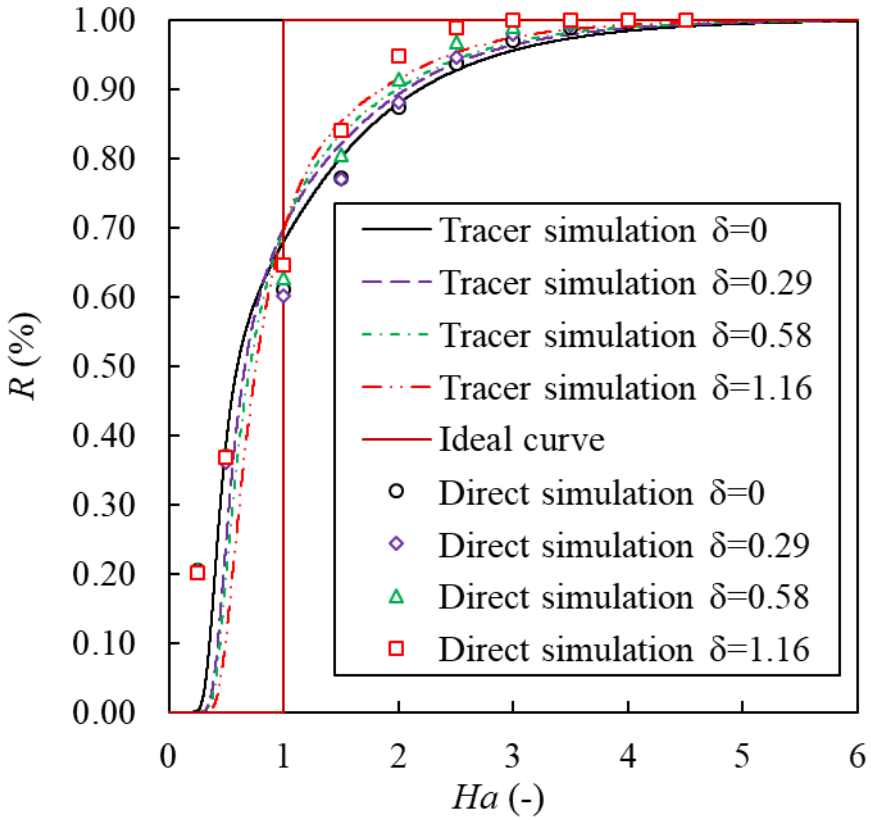

Fig 6.11 Direct simulation results and tracer simulation results

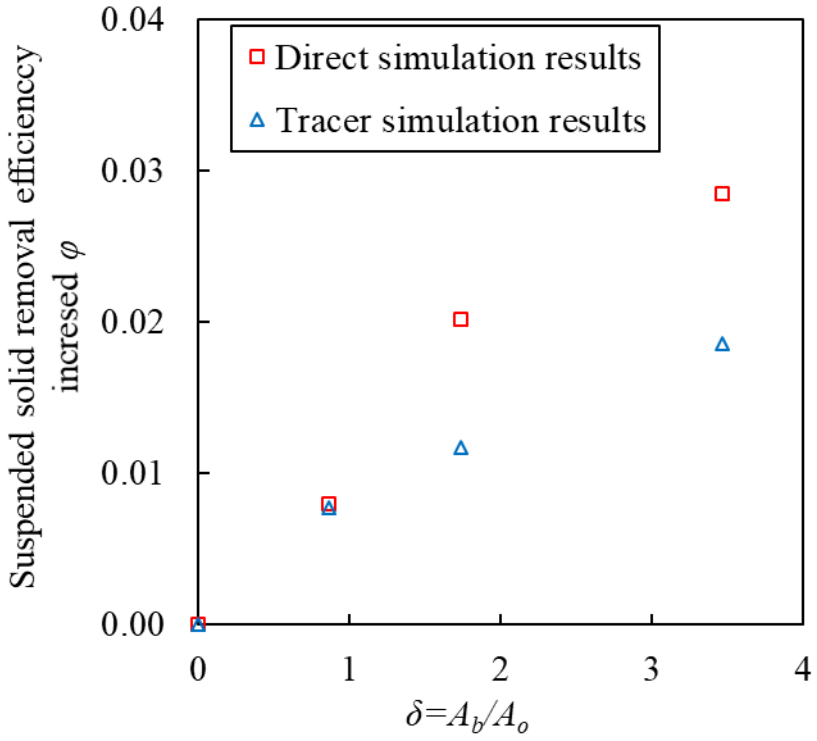

Fig 6.12 Direct simulation results and tracer simulation results with *Ha* = 3.0

Limitation of the simulation: In this study, the influence of other parameters, such as plate spacing and distance to the bottom of the tank, was not investigated. It is expected that the future simulation should consider these matters to reflect the actual profile of lamella settling tanks better.

6.4. CONCLUSION

In this chapter, the effectiveness of inclined plates in lamella settling tanks was investigated. CFD simulation indicated that the maximum of 56% of the horizontal projected area of baffles contributed to better solids settling in lamella settlers, which was significantly lower than traditional design criteria. Inclined plates were efficient for particle groups with Hazen number ranged from 2 to 4. Lamella settlers improved the hydraulic regime, reflected by higher numbers of tanks-in-series compared to settling tanks. The formation of reduced recirculation zone beneath the inclined plates and larger clearwater area at the outlet confirmed the better SS removal efficiency of lamella settlers compared to conventional settling tanks.

References

[5] W. F. Leung, “Lamella and Tube Settlers. 2. Flow Stability,” *Ind. Eng. Chem. Process Des. Dev.*, vol. 22, no. 1, pp. 68–73, 1983.

[6] A. Demir, “Determination of settling efficiency and optimum plate angle for plated settling tanks,” *Water Res.*, vol. 29, no. 2, pp. 611–616, 1995.

[7] K. Fujisaki and M. Terashi, “Improvement of settling tank performance using inclined tube settlers,” vol. 80, pp. 475–484, 2005.

[16] A. I. Stamou, E. W. Adams, and W. Rodi, “Modélisation numérique de l’écoulement et de la sedimentation dans des bassins de décantation primaires de forme rectangulaire,” *J. Hydraul. Res.*, vol. 27, no. 5, pp. 665–682, 1989.

[22] W. P. Kowalski, “The method of calculations of the sedimentation efficiency in tanks with lamella packets,” *Arch. Hydroengineering Environ. Mech.*, vol. 51, no. 4, pp. 371–385, 2004.

[24] R. Tarpagkou and A. Pantokratoras, “The influence of lamellar settler in sedimentation tanks for potable water treatment - A computational fluid dynamic study,” *Powder Technol.*, vol. 268, pp. 139–149, 2014.

[25] M. Weiss, B. G. Plosz, K. Essemiani, and J. Meinhold, “CFD modelling of sludge sedimentation in secondary clarifiers,” *WIT Trans. Eng. Sci.*, vol. 52, pp. 509–518, 2006.

[42] K. Mohanarangam and D. Stephens, “Cfd Modelling of Floating and Settling Phases in Settling Tanks,” *Victoria*, no. December, pp. 1–7, 2009.

[44] A. M. Goula, M. Kostoglou, T. D. Karapantsios, and A. I. Zouboulis, “A CFD methodology for the design of sedimentation tanks in potable water treatment. Case study: The influence of a feed flow control baffle,”

Chem. Eng. J., vol. 140, no. 1–3, pp. 110–121, 2008.

[51] H. Asgharzadeh, B. Firoozabadi, and H. Afshin, "Experimental investigation of effects of baffle configurations on the performance of a secondary sedimentation tank," *Sci. Iran.*, vol. 18, no. 4 B, pp. 938–949, 2011.

[52] M. Shahrokhi and F. Rostami, "The Computational Modeling of Baffle Configuration in the Primary Sedimentation Tanks," *Flow3D2.Propagation.Net*, vol. 6, pp. 392–396, 2011.

[55] M. M. Heydari, M. S. Bajestan, H. A. Kashkuli, and H. Sedghi, "The effect angle of baffle on the performance of settling basin," *World Appl. Sci. J.*, vol. 21, no. 6, pp. 829–837, 2013.

[64] Ghawi, "Application of Computational Fluid Dynamics modelling to a horizontal sedimentation tank," no. April, 2017.

[66] Y. L. Liu, W. L. Wei, B. Lv, and X. F. Yang, "Research on optimal radius ratio of impellers in an oxidation ditch by using numerical simulation," *Desalin. Water Treat.*, vol. 52, no. 13–15, pp. 2811–2816, 2014.

[67] W. Wei, Y. Liu, and B. Lv, "Numerical simulation of optimal submergence depth of impellers in an oxidation ditch," *Desalin. Water Treat.*, vol. 57, no. 18, pp. 8228–8235, 2016.

[68] A. I. Stamou, G. Theodoridis, and K. Xanthopoulos, "Design of secondary settling tanks using a CFD model," *J. Environ. Eng.*, vol. 135, no. 7, pp. 551–561, 2009.

[72] Ghawi and J. Kri, "A Computational Fluid Dynamics Model of Flow and Settling in Sedimentation Tanks," *Appl. Comput. Fluid Dyn.*, 2012.

[73] Japan Sewage Works Association, *Design Standard for Municipal Wastewater Treatment Plants*. Tokyo, Japan: Japan Sewage Works Association, 2013.

[75] M. Terashima, M. Iwasaki, H. Yasui, R. Goel, K. Suto, and C. Inoue,

"Tracer experiment and RTD analysis of DAF separator with bar-type baffles," *Water Sci. Technol.*, vol. 67, no. 5, pp. 942–947, 2013.

CHAPTER 7 IMPROVEMENT OF SLUDGE SETTLING MODELLING IN SECONDARY SEDIMENTATION TANK USING CFD

7.1. INTRODUCTION

The secondary sedimentation tank (SST) is applied in biological wastewater treatment systems to remove activated sludge due to gravity. Many studies have focused on simulation to predict sludge concentration distribution for the effective design and operation of SSTs. The important factor affecting simulation results is the settling velocity model of sludge particles. François [27] studied activated sludge settling mechanisms using the experiment method. The results of a detailed activated sludge velocity profile were applied to build numerical models in the simulation settling process. Weiss [25] investigated the sedimentation of activated sludge using a CFD model to simulate a full-scale circular secondary sedimentation, but the simulation results incorrectly predicted the sludge concentration in a larger distance from the inlet zone. Ramin [26] developed a new settling velocity model that involved the effect of resistance, transient, and compression on sludge distribution. These earlier studies applied settling velocity model for one particle group with settling slope (k_s) and maximum settling velocity (SV_0) from the measurement results. Conventionally, the smallest SV_0 of sludge particle was measured, but the larger SV_0 which should be available and included in the model was not observed. In this study, simulations were performed to compare the conventional model with one particle group and the modified model with multiple particle groups. The CFD model was used to simulate the settling process in the SST. Full-scale measurements were performed in SST at four wastewater treatment plants (WWTPs) to validate the simulation results in the CFD model.

7.2. MATERIALS AND METHODS

7.2.1 Numerical modelling methods

The Algebraic Slip Model was used in this simulation. Turbulence in the liquid phase was modelled using the *k-ε* model, which successfully simulated the sedimentation tank in previous research [64]. In this study, the commercial software CFX 18.0 (in ANSYS) was used to perform CFD modelling. The hydrodynamic and flow behavior in the SST was performed in the two-dimensional model (2D).

Settling velocity was modeled as the function of sludge concentration using Vesilind model

$$SV = SV_0 \cdot e^{-k_s X} \tag{7.1}$$

where

SV_0: Maximum settling velocity (m/h)

k_s: Settling slope (-)

X: sludge concentration (kg/m^3)

The maximum of SV was determined at sludge concentration of 1 kg/m^3 (Goel, Terashima and Yasui, 2004 [81]).

The Vesilind model was applied in the prediction of sludge blanket height in 1-D by calculating the settling velocity of the smallest particle group. In 2-D simulation, the sludge blanket height was affected by the larger particle groups. Therefore, the simulated results were inconsistent with the measured data. In this study, it was obligated to manipulate the coefficient of SV_0 without experimental evidence.

7.2.2 Model geometry and boundary condition simulation

Simulations were performed using SST configurations which located in the K, H, Ko, I, and Ry WWTPs, respectively. Here, a configuration of K SST was used in modelling, as shown in **Fig 7.1**.

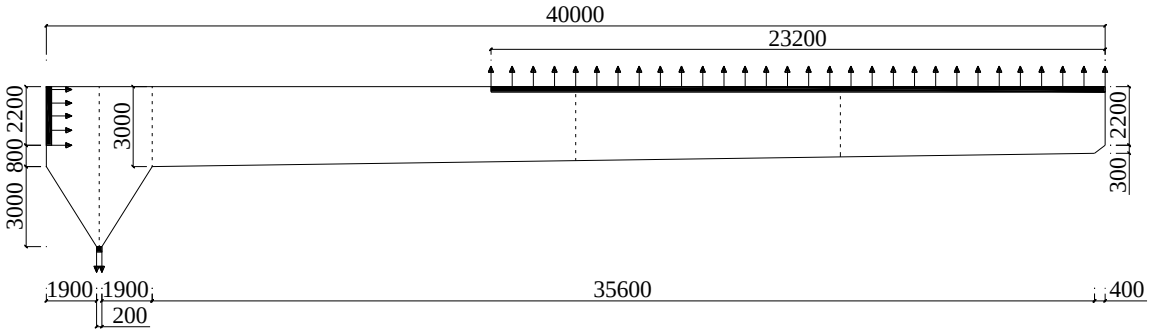

Sludge concentration was monitored at four positions.

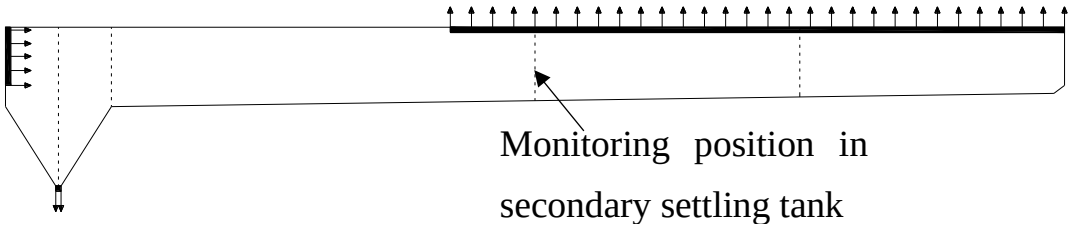

Fig 7.1 Geometry of SST in K WWTP

The K, H, Ko, I, and Ry SST were simulated with the parameters listed in **Table 7.1**.

Table 7.1 Simulation condition for K, H, Ko, I, and Ry SSTs

WWTP		Outlet 1 (m^3/h)	Outlet 2 (m^3/h)	Influent sludge concentration (kg/ m^3)	k_s (-)	SV_0 (m/h)
K		573	411	2.160	0.85	14.26
H	1	287	80	1.060	0.73	19.30
	2	183	51	1.060	0.73	19.30
Ko	1	140	69	1.670	0.85	13.11
	2	179	69	1.670	0.85	13.11

I	1	324	113	1.120	1.02	13.49
	2	378	132	1.060	1.02	13.49
Ry	1	156	45	1.450	0.82	13.20
	2	136	39	1.200	0.82	13.20

7.2.3 Selection of appropriate groups of particles

To verify the sensitivity of group numbers, the simulation of K secondary settling tank was conducted at different particle groups ranging from 1 to 20. The maximum settling velocity (SV_0) for each particle group was defined as the following:

Simulation of single particle group: $SV_{01} = SV_0$ (measured)

Simulation of multiple particle groups (from 2 to 20):

- The smallest $SV_{01} = SV_0$ (measured)
- The largest $SV_{020} = 2.8*SV_0$
- The settling velocities for other particle groups were evenly distributed between SV_0 and $2.8*SV_0$

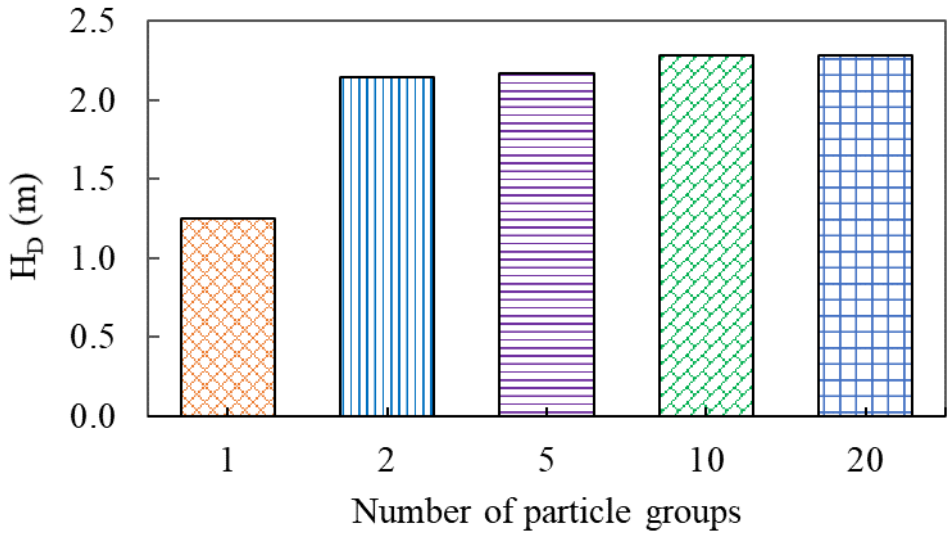

Fig 7.2 The water depth at sludge concentration of 2 kg/m^3 in the middle of the secondary settling tank

By increasing particle groups (**Fig 7.2**), the water depth (H_D) increased from

1.25 to 2.28 m. The groups from 10 to 20 provided results without much difference. Hence, 10 groups of particles were used for the following simulations.

7.2.4 Sludge settling velocity

Two simulation scenarios were carried out with the conventional settling velocity model and the modified settling velocity model. In the first scenario, the conventional settling velocity model with one particle group was simulated with k_s of 0.85 and SV_0 of 14.26 m/h from measurement results in K WWTP. In the second one, the measured k_s was used for simulation with 10 particle groups, the smallest SV_0 was the measured SV_0, and the larger SV_0 distribution was assumed to increase from 1.2 to 2.8SV_0 for particle groups 2 to 10, respectively. The mass fraction was assumed equally for each particle group of 0.0002. These two assumptions were applied for SST simulation at H, Ko, I, and Ry WWTPs.

7.2.5 Tracer simulation method

The tracer simulation was carried out for the Ry secondary settling tank. The configuration of Ry SST was used in modelling, as shown in **Fig 7.3**.

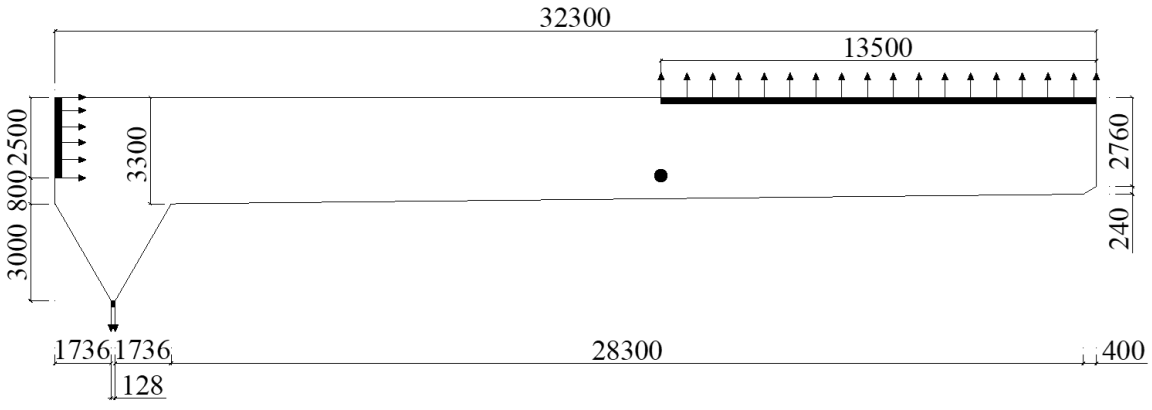

Sludge concentration was monitored at one position.

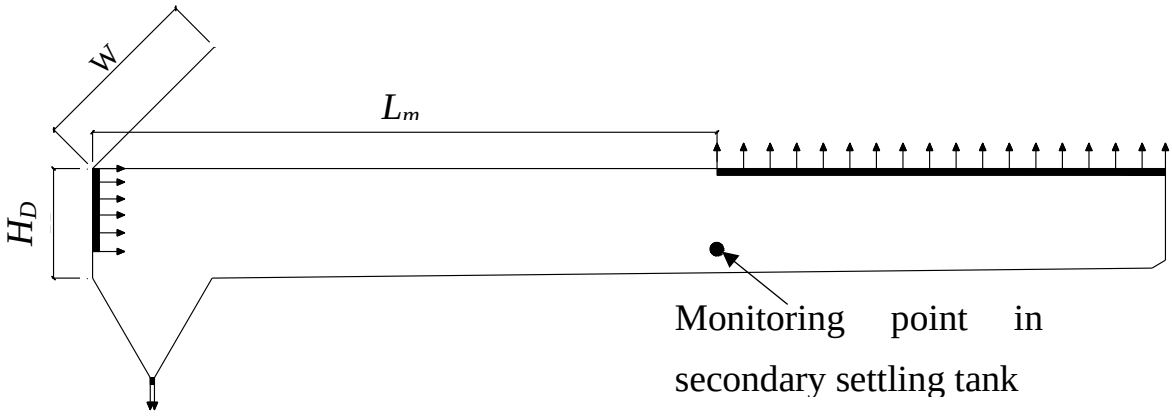

Fig 7.3 Geometry of SST in Ry WWTP

The hydraulic regime of the tanks was assessed using a tracer simulation. A tracer concentration of 0.01 kg/kg was introduced into the inlet (flow rate, Q=175 m^3/h) for a long period (step input). The data for tracer concentrations at the outlet and monitoring position were recorded to plot a residence time distribution and calculated *C/C_0-curve*. The value of 0.1 from *C/C_0-curve* corresponds to the normalized time θ_{10}, indicating that 10% of the C_0 was discharged at the outlet or monitoring position.

Step input method was applied for tracer simulation

θ: Dimensionless time units (-)

$$\theta = t/t^*_m \tag{7.2}$$

t^*_m: Hydraulic retention time at the monitoring position

$$t^*_m = V_m/Q_1 \tag{7.3}$$

where

Q_1: outlet 1 flow rate

V_m: The volume of secondary settling tank from inlet to monitoring position

$$V_m = W \times H_D \times L_m \tag{7.4}$$

where

W: the width of the tank

H_D: the depth of the tank

L_m: the length from inlet to the monitoring position

7.3. RESULTS AND DISCUSSION

7.3.1 Sludge concentration distribution in K secondary settling tank

The results in **Fig 7.4** showed that the sludge distribution in the simulation SST with 10 particle groups was consistent with the settling regime in the tank. The sludge distribution was decreased along the length of the tank. Meanwhile, the simulation with a single particle group indicated that the sludge distribution was not significantly varied along the length of the tank, which was not properly described the reality. The curve of sludge blanket height of 2 kg/m^3 in the case of 10 groups was closer to the experimental data but far different in the case of a single group. Particularly, the settling slope in simulation with 10 groups of particles was agreed with experimental measurement, while this could not obtain in the other case.

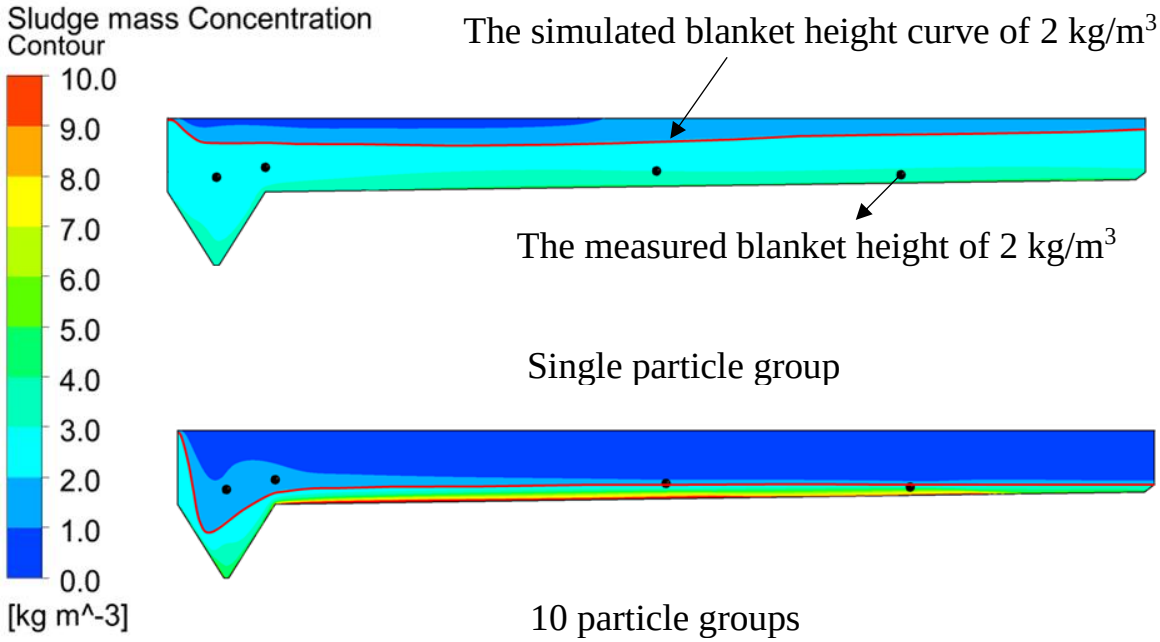

Fig 7.4 The blanket height curve of 2 kg/m^3 in simulation and measurement results

7.3.2 Comparisons on sludge concentration between simulation and measurement results

From the results in **Fig 7.5**, the sludge concentration distribution curves in the simulation with 10 particle groups had a similar trend with these curves in experimental results. Specifically, at positions II, III, and IV (from 0 to 2 m of depth), sludge concentration increased slowly from zero to approximately 2 kg/m^3. However, the curves increased dramatically at 6 kg/m^3 for position II and 12 kg/m^3 for positions III and IV (3 m of depth). On the contrary, the simulation results with one particle group showed that there was a slight increase in sludge concentration from 1 to 4 kg/m^3 at depths from 0 to 3 m. Consequently, the difference between simulation results with 10 particle groups and experimental results was smaller than those in the simulation with one particle group. At position I, the sludge concentration difference between simulation and measurement results was insignificant in both scenarios.

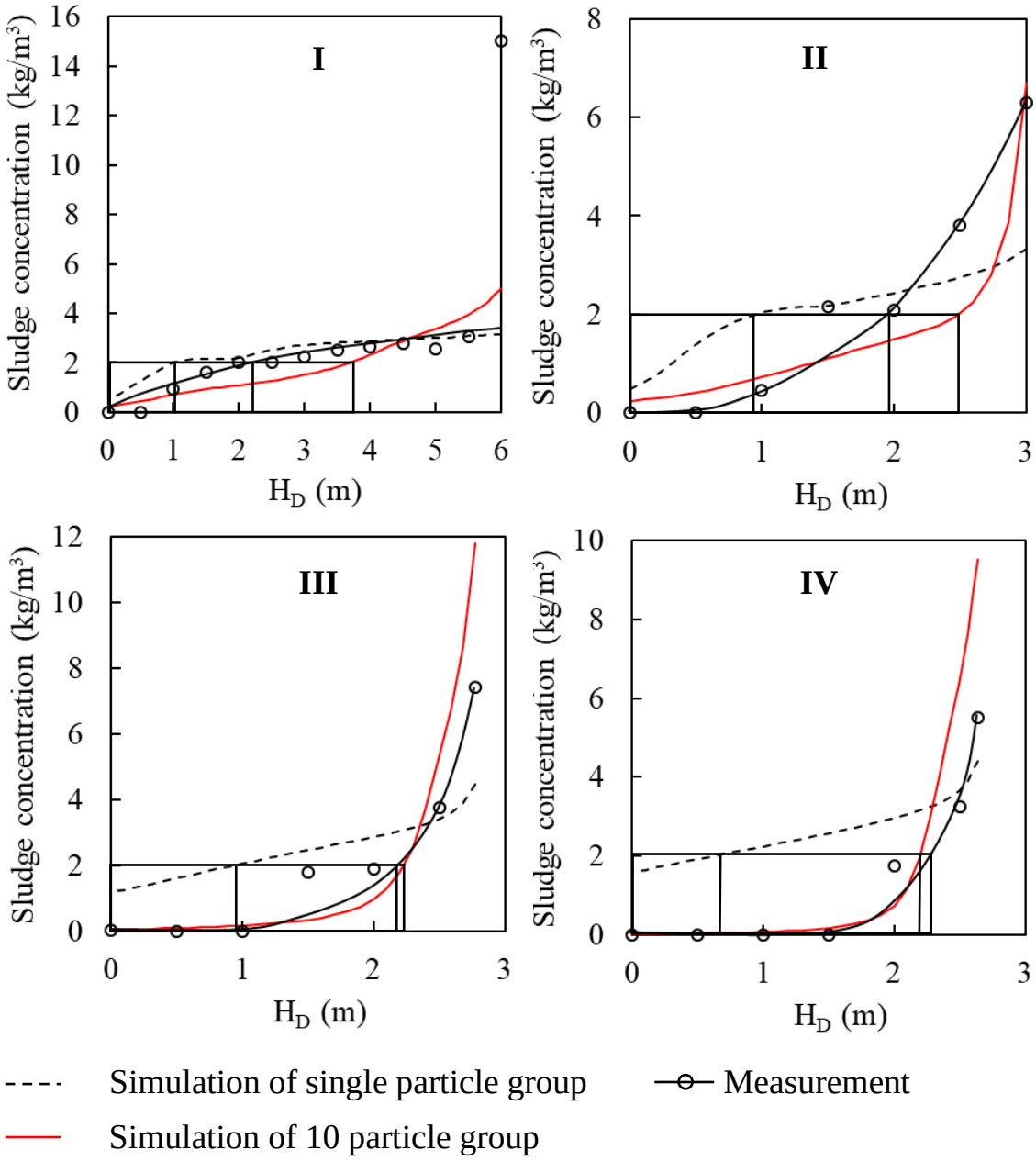

Fig 7.5 Relationship between sludge concentration and water depth in K WWTP

7.3.3 Comparision on water depth between simulation and measurement results

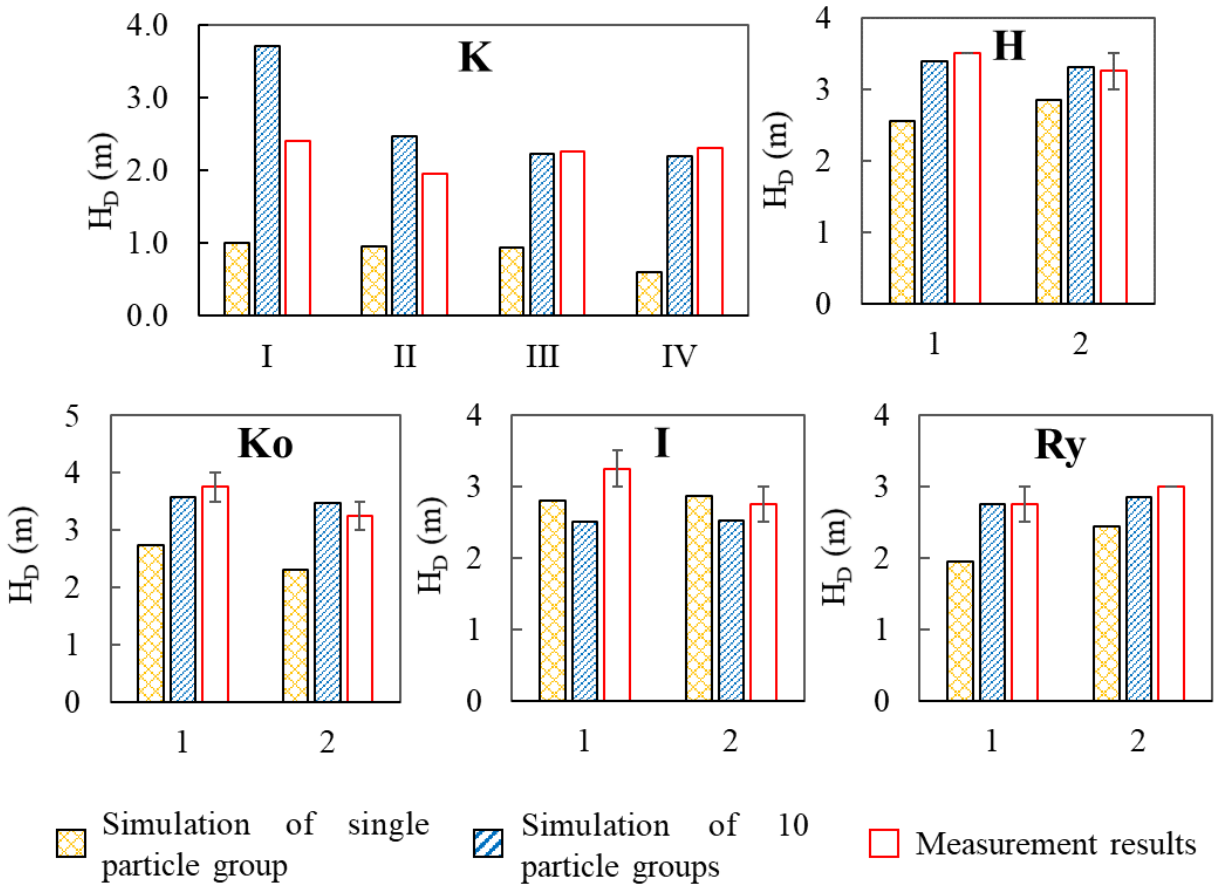

Fig 7.6 Comparison of water depth between measurement and simulation results with a sludge concentration of 2 kg/m^3

At the same sludge concentration of 2 kg/m^3, the significant differences between the simulation water depth with one particle group and experiment water depth in K, H, Ko, and Ry SSTs were shown in **Fig 7.6**. In contrast, there are small differences between simulation water depth with 10 particle groups and experimental water depth in SSTs. Simulation results with 4 data sets showed that the sludge distribution in the SST was better predicted due to the simulating of multiple particle groups compared to the simulating of the single particle group.

However, a larger difference was observed in the simulation with 10 particle groups compared to a single particle group in the I SST. These results indicated that the initial assumption about the settling velocity for each particle group was not reasonable with the actual distribution of sludge. Therefore, the simulation results did not accurately predict the distribution of sludge in the SST.

7.3.4 Tracer simulation results

Tracer simulation results in **Fig 7.7** show that the hydraulic regime in the tank is affected by the density current. At the time $\Theta = 1$, the tracer concentration of 0.01 has passed the observation point (in theory, tracer concentration of 0.01 starts appearing at the observation point with $\Theta = 1$), it means that a short-circuiting occurred in the SST. Thus, the hydraulic regime in the tank is greatly affected by the density current.

Tracer curve simulation results also show the influence of density current in the tank. According to the theory, when the tank is steady-state and unaffected by density current, the tracer curve at the observed locations will overlap. However, in **Fig 7.8**, these lines do not overlap, showing the effect of density current on the flow regime in the tank.

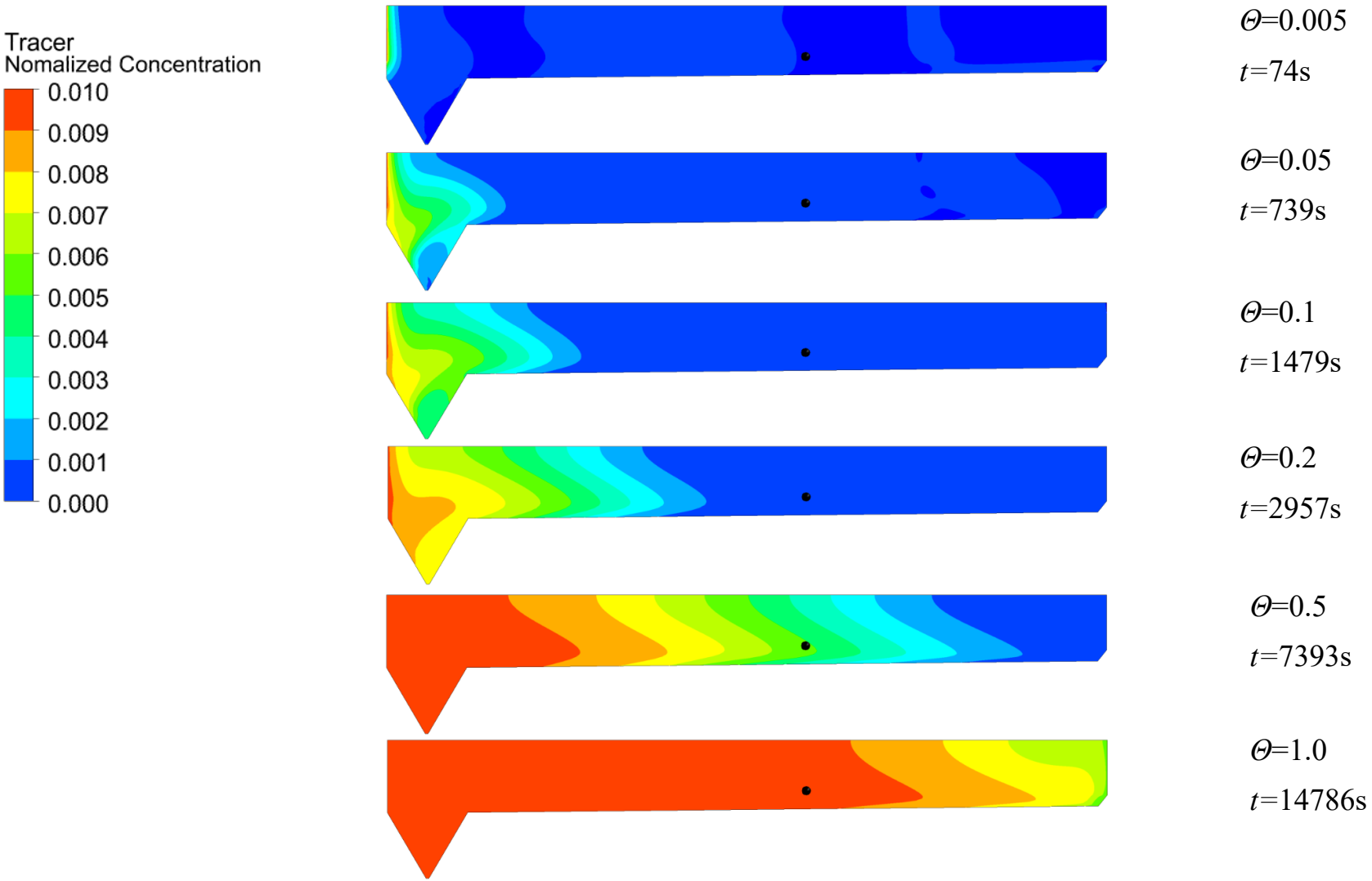

Fig 7.7 Tracer distribution in secondary settling tank at difference Θ

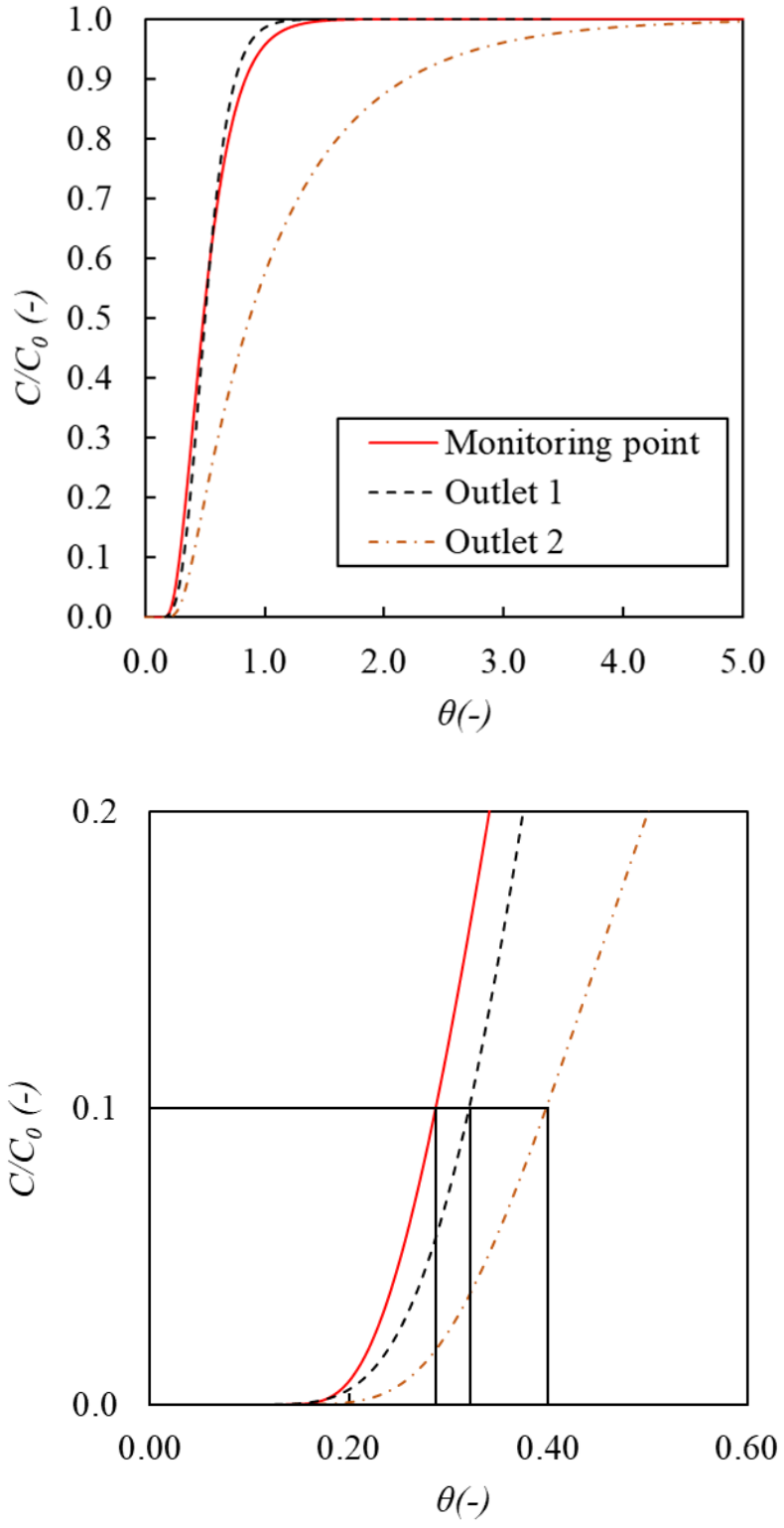

Fig 7.8 Tracer curve for monitoring point, outlet 1 and outlet 2

7.4. CONCLUSION

The study evaluated the effect of the settling velocity model on predicting sludge distribution in SST. In the conventional settling velocity model, only the smallest SV_0 was measured and used for simulation. Therefore, the simulation results did not accurately reflect the settling process occurring in SSTs. In this study, the modified settling velocity model was proposed, which offered a new concept for the SST simulation. Specifically, simulation results indicated that the minor differences between the simulation with modified settling velocity model and sludge concentration measurement results were observed. However, the SV_0 distribution and the mass fraction of multiple particle groups should be measured to improve the simulation accuracy in further research.

References

[25] M. Weiss, B. G. Plosz, K. Essemiani, and J. Meinhold, “CFD modelling of sludge sedimentation in secondary clarifiers,” *WIT Trans. Eng. Sci.*, vol. 52, pp. 509–518, 2006.

[26] E. Ramin *et al.*, “A new settling velocity model to describe secondary sedimentation,” *Water Res.*, vol. 66, pp. 447–458, 2014.

[27] P. François, F. Locatelli, J. Laurent, and K. Bekkour, “Experimental study of activated sludge batch settling velocity profile,” *Flow Meas. Instrum.*, vol. 48, pp. 112–117, 2016.

[64] Ghawi, “Application of Computational Fluid Dynamics modelling to a horizontal sedimentation tank,” no. April, 2017.

[81] R. Goel, M. Terashima, and H. Yasui, “Application of CFD to study the effects of Feed-well configuration on suspended solid concentration profile in settling tank,” in *Hydroinformatics*, World Scientific, 2004, pp. 316–323.

CHAPTER 8 CONCLUSIONS AND RECOMMENDATIONS

The dissertation presented the study of sedimentation tanks in water and wastewater treatment. The study applied the CFD model to simulate sedimentation tanks, which helped reduce the time-spent and cost of the research compared to experimental studies. Many influencing factors are included in the model to assess the effectiveness of the tank. The study focused on simulating the two settling processes in primary and secondary settling tanks. In primary settling tanks, the simulation was performed on lamella settling tanks with a different number of inclined plates and inclined plates configurations. The main purpose of the study is to evaluate the effect of the increased settling area due to the inclined plates on the SS removal efficiency in the tank, thereby proposing solutions to optimize the design and operation of the settling tank. For secondary settling tanks, the study proposes a new concept for the settling model to be used to simulate the settling process instead of the conventional settling model. It aimed at predicting the sludge distribution in the tanks with higher accuracy, which is important for the operation of secondary settling tanks.

8.1. PRINCIPLE FINDINGS

Chapter 4 investigated the effect of inclined plates on the performance of lamella settling tanks. The results showed that the increased settling area due to the inclined plates helped to increase the SS removal efficiency in the tank, in which the removal efficiency varied with each group of particles. The actual effectiveness of the increased settling area attainable flow rate in the tank was only 0.2364, significantly lower than the theoretical calculation of 1. The simulation results with different inclined plate configurations having the same settling area showed that the hydraulic regime in the settling tank also affects the SS removal efficiency.

Chapter 5 studied the influence of increased settling area by installing an inclined plate or increasing the length or width of the tank dimension to SS removal efficiency of small settling velocity particles. The simulation results showed that the SS removal efficiency of small settling velocity particles was improved by increasing the settling area in all three cases. In particular, the increased settling area due to increasing the length had the largest contribution to remove the efficiency of small settling velocity particle groups with the β = 0.74. However, this coefficient was much lower than the ideal coefficient with β = 1. The result would contribute significantly to the renovated design of settling tanks in the water and wastewater treatment plant, in which the tank performance was optimized.

Chapter 6 focused on the simulation of sedimentation tanks with a different number of inclined plates to assess the impact of inclined plates on the hydraulic regime in tanks. In the study, the Hazen number was used to evaluate the ability of SS removal to be increased by inclined plates. The results showed that the Hazen number was increased in each particle group by increasing the number of inclined plates. The actual contribution of the settling area to the Hazen number was recorded as the largest as 0.56, which was significantly

lower than the theoretical value of 1. The results were also consistent with the simulation results in Chapters 4 and 5. The calculation of the N and the tracer curve clarified the effect of the inclined plates on the hydraulic regime and the SS removal efficiency in the tanks.

Chapter 7 proposed a new concept in the simulation of sludge in which ten particle groups were applied for simulation instead of a single particle group as in conventional simulation. The simulation results with ten particle groups showed that the distribution of sludge in the secondary settling tanks was similar to the experimental observation results. In particular, the settling slope in the simulation with ten particle groups had the same tendency to the measurement results, which could not be predicted by simulation with a single particle group. Therefore, the new concept with multiple particle groups was suitable for simulating the distribution of sludge in the secondary settling tanks.

The above findings reflected the difference between the calculation formula in ideal conditions and simulation in operating conditions. The research results provided the basis for the optimal studies in the design, renovation, and operation of sedimentation tanks. At the same time, the study also increased the understanding of the nature of the internal processes of the sedimentation tank by visual images. Moreover, a better understanding of the nature of the processes occurring in the sedimentation tank was clarified by visual images obtained from CFD software.

8.2. FUTURE WORK

In this study, many factors that influence the performance of the sedimentation tank were defined in the CFD model. However, some assumptions were still used in the simulation process. Further studies need to address some of the following issues:

In the primary settling tank, the model eliminated the interaction factor between the suspended solid particles, which may affect the SS removal efficiency of the tank. Temperature and depth were kept as constant values in the simulation, although their variation might directly affect the hydraulic regime in a tank. For optimal design, renovation, and operation, it is necessary to assess the effect of changes in temperature and depth of the tank.

The results in chapter 5 showed that the SS removal efficiency was highest when increasing the length of the tank. However, this option is very difficult to arrange the layout of the tank. Therefore, the layout of the zigzag flow direction is proposed as the optimal selection for the design. Simulation for this type of configuration needs to be simulated to assess the performance of sedimentation tanks.

In the secondary settling tanks, the number of particle groups and the settling velocity of each particle group were based on assumption. If these two parameters were determined, the model could be improved. However, this task might be experimentally challenging. Therefore, based on the measured of sludge blanket height, the number of particle groups and their settling velocities could be obtained using the back-calculation approach. The model, after being corrected with measurement data, will be applied to predict the distribution of sludge under different conditions of the tank.

REFERENCES

[1] G. A. Ekama *et al.*, "Secondary settling tanks: theory, modelling and operation.," in *IAWQ Scientific and Technical Report No. 6.*, London, 1997.

[2] L. Piirtola, B. Hultman, C. Andersson, and Y. Lundeberg, "Activated sludge ballasting in batch tests," vol. 33, no. 8, pp. 3–8, 1999.

[3] D. G. Christoulas, P. H. Yannakopoulos, and A. D. Andreadakis, "An empirical model for primary sedimentation of sewage," *Environ. Int.*, vol. 24, no. 8, pp. 925–934, 1998.

[4] M. Jover-Smet, J. Martín-Pascual, and A. Trapote, "Model of suspended solids removal in the primary sedimentation tanks for the treatment of urban wastewater," *Water (Switzerland)*, vol. 9, no. 6, 2017.

[5] W. F. Leung, "Lamella and Tube Settlers. 2. Flow Stability," *Ind. Eng. Chem. Process Des. Dev.*, vol. 22, no. 1, pp. 68–73, 1983.

[6] A. Demir, "Determination of settling efficiency and optimum plate angle for plated settling tanks," *Water Res.*, vol. 29, no. 2, pp. 611–616, 1995.

[7] K. Fujisaki and M. Terashi, "Improvement of settling tank performance using inclined tube settlers," vol. 80, pp. 475–484, 2005.

[8] T. McKean, "Novel Application of a Lamella Clarifier for Improved Primary Treatment of Domestic Wastewater," no. 118, pp. 119–124, 2010.

[9] G. C. Chintokoma, R. L. Machunda, and K. N. Njau, "Optimization of Sedimentation Tank Coupled with Inclined Plate Settlers as a Pre-treatment for High Turbidity Water," vol. 5, no. 17, pp. 11–24, 2015.

[10] J. Bridgeman, B. Jefferson, and S. A. Parsons, "The development and application of CFD models for water treatment flocculators," *Adv. Eng.*

Softw., vol. 41, no. 1, pp. 99–109, 2010.

[11] M. Terashima *et al.*, "CFD simulation of mixing in anaerobic digesters," *Bioresour. Technol.*, vol. 100, no. 7, pp. 2228–2233, 2009.

[12] Y. Fayolle, A. Cockx, S. Gillot, M. Roustan, and A. Héduit, "Oxygen transfer prediction in aeration tanks using CFD," *Chem. Eng. Sci.*, vol. 62, no. 24, pp. 7163–7171, 2007.

[13] W. B. Rauen, A. Angeloudis, and R. A. Falconer, "Appraisal of chlorine contact tank modelling practices," *Water Res.*, vol. 46, no. 18, pp. 5834–5847, 2012.

[14] D. L. Huggins, R. H. Piedrahita, and T. Rumsey, "Use of computational fluid dynamics (CFD) for aquaculture raceway design to increase settling effectiveness," *Aquac. Eng.*, vol. 33, no. 3, pp. 167–180, 2005.

[15] E. Imam, J. A. McCorquodale, and J. K. Bewtra, "Numerical modeling of sedimentation tanks," *J. Hydraul. Eng.*, vol. 109, no. 12, pp. 1740–1754, 1983.

[16] A. I. Stamou, E. W. Adams, and W. Rodi, "Modélisation numérique de l'écoulement et de la sedimentation dans des bassins de décantation primaires de forme rectangulaire," *J. Hydraul. Res.*, vol. 27, no. 5, pp. 665–682, 1989.

[17] J. A. McCorquodale, "Numerical Simulation of Unsteady Conditions in Clarifiers," *Water Poll. Res. J. Canada*, vol. 26, no. 2, pp. 201–222, 1991.

[18] S. Zhou, J. A. McCorquodale, and Z. Vitasovic, "Influences of density on circular clarifiers with baffles," *J. Environ. Eng. (United States)*, vol. 118, no. 6, pp. 829–847, 1992.

[19] Y. C. Jin, Q. C. Guo, and T. Viraraghavan, "Modeling of Class I settling tanks," *J. Environ. Eng.*, vol. 126, no. 8, pp. 754–760, 2000.

[20] K. Ramalingam *et al.*, "Critical modeling parameters identified for 3D CFD modeling of rectangular final settling tanks for New York City wastewater treatment plants," *Water Sci. Technol.*, vol. 65, no. 6, pp.

1087–1094, 2012.

[21] A. Ghawi and J. Kriš, “Improvement performance of secondary clarifiers by a computational fluid dynamics model,” *Slovak J. Civ. Eng.*, vol. 19, no. 4, pp. 1–11, 2012.

[22] W. P. Kowalski, “The method of calculations of the sedimentation efficiency in tanks with lamella packets,” *Arch. Hydroengineering Environ. Mech.*, vol. 51, no. 4, pp. 371–385, 2004.

[23] Y. Shen and K. Yanagimachi, “CFD-aided cell settler design optimization and scale-up: Effect of geometric design and operational variables on separation performance,” *Biotechnol. Prog.*, vol. 27, no. 5, pp. 1282–1296, 2011.

[24] R. Tarpagkou and A. Pantokratoras, “The influence of lamellar settler in sedimentation tanks for potable water treatment - A computational fluid dynamic study,” *Powder Technol.*, vol. 268, pp. 139–149, 2014.

[25] M. Weiss, B. G. Plosz, K. Essemiani, and J. Meinhold, “CFD modelling of sludge sedimentation in secondary clarifiers,” *WIT Trans. Eng. Sci.*, vol. 52, pp. 509–518, 2006.

[26] E. Ramin *et al.*, “A new settling velocity model to describe secondary sedimentation,” *Water Res.*, vol. 66, pp. 447–458, 2014.

[27] P. François, F. Locatelli, J. Laurent, and K. Bekkour, “Experimental study of activated sludge batch settling velocity profile,” *Flow Meas. Instrum.*, vol. 48, pp. 112–117, 2016.

[28] B. Firoozabadi, “Hydraulic performance of primary settling tanks,” pp. 1–6, 2005.

[29] J. Bridgeman, B. Jefferson, and S. A. Parsons, “Computational Fluid Dynamics Modelling of Flocculation in Water Treatment: A Review,” *Eng. Appl. Comput. Fluid Mech.*, vol. 3, no. 2, pp. 220–241, 2009.

[30] G. Arbat *et al.*, “Hydrodynamic behaviour of the underdrains in microirrigation sand media filters using CFD software,” *Acta Hortic.*,

vol. 1008, pp. 85–90, 2013.

[31] H. Yeung, “Modelling of service reservoirs,” *J. Hydroinformatics*, vol. 3, no. 3, pp. 165–172, 2001.

[32] J.-M. Zhang;, B. C. Khoo;, H. P. Lee;, C. P. Teo;, N. Haja;, and and K. Q. Peng;, “Numerical Simulation and Assessment of the Effects of Operation and Baffling on a Potable Water Service Reservoir,” *J. Environ. Eng.*, vol. 139, no. March, pp. 341–348, 2013.

[33] “No Title.” [Online]. Available: https://researchbank.swinburne.edu.au/file/7b8f18b0-2f6e-4498-87bc-951a77960948/1/Alamgir Hossain Thesis.pdf.

[34] R. W. Samstag *et al.*, “CFD for wastewater treatment: An overview,” *Water Sci. Technol.*, vol. 74, no. 3, pp. 549–563, 2016.

[35] M. So, “Multiscale modelling of biofilm in sponge carrier media,” The University of Kitakyushu, 2014.

[36] D. Zhang, “Optimize sedimentation tank and lab flocculation unit by CFD,” Norwegian University of Life Sciences, 2014.

[37] The open university, “Potable water treatment.” [Online]. Available: https://www.open.edu/openlearn/science-maths-technology/engineering-and technology/technology/potable-water-treatment/content-section-4.4. [Accessed: 03-Feb-2020].

[38] P. Larsen, “On the hydraulics of rectangular settling basins: experimental and theoretical studies,” *Dep. Water Res. Eng. Lund Inst. Technol. Lund, Sweden.*, 1977.

[39] B. S. Zhou and A. M. Godo, “Short circuiting and density interface in primary clarifiers,” vol. 120, no. 9, pp. 1060–1080, 1995.

[40] T. Matko, N. Fawcett, A. Sharp, and T. Stephenson, “Recent progress in the numerical modelling of wastewater sedimentation tanks,” *Process Saf. Environ. Prot.*, vol. 74, no. 4, pp. 245–258, 1996.

[41] B. C. Liu, J. Ma, S. H. Huang, D. H. Chen, and W. X. Chen, "Two-dimensional numerical simulation of primary settling tanks by hybrid finite analytic method," *J. Environ. Eng.*, vol. 134, no. 4, pp. 273–282, 2008.

[42] K. Mohanarangam and D. Stephens, "Cfd Modelling of Floating and Settling Phases in Settling Tanks," *Victoria*, no. December, pp. 1–7, 2009.

[43] P. Krebs, D. Vischer, and W. Gujer, "Inlet-structure design for final clarifiers," *J. Environ. Eng. (United States)*, vol. 121, no. 8, pp. 558–564, 1995.

[44] A. M. Goula, M. Kostoglou, T. D. Karapantsios, and A. I. Zouboulis, "A CFD methodology for the design of sedimentation tanks in potable water treatment. Case study: The influence of a feed flow control baffle," *Chem. Eng. J.*, vol. 140, no. 1–3, pp. 110–121, 2008.

[45] A. H. Ghawi and K. Jozef, "Improving Performance of Horizontal Sedimentation Tanks," *ResearchGate*, no. December, 2008.

[46] X. Wang, L. Yang, Y. Sun, L. Song, M. Zhang, and Y. Cao, "Three-dimensional simulation on the water flow field and suspended solids concentration in the rectangular sedimentation tank," *J. Environ. Eng.*, vol. 134, no. 11, pp. 902–911, 2008.

[47] P. Rodríguez López, A. G. Lavín, M. M. Mahamud López, and J. L. Bueno de las Heras, "Flow models for rectangular sedimentation tanks," *Chem. Eng. Process. Process Intensif.*, vol. 47, no. 9–10, pp. 1705–1716, 2008.

[48] M. Al-Sammarraee and A. Chan, "Large-eddy simulations of particle sedimentation in a longitudinal sedimentation basin of a water treatment plant. Part 2: The effects of baffles," *Chem. Eng. J.*, vol. 152, no. 2–3, pp. 315–321, 2009.

[49] A. Tamayol, B. Firoozabadi, and M. A. Ashjari, "Hydrodynamics of secondary settling tanks and increasing their performance using baffles,"

J. Environ. Eng., vol. 136, no. 1, pp. 32–39, 2010.

[50] B. Liu, J. Ma, L. Luo, Y. Bai, S. Wang, and J. Zhang, "Design of Rectangular Primary Settling Tanks," *J. Environ. Eng.*, no. May, pp. 501–507, 2010.

[51] H. Asgharzadeh, B. Firoozabadi, and H. Afshin, "Experimental investigation of effects of baffle configurations on the performance of a secondary sedimentation tank," *Sci. Iran.*, vol. 18, no. 4 B, pp. 938–949, 2011.

[52] M. Shahrokhi and F. Rostami, "The Computational Modeling of Baffle Configuration in the Primary Sedimentation Tanks," *Flow3D2.Propagation.Net*, vol. 6, pp. 392–396, 2011.

[53] M. Gong *et al.*, "Development of a flocculation sub-model for a 3-D CFD model based on rectangular settling tanks," *Water Sci. Technol.*, vol. 63, no. 2, pp. 213–219, 2011.

[54] M. Shahrokhi, F. Rostami, M. A. Md Said, S. R. Sabbagh Yazdi, and Syafalni, "The effect of number of baffles on the improvement efficiency of primary sedimentation tanks," *Appl. Math. Model.*, vol. 36, no. 8, pp. 3725–3735, 2012.

[55] M. M. Heydari, M. S. Bajestan, H. A. Kashkuli, and H. Sedghi, "The effect angle of baffle on the performance of settling basin," *World Appl. Sci. J.*, vol. 21, no. 6, pp. 829–837, 2013.

[56] B. Lee, "Evaluation of double perforated baffles installed in rectangular secondary clarifiers," *Water (Switzerland)*, vol. 9, no. 6, 2017.

[57] R. Kuoppamäki, "The applicability of tracer techniques for studies on sewage treatment process dynamics," *Int. J. Appl. Radiat. Isot.*, vol. 28, no. 10–11, pp. 833–837, 1977.

[58] S. Conserva, F. Tatti, V. Torretta, N. Ferronato, and P. Viotti, "An integrated approach to the biological reactor-sedimentation tank system," *Resources*, vol. 8, no. 2, 2019.

[59] W. F. Leung and R. F. Probsteln, “Lamella and Tube Settlers. 1. Model and Operation,” *Ind. Eng. Chem. Process Des. Dev.*, vol. 22, no. 1, pp. 58–67, 1983.

[60] B. Lee, “Experimental study to evaluate design procedure and proposed improvement measures for clarifier with inclined plates,” *Environ. Eng. Res.*, vol. 20, no. 3, pp. 298–305, 2015.

[61] S. Sarkar, D. Kamilya, and B. C. Mal, “Effect of geometric and process variables on the performance of inclined plate settlers in treating aquacultural waste,” *Water Res.*, vol. 41, no. 5, pp. 993–1000, 2007.

[62] D. Burgos-Flores, A. Martín-Domínguez, I. R. Martín-Domínguez, M. Pérez-Tello, and M. T. Alarcon-Herrera, “Mathematical modelling of lamella plate settle hydraulics,” *Proc. Inst. Civ. Eng. Water Manag.*, vol. 162, no. 4, pp. 251–259, 2009.

[63] Y. Yu, D. Liu, and X. Cui, “Study on Hydraulic Characteristic of the Tube Settler,” no. Mcae, pp. 128–131, 2016.

[64] Ghawi, “Application of Computational Fluid Dynamics modelling to a horizontal sedimentation tank,” no. April, 2017.

[65] A. Stamou and A. Gkesouli, “Modeling settling tanks for water treatment using computational fluid dynamics,” *J. Hydroinformatics*, vol. 17, no. 5, pp. 745–762, 2015.

[66] Y. L. Liu, W. L. Wei, B. Lv, and X. F. Yang, “Research on optimal radius ratio of impellers in an oxidation ditch by using numerical simulation,” *Desalin. Water Treat.*, vol. 52, no. 13–15, pp. 2811–2816, 2014.

[67] W. Wei, Y. Liu, and B. Lv, “Numerical simulation of optimal submergence depth of impellers in an oxidation ditch,” *Desalin. Water Treat.*, vol. 57, no. 18, pp. 8228–8235, 2016.

[68] A. I. Stamou, G. Theodoridis, and K. Xanthopoulos, “Design of secondary settling tanks using a CFD model,” *J. Environ. Eng.*, vol. 135,

no. 7, pp. 551–561, 2009.

[69] M. Weiss, B. G. Plosz, K. Essemiani, and J. Meinhold, "CFD modelling of sludge sedimentation in secondary clarifiers," *WIT Trans. Eng. Sci.*, vol. 52, no. January 2009, pp. 509–518, 2006.

[70] Degrémont, *Water treatment handbook*, 7th editio. France, 2007.

[71] I. Metcalf and Eddy, *Wastewater Engineering: Treatment and Reuse*, Fourth edi. New York, USA: Mc Gram-Hill, 2003.

[72] Ghawi and J. Kri, "A Computational Fluid Dynamics Model of Flow and Settling in Sedimentation Tanks," *Appl. Comput. Fluid Dyn.*, 2012.

[73] Japan Sewage Works Association, *Design Standard for Municipal Wastewater Treatment Plants*. Tokyo, Japan: Japan Sewage Works Association, 2013.

[74] A. I. Stamou, "Verification and application of a mathematical model for the assessment of the effect of guiding walls on the hydraulic efficiency of chlorination tanks," *J. Hydroinformatics*, vol. 4, no. 4, pp. 245–254, 2002.

[75] M. Terashima, M. Iwasaki, H. Yasui, R. Goel, K. Suto, and C. Inoue, "Tracer experiment and RTD analysis of DAF separator with bar-type baffles," *Water Sci. Technol.*, vol. 67, no. 5, pp. 942–947, 2013.

[76] T. A. Nguyen, N. T. M. Dao, B. Liu, M. Terashima, and H. Yasui, "Computational fluid dynamics study on attainable flow rate in a lamella settler by increasing inclined plates," *J. Water Environ. Technol.*, vol. 17, no. 2, pp. 76–88, 2019.

[77] Y. Liu, P. Zhang, and W. Wei, "Simulation of effect of a baffle on the flow patterns and hydraulic efficiency in a sedimentation tank," *Desalin. Water Treat.*, vol. 57, no. 54, pp. 25950–25959, 2016.

[78] M. Patziger, H. Kainz, M. Hunze, and J. Józsa, "Influence of secondary settling tank performance on suspended solids mass balance in activated sludge systems," *Water Res.*, vol. 46, no. 7, pp. 2415–2424, 2012.

[79] JFE Engineering Corporation, “Pretreatment sedimentation equipment - Inclined plate settling device,” 2019. [Online]. Available: http://www.jfe-eng.co.jp/products/environment/water_supply/sup02.html. [Accessed: 20-Sep-2008].

[80] SUEZ’s degremont, “SUEZ’s degremont® water handbook, Lamella sedimentation,” 2019. [Online]. Available: https://www.suezwaterhandbook.com/water-and-generalities/fundamental-physical-chemical-engineering-processes-applicable-to-water-treatment/sedimentation/lamellar-sedimentation. [Accessed: 20-Sep-2008].

[81] R. Goel, M. Terashima, and H. Yasui, “Application of CFD to study the effects of Feed-well configuration on suspended solid concentration profile in settling tank,” in *Hydroinformatics*, World Scientific, 2004, pp. 316–323.

RESEARCH PUBLICATIONS BIBLIOGRAPHY

1. The-anh Nguyen, Nguyet Thi-minh Dao, Mitsuharu Terashima, Hidenari Yasui. Improvement of Suspended Solids Removal Efficiency in Sedimentation Tanks by Increasing Settling Area Using Computational Fluid Dynamics. *J. Water Environ. Technol.*,17(6), 420–431, 2019.

2. The-anh Nguyen, Nguyet Thi-minh Dao, Bing Liu, Mitsuharu Terashima, Hidenari Yasui. Computational Fluid Dynamics Study on Attainable Flow Rate in a Lamella Settler by Increasing Inclined Plates. *J. Water Environ. Technol.*, 17(2), 76–88, 2019.

CONFERENCE PARTICIPATION

International conferences

1. The-anh Nguyen, Nguyet Thi-minh Dao, Yutaka Kanza, Mitsuharu Terashima, Hidenari Yasui. Improvement of Sludge Settling Modelling in Secondary Sedimentation Tank Using CFD. Proceeding of "*The 56th Japan Annual Technical Conference on Sewerage"*, p66–68, 7-8 August, Yokohama, Japan, 2019.

2. The-anh Nguyen, Nguyet Thi-minh Dao, Mitsuharu Terashima, Hidenari Yasui. CFD Study on Improvement of Suspended Solids Removal Efficiency in Sedimentation Tank Using Inclined Plates. *Water and Environment Technology Conference 2019,* 13-14 July, Osaka, Japan, 2019.

3. The-anh Nguyen, Mitsuharu Terashima, Nguyet Thi-minh Dao, Bing Liu, Hidenari Yasui. CFD Study on Attainable Flow Rate of Lamella Settler by Increasing Inclined Plates. *Water and Environment Technology Conference 2018,* 14-15 July, Ehime, Japan, 2018.